AD-A130 533 PARAMETRIC ACOUSTIC ARRAY FORMATION VIA WEAK COLLINEAR AND NONCOLLINEAR I..(U) TEXAS UNIV AT AUSTIN APPLIED RESEARCH LABS M F HAMILTON JUN 83 ARL-TR-83-19 1/3

UNCLASSIFIED N00014-79-C-0624 F/G 17/1 NL

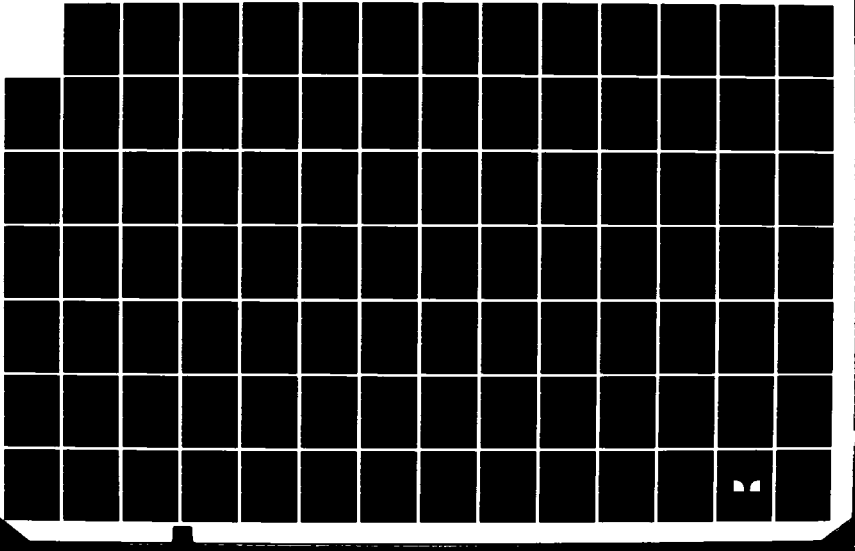

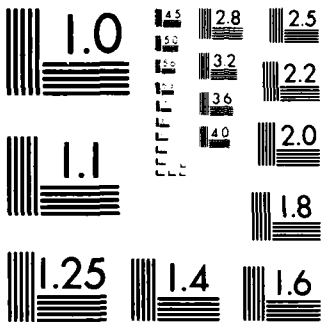

MICROCOPY RESOLUTION TEST CHART
NATIONAL BUREAU OF STANDARDS-1963-A

PARAMETRIC ACOUSTIC ARRAY FORMATION VIA WEAK COLLINEAR AND NONCOLLINEAR INTERACTION IN DISPERSIVE FLUIDS

by

MARK F. HAMILTON

GRADUATE PROGRAM IN ACOUSTICS
THE PENNSYLVANIA STATE UNIVERSITY
UNIVERSITY PARK, PA 16802

APPLIED RESEARCH LABORATORIES
THE UNIVERSITY OF TEXAS AT AUSTIN
AUSTIN, TX 78712

ARL-TR-83-19

JUNE 1983

OFFICE OF NAVAL RESEARCH
DEPARTMENT OF THE NAVY
ARLINGTON, VA 22217

N00014-79-C-0624

N00014-75-C-0867

UNCLASSIFIED

SECURITY CLASSIFICATION OF THIS PAGE *(When Data Entered)*

REPORT DOCUMENTATION PAGE		READ INSTRUCTIONS BEFORE COMPLETING FORM
1. REPORT NUMBER	2. GOVT ACCESSION NO. AD-A130553	3. RECIPIENT'S CATALOG NUMBER
4. TITLE *(and Subtitle)* PARAMETRIC ACOUSTIC ARRAY FORMATION VIA WEAK COLLINEAR AND NONCOLLINEAR INTERACTION IN DISPERSIVE FLUIDS		5. TYPE OF REPORT & PERIOD COVERED Technical Report 6. PERFORMING ORG. REPORT NUMBER ARL-TR-83-19
7. AUTHOR(s) Mark F. Hamilton		8. CONTRACT OR GRANT NUMBER(s) N00014-79-C-0624 N00014-75-C-0867
9. PERFORMING ORGANIZATION NAME AND ADDRESS Applied Research Laboratories The University of Texas at Austin Austin, Texas 78712		10. PROGRAM ELEMENT, PROJECT, TASK AREA & WORK UNIT NUMBERS
11. CONTROLLING OFFICE NAME AND ADDRESS The Pennsylvania State University University Park, Pennsylvania 16802		12. REPORT DATE June 1983 13. NUMBER OF PAGES 230
14. MONITORING AGENCY NAME & ADDRESS *(if different from Controlling Office)* Office of Naval Research Department of the Navy Arlington, Virginia 22217		15. SECURITY CLASS. *(of this report)* UNCLASSIFIED 15a. DECLASSIFICATION DOWNGRADING SCHEDULE

16. DISTRIBUTION STATEMENT *(of this Report)*

Approved for public release; distribution unlimited.

17. DISTRIBUTION STATEMENT *(of the abstract entered in Block 20, if different from Report)*

18. SUPPLEMENTARY NOTES

19. KEY WORDS *(Continue on reverse side if necessary and identify by block number)*

parametric array noncollinear interaction dispersion Gaussian beams
dissipation diffraction phase matching paraxial virtual sources

20. ABSTRACT *(Continue on reverse side if necessary and identify by block number)*

The effect of dispersion on parametric arrays formed by Gaussian beams is investigated via solutions of the nonlinear paraxial wave equation. Analytical solutions are obtained by employing the quasilinear approximation; the results are thus restricted to weakly nonlinear interactions. Both (i) collinear and (ii) noncollinear interactions of the primary beams are considered.

(i) Axial field curves and farfield directivity patterns are presented for the difference-frequency signal resulting from collinear interaction of Gaussian

DD FORM 1 JAN 73 1473 EDITION OF 1 NOV 65 IS OBSOLETE

UNCLASSIFIED

SECURITY CLASSIFICATION OF THIS PAGE *(When Data Entered)*

beams. The effects of dispersion, dissipation, and diffraction are considered in detail. Discrepancies with previous work are discussed. Dispersion is found to noticeably affect nonlinear interaction only when $|\delta| > \alpha_T/k_-$, where $\delta = 1 - (k_1 - k_2)/k_-$ is the dispersion parameter, k_j $(j = 1,2)$ and k_- are the primary and difference-frequency wave numbers, respectively, and $\alpha_T = \alpha_1 + \alpha_2 - \alpha_-$ is the combined attenuation coefficient. For an absorption-limited array, the interaction region behaves as a line array whose phasing depends on δ. When $\delta \geq 0$, the direction of maximum radiation is shifted off axis to the angle $\cos^{-1}(1 - \delta)$, whereas when $\delta < 0$, the field is evanescent and the maximum, although diminished in amplitude, remains on axis. Diffraction of the primaries also introduces slight phase mismatching, the effect of which is reduced for an appropriate positive value of δ.

(ii) Noncollinear interaction of collimated plane waves as well as Gaussian beams is investigated. When $\delta > 0$, it is well known that compensation for the detrimental effects of dispersion in plane-wave interaction is attained when the primaries intersect at the angle where $\vec{k}_1 - \vec{k}_2 = \vec{k}_-$. However, for arrays formed by narrow, noncollinear primaries, it is found that no amount of compensation is possible when $\delta > 0$. When $\delta < 0$, slight compensation is sometimes possible for highly collimated plane waves, for which the phase matching angle is $\sqrt{-8\delta}$ radians. No similar compensation is possible with Gaussian beams. The price paid for phase matching via noncollinear interaction is reduction in size of the interaction region, and therefore only marginal compensation for dispersion is ever possible.

FOREWORD

This report is an adaptation of Mark F. Hamilton's Ph.D. thesis (same title). The degree was granted in May 1983 by The Pennsylvania State University, where the author was enrolled in the Graduate Program in Acoustics.

Dr. Hamilton began his research at Penn State in 1980 under the supervision of the late Francis H. Fenlon. After Professor Fenlon's death in 1981, Hamilton came to Applied Research Laboratories, The University of Texas at Austin, to complete the work.

Primary support for the research came from the Office of Naval Research (ONR) under Contract N00014-79-C-0624 at Penn State; F. H. Fenlon, later J. D. Maynard, was principal investigator. Additional support came from ONR Contract N00014-75-C-0867 at Applied Research Laboratories, The University of Texas at Austin. ONR Scientific Officer was L. E. Hargrove for both contracts.

The good will and cooperation of many persons at the two universities and at ONR are gratefully acknowledged.

David T. Blackstock

Supervisor

TABLE OF CONTENTS

TABLE OF CONTENTS (continued)

LIST OF FIGURES

LIST OF FIGURES (continued)

LIST OF FIGURES (continued)

LIST OF FIGURES (continued)

LIST OF SYMBOLS

1 , 2 , $+$, $-$, $\pm$	subscripts representing ω_1 , ω_2 , etc.; e.g., $k_1 = k_{\omega_1}$
$*$	i) z^* : complex conjugate of z ii) $p_\omega * p_\omega$: convolution over ω
a	circular piston radius
a , b	rectangular beam half-widths in x and y directions, respectively
$a_\omega = \alpha_\omega z_o$	absorption loss at frequency ω and range z_o
$a'_\omega = \alpha'_\omega z_o$	complex absorption coefficient
$a_{T_\pm} = \alpha_{T_\pm} z_o$	combined absorption coefficient ($a_T = a_{T_-}$)
$a'_{T_\pm} = \alpha'_{T_\pm} z_o$	complex combined absorption coefficient
$A_\omega(\theta,z)$, $A_\omega(k_\varepsilon,z)$	angular spectrum
$A_{12}(\theta)$, $A_{12}(k_\varepsilon)$	aperture factor
$A_G(\theta_x,\theta_y;\phi)$	normalized aperture factor for non-diffracting Gaussian beams
b	thermoviscous coefficient
B/A	ratio of coefficients in the equation of state
c_o	reference sound speed
c_ω	sound speed at frequency ω
c_o , c_∞	equilibrium and frozen sound speeds, respectively, in a monorelaxing fluid
c_g	group velocity of the primaries
$D = \omega_o \varepsilon_o / 2c_o = \pi\varepsilon_o/\lambda_o$	effective Gaussian source diameter in mean primary wavelengths
$D(\cdot)$	dispersion operator
$D_1(\theta)$, $D_2(\theta)$	primary beam directivities

$D_\delta(\theta)$	difference-frequency directivity for collinear interaction
$D_\delta(\theta_x,\theta_y;\phi)$	difference-frequency directivity for noncollinear interaction
$D_o^W(\theta)$	Rutherford directivity
$D_\delta^W(\theta)$, $D_\delta^W(\theta_x,\theta_y)$	modified Westervelt directivity
$D_\delta^G(\theta;\phi)$	Westervelt-type directivity for nondiffracting Gaussian primaries
$D_\delta^G(\theta_x,\theta_y;\phi)$	Westervelt-type directivity for Gaussian primaries
$\mathrm{erfc}(z)$	complementary error function
$E_n(z)$	exponential integral
$E_n(\varepsilon,z;\omega)$	eigenfunction of paraxial wave equation for axisymmetric radiation
$E_{mn}(x,y,z;\omega)$	eigenfunction of paraxial wave equation
$F_\delta^R(\theta_x,\theta_y;\phi_1,\phi_2)$	component of difference-frequency directivity for noncollinear interaction of rectangular beams
$F_\omega\{p(t)\} = \int_{-\infty}^{\infty} p(t)e^{-i\omega t}\,dt$	Fourier transform of $p(t)$
$g_\omega(\vec{r}\,\vert\,\vec{r}\,')$	Green's function
$G_\omega(k_x,k_y,z)$, $G_\omega(k_\varepsilon,z)$	angular spectrum of the Green's function
$H(x)$	Heaviside unit step function
$H_n(x)$	Hermite polynomial of order n
$i = \sqrt{-1}$	imaginary unit
$I_n(x)$	modified Bessel function of order n
$J_n(x)$	Bessel function of order n
$k_\omega = \omega/c_\omega = \vert\vec{k}_\omega\vert$	wave number at frequency ω
$\vec{k}_\omega$	wave vector at frequency ω
$k_o = (k_1 + k_2)/2$	mean primary wave number

k_x , k_y , k_z , k_ε	wave vector components
L	length of finite array
$L_n(x)$	Laguerre polynomial of order n
$m = (c_\infty^2 - c_o^2)/c_o^2$	dispersivity of monorelaxing fluid
$O(\cdot)$	order function
$p(x,y,z,t)$	acoustic pressure
$p_\omega(x,y,z) = F_\omega\{p(x,y,z,t)\}$	acoustic pressure spectral amplitude
$P_1(x,y)$, $P_2(x,y)$	amplitude of primaries at $z = 0$.
p_{01} , p_{02}	peak pressure of Bessel primary beams at the face of the projector
p_{G1} , p_{G2}	peak pressure of Gaussian primary beams at the face of the projector
$P_o = \beta p_{G1} p_{G2}/\rho_o c_o^2$	reference pressure
P_n , P_{mn} , P_{mnpq}	series expansion coefficients having units of pressure
$Q_\omega(x,y,z) = p_\omega(x,y,z) * p_\omega(x,y,z)$	volume distributed source excitation at frequency ω
$r = \lvert\vec{r}\rvert$	range from projector
$\vec{r}$	position vector
$Re(\cdot)$	real part of a complex number
$rect(x)$	rectangle function
t , $t' = t - z/c_o$	time and retarded time, respectively
$u = \lvert\vec{u}\rvert$	particle velocity
$\vec{u}$	particle velocity vector
u_x , u_y	particle velocity components
V'	volume containing virtual sources
x , y , z	Cartesian coordinates
x_o , y_o	Gaussian source dimensions
$X = x/\varepsilon_o$	normalized coordinate

$Y = y/\varepsilon_o$	normalized coordinate
$z_o = \omega_o \varepsilon_o^2/2c_o$	mean primary frequency collimation distance for a Gaussian beam
$Z = z/z_o$	normalized range coordinate
$Z_\pm$	field integral coefficient
α_ω	attenuation coefficient at frequency ω
$\alpha'_\omega = \alpha_\omega + i(k_\omega - \omega/c_o)$	complex attenuation coefficient
$\alpha_{T_\pm} = \alpha_1 + \alpha_2 - \alpha_\pm$	combined attenuation coefficient ($\alpha_T = \alpha_{T_-}$)
$\alpha'_{T_\pm} = \alpha_{T_\pm} - ik_\pm\delta_\pm$	complex combined attenuation coefficient
β	coefficient of nonlinearity
$\beta_\pm(\phi)$	modified coefficient of nonlinearity
γ	ratio of specific heats
$\delta_\pm = 1 - (k_1 \pm k_2)/k_\pm$	dispersion coefficient ($\delta = \delta_-$)
$\delta(x)$	Dirac delta function
δ_{mn}	Kronecker delta function
$\Delta\phi$	phase mismatch between primaries resulting from diffraction
$\varepsilon = (x^2 + y^2)^{1/2}$	radial coordinate in plane transverse to beam axis
ε_o	spot size of Gaussian beam
ϕ	azimuthal angle
θ_o	angle of maximum difference-frequency radiation
ϕ_x, ϕ_y	azimuthal angles in x-z and y-z planes, respectively
θ_{HP}	half-power angle of difference-frequency radiation
λ_ω	wavelength at frequency ω

$\lambda_o = 2\pi c_o/\omega_o$	approximate wavelength at mean primary frequency
$\lambda_q = 2\pi/(\lvert\vec{k}_1 - \vec{k}_2\rvert - k_-)$	difference-frequency field spatial oscillation period for plane-wave interaction
$\xi = \varepsilon/\varepsilon_o$	normalized radial coordinate
ρ , ρ_o	total and ambient density, respectively
τ	relaxation time of monorelaxing fluid
$\phi = \phi_1 - \phi_2$	angle between primaries
ϕ_o	angle at which resonance occurs within interaction region
ϕ_1 , ϕ_2	angles formed by primaries and the z axis
$\chi_\omega = k_\omega - i\alpha_\omega$	complex wave number
$\vec{\chi}_\omega$	complex wave vector
χ_z	z component of $\vec{\chi}_\omega$
ψ	angle formed by $\vec{k}_1 - \vec{k}_2$ and z axis when $\phi_1 = \phi/2$, $\phi_2 = -\phi/2$
Ψ	angle formed by $\vec{k}_1 - \vec{k}_2$ and z axis when $\phi_1 = \phi$, $\phi_2 = 0$
ω	angular frequency
$\omega_o = (\omega_1 + \omega_2)/2$	mean primary frequency
ω_1 , ω_2	primary frequencies
$\omega_\pm = \omega_1 \pm \omega_2$	sum and difference frequencies
$\Omega = \omega/\omega_o$	normalized frequency
$\nabla^2 = \partial_x^2 + \partial_y^2 + \partial_z^2$	Laplacian operator
$\nabla_\perp^2 = \partial_x^2 + \partial_y^2$	Laplacian operator in plane transverse to beam axis

ACKNOWLEDGMENTS

This research is dedicated to the memory of the late Dr. Francis H. Fenlon. Words cannot express the extent of his effect on the author. The encouragement and understanding provided by Dr. Fenlon's family were, and still are, beyond thanks.

It is with deepest appreciation that the essential contributions of Dr. David T. Blackstock of Applied Research Laboratories of The University of Texas at Austin (ARL:UT) are gratefully acknowledged. After the death of Dr. Fenlon, Dr. Blackstock assumed the role of the author's major thesis supervisor. Were it not for his generosity and southern hospitality, it is questionable whether this project would have been completed.

Drs. Jacqueline and Sigve Tjøtta of The University of Bergen, Norway, provided invaluable criticism of Chapter IV. Moreover, they checked many of the results obtained in that chapter against those obtained from their computer program which solves the nonlinear paraxial wave equation.

Drs. J. Tichy and M. T. Pigott of The Pennsylvania State University played important roles in solving both administrative and logistic problems resulting from the author's stay at ARL:UT. The assistance of the author's doctoral committee, namely Drs. S. I. Hayek, J. D. Maynard, S. T. McDaniel, and A. D. Stuart, is gratefully acknowledged.

A number of people at ARL:UT deserve special recognition for their contributions to this project. Above all, Mr. J. M. Estes is acknowledged for his assistance concerning numerical computation, as well as for playing the devil's advocate throughout the course of the author's research. Also, for many helpful discussions, are thanked, Dr. H. L. Kuntz, and Messrs. J. A. TenCate, Y. H. Berthelot, and D. A. Nelson.

Typing was performed primarily by Miss Rebecca G. Messer, with final revisions typed by Mrs. Dorothy Tindal.

Last, but certainly not least, thanks are extended to Dr. Cyril M. Harris of Columbia University for encouraging the author to enter the field of acoustics.

This work was supported by the United States Office of Naval Research.

CHAPTER I

INTRODUCTION

The parametric array involves simultaneous radiation of two acoustic signals having frequencies ω_1 and ω_2 from a single source. If the amplitudes of these two signals, which are called the primary waves, are sufficiently high that the medium responds nonlinearly to the propagation of the signals, intermodulation distortion occurs. Components having frequencies $n\omega_1 \pm m\omega_2$, where $n,m = 0,1,2, \ldots$, are thus generated during the course of propagation. Of greatest interest is the component whose frequency, ω_-, is given by the difference between the frequencies of the primary waves, $\omega_1 - \omega_2$. The primary frequencies are usually selected whereby $\omega_1 \simeq \omega_2$, and therefore $\omega_- << \omega_1,\omega_2$. Because absorption of a sound wave usually increases with frequency, the difference-frequency signal outlasts not only all other intermodulation components, but the primaries as well. A remarkable consequence of generating the difference-frequency signal in this fashion is that the directivity function is roughly equivalent to those of the primaries, despite the fact that $\omega_- << \omega_1,\omega_2$. The parametric array thus offers a means of radiating a signal in a far narrower beam than is possible by conventional radiation.

Beginning with Westervelt's landmark paper in 1963,[1] analyses of the parametric acoustic array have, with few exceptions, been restricted to arrays formed by wave interaction in dispersionless fluids. When two finite-amplitude primary beams interact collinearly in a dispersionless fluid to generate a difference-frequency excitation, the virtual sources assume a phase distribution corresponding to the propagation

speed of the primaries. Because the difference-frequency signal propagates at the same speed, it is coherently amplified along the length of the array. It is precisely this phase coherence which gives rise to the end-fire radiation pattern, which is the hallmark of the parametric array.

In a dispersive fluid the phasing of the virtual sources does not in general match the propagation speed of the difference-frequency wave. An indication of how the phase mismatch affects parametric array formation is revealed by considering the lossless collinear interaction of two plane primary waves described by $e^{i(\omega_1 t - k_1 z)}$ and $e^{i(\omega_2 t - k_2 z)}$, where $k_j = \omega_j/c_j$ is the wave number of the wave having frequency ω_j and propagating at speed c_j. To a first approximation, where the interaction is confined to the waves k_1, k_2, and k_-, and where $k_- = \omega_-/c_-$, the frequency-domain wave equation that the difference-frequency pressure field must satisfy is of the form

$$\left(\frac{\partial^2}{\partial z^2} + k_-^2\right) p_- = Ke^{-i(k_1 - k_2)z} .$$

Resonance occurs when the wave number $(k_1 - k_2)$ of the forcing function, i.e., of the virtual-source distribution, is the same as the wave number (k_-) of the difference-frequency field. The amplitude of $p_-(z)$ is found to be proportional to[2]

$$\left|\frac{\sin (k_1 - k_2 - k_-)z/2}{k_1 - k_2 - k_-}\right| .$$

In the absence of dispersion $(k_1 - k_2 = k_-)$, the amplitude increases linearly with range. This growth is unbounded because we have neglected any losses (dissipative and finite-amplitude) ordinarily suffered by the

primaries. When the fluid is dispersive $(k_1 - k_2 \neq k_-)$, the amplitude oscillates in space with period $2\pi/|k_1 - k_2 - k_-|$. Energy transferred from the primaries to the difference-frequency signal in the first half spatial period is thus withdrawn in the second half period. The cycle is repeated in each subsequent period. As a result, if the interaction region extends beyond $\pi/|k_1 - k_2 - k_-|$, which it does in the absence of losses, the efficiency of the parametric interaction is severely diminished.

The effect of dispersion and in particular the concept of phase matching in parametric interactions has received considerable attention in the field of nonlinear optics because of the strong dispersivity of most optical dielectrics. (See, for example, References 3 and 4.) Since, on the contrary, most acoustical media exhibit weak dispersion, there has been comparatively little interest in the effect of dispersion on the performance of the parametric acoustic array. The most common cause of dispersion is relaxation, for which the dispersivity is measured by $m = (c_\infty^2 - c_o^2)/c_o^2$, where c_o and c_∞ are the sound speeds at zero and infinite frequency, respectively. For example, in sea water the value of m is in general less than 10^{-4}. We will find that greater dispersion is necessary for observation of the spatial oscillations described above. In various liquid polymers, m can be as large as 0.1. However, such large dispersion in relaxing fluids is accompanied by extraordinarily high sound attenuation, which prohibits observation of the effects of the dispersion.

Inhomogeneous fluids, examples of which are bubbly liquids and aerosols, provide alternative sources of dispersion. Virtually

unlimited dispersion is easily obtained with bubbly water, where excess attenuation of sound due to the bubbles is maximized near the resonance frequency of the bubble oscillations. If the primary frequencies and the difference frequency are respectively much higher and lower than the bubble resonance frequency, most excess attenuation is avoided and the effects of dispersion on the parametric array should be easily observed. Zabolotskaya and Soluyan[5] suggested the use of bubbles for enhancing parametric amplification via dispersive wave filtering. Recall that not only the difference frequency is generated by intermodulation distortion of the primaries; all other nonlinearly generated components draw energy from the primaries, thereby reducing the amount of energy available for amplification of the difference-frequency signal. Also, interaction of the sum-frequency component $(\omega_1 + \omega_2)$ with the second harmonic of the lower-frequency primary $(2\omega_2)$ causes degenerative coupling with, and thus attenuation of, the difference-frequency signal. Dispersive wave filtering refers to conditions where all nonlinearly generated components except the difference-frequency signal suffer the detrimental effects of dispersion.

So far only the Soviets have considered the matter of parametric array formation in a dispersive fluid. Novikov,[6] the first to address the problem, analyzed the interaction of nondiffracting primary waves in a relaxing fluid and obtained expressions for the axial nearfield and the farfield radiation pattern. He showed that maximum radiation occurs at an angle given by $\theta_o = \cos^{-1}[(k_1 - k_2)/k_-]$. Karamzin, Sukhorukov, and Sukhorukova[7] followed with a numerical analysis that illustrates the way in which dispersion can be employed to offset the small phase mismatch caused by diffraction. They demonstrated that the axial intensity

of the difference-frequency signal can be thus increased slightly at certain locations within the parametric array field. A more significant contribution is that of Kozyaev and Naugol'nykh,[8] who investigated parametric array formation in bubbly water. Although their analysis is confined to collimated plane primary waves, it is novel in that they consider the possibility of phase matching by having the beams intersect at a suitable angle. For collinear interaction, they showed the directivity function to be a version of Westervelt's result[1] for an absorption-limited array, but with the maximum radiation occurring at the angle θ_o obtained by Novikov.[6] More recently, Novikov[9] extended his previous analysis[6] to include diffraction of the primary beams. He demonstrated that a Gaussian beam model also yields a modified Westervelt directivity function for absorption-limited arrays. Without dispersion, his results reduce to those originally obtained by Fenlon and McKendree.[10]

A peculiar mistake has apparently arisen and propagated through the Soviet literature.[6,7,8,9] The error is associated with the sign of the parameter that measures dispersion, which we define here as $\delta = 1 - (k_1 - k_2)/k_-$. We obtain $\delta = 0$ for no dispersion $(c_1 = c_2 = c_-)$, $\delta > 0$ for normal dispersion $(c_1 \geq c_2 > c_-)$, and $\delta < 0$ for anomalous dispersion $(c_1 \leq c_2 < c_-)$. Novikov[6] initially analyzed the axial nearfield of an array formed in a weakly relaxing fluid, where for $c_1 = c_2 = c_\infty$ and $c_- = c_o$, m can be approximated by 2δ . While he began with the proper wave equation, he obtained a solution which contains m with the wrong sign. However, as shown below, because Novikov[6] neglected diffraction in the primary beams and considered only cases of high absorption, his error in the axial

solution is insignificant and hence academic. On the other hand, a similar mistake by Karamzin, Sukhorukov, and Sukhorukova[7] led to the erroneous conclusion that anomalous dispersion, not normal dispersion, is necessary for increasing the conversion efficiency of the parametric array. Kozyaev and Naugol'nykh,[8] while deriving the proper directivity function which has a maximum at $\theta_o = \cos^{-1}[(k_1 - k_2)/k_-]$, failed to correctly interpret it. They stated that the direction of maximum radiation is shifted off-axis when $k_1 - k_2 > k_-$ $(\delta < 0)$, while clearly this shift can occur only when $k_1 - k_2 < k_-$ $(\delta > 0)$. Finally, Novikov[9] introduced δ with the wrong sign in his wave equation and subsequently carried the mistake through his entire analysis. Incorrect conclusions were thus reached regarding both the behavior of the axial field and the farfield directivity pattern.

Analysis of the parametric array is complicated by the need for adequate descriptions of the primary wave fields, since the product of the primaries constitutes the distribution of virtual sources which radiates the difference-frequency signal. When the amplitudes of the primaries are sufficiently weak that shock formation does not occur, the nonlinear wave equation may be solved by successive approximations. Such is usually the case in practice, i.e., it is assumed that the primaries remain relatively unaffected by the nonlinear interaction. Therefore, once the primary wave fields are known, the difference-frequency field can be evaluated, to a first approximation, by the method of Green's functions. Westervelt[1] considered primary beams which are so narrow that their width can be neglected. He obtained a directivity function for the difference-frequency signal which describes the radiation pattern resulting from a semi-infinite end-fire line array.

The Tjøttas[11] extended Westervelt's farfield analysis to primaries radiated by a finite aperture. In both cases, no account was taken for spreading of the primary beams. Muir[12] accounted for the directivity of the primaries by assuming that most nonlinear interaction occurs beyond the nearfield, and thus integrated over the product of the primary-beam directivity functions. His result, which he demonstrated may be used in the nearfield, requires numerical integration. A number of authors[13,14,15] considered the effect of the primary-wave nearfield by matching plane-wave and spherical-wave solutions. More sophisticated solutions which are valid for the nearfield of the array require numerical integration. An exception is the closed-form analytical nearfield solution obtained by Novikov, Rudenko, and Soluyan,[16] who solved Kuznetsov's[17] nonlinear paraxial wave equation for Gaussian primary beams. Their analysis was subsequently extended by Novikov, Rybachek, and Timoshenko[18] to encompass the entire paraxial field, for which a simple analytical solution exists along the acoustic axis. The utility of using Gaussian primary beams was demonstrated by Fenlon's[10,19] detailed analyses where, by appropriate scaling, he developed approximate analytical solutions for fields radiated by uniformly excited circular and rectangular projectors.

Our analysis begins with a discussion in Chapter II of the effect of dispersion on parametric arrays formed by collinear interaction of collimated plane primary waves. In Chapter II much of the basic analysis is laid out for the remainder of the thesis. Specifically, we discuss in Section 2.2 the region in which nonlinear interaction occurs. It is in the interaction region that dispersion is manifested via spatial oscillations of the difference-frequency signal. The interaction

region is terminated when the primaries become sufficiently weak that they no longer sustain significant nonlinear interaction. We assume in Chapter II that the primaries do not experience spreading losses. Moreover, we assume throughout the thesis that the primaries are of sufficiently weak finite amplitudes that they impart only a small percentage of their energy to the nonlinearly generated signals. These losses from the primaries are called finite-amplitude losses. Therefore, in the absence of both spreading and finite-amplitude losses, dissipation eventually terminates the interaction region. An array terminated in this way is called an absorption-limited array. In Section 2.3 we discuss the effect of dispersion on the farfield radiation pattern of an absorption-limited array.

The subsequent analysis is an extension of Fenlon and McKendree's[10] Gaussian beam model for parametric arrays, to the case of dispersive fluids as discussed by Fenlon and Hamilton.[20,21] By way of Gaussian primary beams, diffraction as well as dispersion and dissipation is taken into account. Not only does diffraction induce spreading losses and thus compete with dissipation in terms of attenuation of the primaries; it also introduces slight phase mismatching beyond that created by dispersion. Diffraction also has a significant effect on the directivity pattern. Assuming weak finite-amplitude conditions, we use the method of successive approximations to solve a modification of Kuznetsov's[17] paraxial wave equation. Chapter III is devoted to a derivation of Green's functions and eigenfunctions of the paraxial wave equation. In Chapter IV we present a detailed analysis of parametric arrays formed by collinear interaction of Gaussian primary beams. Attention is restricted in Section 4.2 to the

axial difference-frequency field, after which we discuss the farfield radiation pattern in Section 4.3. We conclude Chapter IV with a discussion of the sum-frequency signal, which behaves quite differently from the difference-frequency signal. In Appendix C, the field equations derived in Chapter IV are transformed for application to sum- and difference-frequency fields resulting from primaries radiated by circular piston projectors. Predictions made with the transformed equations are compared with data reported in the literature for components generated by finite-amplitude beams in dispersionless fluids.

Phase mismatching occurs not only because of dispersion, but also as a result of noncollinear interaction of the primaries. When plane primary waves intersect at such an angle that $\vec{k}_1 - \vec{k}_2 = \vec{k}_-$, phase matching with the difference-frequency signal is accomplished. Phase matching in a dispersionless fluid is therefore possible only for collinear interaction where $\vec{k}_1$ and $\vec{k}_2$ have the same direction. However, noncollinear interaction presents the possibility of phase matching in dispersive fluids, which is the motivation behind Chapters V and VI. In any event, the analysis presented here for parametric arrays formed by noncollinear interaction is entirely new. In Chapter V we parallel the analysis in Chapter II of parametric arrays formed by nondiffracting primaries, except that we consider the case of noncollinear interaction. In Chapter VI we again resort to Gaussian beams where the effect of diffraction on noncollinear interaction in a dispersive fluid is examined.

CHAPTER II

PARAMETRIC ARRAYS FORMED BY NONDIFFRACTING COLLINEAR PRIMARY WAVES

In this chapter we neglect the effect of diffraction on the primaries, and analyze the effect of dispersion on parametric arrays formed by collinear interaction of collimated primary waves. Simple analytical solutions are thus obtained from which physical interpretation of the effects of dispersion are easily deduced. We begin in Section 2.1 with a discussion of the second-order wave equation, as well as the method of solution, which will be used in this chapter. In Section 2.2 we analyze the behavior within the interaction region by considering the problem of plane-wave interaction. The farfield is investigated in Section 2.3 by way of Fresnel approximations of the Green's function solution.

2.1 The Wave Equation and the Parametric Array

During the past two decades, a vast number of articles pertaining to parametric array formation in dispersionless fluids has appeared in the literature. Excellent concise surveys may be found in the introductions of References 10 and 13, which together bring the reader up to 1979, and direct him to other, less accessible reviews. We thus restrict our attention primarily to that work which relates to the problem at hand, namely the effect of dispersion on the parametric array.

The parametric array is perhaps the most well-known application of nonlinear acoustics. Westervelt conceived the parametric array (first reported[22] in 1960, but not published[1] until 1963) as a consequence of Lighthill's[23] acoustic analog equation, which was originally

derived to describe the radiation of sound by turbulent flow. By manipulating Lighthill's exact equation, Westervelt derived the following approximate wave equation:

$$\nabla^2 p - \frac{1}{c_o^2} \frac{\partial^2 p}{\partial t^2} = - \frac{\beta}{\rho_o c_o^4} \frac{\partial^2 p^2}{\partial t^2} \quad , \tag{2.1}$$

where $p(x,y,z,t)$ is the acoustic pressure, c_o is the small-signal sound speed, ρ_o is the ambient density of the fluid, and β is the coefficient of nonlinearity. For liquids we have

$$\beta = 1 + B/2A \quad ,$$

where,[24] if P is the total pressure (static plus acoustic),

$$\frac{B}{A} = \frac{\rho_o}{c_o^2} \left(\frac{\partial^2 P}{\partial \rho^2} \right)_o \quad ;$$

the derivative is taken at $\rho = \rho_o$ and constant entropy. For an ideal gas B/A is $\gamma - 1$, where γ is the ratio of specific heats, and therefore β is $(\gamma + 1)/2$. As pointed out recently by Tjøtta and Tjøtta,[25] the approximations which lead to Equation (2.1) restrict its application to waves whose surfaces of constant phase possess large radii of curvature. Such waves are referred to as quasi-plane waves, an example of which is a spherical wave when $kr >> 1$. However, this restriction does not affect our analysis because we are concerned primarily with the paraxial region of highly collimated beams.

The quadratic nonlinearity in Equation (2.1) arises from nonlinearities in the equations of state and motion. As discussed in greater detail in Section 5.1, β accounts for the relative importance of the sources of nonlinearity. The term $B/2A$ represents the

quadratic nonlinearity in the equation of state relating the pressure and density. The factor of unity represents convection of the fluid which results from the finite amplitude of the particle velocity, u. In fact, the propagation speed varies from point to point on a waveform, and is given by

$$c_o + \beta u \quad ,$$

where c_o here refers to the small-signal sound speed, i.e., the propagation speed of the zero crossings of the wave. A waveform therefore becomes increasingly distorted during the course of propagation. The nature of the distortion can be understood from Equation (2.1). Components are generated having frequencies which result from the continuous squaring of the propagating signal. For example, a sinusoidal waveform becomes enriched with every harmonic of its original (fundamental) frequency. Of course, the nonlinearly generated components are created at the expense of energy in the fundamental. This energy drain from the fundamental is referred to as finite-amplitude losses.

Westervelt exploited the quadratic nonlinearity in the interaction of two highly directional collinear sound beams of different frequencies. Specifically, if the two beams, called primaries, have frequencies ω_1 and ω_2 $(\omega_1 > \omega_2)$, then the nonlinearity in Equation (2.1) gives rise to secondary components having frequencies $2\omega_1$, $2\omega_2$, $\omega_+ = \omega_1 + \omega_2$, and $\omega_- = \omega_1 - \omega_2$. Until they are sufficiently attenuated by dissipative, spreading, or finite-amplitude losses, the primaries continuously pump energy, during the course of propagation, into the secondary-frequency components. The region in which the energy transfer takes place is called the interaction region.

In a dispersionless fluid, the primaries propagate at the same speed as the secondary components. The interaction is then synchronous in the sense that, because the primaries do not shift in phase relative to the secondary components, the latter are amplified coherently over the entire length of the interaction region. Indeed, the phasing is such that the interaction region resembles an end-fire array which is radiating at the secondary frequencies. Westervelt named this interaction region the parametric array.

The remarkable feature of the parametric array is that the directivity of the difference-frequency signal is determined not so much by the source which radiates the primaries, but by the length of the interaction region, i.e., of the virtual end-fire array. The difference-frequency signal can thus be radiated as a far narrower beam than would be possible if it were radiated directly by the source. In general, absorption of sound increases with frequency. For example, the viscous attenuation coefficient of sound is roughly proportional to the square of the frequency. If $\omega_1 \approx \omega_2$, then $\omega_- << \omega_1, \omega_2$, whereby the attenuation coefficients of the components having frequencies ω_1, ω_2, $2\omega_1$, $2\omega_2$, and ω_+, are at least an order of magnitude greater than that for the difference-frequency component. As a result, the difference-frequency component outlasts all of the other frequency components radiated by the parametric array, including the primaries despite their high initial amplitudes.

In the frequency domain, Equation (2.1) becomes

$$\nabla^2 p_\omega + \left(\frac{\omega}{c_o}\right)^2 p_\omega = \frac{\beta\omega^2}{\rho_o c_o^4} Q_\omega \quad , \tag{2.2}$$

where

$$p_\omega(x,y,z) = \int_{-\infty}^{\infty} p(x,y,z,t)\, e^{-i\omega t}\, dt$$

and

$$Q_\omega = \int_{-\infty}^{\infty} p^2(t) e^{-i\omega t}\, dt = \int_{-\infty}^{\infty} p_{\omega'} p_{\omega-\omega'}\, d\omega' = p_\omega * p_\omega \quad . \qquad (2.3)$$

Even though $Q_\omega(x,y,z)$ is a function of p_ω, Equation (2.2) has the form of an inhomogeneous Helmholtz equation. Moreover, Equation (2.1) is commonly referred to as the inhomogeneous wave equation. This description follows from the interpretation of Q_ω as a volume-distributed source term. In fact, because of this interpretation, Berktay and his coworkers[26,27] used the term "virtual sources" to describe the interaction region.

We now account for dissipation and dispersion in an ad hoc manner. Suppose ε characterizes the scale of the acoustic pressure amplitude and μ the scale of the combined effects of dissipation and dispersion. Linear lossless terms are then of order ε, linear lossy terms are of order $\mu\varepsilon$, most significant nonlinear lossless terms are of order ε^2, and nonlinear lossy terms are of order $\mu\varepsilon^2$ and higher. If we regard the effects of nonlinearity, dissipation, and dispersion as each being small, none of which we wish to neglect entirely, the ordering hierarchy becomes as follows: first-order terms are of order ε, second-order terms are of order ε^2 and $\mu\varepsilon$, and all remaining terms are third- and higher-order. Therefore, in a second-order wave equation, terms accounting for either dissipation or dispersion do not

appear in combination with Q_ω, since such products constitute third-order quantities. We thus include the effects of dissipation and dispersion by rewriting Equation (2.2) as

$$\nabla^2 p_\omega + \chi_\omega^2 p_\omega = \frac{\beta\omega^2}{\rho_o c_o^4} Q_\omega \quad , \tag{2.4}$$

where

$$\chi_\omega = k_\omega - i\alpha_\omega \quad .$$

The wave number $k_\omega = \omega/c_\omega$ depends on the frequency-dependent sound speed c_ω, α_ω is the attenuation coefficient, and c_o is an arbitrary reference sound speed, i.e., c_ω evaluated at an arbitrary frequency.

In this thesis we use the method of successive approximations to obtain second-order solutions of Equation (2.4). For sufficiently high source amplitudes, the second-order solutions become unsuitable, and higher-order approximations become necessary. Our analysis is therefore valid only when we can safely ignore finite-amplitude losses incurred by the primaries as a result of energy transfer to the secondary-frequency components. To ensure acceptable accuracy of the second-order solutions, we consider only sources which emit waves of sufficiently weak finite amplitudes that shock formation does not occur.[13] For example, at the point where an initially sinusoidal plane wave forms a shock front in an inviscid fluid, the amplitude of the fundamental is only down to 88% of its original value.

We are interested in this chapter only in axisymmetric source excitations. We also assume in this chapter that the primaries do not experience diffraction. For a source which is located in the center of

the x-y plane and radiating in the positive z direction, the boundary conditions for the two primaries are given by $p_j(\varepsilon,0)$, where $j = 1,2$ represents ω_1 and ω_2, respectively, and $\varepsilon^2 = x^2 + y^2$. In the first approximation, the primaries obey the linear wave equation, that is, Equation (2.4) with $Q_\omega = 0$. The linear form of Equation (2.4) which is to be solved for plane primary waves thus becomes

$$\left(\frac{\partial^2}{\partial z^2} + \chi_j^2\right) p_j(\varepsilon,z) = 0 \quad . \tag{2.5}$$

For wave propagation in the positive z direction, the solution of Equation (2.5) is simply

$$p_j(\varepsilon,z) = p_j(\varepsilon,0)e^{-i\chi_j z} \quad . \tag{2.6}$$

In the second approximation, the source term Q_ω is a function of only the primary wave fields. Effects resulting from interaction of the secondary-frequency components with either the primaries or other second- or higher-order frequency components are therefore not taken into account. For the difference frequency, Equation (2.3) becomes

$$Q_-(\varepsilon,z) = p_1(\varepsilon,z)\, p_2^*(\varepsilon,z) \quad , \tag{2.7}$$

where p_2^* is the complex conjugate of p_2. Combining Equations (2.4), (2.6), and (2.7), we obtain for the inhomogeneous wave governing the difference-frequency pressure field,

$$(\nabla^2 + \chi_-^2)\, p_-(\varepsilon,z) = \frac{\beta\omega_-^2}{\rho_o c_o^4}\, p_1(\varepsilon,0)\, p_2^*(\varepsilon,0)\, e^{-i(\chi_1 - \chi_2^*)z} \quad . \tag{2.8}$$

An interesting analogy may be made if we now rewrite Equation (2.8) in the following one-dimensional form:

$$\left(\frac{\partial^2}{\partial z^2} + k_-^2\right) p_-(z) = Ae^{-i(k_1 - k_2)z} \quad , \tag{2.9}$$

where we have neglected dissipation. Equation (2.9) is an inhomogeneous Helmholtz equation of the functional form which governs the response of a simple harmonic oscillator to an external harmonic driving force. We obtain the equation for the oscillator by replacing spatial variables in Equation (2.9) with temporal variables, i.e., by replacing z by t and k by ω, so that we have

$$\left(\frac{\partial^2}{\partial t^2} + \omega_-^2\right) w(t) = Ae^{-i\omega_e t} \quad ,$$

where w is the displacement of the oscillator, ω_e is the excitation frequency, and ω_- is the natural frequency of the system. When $\omega_e = \omega_-$, we say that resonance occurs, and the displacement amplitude of the oscillator increases linearly with time. However, when the excitation frequency is close but not equal to the natural frequency of the oscillator, the oscillator responds by beating.

By analogy, we can expect a similar behavior of the pressure amplitude obtained from Equation (2.9). When $k_1 - k_2 = k_-$, the pressure amplitude grows linearly with range, whereas if $k_1 - k_2 \neq k_-$, it undergoes beating. The phenomena of linear growth and beating of the pressure amplitude are therefore exhibited in space rather than time. Here we are interested in the relation of the spatial frequency of the forcing function $(k_1 - k_2)$, i.e., of the virtual-source distribution, to the natural spatial frequency of the difference-frequency

signal (k_-) . This relation depends of course on the dispersivity of the fluid. However, whereas the response of the oscillator is a function only of time, p_- is in general a function of two or three spatial variables. We can thus anticipate greater flexibility in the response of p_- to the excitation due to the virtual sources.

2.2 Interaction Region

Here we investigate nonlinear interaction between the primaries and the difference-frequency signal by obtaining exact solutions for the angular spectrum of the pressure field governed by Equation (2.8). The procedure we follow to obtain solutions of Equation (2.8) is similar to that given by Novikov.[6] By way of the Hankel transform, we may expand the pressure field in an angular spectrum of cylindrical wave modes:

$$p_\omega(\varepsilon,z) = \int_0^\infty A_\omega(k_\varepsilon,z)\, J_o(k_\varepsilon \varepsilon)\, k_\varepsilon dk_\varepsilon \quad , \tag{2.10}$$

$$A_\omega(k_\varepsilon,z) = \int_0^\infty p_\omega(\varepsilon,z)\, J_o(k_\varepsilon \varepsilon)\, \varepsilon d\varepsilon \quad . \tag{2.11}$$

In terms of $A_\omega(k_\varepsilon)$, Equation (2.8) becomes

$$\left(\frac{\partial^2}{\partial z^2} + \chi_z^2\right) A_-(k_\varepsilon,z) = \frac{\beta\omega_-^2}{\rho_o c_o^4} A_{12}(k_\varepsilon)\, e^{-i(\chi_1 - \chi_2^*)z} \quad , \tag{2.12}$$

where

$$\chi_z^2 = \chi_-^2 - k_\varepsilon^2 \quad , \tag{2.13}$$

and

$$A_{12}(k_\varepsilon) = \int_0^\infty p_1(\varepsilon,0)\ p_2^*(\varepsilon,0)\ J_o(k_\varepsilon\varepsilon)\ \varepsilon d\varepsilon \quad . \tag{2.14}$$

The solution of Equation (2.12) is given by

$$A_-(k_\varepsilon,z) = \frac{\beta\omega_-^2 A_{12}(k_\varepsilon)}{\rho_o c_o^4[\chi_z^2 - (\chi_1 - \chi_2^*)^2]} e^{-i(\chi_1 - \chi_2^*)z} + B_1 e^{-i\chi_z z} + B_2 e^{i\chi_z z} \quad , \tag{2.15}$$

where B_1 and B_2 are constants of the homogeneous solution. For progressive wave propagation in the positive z direction, we must have $B_2 = 0$. If in addition we assume that the difference-frequency signal is not radiated directly by the source (i.e., $p_-(\varepsilon,0) = 0$), then B_1 is determined and Equation (2.15) becomes

$$A_-(k_\varepsilon,z) = \frac{\beta\omega_-^2 A_{12}(k_\varepsilon)}{\rho_o c_o^4[\chi_z^2 - (\chi_1 - \chi_2^*)^2]} [e^{-i(\chi_1 - \chi_2^*)z} - e^{-i\chi_z z}] \quad . \tag{2.16}$$

Simple rearrangement of Equation (2.16) yields

$$A_-(k_\varepsilon,z) = \frac{i2\beta\omega_-^2 A_{12}(k_\varepsilon)}{\rho_o c_o^4(\chi_1 - \chi_2^* + \chi_z)} \frac{\sin[(\chi_1 - \chi_2^* - \chi_z)z/2]}{\chi_1 - \chi_2^* - \chi_z} e^{-i(\chi_1 - \chi_2^* + \chi_z)z/2} \quad . \tag{2.17}$$

In general, $p_-(\varepsilon,z)$ is difficult to obtain via Equations (2.10) and (2.17) because of the complicated dependence of $A_-(k_\varepsilon,z)$ on χ_z , since χ_z is a function of k_ε .

A simple yet important exception is the case in which the primaries are plane waves with initial amplitudes $p_j(\varepsilon,0) = p_{0j}$. We thus obtain $k_\varepsilon = 0$ and $\chi_z = \chi_-$, and Equation (2.17) becomes

$$p_-(z) = \frac{i\beta k_- p_{01} p_{02}}{\rho_o c_o^2} e^{-(\alpha_- + \alpha_T/2)z} \frac{\sin[(k_1 - k_2 - k_- - i\alpha_T)z/2]}{k_1 - k_2 - k_- - i\alpha_T} e^{-i(k_1 - k_2 + k_-)z/2} , \tag{2.18}$$

where

$$\alpha_T = \alpha_1 + \alpha_2 - \alpha_- .$$

In Equation (2.18) we replaced $2\omega_-^2/(\chi_1 - \chi_2^* + \chi_-)c_o^2$ by k_-. The justification is the assumption that dispersion is small and $k >> \alpha$, whereby the amplitude of $p_-(z)$ is relatively unaffected by the approximation. However, the same approximation cannot be made in the exponentials.

We begin with an analysis of Equation (2.18) where we neglect absorption. Of course, absorption and dispersion are not physically independent parameters; their interdependence can be determined from the Kramers-Kronig relations.[28] However, we vary absorption and dispersion independently in this thesis for the purpose of illustrating their effects on nonlinear interaction. In the absence of absorption, Equation (2.18) reduces to

$$p_-(z) = \frac{i\beta p_{01} p_{02}}{\delta \rho_o c_o^2} \sin(\delta k_- z/2) e^{-i(k_1 - k_2 + k_-)z/2} , \tag{2.19}$$

where

$$\delta = 1 - \frac{k_1 - k_2}{k_-} . \tag{2.20}$$

The dispersion parameter δ is zero when $k_1 - k_2 = k_-$, positive when $k_1 - k_2 < k_-$, and negative when $k_1 - k_2 > k_-$. By normal dispersion we mean that the speed of sound increases with frequency, whereas by

anomalous dispersion, we mean that the speed of sound decreases with frequency. Therefore, δ is positive for normal dispersion ($c_1 \geq c_2 > c_-$) and negative for anomalous dispersion ($c_1 \leq c_2 < c_-$).

The behavior of Equation (2.19) is illustrated in Figure 1. From Equation (2.19) we find that the period of spatial oscillation in amplitude, λ_q, is

$$\lambda_q = \frac{2\pi}{|k_1 - k_2 - k_-|} \quad , \tag{2.21}$$

which in terms of δ is $\lambda_q = 2\pi/|\delta|k_-$. The reason for the oscillations is that the phasing of the virtual sources does not always coincide with the phase of the difference-frequency signal. Since the wave number of the virtual-source excitation is $k_1 - k_2$ and the frequency of radiation is ω_-, the propagation speed of the excitation due to the virtual sources, c_g, is

$$c_g = \frac{\omega_-}{k_1 - k_2} \quad , \tag{2.22}$$

which is different from that of the difference-frequency signal, $c_- = \omega_-/k_-$.

Referring to Figure 2, we identify c_g as the group velocity of the signal formed by the two primaries. When there is no dispersion, $c_g = c_-$, and the virtual sources interact synchronously with the difference-frequency wave. The result is a continuous transfer of energy from the primaries to the difference-frequency signal, which results in coherent amplification of the latter. Such is the case where $\delta = 0$ in Figure 1. In general, with dispersion we have $c_g \neq c_-$. In this case, the phase of the excitation due to the virtual

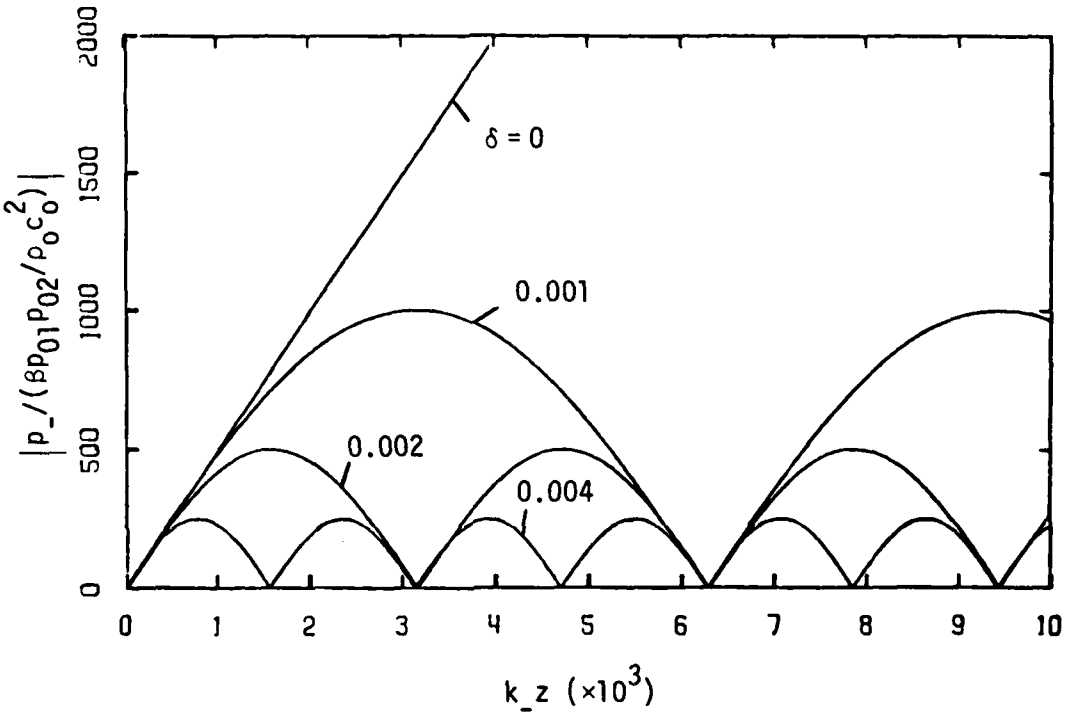

Figure 1. Effect of Dispersion on the Difference-Frequency Field Resulting from Collinear Interaction of Plane Waves in a Nondissipative Fluid.

AS-83-699

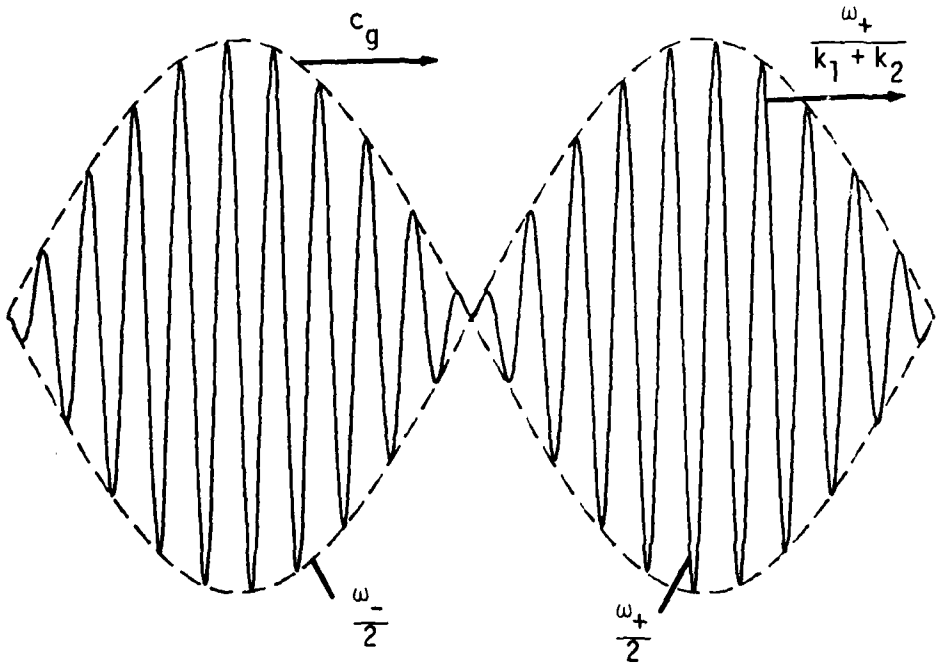

Figure 2. Illustration of the Group Velocity, $c_g = \omega_-/(k_1 - k_2)$, Associated with the Collinear Propagation of Two Primary Waves ($\omega_+/\omega_- = 20$).

AS-83-700

sources, relative to that of the difference-frequency signal, passes through 360° over the distance λ_q. It is because of the consequent cyclic behavior of the energy flow between the primaries and the difference-frequency signal that the amplitude of the latter experiences the oscillations illustrated in Figure 1. The direction of energy flow in the region $0 < z < \lambda_q/2$ is from the primaries to the difference-frequency signal. Rudenko and Soluyan[2] refer to $\lambda_q/2$ as the coherence length of the interaction.

An interesting physical interpretation can be made by realizing that the solution in the form of Equation (2.16) represents the homogeneous plus the particular solution of Equation (2.12). For the case of infinite plane waves, we thus obtain

$$p_-(z) \propto e^{-(\alpha_1 + \alpha_2)z} e^{-i(k_1 - k_2)z} - e^{-\alpha_- z} e^{-ik_- z} .$$

For no dispersion we have, from Equation (2.16),

$$|p_-(z)| \propto \left| e^{-(\alpha_1 + \alpha_2)z} - e^{-\alpha_- z} \right| , \qquad (2.23a)$$

$$|p_-(z)| \propto z , \quad \alpha = 0 . \qquad (2.23b)$$

For no dispersion and little to no dissipation, the amplitude of the difference-frequency signal grows linearly with range, at least so long as our approximations in the derivation of Equation (2.8) remain valid. For a dispersionless, dissipative fluid, however, the amplitude is governed by Equation (2.23a). The factors $e^{-(\alpha_1 + \alpha_2)z}$ and $e^{-\alpha_- z}$ arise from the particular and homogeneous solutions of Equation (2.8), respectively. In general, $\alpha_- < \alpha_1 + \alpha_2$, and therefore the difference-frequency signal decays at sufficiently great distances as $e^{-\alpha_- z}$.

In Section 2.1 we noted that because α_- is small compared to α_1, α_2, etc., p_- is the sole survivor of the components radiated by the parametric array. There is, however, dichotomy in the coexistence of the homogeneous and particular solutions.[29] The homogeneous solution is a freely propagating difference-frequency wave having wave number k_- and attenuation coefficient α_-. The particular solution, on the other hand, is a forced difference-frequency wave which corresponds to the excitation due to the virtual sources. The forced wave is governed by the wave number $k_1 - k_2$ and attenuation coefficient $\alpha_1 + \alpha_2$. A manifestation of the coexistence of the two waves is the wave number of p_- in Equation (2.18). We find that the wave number is neither k_- nor $k_1 - k_2$, but the average of the two.

In Figure 3 we see the way the effects of dissipation compete with those of dispersion. For sufficiently high attenuation, the spatial oscillations are entirely damped out, and the effects of dispersion may for all practical purposes be neglected.

We now consider the behavior of the interaction region for source excitations having arbitrary amplitude distributions. When dissipation is omitted, Equation (2.13) yields

$$k_-^2 = k_\varepsilon^2 + k_z^2 \quad .$$

If we let θ denote the angle formed with the z axis by the direction of propagation of any particular mode, we have

$$k_\varepsilon = k_- \sin\theta \quad , \quad k_z = k_- \cos\theta \quad .$$

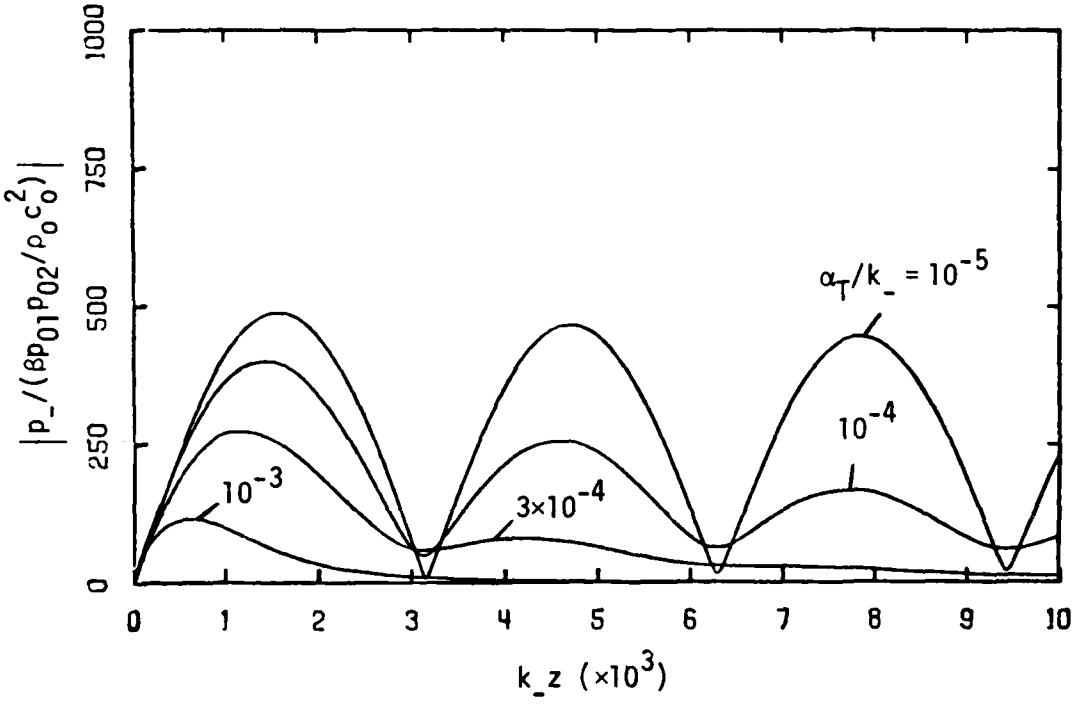

Figure 3. Effect of Dissipation on the Difference-Frequency Field Resulting from Collinear Interaction of Plane Waves in a Dispersive Fluid ($\delta = 0.002$, $\alpha_1 = \alpha_2 = \alpha_- = \alpha_T$).

AS-83-701

Equation (2.17) may thus be rewritten as

$$A_-(\theta,z) = \frac{i2\beta\omega_-^2}{\rho_o c_o^4} A_{12}(\theta) \frac{\sin[(k_1 - k_2 - k_- \cos\theta)z/2]}{[(k_1 - k_2)^2 - (k_- \cos\theta)^2]} e^{-i(k_1 - k_2 + k_- \cos\theta)z/2} . \tag{2.24}$$

From Equation (2.24) we find that only the angular component which propagates in the direction θ_o given by

$$\theta_o = \cos^{-1}\left(\frac{k_1 - k_2}{k_-}\right) \tag{2.25}$$

interacts synchronously with the primaries and thus grows linearly throughout the interaction region. Novikov[6] describes Equation (2.25) as the condition for Cerenkov radiation of the difference-frequency wave. Cerenkov radiation refers to the light emitted by charged particles which travel faster than the speed of light. For Equation (2.25) to possess a real solution for θ_o, it is required that $k_1 - k_2 \leq k_-$. Thus, when the virtual-source excitation propagates faster than a difference-frequency signal, we have the analogy with Cerenkov radiation insofar as the virtual source excitation behaves as an independent moving source.

2.3 Farfield of the Parametric Array

The analysis in the previous section is not suitable for investigation of the farfield radiation pattern, specifically because expressions for $p_-(\varepsilon,z)$ cannot in general be obtained from Equation (2.17). Instead, to solve Equation (2.8), we shall use the Green's function, which lends itself to the appropriate farfield approximations. In this section the procedure is followed which was originally employed by Westervelt.[1]

It is well known that the Green's function for Equation (2.8) is

$$g_-(\vec{r}|\vec{r}') = \frac{e^{-i\chi_-|\vec{r} - \vec{r}'|}}{4\pi|\vec{r} - \vec{r}'|} \quad ,$$

where $\vec{r}$ and $\vec{r}'$ are the position vectors of the observation and source points, respectively. The solution of Equation (2.8) can thus be written

$$p_-(r,\theta) = \frac{\beta\omega_-^2}{4\pi\rho_o c_o^4} \int_{V'} p_1(\varepsilon',0)p_2^*(\varepsilon',0)e^{-i(\chi_1-\chi_2^*)z'} \frac{e^{-i\chi_-|\vec{r} - \vec{r}'|}}{|\vec{r} - \vec{r}'|} dV' \quad , \tag{2.26}$$

where V' is the volume of integration containing the virtual-source distribution, and θ is the azimuthal angle subtended by $\vec{r}$ and the z axis.

Evaluation of $|\vec{r} - \vec{r}'|$ is similar to that usually performed when calculating the radiation pattern of a circular piston. Referring to Figure 4, we have for the right triangle

$$|\vec{r} - \vec{r}'|^2 = \sigma^2 + (z - z')^2 \quad ,$$

and by the law of cosines

$$\sigma^2 = \varepsilon^2 + \varepsilon'^2 - 2\varepsilon\varepsilon' \cos\psi \quad .$$

After eliminating σ and replacing $\varepsilon^2 + z^2$ by r^2, we get

$$|\vec{r} - \vec{r}'| = r\sqrt{1 - \frac{2\varepsilon\varepsilon'}{r^2}\cos\psi - \frac{2zz'}{r^2} + \left(\frac{\varepsilon'}{r}\right)^2 + \left(\frac{z'}{r}\right)^2} \quad . \tag{2.27}$$

If the observation points are far removed from the interaction region, (ε'/r) and (z'/r) are small quantities of order (r'/r). We thus

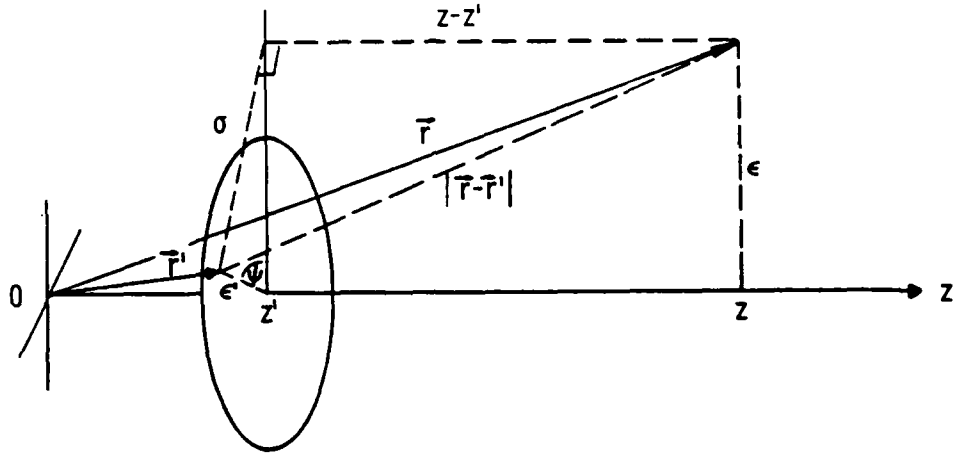

Figure 4. Relation Between Virtual Source Location $(\vec{r}')$ and Observation Points $(\vec{r})$.

AS-83-702

expand Equation (2.27) and discard terms of order $(r'/r)^2$ and higher to obtain

$$|\vec{r} - \vec{r}'| \simeq r - \varepsilon' \sin\theta \cos\psi - z' \cos\theta \quad , \tag{2.28}$$

where the relations $\varepsilon = r \sin\theta$ and $z = r \cos\theta$ have been used. Equation (2.28) is no more than the Fresnel approximation of Equation (2.27) (see, e.g., Reference 30).

For the geometry in Figure 4 we have $dV' = \varepsilon' d\varepsilon' d\psi dz'$, where the ranges of integration are

$$0 < \varepsilon' < \infty \quad , \quad 0 < \psi < 2\pi \quad , \quad 0 < z' < z \quad .$$

After replacing $|\vec{r} - \vec{r}'|$ by r in the denominator of Equation (2.26) while employing Equation (2.28) in the exponential, we obtain

$$p_-(r,\theta) = \frac{\beta\omega_-^2}{4\pi\rho_o c_o^4} \frac{e^{-i\chi_- r}}{r} \int_0^z e^{-i(\chi_1 - \chi_2^* - \chi_- \cos\theta)z'} \, dz'$$

$$\cdot \int_0^\infty p_1(\varepsilon',0) p_2^*(\varepsilon',0) \int_0^{2\pi} e^{i\chi_- \varepsilon' \sin\theta \cos\psi} \, d\psi \varepsilon' d\varepsilon' \quad . \tag{2.29}$$

The integral over z' yields

$$\int_0^z e^{-i(\chi_1 - \chi_2^* - \chi_- \cos\theta)z'} \, dz' = \frac{1 - \exp\{-[\alpha_T + i(k_1 - k_2 - k_- \cos\theta)]z\}}{\alpha_T + i(k_1 - k_2 - k_- \cos\theta)} \quad ,$$

which for large $\alpha_T z$ reduces to

$$\frac{1}{\alpha_T + i(k_1 - k_2 - k_- \cos\theta)} \quad .$$

As before, we have $\alpha_T = \alpha_1 + \alpha_2 - \alpha_-$, because $\alpha_- \cos\theta$ has been replaced by α_- . The substitution is acceptable because we are concerned primarily with the paraxial field where θ is small. Moreover, α_- is generally much smaller than both α_1 and α_2 , and therefore $\alpha_T \simeq \alpha_1 + \alpha_2$. Integrating over ψ , we have

$$\int_0^{2\pi} e^{i\chi_- \varepsilon' \sin\theta \cos\psi} \, d\psi = 2\pi J_o(\chi_- \varepsilon' \sin\theta) \quad .$$

Because $\chi_- = k_- - i\alpha_-$ and $k_- >> \alpha_-$, the Bessel function is conveniently expanded about $k_- \varepsilon' \sin\theta$:

$$J_o(\chi_- \varepsilon' \sin\theta) = J_o(k_- \varepsilon' \sin\theta) - i\alpha_- \varepsilon' \sin\theta \; J_o'(k_- \varepsilon' \sin\theta) + \ldots$$

$$= J_o(k_- \varepsilon' \sin\theta) + i\alpha_- \varepsilon' \sin\theta \; J_1(k_- \varepsilon' \sin\theta) + \ldots \quad ,$$

where $J_o'(x) = dJ_o(x)/dx$. Therefore, when $k_- \varepsilon' \sin\theta << 1$ as is the case in the paraxial field, we obtain

$$J_o(\chi_- \varepsilon' \sin\theta) \simeq J_o(k_- \varepsilon' \sin\theta) \quad .$$

Equation (2.29) now becomes

$$p_-(r,\theta) = \frac{\beta\omega_-^2}{2\alpha_T \rho_o c_o^4} \frac{e^{-i\chi_- r}}{r} A_{12}(\theta) \; D_\delta^W(\theta) \quad , \tag{2.30}$$

where $A_{12}(\theta)$ is given by Equation (2.14) with $k_\varepsilon = k_- \sin\theta$, and

$$D_\delta^W(\theta) = \frac{\alpha_T}{\alpha_T + i(k_1 - k_2 - k_- \cos\theta)} \tag{2.31a}$$

$$= \frac{1}{1 + i2(k_-/\alpha_T)[\sin^2(\theta/2) - \delta/2]} \quad , \tag{2.31b}$$

where again $\delta = 1 - (k_1 - k_2)/k_-$.

We recognize $A_{12}(\theta)$ in Equation (2.30) as the aperture factor referred to first and again recently by Tjøtta and Tjøtta.[11,31] The aperture factor accounts for the effect of finite source aperture on nonlinear generation of the difference-frequency signal. For example, if both primaries are radiated by a circular piston of radius a , i.e.,

$$p_j(\varepsilon,0) = p_{0j} \quad , \quad 0 < \varepsilon < a$$

$$= 0 \quad , \quad \varepsilon > a \quad ,$$

evaluation of Equation (2.14) leads to

$$p_-(r,\theta) = \frac{\beta\omega_-^2 a^2 p_{01} p_{02}}{4\alpha_T \rho_o c_o^4} \frac{e^{-i\chi_- r}}{r} \left[\frac{2J_1(k_- a \sin\theta)}{k_- a \sin\theta}\right] D_\delta^W(\theta) \quad . \qquad (2.32)$$

When $\delta = 0$, Equation (2.32) reduces to the result obtained by Tjøtta and Tjøtta.[11] Similarly, for Gaussian primary beams where

$$p_j(\varepsilon,0) = p_{Gj} e^{-(\varepsilon/\varepsilon_o)^2} \quad ,$$

Equation (2.30) becomes

$$p_-(r,\theta) = \frac{\beta\omega_-^2 \varepsilon_o^2 p_{G1} p_{G2}}{8\alpha_T \rho_o c_o^4} \frac{e^{-i\chi_- r}}{r} \exp\{-\frac{1}{8} k_-^2 \varepsilon_o^2 \sin^2\theta\} D_\delta^W(\theta) \quad . \qquad (2.33)$$

Inspection of Equations (2.32) and (2.33) shows that $A_{12}(\theta)$, when properly normalized, represents the directivity function of a difference-frequency signal which is radiated linearly from a source defined by $p_1(\varepsilon,0)p_2^*(\varepsilon,0)$. Such a result is consistent with the concept of difference-frequency radiation by a volume distribution of

virtual sources, and becomes obvious when we consider the so-called product theorem of array theory (see, e.g., Reference 32). According to the product theorem, the directivity function of an array composed of directive elements (all elements the same) is given by the product of the element directivity function and the directivity function of the array when the elements are replaced by point sources.

As an example, we consider the case where the primaries are radiated by a circular piston of radius a. Since we assumed that the primaries do not experience diffraction, the virtual sources acquire the shape of disks of radius a which are stacked coaxially along the z axis, as shown in Figure 5a. The directivity function for each differential element of the array is, of course,

$$\frac{2J_1(k_- a \sin\theta)}{k_- a \sin\theta} \quad , \tag{2.34}$$

since each element is radiating at the difference frequency. If we replace each of the elements by a point source, we obtain the line array depicted in Figure 5b. The line array is semi-infinite, beginning at the origin and extending to $z = \infty$, and possesses an amplitude distribution given by $e^{-\alpha_T z}$. Recall from Equation (2.22) that the phasing of the virtual sources corresponds to a wave propagating at speed $c_g = \omega_-/(k_1 - k_2)$ in the positive z direction. The phase delay associated with each differential virtual source is thus given by $-(\omega_-/c_g)z$. When there is no dispersion, the phase delay reduces to $-k_- z$. Calculation of the directivity function for this semi-infinite, amplitude-tapered, phase-shaded, line array is not difficult, and the result is

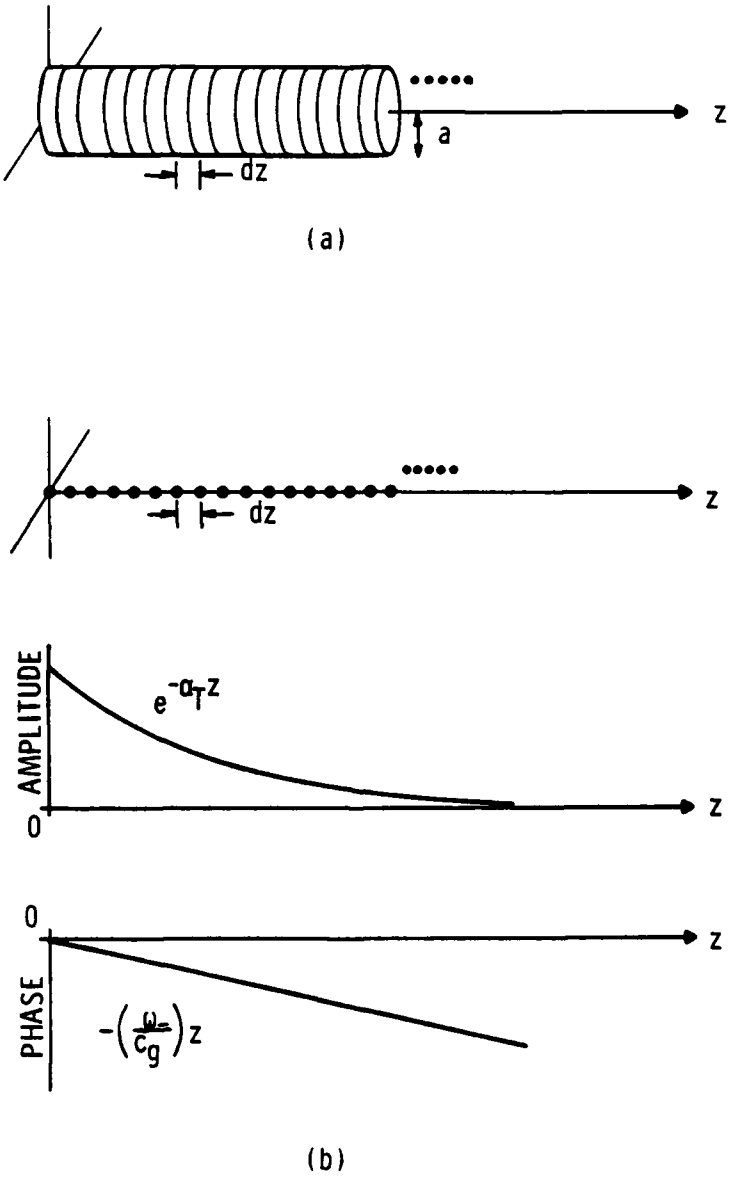

Figure 5. Parametric Array Decomposed Into (a) Disks of Radius a and (b) an Array of Point Sources Having Exponential Amplitude Taper and Linear Phase Shading.

AS-83-703

$$D(\theta) = \frac{1}{1 + i(k_-/\alpha_T)(c_-/c_g - \cos\theta)} \quad . \tag{2.35}$$

Replacing c_g by $\omega_-/(k_1 - k_2)$ in Equation (2.35) we again obtain Equation (2.31), while the product of Equations (2.34) and (2.35) yields the directivity function in Equation (2.32), as required. The preceding analysis is of course general and can thus be extended to any source geometry, as seen by inspection of Equation (2.30). In all cases the function $D_\delta^W(\theta)$ is recovered.

When the difference-frequency wavelength is large compared to the size of a virtual source (e.g., when $k_-a < 1$ or $k_-\varepsilon_o < 1$), the aperture factor depends weakly on θ, and the directivity function in Equation (2.30) is given primarily by $D_\delta^W(\theta)$. This is the case considered by Westervelt for a dispersionless fluid. That is, he obtained the function $D_o^W(\theta)$, which is $D_\delta^W(\theta)$ when evaluated at $\delta = 0$. Westervelt referred to $D_o^W(\theta)$ as the Rutherford directivity because of its similarity to the function describing Rutherford scattering of α particles. Westervelt's result is said to apply to absorption-limited arrays, which are parametric arrays formed by highly collimated primary beams where dissipation restricts nonlinear interaction to the nearfield of the primaries. Hereafter we shall refer to $D_\delta^W(\theta)$ as a modified Westervelt directivity function. Strictly speaking, $D_\delta^W(\theta)$ is not a true directivity function in the sense that it is not normalized to unity when $\delta < 0$. It is worth mentioning that $D_o^W(\theta)$ produces a directivity pattern which has no sidelobes. This remarkable property is a consequence of the infinite extent of the parametric array, whose termination is in the form of an exponential amplitude taper.

The phasing of the virtual sources strongly affects the directivity of the parametric array. At an angle θ_o given by

$$\theta_o = \cos^{-1}\left(\frac{k_1 - k_2}{k_-}\right) \quad , \tag{2.36}$$

$D_\delta^W(\theta)$ attains its maximum value of unity. Equation (2.36) is the same condition given by Equation (2.25) for the component of the angular spectrum which experiences synchronous interaction with the primaries. However, the interpretation here is somewhat different. Equation (2.25) gives the synchronism condition for a specific angular component of the difference-frequency signal propagating within the nonlinear interaction region. Equation (2.36), on the other hand, gives the direction of maximum radiation from a line array which is phased in the manner discussed above, and which radiates at frequency ω_- into a fluid where the sound speed is c_-. Of course, the latter behavior is manifested only for highly collimated primary beams where the aperture factor can be neglected. The discussion which follows addresses this case, i.e., we assume the primaries are sufficiently collimated that the directivity function of the difference-frequency signal is given by $D_\delta^W(\theta)$.

When there is no dispersion, $c_g = c_-$. The phasing of the virtual sources thus corresponds with the speed of the sound being radiated, and we recover the result obtained by Westervelt[1] for the end-fire array. When there is dispersion, maximum radiation occurs at the angle $\theta_o = \cos^{-1}(c_-/c_g)$, which is the same as that given in Equation (2.36). When $c_g \geq c_-$, θ_o is the direction of propagation of a difference-frequency wave which travels at speed c_- and projects a phase speed c_g along the direction of the array. Radiation from

the interaction region is thus analogous to that from bending waves on an infinite plate (see, e.g., Reference 33). When $c_g < c_-$, the equation $\theta_o = \cos^{-1}(c_-/c_g)$ no longer admits a real solution, and the radiation is of an evanescent nature. Plots of $|D_\delta^W(\theta)|$ for both normal ($\delta > 0$) and anomalous ($\delta < 0$) dispersion are presented in Figure 6. In both cases, the axial farfield level is significantly attenuated according to how much δ differs from zero. Specifically, we find that

$$D_\delta^W(0) = \frac{1}{1 - i\delta k_-/\alpha_T} \quad .$$

The broadening of the beam is indicated by the half-power angle, defined here as the angle beyond which the pressure squared is always 3 dB below its maximum at θ_o ($\theta_o = 0$ when $\delta \leq 0$) :

$$\theta_{HP} \simeq \sqrt{2\left(\frac{\alpha_T}{k_-} + \delta\right)} \quad , \quad \delta \geq 0 \qquad (2.37a)$$

$$\theta_{HP} \simeq \sqrt{2\delta + \sqrt{\left(2\frac{\alpha_T}{k_-}\right)^2 + 8\delta^2}} \quad , \quad \delta \leq 0 \quad . \qquad (2.37b)$$

When there is no dispersion we have the well-known result[1] $\theta_{HP} \simeq \sqrt{2\alpha_T/k_-}$. The beam gets wider as α_T increases because the array becomes shorter by virtue of higher attenuation of the primaries. The beamwidth also increases with $|\delta|$ as the phasing of the array departs from conditions required for end-fire radiation. Note that the beamwidth does not (for narrow primary beams) depend on source dimensions.

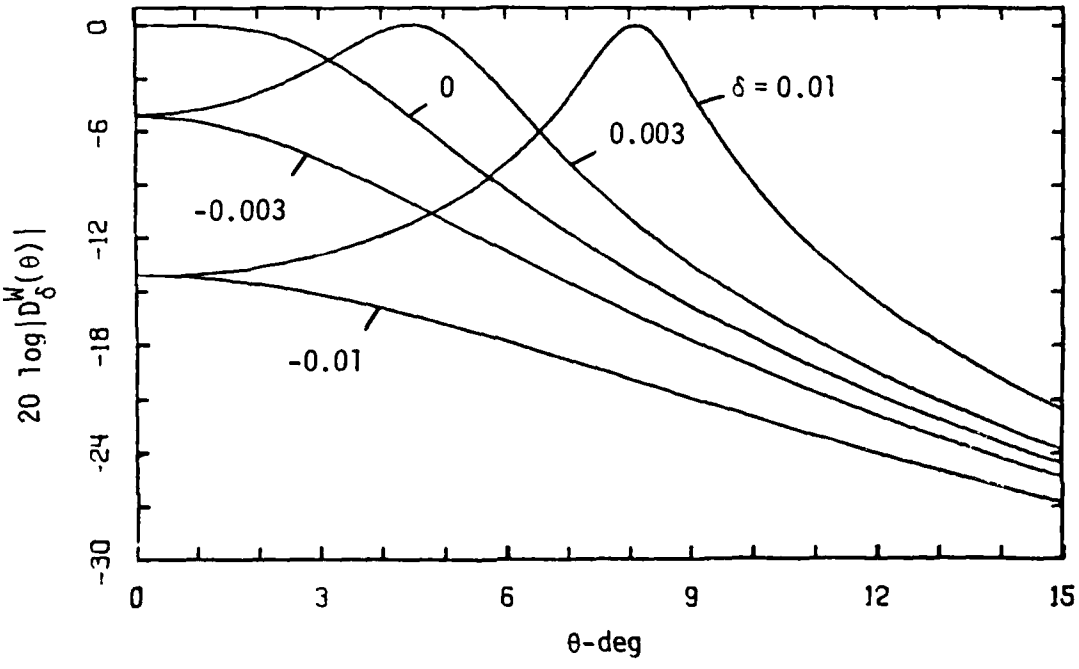

Figure 6. Modified Westervelt Directivity Function, $D_\delta^W(\theta)$, $(k_-/\alpha_T = 500)$.

AS-83-704

A useful description of the shift in the direction of maximum radiation is provided by the use of vectors. Specifically, the direction of maximum radiation is determined by the orientation of the difference-frequency wave vector $\vec{k}_-$ so that its component in the z direction is given by $k_1 - k_2$. Three situations ($\delta = 0$, $\delta > 0$, $\delta < 0$) for a highly collimated parametric array are presented in Figure 7. When there is no dispersion, $\vec{k}_-$ is aligned with the z axis, and the end-fire radiation pattern results. For normal dispersion ($\delta > 0$), $\vec{k}_-$ sweeps out a cone forming an angle θ_o with the z axis. For anomalous dispersion ($\delta < 0$) there is no orientation of $\vec{k}_-$ for which its z component is $k_1 - k_2$; the directivity function is then maximized when $\vec{k}_-$ is aligned with the z axis.

In conclusion we note that Kozyaev and Naugol'nykh[8] derived an expression which for collinear primary beams reduces to Equation (2.31), if in Equation (16) in their article we replace the typographical error $k_1 + k_2$ by $k_1 - k_2$. However, in their Equations (19) and (20) they state that the direction of maximum radiation is shifted off axis when $\delta < 0$, but not when $\delta > 0$. Such a conclusion is clearly, in light of the above discussion, in error.

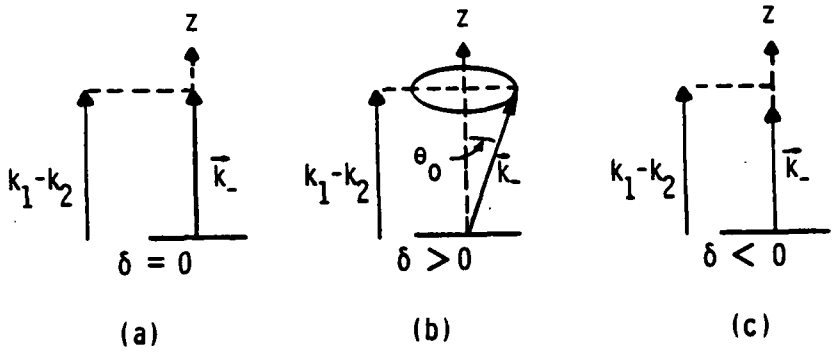

Figure 7. Vector Representation of Difference-Frequency Radiation from an Absorption-Limited Array for (a) No Dispersion, (b) Normal Dispersion, and (c) Anomalous Dispersion.

AS-83-705

CHAPTER III

THE PARAXIAL WAVE EQUATION

In this chapter we introduce an approximation of Westervelt's equation which accurately describes the wave field in highly collimated beams, but is easier to solve than Equation (2.1). Tjøtta and Tjøtta[25] maintain that this approximate equation, called the paraxial wave equation, accounts for nonlinear effects in beams no less accurately than does Westervelt's equation. The reason stems from assumptions made when combining nonlinear terms to obtain the form given by the right-hand side of Equation (2.1). We proceed to write the nonlinear paraxial wave equation in such a way that it accounts for the effects of both dispersion and dissipation. Next we derive the Green's function, which enables us to rewrite the nonlinear paraxial wave equation in integral form. The resulting integral equation is then solved by successive approximations. In the first approximation we obtain the solution for the linearized (homogeneous) paraxial wave equation. The homogeneous solution requires integration over the product of the boundary condition, i.e., the source excitation, and the Green's function. Analytical evaluation of the integral is possible when the boundary condition is expanded in terms of an appropriate set of orthogonal functions. The resulting solution, which is a new set of orthogonal functions, constitutes the eigenfunctions of the linearized paraxial wave equation. Combinations of the eigenfunctions thus yield solutions for primary wave fields resulting from arbitrary source excitations. As in Chapter II, the second approximation involves replacing the quadratic term by the square of the

first-order solution. The resulting integral solution for the sum- as well as difference-frequency components is therefore valid throughout the entire paraxial field of arbitrary primary beams.

3.1 Kuznetsov's Equation with Dispersion Included

It became evident in the last chapter that we must employ various approximations to obtain nontrivial analytical solutions of the wave equation. The approximations can be applied either to the exact integral solutions or to the governing wave equation. To study nonlinear effects in beams, Zabolotskaya and Khokhlov[34] derived an approximation of Equation (2.1) that is valid throughout the paraxial field. By writing their equations in terms of the retarded time $t' = t - z/c_o$, they effectively factor out the strong time dependence, which causes rapid variations in the acoustic waveform. Terms involving two z derivatives are then discarded on the basis that, along the direction of propagation of a beam, variations in the shape of the waveform due to the effects of nonlinearity and diffraction are small. In other words, in a coordinate system that travels along with the waveform, changes with distance in the direction of propagation are gentle. Kuznetsov[17] subsequently extended Zabolotskaya and Khokhlov's paraxial nonlinear wave equation, called the ZK equation in the literature, to encompass thermoviscous fluids. For progressive wave propagation in the positive z direction, Kuznetsov's equation is

$$\frac{\partial^2 p}{\partial z \partial t'} - b \frac{\partial^3 p}{\partial t'^3} - \frac{c_o}{2} \nabla_\perp^2 p = \frac{\beta}{2\rho_o c_o^3} \frac{\partial^2 p^2}{\partial t'^2} \quad , \tag{3.1}$$

where $p(x,y,z,t')$ is the acoustic pressure, $t' = t - z/c_o$ is retarded time, c_o is a reference sound speed, and

$$\nabla_\perp^2 = \frac{\partial^2}{\partial x^2} + \frac{\partial^2}{\partial y^2} \quad .$$

Coefficients describing the thermal and viscous properties of the fluid are included in

$$b = \frac{\nu}{2c_o^3}\left(V + \frac{\gamma - 1}{Pr}\right) \quad ,$$

where ν is the kinematic viscosity, $V = 2 + \lambda/\mu$ is the viscosity number, λ and μ are the dilatational and shear viscosity coefficients, respectively, γ is the ratio of specific heats, and Pr is the Prandtl number.

Using perturbation techniques, Tjøtta and Tjøtta[25] argue that Equation (3.1) possesses the same degree of accuracy as Westervelt's wave equation[1] when losses are included, which can be written as

$$(1 - 2c_o b \frac{\partial}{\partial t}) \frac{\partial^2 p}{\partial t^2} - c_o^2 \nabla^2 p = \frac{\beta}{\rho_o c_o^2} \frac{\partial^2 p^2}{\partial t^2} \quad . \tag{3.2}$$

Note that Equation (3.2) contains two z derivatives whereas Equation (3.1) contains only one. The Tjøttas[25] contend that Equation (3.2), like Equation (3.1), is restricted to quasi-plane waves which can be expressed as

$$p(x,y,z,t) = p_\omega(x,y,z)e^{i\omega(t - z/c_o)} \quad , \tag{3.3}$$

where $p_\omega(x,y,z)$ varies slowly in the z direction. Indeed, if we insert Equation (3.3) into Equation (3.2) and assume that

$$\left|\frac{\partial^2 p_\omega}{\partial z^2}\right| << \frac{2\omega}{c_o}\left|\frac{\partial p_\omega}{\partial z}\right| ,$$

then, if the nonlinear term is omitted, Equation (3.2) reduces to

$$\frac{\partial p_\omega}{\partial z} + b\omega^2 p_\omega + \frac{ic_o}{2\omega}\nabla_\perp^2 p_\omega = 0 \quad . \tag{3.4}$$

Equation (3.4) is of the exact form assumed by the linear terms in Equation (3.1) for a waveform described by Equation (3.3). Any restrictions imposed upon Equation (3.2) result from approximations in the derivation of the nonlinear term. Westervelt[35] maintains that retaining the complete Laplacian in (the lossless version of) Equation (3.2), and hence asserting the applicability of Equation (3.2) to arbitrary acoustic fields, is justified under one condition. The condition is that when Equation (3.2) is solved for non-planar waves in the second approximation, the solution for the secondary components is sought only for regions which are far removed from the virtual sources. From the above considerations, it thus appears that for the analysis of collimated beams, no loss of accuracy results from using Equation (3.1) instead of Equation (3.2).

Equation (3.1) is especially well suited for the analysis of Gaussian beams. When linearized, Equation (3.1) provides a nearly exact description of the paraxial field. Moreover, within the near-field of Gaussian primaries, where substantial nonlinear interaction occurs, the term containing the diffraction operator (i.e., $\nabla_\perp^2 p$) tends to zero, and Equation (3.1) reduces to the Burgers equation. The

Burgers equation is an excellent approximation of the exact equations that govern plane wave propagation in weakly nonlinear and dissipative fluids.[36] Solutions obtained from Equation (3.1) for the difference-frequency field resulting from Gaussian primaries are therefore valid for the entire paraxial field. Thus, despite the subtle controversial discrepancies between Equations (3.1) and (3.2), Equation (3.1) is adequate for the purposes of our analysis.

We now proceed to introduce dispersion in the paraxial wave equation. If diffraction is neglected in Equation (3.4), which is the linearized version of Equation (3.1) when a solution of the form of Equation (3.3) is assumed, we obtain

$$\frac{\partial p_\omega}{\partial z} + b\omega^2 p_\omega = 0 \quad . \tag{3.5}$$

For boundary condition $e^{i\omega_o t}$ at $z = 0$ the solution of Equation (3.5) is simply $2\pi\delta(\omega - \omega_o)\, e^{-b\omega^2 z}$, which in the time domain becomes

$$p = e^{-b\omega_o^2 z}\, e^{i\omega_o(t - z/c_o)} \quad . \tag{3.6}$$

Hereafter we shall omit the subscript on ω_o. From Equation (3.6) we identify $b\omega^2$ as the small-signal attenuation coefficient α_ω. In the derivation[17,25] of Equation (3.1), the effects of dissipation, diffraction, and nonlinearity are each accounted for to the same order of magnitude. It is therefore consistent to introduce dispersion via a modification of the dissipation term since, as discussed in Section 2.1, dispersion and dissipation are competitive with respect to their effect on the waveform. Consequently, dispersion, like dissipation, is neglected in the x and y directions.

Dispersion is thus introduced in Equation (3.6), and hence Equation (3.1), by replacing the attenuation coefficient by

$$\alpha'_\omega = \alpha_\omega + i(k_\omega - \frac{\omega}{c_o}) \quad , \tag{3.7}$$

where

$$k_\omega = \frac{\omega}{c_\omega} \quad ,$$

and c_ω is the frequency-dependent sound speed. In the absence of dispersion, the imaginary part of α'_ω vanishes, leaving only the attenuation coefficient α_ω. Equation (3.6) now becomes

$$p = e^{-\alpha'_\omega z} e^{i\omega t'}$$

$$= e^{-\alpha_\omega z} e^{i\omega(t - z/c_\omega)} \quad . \tag{3.8}$$

As required, Equation (3.8) describes a plane wave traveling at speed c_ω and being attenuated as $e^{-\alpha_\omega z}$. We wish now to write Equation (3.1) in a general form that accounts for arbitrary attenuation and dispersion. Note that the attenuation coefficient $b\omega^2$, which is associated with Equation (3.1), results from the factor of b times two time derivatives of the pressure. Following Blackstock,[37] we introduce an operator D which is defined according to the relation

$$D\{p_\omega(x,y,z)\ e^{i\omega t'}\} = -\alpha'_\omega p_\omega(x,y,z)\ e^{i\omega t'} \quad , \tag{3.9}$$

and rewrite Equation (3.1) in the following general form:

$$\frac{\partial^2 p}{\partial z \partial t'} - \frac{\partial}{\partial t'} D(p) - \frac{c_o}{2} \nabla_\perp^2 p = \frac{\beta}{2\rho_o c_o^3} \frac{\partial^2 p^2}{\partial t'^2} \quad . \tag{3.10}$$

By comparing Equations (3.1) and (3.10), we find that

$$D(p) = b \frac{\partial^2 p}{\partial t'^2} \tag{3.11}$$

for thermoviscous fluids, whereby using Equations (3.7) and (3.9), we obtain

$$\alpha_\omega = b\omega^2 \quad , \quad k_\omega = \frac{\omega}{c_o} \quad , \tag{3.12}$$

as required. For monorelaxing fluids we have

$$D(p) = \frac{m}{2c_o} \frac{\partial}{\partial t'} \int_{-\infty}^{t'} \frac{\partial p}{\partial \eta} e^{-(t'-\eta)/\tau} \, d\eta \quad , \tag{3.13}$$

which we deduce by comparing Equation (3.10) with the paraxial wave equation derived by Rudenko, Soluyan, and Khokhlov.[38] The dispersivity of a monorelaxing fluid is

$$m = \frac{c_\infty^2 - c_o^2}{c_o^2} \quad ,$$

where c_o and c_∞ are the respective sound speeds at zero and infinite frequency (also called the equilibrium and frozen sound speeds, respectively), and τ is the relaxation time. From Equations (3.9) and (3.13) we thus obtain

$$\alpha_\omega = \frac{m}{2c_o\tau} \frac{(\omega\tau)^2}{1 + (\omega\tau)^2} \quad , \quad k_\omega = \frac{\omega}{c_o} \left[1 - \frac{m}{2} \frac{(\omega\tau)^2}{1 + (\omega\tau)^2} \right] , \tag{3.14}$$

for monorelaxing fluids. Extensions of Equation (3.14) to multi-relaxing fluids are provided by Klinman.[39]

In general, we do not need an explicit analytical expression for D, as given for example in Equations (3.11) and (3.13). It is sufficient to know α_ω and c_ω for the frequencies of interest. For instance, a common source of dispersion in fluids is bubbles, for which an adequate mathematical description is extremely involved. In fact, for liquids containing bubbles in concentrations sufficient to induce dispersion, the nonlinear effects arising from the dynamic nonlinearity of the bubble oscillations exceed those due to the hydrodynamic contribution. It then becomes necessary to replace β in Equation (3.1) by a suitable expression which accounts for the additional nonlinearity. Discussions of the parameters α_ω, k_ω, and β for bubbly water can be found in References 8 and 40.

The effect of the operator D on wave propagation is illustrated more clearly after we transform Equation (3.10) into the frequency domain to obtain

$$\frac{\partial p_\omega}{\partial z} + (\alpha'_\omega + \frac{ic_o}{2\omega} \nabla_\perp^2) p_\omega = \frac{i\beta\omega}{2\rho_o c_o^3} Q_\omega \quad , \tag{3.15}$$

where

$$Q_\omega(x,y,z) = p_\omega(x,y,z) * p_\omega(x,y,z) \quad . \tag{3.16}$$

Note that a distinction is made between the Fourier transformation which gives rise to Equation (2.2) and that which gives rise to Equation (3.15). In the former, the transform involves t, whereas in the latter it involves the retarded time t'. Equation (3.15) therefore yields solutions containing the exponentials given in Equation (3.8).

3.2 Green's Functions

As in Chapter II, we will solve our governing nonlinear wave equation by the method of successive approximations. In the first approximation the nonlinear term is neglected. We thus let $Q_\omega = 0$, whereby Equation (3.15) assumes the form of a diffusion equation where the time derivative is replaced by a spatial derivative. Because the sound field is unbounded in the x and y directions, we require only one boundary condition to satisfy the single z derivative. The boundary condition, which we prescribe at $z = 0$, defines the source excitation of the primary beams. Solving Equation (3.15) when $Q_\omega = 0$ subject to the boundary condition at $z = 0$, we thus obtain the solution for the primary wave field. As before, the second approximation involves evaluating Q_ω with the solution derived from the first approximation, and then solving the resulting linear inhomogeneous differential equation. Since the homogeneous solution is the same as before, it is the particular solution of this inhomogeneous equation that provides the correction to the first approximation, and is the solution for the secondary field components which result from squaring the primary field. Both homogeneous and particular solutions are easily obtained once the Green's function is known. Moreover, by using the Green's function we can express Equation (3.15) in integral form, which lends itself more readily to solution via successive approximations.

The Green's function problem associated with Equation (3.15) is

$$\frac{\partial g_\omega}{\partial z} + (\alpha'_\omega + \frac{ic_o}{2\omega} \nabla_\perp^2) g_\omega = \delta(x - x') \, \delta(y - y') \, \delta(z - z') \quad , \quad (3.17)$$

with

$$g_\omega(x,y,z|x',y',z') = 0 \quad , \quad \text{for } z \leq 0 \quad , \tag{3.18}$$

where $g_\omega(\vec{r}|\vec{r}')$ is the Green's function, $\delta(\cdot)$ is the Dirac delta function, $\vec{r} = (x,y,z)$ is the observation point, and $\vec{r}' = (x',y',z')$ is the source point. Equation (3.17) can be solved with the same techniques which are used to solve the diffusion equation,[41] the only essential difference being the factor α'_ω.

We thus proceed to express $g_\omega(\vec{r}|\vec{r}')$ in terms of its angular spectrum:

$$g_\omega(\vec{r}|\vec{r}') = \left(\frac{1}{2\pi}\right)^2 \int\int_{-\infty}^{\infty} G_\omega(k_x,k_y,z)\, e^{ik_x x + ik_y y}\, dk_x dk_y \quad , \tag{3.19}$$

$$G_\omega(k_x,k_y,z) = \int\int_{-\infty}^{\infty} g_\omega(\vec{r}|\vec{r}')\, e^{-ik_x x - ik_y y}\, dxdy \quad . \tag{3.20}$$

In terms of G_ω, Equation (3.17) becomes

$$\frac{\partial G_\omega}{\partial z} + \left[\alpha'_\omega - \frac{ic_o}{2\omega}(k_x^2 + k_y^2)\right]G_\omega = e^{-ik_x x' - ik_y y'}\, \delta(z - z') \quad . \tag{3.21}$$

The solution of Equation (3.21) that satisfies Equation (3.18) is

$$G_\omega(k_x,k_y,z) = e^{-ik_x x' - ik_y y'} \int_0^z e^{-\gamma(z - \eta)}\, \delta(\eta - z')\, d\eta \quad , \tag{3.22}$$

where

$$\gamma = \alpha'_\omega - \frac{ic_o}{2\omega}(k_x^2 + k_y^2) \quad . \tag{3.23}$$

The integral in Equation (3.22) is elementary, yielding

$$G_\omega(k_x,k_y,z) = \exp\{-ik_x x' - ik_y y' - \gamma(z - z')\}\, H(z - z') \quad , \tag{3.24}$$

where $H(z)$ is the Heaviside function defined by

$$H(z) = 1 \quad , \quad z > 0$$

$$= 0 \quad , \quad z < 0 \quad .$$

Combining Equations (3.19) and (3.24) gives the solution,

$$g_\omega(\vec{r}|\vec{r}') = \left(\frac{1}{2\pi}\right)^2 H(z - z') \int\int_{-\infty}^{\infty} \exp\{ik_x(x - x') + ik_y(y - y') - \gamma(z - z')\}dk_x dk_y \quad ,$$

which we write using Equation (3.23) as follows:

$$g_\omega(\vec{r}|\vec{r}') = \left(\frac{1}{2\pi}\right)^2 e^{-\alpha'_\omega(z - z')} H(z - z')\, I_x I_y \quad , \tag{3.25}$$

where

$$I_x = \int_{-\infty}^{\infty} \exp\left\{\frac{ic_o}{2\omega}(z - z')k_x^2 + i(x - x')k_x\right\} dk_x \quad ,$$

and

$$I_y = \int_{-\infty}^{\infty} \exp\left\{\frac{ic_o}{2\omega}(z - z')k_y^2 + i(y - y')k_y\right\} dk_y \quad .$$

Evaluation of I_x and I_y is easy, and Equation (3.25) becomes

$$g_\omega(\vec{r}|\vec{r}') = \frac{i\omega}{2\pi c_o} \frac{e^{-\alpha'_\omega(z-z')}}{z-z'} \exp\left\{-\frac{i\omega}{2c_o}\left[\frac{(x-x')^2+(y-y')^2}{z-z'}\right]\right\} H(z-z') \quad . \tag{3.26}$$

Equation (3.26) is simply the Fresnel approximation of the Green's function for the Helmholtz equation.[30] Homogeneous solutions, i.e., primary wave fields derived from Equations (3.1) and (3.15) are therefore excellent approximations of the exact solutions obtained from the Helmholtz equation, insofar as the Fresnel approximations remain valid.

The homogeneous solution of Equation (3.15) is obtained by integrating over the product of the boundary condition and the Green's function as follows:

$$p^h_\omega(x,y,z) = \int_{-\infty}^{\infty}\int p_\omega(x',y',0)\, g_\omega(x,y,z|x',y',0)\, dx'dy' \quad . \tag{3.27}$$

Likewise, the particular solution of Equation (3.15) is obtained by integrating over the product of the forcing function and the Green's function:

$$p^p_\omega(x,y,z) = \frac{i\beta\omega}{2\rho_o c_o^3} \int_0^{\infty}\int_{-\infty}^{\infty}\int Q_\omega(x',y',z')\, g_\omega(x,y,z|x',y',z')\, dx'dy'dz' \quad . \tag{3.28}$$

Note that no approximations are assumed by writing Equation (3.28), because Q_ω is still a function of p_ω. Since the complete solution of Equation (3.15) is given by the sum of the homogeneous and particular solutions,

$$p_\omega = p^h_\omega + p^p_\omega \quad ,$$

we have, using Equations (3.26), (3.27), and (3.28),

$$p_\omega(x,y,z) = \frac{i\omega}{2\pi c_o}\frac{e^{-\alpha'_\omega z}}{z}\int_{-\infty}^{\infty}\int p_\omega(x',y',0)\exp\left\{-\frac{i\omega}{2c_o z}\left[(x-x')^2+(y-y')^2\right]\right\}dx'dy'$$

$$-\frac{\beta\omega^2}{4\pi\rho_o c_o^4}\int_0^z\int_{-\infty}^{\infty}\int Q_\omega(x',y',z')\,\frac{e^{-\alpha'_\omega(z-z')}}{z-z'}$$

$$\cdot\exp\left\{-\frac{i\omega}{2c_o}\left[\frac{(x-x')^2+(y-y')^2}{z-z'}\right]\right\}dx'dy'dz' \quad . \qquad (3.29)$$

Equation (3.29), which was first derived by Fenlon,[13,19] is an exact integral representation of Equation (3.15). In the first approximation the integral over Q_ω is omitted, and the remaining integral over the boundary condition, $p_\omega(x,y,0)$, yields the primary wave field. This is just the homogeneous solution. In the second approximation Q_ω is evaluated with the field obtained in the first approximation. The resulting integral over Q_ω thus provides a correction to the solution obtained from the integral over $p_\omega(x,y,0)$, the latter being the same homogeneous solution which is obtained in the first approximation. In the second approximation, it is the integral over Q_ω that yields solutions for the secondary field components.

Similar, and somewhat simpler, results may be derived for fields resulting from axisymmetric radiation. As shown in Appendix A, the Green's function for Equation (3.15) when the field can be expressed as $p_\omega(\varepsilon,z)$, where $\varepsilon^2 = x^2 + y^2$, is given by

$$g_\omega(\varepsilon,z|\varepsilon',z') = \frac{i\omega}{c_o}\,\frac{e^{-\alpha'_\omega(z-z')}}{z-z'}\,J_o\left\{\frac{\omega\varepsilon\varepsilon'}{c_o(z-z')}\right\}\exp\left\{-\frac{i\omega}{2c_o}\left(\frac{\varepsilon^2+\varepsilon'^2}{z-z'}\right)\right\}H(z-z')\ . \tag{3.30}$$

For axisymmetric radiation, the integral form of Equation (3.15) thus becomes

$$p_\omega(\varepsilon,z) = \frac{i\omega}{c_o}\,\frac{e^{-\alpha'_\omega z}}{z}\int_0^\infty p_\omega(\varepsilon',0)J_o\left\{\frac{\omega\varepsilon\varepsilon'}{c_o z}\right\}\exp\left\{-\frac{i\omega}{2c_o z}\,(\varepsilon^2+\varepsilon'^2)\right\}\,\varepsilon'd\varepsilon'$$

$$-\frac{\beta\omega^2}{2\rho_o c_o^4}\int_0^z\int_0^\infty Q_\omega(\varepsilon',z')\,\frac{e^{-\alpha'_\omega(z-z')}}{z-z'}\,J_o\left\{\frac{\omega\varepsilon\varepsilon'}{c_o(z-z')}\right\}\exp\left\{-\frac{i\omega}{2c_o}\left(\frac{\varepsilon^2+\varepsilon'^2}{z-z'}\right)\right\}\varepsilon'd\varepsilon'dz'\ , \tag{3.31}$$

as given by Fenlon and McKendree.[10] Equation (3.31) may also be obtained from Equation (3.29) by letting $x = \varepsilon\cos\psi$ and $y = \varepsilon\sin\psi$.

3.3 Eigenfunctions and the Second-Order Solution

We now derive the eigenfunctions for the linearized paraxial wave equation,

$$\frac{\partial p_\omega}{\partial z} + \left(\alpha'_\omega + \frac{ic_o}{2\omega}\nabla_\perp^2\right)p_\omega = 0\ . \tag{3.32}$$

As demonstrated by Kogelnik,[42,43] Gauss-Hermite functions of the form

$$H_n(x)e^{-x^2/2}\ , \tag{3.33}$$

where[41]

$$H_n(x) = (-1)^n\,e^{x^2}\,\frac{d^n}{dx^n}\,e^{-x^2}$$

is a Hermite polynomial of order n, are solutions of Equation (3.32) when $\alpha'_\omega = 0$, and form a complete orthogonal set. The orthogonality relation satisfied by Equation (3.33) is[41]

$$\int_{-\infty}^{\infty} H_m(x)\, H_n(x)\, e^{-x^2}\, dx = \delta_{mn} 2^n n! \sqrt{\pi} \quad . \tag{3.34}$$

By way of the following derivation, we introduce the dimensionless parameters that will be used extensively in Chapters IV and VI.

We begin by expressing our boundary condition as

$$p_\omega(X,Y,0) = \sum_{m=0}^{\infty} \sum_{n=0}^{\infty} P_{mn} H_m(\sqrt{2}X)\, H_n(\sqrt{2}Y)\, e^{-X^2 - Y^2} \quad , \tag{3.35}$$

where

$$X = \frac{x}{\varepsilon_o} \quad , \quad Y = \frac{y}{\varepsilon_o} \quad .$$

The significance of ε_o, which is an arbitrary constant, is derived from the lowest order mode of $p_\omega(X,Y,0)$ where $m = n = 0$. Since $H_o = 1$, the fundamental mode is Gaussian, and ε_o is thus the initial spot size of the resulting Gaussian beam which is the fundamental mode of radiation. Using the orthogonality relation in Equation (3.34), we find that the coefficients in Equation (3.35) are given by

$$P_{mn} = (\pi m! n! 2^{m+n-1})^{-1} \iint_{-\infty}^{\infty} p_\omega(X,Y,0)\, H_m(\sqrt{2}X)\, H_n(\sqrt{2}Y)\, e^{-X^2 - Y^2}\, dX dY \quad . \tag{3.36}$$

We obtain our solution of Equation (3.32) from Equation (3.27), which in dimensionless form becomes

$$p_\omega(X,Y,Z) = i\frac{\Omega}{\pi}\frac{e^{-a'_\omega Z}}{Z}\int_{-\infty}^{\infty}\int p_\omega(X',Y',0)\exp\{-i\frac{\Omega}{\pi}[(X-X')^2+(Y-Y')^2]\}\,dX'dY' \quad , \tag{3.37}$$

where

$$Z = \frac{z}{z_o} \quad , \quad a'_\omega = \alpha'_\omega z_o \quad , \quad z_o = \frac{\omega_o \varepsilon_o^2}{2c_o} \quad , \quad \Omega = \frac{\omega}{\omega_o} \quad ,$$

and ω_o is an arbitrary reference frequency. Thus, z_o is the collimation distance of the fundamental mode at frequency ω_o, so that $Z = 1$ marks the transition region where that mode passes from its nearfield to its farfield. The normalized parameters become extremely useful when we analyze in detail parametric arrays formed by Gaussian primary beams. Inserting Equation (3.35) into Equation (3.37), we obtain for the homogeneous solution

$$p_\omega(X,Y,Z) = i\frac{\Omega}{\pi}\frac{e^{-a'_\omega Z}}{Z}\sum_{m=0}^{\infty}\sum_{n=0}^{\infty} P_{mn} I_m(X,Z)\, I_n(Y,Z) \quad , \tag{3.38}$$

where

$$I_m(X,Z) = \int_{-\infty}^{\infty} H_m(\sqrt{2}X')\exp\{-X'^2 - i\frac{\Omega}{Z}(X-X')^2\}\,dX' \quad ,$$

and

$$I_n(Y,Z) = \int_{-\infty}^{\infty} H_n(\sqrt{2}Y')\exp\{-Y'^2 - i\frac{\Omega}{Z}(Y-Y')^2\}\,dY' \quad .$$

After some manipulation, we can evaluate I_m and I_n with the help of integral tables.[44] Equation (3.38) becomes

$$p_\omega(X,Y,Z) = \sum_{m=0}^{\infty} \sum_{n=0}^{\infty} P_{mn} E_{mn}(X,Y,Z;\Omega) \quad , \tag{3.39}$$

where

$$E_{mn}(X,Y,Z;\Omega) = \frac{e^{-a'_\omega Z}}{1 - iZ/\Omega} H_m\left\{\frac{\sqrt{2}X}{\sqrt{1 + (Z/\Omega)^2}}\right\} H_n\left\{\frac{\sqrt{2}Y}{\sqrt{1 + (Z/\Omega)^2}}\right\}$$

$$\cdot \exp\left\{-\frac{X^2 + Y^2}{1 - iZ/\Omega} + i(m + n) \tan^{-1}(Z/\Omega)\right\} \quad . \tag{3.40}$$

The orthogonality relation satisfied by the eigenfunctions is

$$\int_{-\infty}^{\infty}\int E_{mn}(X,Y,Z;\Omega) E^*_{pq}(X,Y,Z;\Omega)\, dXdY = \delta_{mp}\delta_{nq}\pi m!n!2^{m+n-1} e^{-2a_\omega Z} \quad , \tag{3.41}$$

where $a'_\omega + a'^*_\omega = 2a_\omega$, and $a_\omega = \alpha_\omega z_o$. When $a'_\omega = 0$, the eigenfunctions reduce to those presented by Cook and Arnoult[45] in their analysis of radiation from ultrasonic transducers.

For weak interactions, the source term for the sum and difference frequency is approximated by

$$Q_\pm(X,Y,Z) = p_1(X,Y,Z)\, p_2^{(*)}(X,Y,Z) \quad , \tag{3.42}$$

where (*) indicates that the complex conjugate applies only for the difference frequency. The relation in Equation (3.42) is easily deduced by recognizing that only the real part (or else only the imaginary part) of a solution is used to describe the acoustic field. Use of complex

notation is only a convenience, and must be abandoned when performing nonlinear operations. That is, to square the primary field we must square the quantity $\mathrm{Re}(p_1 + p_2)$, after which we identify the terms containing the sum and difference frequencies. Returning then to complex notation, Equation (3.42) follows immediately. In terms of the eigenfunctions, Equation (3.42) becomes

$$Q_{\pm}(X,Y,Z) = \sum_{m,n,p,q=0}^{\infty} P_{mn} P_{pq}^{(*)} E_{mn}(X,Y,Z;\Omega_1) E_{pq}^{(*)}(X,Y,Z;\Omega_2) \quad . \tag{3.43}$$

Combining Equations (3.28) and (3.43) and assuming $p_{\pm}(X,Y,0) = 0$, we obtain for the sum- and difference-frequency pressure fields, in dimensionless form,

$$p_{\pm}(X,Y,Z) = -\frac{1}{\pi}\Omega_{\pm}^2 D^2 \sum_{m,n,p,q=0}^{\infty} P_{mnpq} \int_0^Z \iint_{-\infty}^{\infty} E_{mn}(X',Y',Z';\Omega_1) E_{pq}^{(*)}(X',Y',Z';\Omega_2)$$

$$\cdot \frac{e^{-a_{\pm}'(Z-Z')}}{Z-Z'} \exp\left\{-i\Omega_{\pm}\left[\frac{(X-X')^2 + (Y-Y')^2}{Z-Z'}\right]\right\} dX'dY'dZ' \quad , \tag{3.44}$$

where

$$P_{mnpq} = \frac{\beta P_{mn} P_{pq}^{(*)}}{\rho_o c_o^2} \quad , \quad D = \frac{\omega_o \varepsilon_o}{2c_o} \quad .$$

P_{mnpq} has units of pressure, while D is a dimensionless quantity which is a measure of the beam diameter of the fundamental mode in terms of wavelengths associated with the reference frequency ω_o. For example, if we let $\lambda_o = 2\pi c_o/\omega_o$, then $D = \pi\varepsilon_o/\lambda_o$.

Similar results may be derived for axisymmetric radiation. As shown in Appendix A, the Gauss-Laguerre eigenfunctions for Equation (3.32) are

$$E_n(\xi,Z;\Omega) = \frac{e^{-a'_\omega Z}}{1 - iZ/\Omega} L_n\left\{\frac{2\xi^2}{1 + (Z/\Omega)^2}\right\} \exp\left\{-\frac{\xi^2}{1 - iZ/\Omega} + i2n \tan^{-1}(Z/\Omega)\right\} \quad , \tag{3.45}$$

where

$$\xi = \frac{\varepsilon}{\varepsilon_o} = \sqrt{X^2 + Y^2} \quad ,$$

and where the Laguerre polynomials are defined by[41]

$$L_n(x) = e^x \frac{d^n}{dx^n}(x^n e^{-x}) \quad .$$

The primaries are thus given by

$$p_\omega(\xi,Z) = \sum_{n=0}^{\infty} P_n E_n(\xi,Z;\Omega) \quad , \tag{3.46}$$

while for the sum- and difference-frequency pressure fields, we have

$$p_\pm(\xi,Z) = -2\Omega_\pm^2 D^2 \sum_{m,n=0}^{\infty} P_{mn} \int_0^Z \int_0^\infty E_m(\xi',Z';\Omega_1)\, E_n^{(*)}(\xi',Z';\Omega_2)$$
$$\cdot \frac{e^{-a'_\pm(Z - Z')}}{Z - Z'} J_o\left(\frac{2\Omega_\pm \xi\xi'}{Z - Z'}\right) \exp\left\{-i\Omega_\pm\left(\frac{\xi^2 + \xi'^2}{Z - Z'}\right)\right\} \xi' d\xi' dZ' \quad , \tag{3.47}$$

where

$$P_{mn} = \frac{\beta P_m P_n^{(*)}}{\rho_o c_o^2} \quad ,$$

and

$$P_n = \left(\frac{2}{n!}\right)^2 \int_0^\infty p_\omega(\xi,0)\ E_n(\xi,0;\Omega)\ \xi d\xi \quad . \tag{3.48}$$

Thus, for axisymmetric fields we need only perform half the number of summations and integrations which are required for the general case described by Equation (3.44).

Neither Equation (3.44) nor Equation (3.47) can be reduced any further by means of analytical integration. According to Fenlon and McKendree,[10] however, the off-diagonal terms in Equations (3.44) and (3.47) may be omitted when the primary beams have nearly identical shapes. This is usually the case for parametric arrays because the primaries are typically radiated from the same aperture with the frequencies chosen so that $\omega_1 \simeq \omega_2$. Equation (3.47) may then be reduced[10] to a single, although more complicated, integral over Z' . Aside from neglecting off-diagonal terms, we cannot obtain a similar reduction of Equation (3.44).

In summary, we have modified Kuznetsov's nonlinear paraxial wave equation[17] to account for arbitrary attenuation and dispersion. This modified differential equation was rewritten in integral form by way of the Green's function. Using the integral over the boundary condition, which yields the homogeneous solution of the linearized paraxial wave equation, we generated a set of eigenfunctions. These eigenfunctions were combined to describe the primary wave field resulting from an arbitrary source excitation. By squaring the solution for the primary wave field and then integrating over Q_ω , we obtained

a first approximation of the secondary field generated as a result of nonlinear interaction of the primary wave field.

CHAPTER IV

PARAMETRIC ARRAYS FORMED BY COLLINEAR GAUSSIAN PRIMARY BEAMS

In this chapter is presented a detailed analysis of parametric arrays formed by collinear interaction of axisymmetric Gaussian primary beams. The reasons for restricting our analysis to Gaussian primaries are twofold. First is the fact that exact analytical solutions can be obtained from Equation (3.47) when $m = n = 0$. Analytical solutions are useful because they yield asymptotic relations which are easily interpreted. Second, Fenlon[19] and McKendree[10] have demonstrated that Gaussian beams, with proper scaling, yield solutions which are in excellent agreement with results from experiments where the arrays are formed by radiation from uniformly excited circular sources. In Appendix C is introduced the scaling needed to make our results applicable to circular piston radiators.

4.1 Solutions for Primary and Secondary Components

We thus consider the following boundary condition for the primaries:

$$p_j(\xi,0) = p_{Gj} e^{-\xi^2} \quad , \tag{4.1}$$

where $\xi = \varepsilon/\varepsilon_o$ and $\varepsilon^2 = x^2 + y^2$. When Equation (4.1) is substituted into Equation (3.48), the integral vanishes except for $n = 0$. The series in Equation (3.46) therefore reduces to the first term. Combining Equations (3.45), (3.46), and (3.48), we thus obtain for the primary wave fields

$$p_j(\xi,Z) = p_{Gj} \frac{e^{-a_j' Z}}{1 - iZ/\Omega_j} \exp\left\{ - \frac{\xi^2}{1 - iZ/\Omega_j} \right\} \quad . \qquad (4.2)$$

The dimensionless coefficients in Equation (4.2) are $\Omega_j = \omega_j/\omega_o$, $Z = z/z_o$, and $a_j' = \alpha_j' z_o$, where $z_o = \omega_o \varepsilon_o^2/2c_o$ is the collimation distance, as defined in Section 3.3. We now define the reference frequency ω_o by

$$\omega_o = \frac{\omega_1 + \omega_2}{2} \quad ,$$

where ω_1 and ω_2 are the two primary frequencies. For $\omega_1 \simeq \omega_2$ we have $\Omega_1 \simeq \Omega_2 \simeq 1$, and z_o thus represents the collimation length for both primaries.

We first examine the limiting forms of Equation (4.2). For the nearfield, Equation (4.2) reduces to

$$p_j(\xi,Z) \sim p_{Gj} e^{-a_j' Z} e^{-\xi^2} \quad , \quad Z << 1 \quad , \qquad (4.3)$$

which describes the propagation of a plane wave that is subject to attenuation but always maintains the same transverse amplitude distribution. Note that the nearfield of a Gaussian beam is much simpler than that resulting from a circular piston. Treating the nearfield of a Gaussian beam as a plane wave region therefore has real physical meaning.

For the farfield, Equation (4.2) reduces to

$$p_j(\xi,Z) \sim i\Omega_j p_{Gj} \frac{e^{-a_j' Z}}{Z} \exp\left\{ - \left(\frac{\Omega_j \xi}{Z} \right)^2 - i \frac{\Omega_j \xi^2}{Z} \right\} \quad , \quad Z >> 1 \ . \qquad (4.4)$$

There are three factors in Equation (4.4) which together define a spherically spreading wave field. First, the amplitude of p_j suffers spherical spreading losses by virtue of its $1/Z$ dependence. In addition, the term $(\Omega_j \xi/Z)^2$ gives rise to the directivity function. Within the paraxial field, we can let $\xi = DZ\theta$, where $D = \omega_o \varepsilon_o / 2c_o$, so that we have for the directivity function of the primaries

$$D_j(\theta) = \exp\left\{-\Omega_j^2 D^2 \theta^2\right\} \quad . \tag{4.5}$$

Finally, the spherical curvature of the wavefronts is manifested through the phase factor, $-i\Omega_j \xi^2/Z$. By way of Figure 8, the phase delay can be calculated which is required at point Q relative to that at point P, for a wave propagating in the z direction, to establish a spherical wavefront. First we write

$$z^2 = (z - d)^2 + \varepsilon^2 \quad ,$$

which may be rearranged to yield

$$d = \frac{\varepsilon^2 + d^2}{2z} \quad .$$

If only the paraxial field of quasi-plane waves (e.g., highly collimated beams) is considered, then $d << \varepsilon$, so that

$$d \simeq \frac{\varepsilon^2}{2z}$$

in the Fresnel approximation.[30] The necessary phase delay at Q relative to P is thus, for a wave having frequency ω_j and traveling in the z direction,

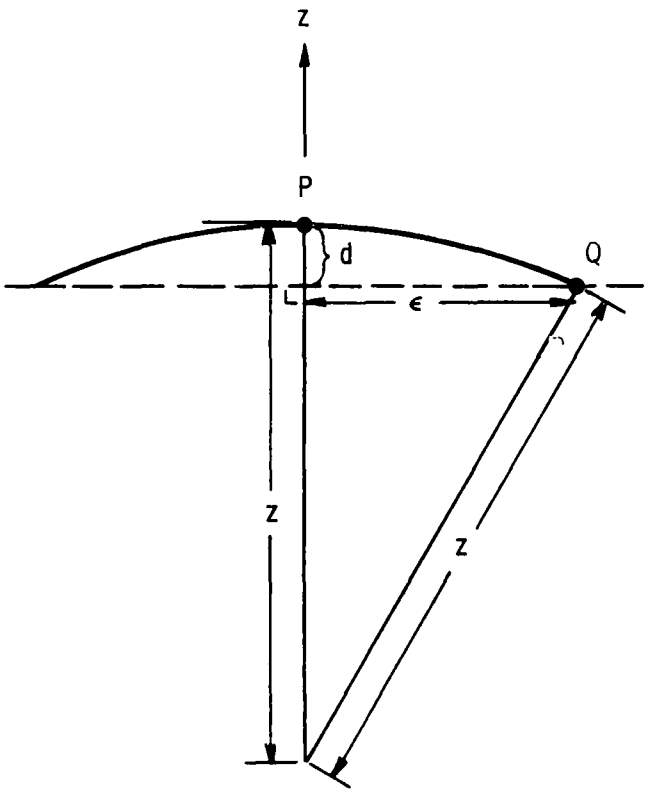

Figure 8. Geometry of a Spherical Wave.

AS-83-706

$$\frac{\omega_j}{c_o} d \approx \frac{\omega_j \varepsilon^2}{2c_o z} \quad ,$$

which may be written in dimensionless form as $\Omega_j \xi^2 / Z$.

To calculate the sum- and difference-frequency fields, we combine Equations (3.47) and (4.2) to obtain

$$p_{\pm}(\xi, Z) = -2\Omega_{\pm}^2 D^2 P_o e^{-a'_{\pm} Z} \int_0^Z \exp\left\{ - \frac{i\Omega_{\pm} \xi^2}{Z - Z'} - a'_{T_{\pm}} Z' \right\} \frac{dZ'}{(Z - Z') g(Z')}$$

$$\int_0^{\infty} \exp\left\{ - \left[\frac{f(Z')}{g(Z')} + \frac{i\Omega_{\pm}}{Z - Z'} \right] \xi'^2 \right\} J_o\left(\frac{2\Omega_{\pm} \xi}{Z - Z'} \xi' \right) \xi' d\xi' \quad , \tag{4.6}$$

where

$$f(Z) = 2 \mp \frac{i\Omega_{\pm}}{\Omega_1 \Omega_2} Z \quad ,$$

$$g(Z) = 1 \mp \frac{i\Omega_{\pm}}{\Omega_1 \Omega_2} Z \mp \frac{1}{\Omega_1 \Omega_2} Z^2 \quad ,$$

and

$$P_o = \frac{\beta p_{G1} p_{G2}}{\rho_o c_o^2} \quad .$$

Both attenuation and dispersion are combined in the factor

$$a'_{T_{\pm}} = a_{T_{\pm}} - i2\delta_{\pm} \Omega_{\pm} D^2 \quad , \tag{4.7}$$

where

$$a_{T_{\pm}} = \alpha_{T_{\pm}} z_o = (\alpha_1 + \alpha_2 - \alpha_{\pm}) z_o$$

and

$$\delta_{\pm} = 1 - \frac{k_1 \pm k_2}{k_{\pm}} \quad .$$

In Equation (4.7), $c_o/c_{\pm}$ has been replaced by unity on the basis that the dispersion is small. This approximation can, of course, be made exact by choosing either $c_o = c_+$ or $c_o = c_-$, which for convenience we will do when discussing either the sum or the difference frequency, respectively. Effects of dispersion are of course still accounted for by $\delta_{\pm}$.

The integral over ξ' in Equation (4.6) can be evaluated, and yields the following expression:

$$p_{\pm}(\xi,Z) = \Omega_{\pm}^2 D^2 P_o e^{-a'_{\pm} Z} \int_0^Z \exp\left\{\frac{i2\Omega_{\pm} \pm \Omega_{\pm}^2 Z'/\Omega_1\Omega_2}{A_z(Z' - Z_{\pm})} \xi^2 - a'_{T_{\pm}} Z'\right\} \frac{dZ'}{A_z(Z' - Z_{\pm})} \quad , \tag{4.8}$$

where

$$A_z = 2 \mp \frac{\Omega_{\pm}^2}{\Omega_1\Omega_2} \pm \frac{i\Omega_{\pm}}{\Omega_1\Omega_2} Z$$

and

$$Z_{\pm} = \frac{2Z + i\Omega_{\pm}}{2 \mp \frac{\Omega_{\pm}^2}{\Omega_1\Omega_2} \pm \frac{i\Omega_{\pm}}{\Omega_1\Omega_2} Z} \quad .$$

After letting $Z' = Z_+(1 - \chi)$, we can rewrite Equation (4.8) as

$$p_{\pm}(\xi,Z) = \Omega_{\pm}^2 D^2 P_o A_z^{-1} e^{-a'_{\pm}Z} \exp\left\{-\left(a'_{T_{\pm}} \mp \frac{\Omega_{\pm}^2\xi^2}{2Z + i\Omega_{\pm}}\right) Z_{\pm}\right\}$$

$$\cdot \int_1^{1 - Z/Z_{\pm}} \exp\left\{a'_{T_{\pm}} Z_{\pm}\chi - \frac{i\Omega_{\pm} Z_{\pm}(4 \mp \Omega_{\pm}^2/\Omega_1\Omega_2)\xi^2}{(2Z + i\Omega_{\pm})^2} \frac{1}{\chi}\right\} \frac{d\chi}{\chi} \quad . \tag{4.9}$$

The sum- and difference-frequency cases will now be considered separately. First note that

$$\Omega_1 = 1 + \Omega_-/2 \quad , \quad \Omega_2 = 1 - \Omega_-/2 \quad ,$$

where $\Omega_- = \Omega_1 - \Omega_2$. Since $\Omega_-^2 << 1$, then $\Omega_1\Omega_2 \simeq 1$ so that for the difference frequency, where $A_z \simeq 2 - i\Omega_- Z$, Equation (4.9) reduces to

$$p_-(\xi,Z) = \Omega_-^2 D^2 P_o \frac{e^{-a'_- Z}}{2 - i\Omega_- Z} \exp\left\{-\left(a'_{T_-} + \frac{\Omega_-^2\xi^2}{2Z + i\Omega_-}\right) Z_-\right\}$$

$$\cdot \int_1^{1 - Z/Z_-} \exp\left\{a'_{T_-} Z_-\chi - \frac{i\Omega_- Z_-(4 + \Omega_-^2)\xi^2}{(2Z + i\Omega_-)^2} \frac{1}{\chi}\right\} \frac{d\chi}{\chi} \quad , \tag{4.10}$$

where

$$Z_- = \frac{2Z + i\Omega_-}{2 + \Omega_-^2 - i\Omega_- Z} \quad .$$

Equation (4.10) becomes formally equivalent to the integral obtained by Novikov[9] if a'_{T_-} is replaced by its complex conjugate, i.e., if the sign of δ_- is reversed. Discussion of the apparent error in Novikov's result is postponed until Section 4.2. The quantity Ω_-^2 which appears in the integral in Equation (4.10) gives rise to the aperture factor. In their analysis of parametric arrays operating in dispersionless fluids, Fenlon and McKendree[10] omitted this factor of Ω_-^2, and therefore obtained no aperture factor. On the other hand, we find in Section 4.3 that the aperture factor for the difference frequency is typically close to unity throughout the paraxial field.

By way of the generating function for modified Bessel functions,

$$e^{\frac{x}{2}\left(t+\frac{1}{t}\right)} = \sum_{n=-\infty}^{\infty} t^n I_n(x) \quad , \tag{4.11}$$

we can express Equation (4.10) in terms of complex exponential integrals:

$$p_-(\xi,Z) = \Omega_-^2 D^2 P_o \frac{e^{-a'_- Z}}{2 - i\Omega_- Z} \exp\left\{-\left(a'_{T_-} + \frac{\Omega_-^2 \xi^2}{2Z + i\Omega_-}\right) Z_-\right\}$$

$$\sum_{n=-\infty}^{\infty} I_n\left\{-\frac{i2\Omega_- Z_- (4+\Omega_-^2)\xi^2}{(2Z+i\Omega_-)^2}\right\}\left[E_{1-n}\left\{-\left[a'_{T_-} + \frac{i\Omega_-(4+\Omega_-^2)\xi^2}{(2Z+i\Omega_-)^2}\right] Z_-\right\}\right.$$

$$\left. - \left(1 - \frac{Z}{Z_-}\right)^n E_{1-n}\left\{-\left[a'_{T_-} + \frac{i\Omega_-(4+\Omega_-^2)\xi^2}{(2Z+i\Omega_-)^2}\right](Z_- - Z)\right\}\right] \quad . \tag{4.12}$$

The complex exponential integrals are defined by[46]

$$E_n(z) = \int_1^\infty \frac{e^{-zt}}{t^n}\, dt \quad , \quad \mathrm{Re}(z) > 0 \quad , \tag{4.13}$$

$$\sim \frac{e^{-z}}{z} \quad , \quad |z| >> |n| \quad . \tag{4.14}$$

A discussion of exponential integrals, in particular with respect to the requirement that the real part of the argument be greater than zero, is given in Appendix B.

Equation (4.9) can be reduced even further for the sum frequency. Since $\Omega_+ = 2$ and $\Omega_1\Omega_2 \simeq 1$, we have

$$4 - \frac{\Omega_+^2}{\Omega_1\Omega_2} \simeq 0 \quad . \tag{4.15}$$

If we neglect the term in Equation (4.9) which contains the left-hand side of Equation (4.15), then we obtain for the sum-frequency pressure field

$$p_+(\xi,Z) = -2D^2P_o \frac{e^{-a_+'Z}}{1-iZ} \exp\left\{ia_{T_+}' - \frac{2\xi^2}{1-iZ}\left\{\left[E_1\{ia_{T_+}'\} - E_1\{ia_{T_+}'(1-iZ)\}\right]\right.\right. . \tag{4.16}$$

More will be said in Section 4.4 regarding the use of Equation (4.15) to obtain Equation (4.16).

As $\omega_1 \to \omega_2$, the approximate relation in Equation (4.15) becomes exact. Indeed, Equation (4.16) is easily modified for application to the second-harmonic fields. Squaring the field given

by $\mathrm{Re}(p_j)$ and then returning to complex notation, we find that the source term for the second-harmonic field is given, to a first approximation, by

$$Q_{2\omega_j}(\xi,Z) = \frac{1}{2}\, p_j^2(\xi,Z) \quad .$$

A factor of $1/2$ must therefore be introduced in Equation (4.16). Equation (4.16) thus becomes an exact analytical solution of the inhomogeneous paraxial wave equation for the second harmonics if $P_o = \beta p_{Gj}^2/2\rho_o c_o^2$, $a_+ = a_{2\omega_j}$, and $\delta_+ = 1 - 2k_{\omega_j}/k_{2\omega_j}$. The result for the second-harmonic field is, of course, valid even if the source emits only a single frequency.

As we noted above, Gaussian beams can be used to model the paraxial field of uniformly excited circular projectors. In Appendix C, the appropriate transformation is made which permits application of not only the field equations derived in this section, but also the asymptotic relations considered in Sections 4.2 and 4.3, to arrays formed by primary beams exhibiting "Bessel" directivity patterns. Note, however, that the distinctive diffraction effects within the nearfield of a circular piston projector, that is, the peaks and nulls, are not modeled by Gaussian beams. However, in Appendix C we demonstrate the utility of the transformed equations by showing the excellent agreement with data obtained from parametric arrays formed by Bessel beams in water, where the dispersion is negligible.

4.2 Axial Difference-Frequency Field

Along the z axis $\xi = 0$, and Equation (4.12) reduces to

$$p_-(0,Z) = \Omega_-^2 D^2 P_o \frac{e^{-a_- Z}}{2-i\Omega_- Z} e^{-a_T' Z_-}\left[E_1\{-a_T' Z_-\} - E_1\{-a_T'(Z_- - Z)\}\right]$$

$$= \Omega_-^2 D^2 P_o \frac{e^{-a_- Z}}{2-i\Omega_- Z} \exp\left\{-(\delta\Omega_-^2 D^2 + i\Omega_- a_T/2)\left(\frac{1-i2Z/\Omega_-}{1-i\Omega_- Z/2}\right)\right\}$$

$$\cdot\left[E_1\left\{-(\delta\Omega_-^2 D^2 + i\Omega_- a_T/2)\left(\frac{1-i2Z/\Omega_-}{1-i\Omega_- Z/2}\right)\right\}\right.$$

$$\left. - E_1\left\{-(\delta\Omega_-^2 D^2 + i\Omega_- a_T/2)\left(\frac{1+Z^2+i\Omega_- Z}{1-i\Omega_- Z/2}\right)\right\}\right] \quad . \tag{4.17}$$

The subscript "-" on a_T, a_T', and δ has been omitted in this and the next section for simplicity. It is understood that for the difference frequency,

$$a_T' = a_T - i2\delta\Omega_- D^2 \quad ,$$

where

$$a_T = a_1 + a_2 - a_-$$

and

$$\delta = 1 - \frac{k_1 - k_2}{k_-} \quad .$$

We also let

$$c_o = c_-$$

so that $a_-' = a_-$. When there is no dispersion (i.e., $\delta = 0$), Equation (4.17) reduces to a form obtained previously by others.[10,18,19] Within the nearfield of the primaries where $Z^2 << 1$, Equation (4.17) assumes the asymptotic form

$$p_-(0,Z) \sim \tfrac{1}{2}\Omega_-^2 D^2 P_o e^{-a_- Z} \exp\{-(\delta\Omega_-^2 D^2 + i\Omega_- a_T/2)(1-i2Z/\Omega_-)\}$$

$$\cdot [E_1\{-(\delta\Omega_-^2 D^2 + i\Omega_- a_T/2)(1-i2Z/\Omega_-)\} - E_1\{-(\delta\Omega_-^2 D^2 + i\Omega_- a_T/2)\}] \ , Z^2 << 1 \ , \tag{4.18}$$

which in the absence of dispersion reduces to the nearfield result of Novikov, Rudenko, and Soluyan.[16]

Novikov[6] was the first to investigate the effect of dispersion on the parametric array. He obtained a nearfield result for mono-relaxing fluids which is similar to Equation (4.18), where α_- and k_- are given by Equations (3.14), and where for small dispersion, $\delta \simeq m/2$. There are, however, a number of inconsistencies in Novikov's derivation. Of minor significance is the fact that he should have mc_o^2 instead of mc_∞^2 in his equation of state, which is an error that propagates through subsequent equations. It is more important that, in going from his wave equation to the integral solution, he changes the sign associated with the dispersivity, m . Finally, to write the axial solution as he does requires an unconventional definition of the exponential integral.

Not only is the sign of m wrong in Novikov's first analysis,[6] but in a subsequent analysis[9] which led to a result like Equation (4.10), he again has an error in the sign of his dispersion coefficient. Examination of Equations (4.17) and (4.18) reveals that the axial amplitude of the difference-frequency wave is indeed sensitive to whether δ is positive or negative. Although energy considerations indicate that $c_\infty > c_o$, there can be wiggles in the dispersion curve that make $\delta < 0$ for a particular choice of frequencies. Indeed, the dispersion characteristics of bubbly water allow for anomalous dispersion ($\delta < 0$).

Placing additional restrictions on Equation (4.18) yields an interesting result. Assuming $|\Omega_- a_T'/2| \gg 1$ in Equation (4.18) and using Equation (4.14), we obtain

$$p_-(0,Z) \sim i \frac{\Omega_-}{a_T'} D^2 P_o e^{-a_- Z} \left(\frac{1}{1 - i2Z/\Omega_-} - e^{-a_T' Z} \right), \quad Z^2 \ll 1 \quad , \quad |\Omega_- a_T'/2| \gg 1 \quad . \tag{4.19}$$

As discussed in Section 4.3, the condition $|\Omega_- a_T'/2| \gg 1$ gives rise to an absorption-limited array, where nonlinear interaction is restricted to the nearfield of the primaries. Now, since z_o is the collimation distance of the primaries, $\Omega_- z_o$ is then the collimation distance of a difference-frequency signal radiated by the source of the primaries. Therefore, when $Z \ll \Omega_-/2$, even the difference-frequency signal behaves as a plane wave, and Equation (4.19) reduces to

$$p_-(0,Z) \sim \frac{2\Omega_-}{a_T'} D^2 P_o e^{-(a_- + a_T'/2)Z} \sin(i a_T' Z/2) \quad , \quad Z \ll \Omega_-/2 \quad , \quad |\Omega_- a_T'/2| \gg 1 \quad . \tag{4.20}$$

Equation (4.20) is identical to Equation (2.18), and we have thus recovered the result for plane-wave interaction. What makes Equation (4.20) particularly interesting is that the amplitude of p_- does not depend on the sign of δ, in contrast to the behavior of Equations (4.17) and (4.18). As shown in Appendix D, the difference-frequency field resulting from spherical primary waves which are radiated by a spherical source of radius a is given by

$$p_-(r) = \frac{ik_-a^2\beta p_{01}p_{02}}{2\rho_o c_o^2}\,\frac{e^{-i\chi_- r}}{r}\,[E_1\{i(\chi_1-\chi_2^*-\chi_-)r\}-E_1\{i(\chi_1-\chi_2^*-\chi_-)a\}] \quad , \tag{4.21}$$

where p_{01} and p_{02} are the amplitudes of the primaries at $r = a$. Because of the fact that[46]

$$E_1(z^*) = [E_1(z)]^* \quad ,$$

the amplitude of p_- in Equation (4.21) is also insensitive to the sign of δ. We thus conclude that diffraction is responsible for the dependence of the difference-frequency field on the sign of δ.

It has been shown both analytically[47,48] and experimentally[49] that diffraction induces asymmetries in finite-amplitude waves which are initially sinusoidal. That is, diffraction causes sharpening of the peaks and rounding of the troughs in the pressure waveform. The asymmetrical distortion occurs because diffraction affects each of the harmonic components differently. Specifically, diffraction alters the phase relations which lead to symmetrical sawtooth formation in one-dimensional wave propagation. Similarly, diffraction induces a

slight phase mismatch between the primaries and the difference-frequency signal.

The phase mismatch caused by diffraction may be discussed more quantitatively if Equation (4.2) is rewritten as

$$p_j(\xi,Z) = p_{G_j} \frac{e^{-a_j'Z + i\phi_j}}{\sqrt{1 + (Z/\Omega_j)^2}} \exp\left\{- \frac{\xi^2}{1 + (Z/\Omega_j)^2}\right\} , \qquad (4.22)$$

where

$$\phi_j(\xi,Z) = \arctan\left(\frac{Z}{\Omega_j}\right) - \frac{Z/\Omega_j}{1 + (Z/\Omega_j)^2} \xi^2 . \qquad (4.23)$$

Transformation of Equation (4.22) into the time domain requires multiplication by $e^{i\omega_j t'}$, which gives rise to the factor

$$e^{-\alpha_j' z + i\phi_j} e^{i\omega_j t'} = e^{-\alpha_j z} e^{i(\omega_j t - k_j' z)} , \qquad (4.24)$$

where

$$k_j' = k_j - \phi_j/z .$$

The modified wave number k_j' accounts for contributions to the phase of the wave, at any time, which result from both the sound speed c_j and the effect of diffraction. Since the latter affects the phase speed and is dependent on frequency, we shall refer to it as diffraction-induced dispersion. A modified dispersion coefficient may therefore be defined as

$$\delta' = 1 - \frac{k_1' - k_2'}{k_-}$$

$$= + \frac{\Delta\phi}{k_- z} , \qquad (4.25)$$

where

$$\Delta\phi = \phi_1 - \phi_2 \quad . \tag{4.26}$$

The total phase mismatch between the primaries and the difference-frequency signal is taken into account by δ' . Inherent dispersion is represented by δ , and diffraction-induced dispersion is represented by $\Delta\phi/k_z$. In the absence of inherent dispersion ($\delta = 0$) , the modified dispersion coefficient reduces to $\delta' = \Delta\phi/k_z$. Positive values of $\Delta\phi$ therefore create an effect which resembles that due to normal inherent dispersion, whereas the effect of negative values of $\Delta\phi$ resembles that of anomalous dispersion.

As illustrated in Figure 9, $\Delta\phi$ is negative throughout the paraxial region, where nonlinear interaction occurs, and it is zero at $Z = 0$ and $Z = \infty$. Along the z axis, $\Delta\phi$ has its minimum value at $Z = \sqrt{\Omega_1\Omega_2} \simeq 1$. That $\Delta\phi$ is negative in the nonlinear interaction region suggests that normal inherent dispersion (i.e., $\delta > 0$) is necessary for compensation of the diffraction-induced dispersion.

Suppose, now, that Equation (4.24) is used to calculate the phase speed in the z direction. The complex exponential in Equation (4.24) may be written as

$$e^{i[\omega_j t - f(z)]} \quad ,$$

where

$$f(z) = k_j z - \phi_j \quad . \tag{4.27}$$

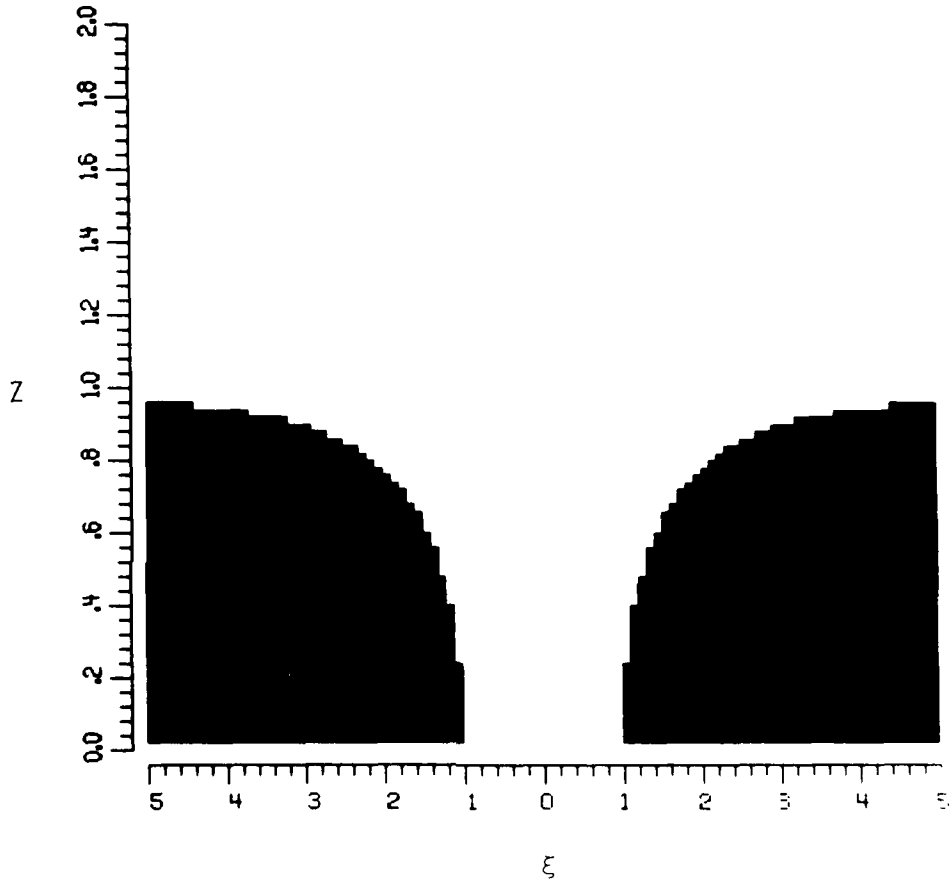

Figure 9. Diffraction-Induced Dispersion for $\Omega_- = 0.1$. Black and White Represent $\Delta\phi > 0$ and $\Delta\phi < 0$, Respectively.

AS-83-707

For a point of constant phase traveling with the wave, we have

$$\omega_j t - f(z) = \text{constant.} \tag{4.28}$$

The phase speed of that point, $v = dz/dt$, is found by differentiating Equation (4.28) with respect to time:

$$v_j = \omega_j \left(\frac{\partial f}{\partial z} \right)^{-1} . \tag{4.29}$$

Therefore, the phase speed in the z direction of a wave of frequency ω_j is, from Equations (4.23), (4.27), and (4.29),

$$v_j(\xi,Z) = c_j \left\{ 1 - \frac{c_j/c_o}{2D^2} \left[\frac{1 - \xi^2}{\Omega_j^2 + Z^2} + \frac{2Z^2\xi^2}{(\Omega_j^2 + Z^2)^2} \right] \right\}^{-1} . \tag{4.30}$$

In the absence of inherent dispersion ($\delta = 0$) and along the z axis ($\xi = 0$), Equation (4.30) reduces to

$$v_j(0,Z) = c_o \left\{ 1 - \frac{1}{2D^2} \frac{1}{\Omega_j^2 + Z^2} \right\}^{-1} . \tag{4.31}$$

It is easily seen from Equation (4.31) that if $\Omega_1 > \Omega_2$, then $v_1(0,Z) < v_2(0,Z)$, which corresponds to the same situation that results from anomalous inherent dispersion. Again, it follows that only normal inherent dispersion ($\delta > 0$) can compensate for diffraction-induced dispersion.

In the farfield of the parametric array, Equation (4.17) reduces to

AD-A130 533 PARAMETRIC ACOUSTIC ARRAY FORMATION VIA WEAK COLLINEAR AND NONCOLLINEAR I. (U) TEXAS UNIV AT AUSTIN APPLIED RESEARCH LABS M F HAMILTON JUN 83 ARL-TR-83-19 2/3

UNCLASSIFIED N00014-79-C-0624 F/G 17/1 NL

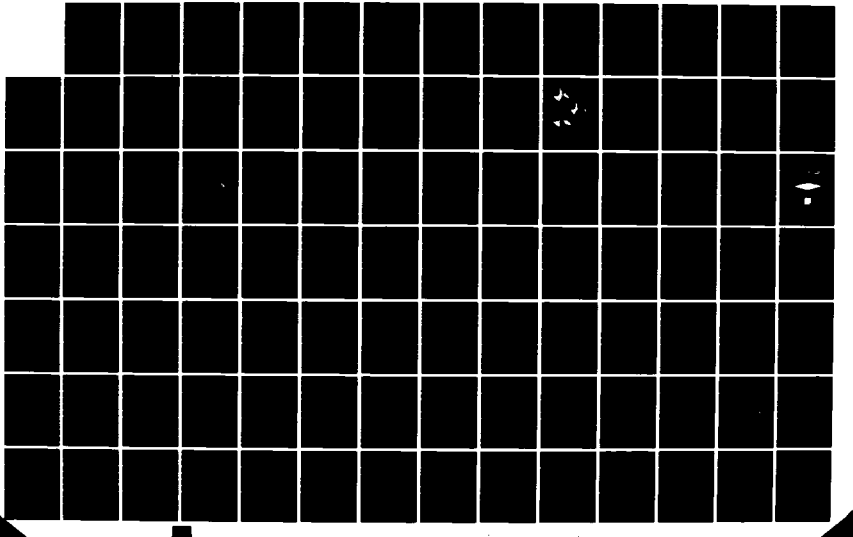

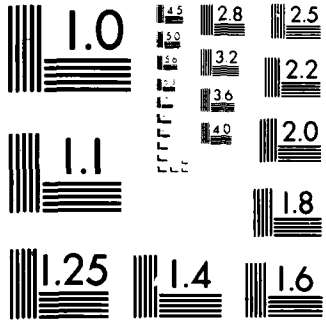

$$p_-(0,Z) \sim i\Omega_- D^2 P_o \frac{e^{-a_- Z}}{Z} \exp\{-4\delta D^2 - i2a_T/\Omega_-\} E_1\{-4\delta D^2 - i2a_T/\Omega_-\} \ , \ Z \to \infty \ . \tag{4.32}$$

Note that the only effect of dispersion in the farfield is additional attenuation. For $|2a_T'/\Omega_-| >> 1$, Equation (4.32) reduces further to

$$p_-(0,Z) \sim - \frac{\Omega_-^2 D^2 P_o}{2a_T - i4\delta\Omega_- D^2} \frac{e^{-a_- Z}}{Z} \ , \ Z \to \infty \ , \quad |2a_T'/\Omega_-| >> 1 \ . \tag{4.33}$$

Presented in Figures 10a-10c are axial difference-frequency field curves which were calculated with Equation (4.17). We assumed a source diameter of $D = 30$ and a frequency-downshift ratio of $\Omega_-^{-1} = 10$, with $a_T = 0.01, 0.1, 1.0$ and δ ranging from 0 to 0.01 . Although a mutual physical dependence exists between dissipation and dispersion, the parameters a_T and δ are treated here as though they are independent for the purpose of illustrating phenomenologically the effect of varying either one separately. Since fluids typically exhibit normal dispersion for which $\delta > 0$, attention is focused primarily on positive values of δ . The pressure is referred to $P_o e^{-a_- Z}$ so that exponential attenuation is factored out. This is done to emphasize the farfield of the parametric array where the difference-frequency component experiences spherical spreading.

Referring to Figure 10, we see that dispersion causes spatial oscillations that occur with greater spatial frequency as $|\delta|$ increases. As discussed in Section 2.2, the oscillations result from virtual sources radiating out of phase with the waves arriving from other virtual sources. The phase mismatch increases with $|\delta|$, and

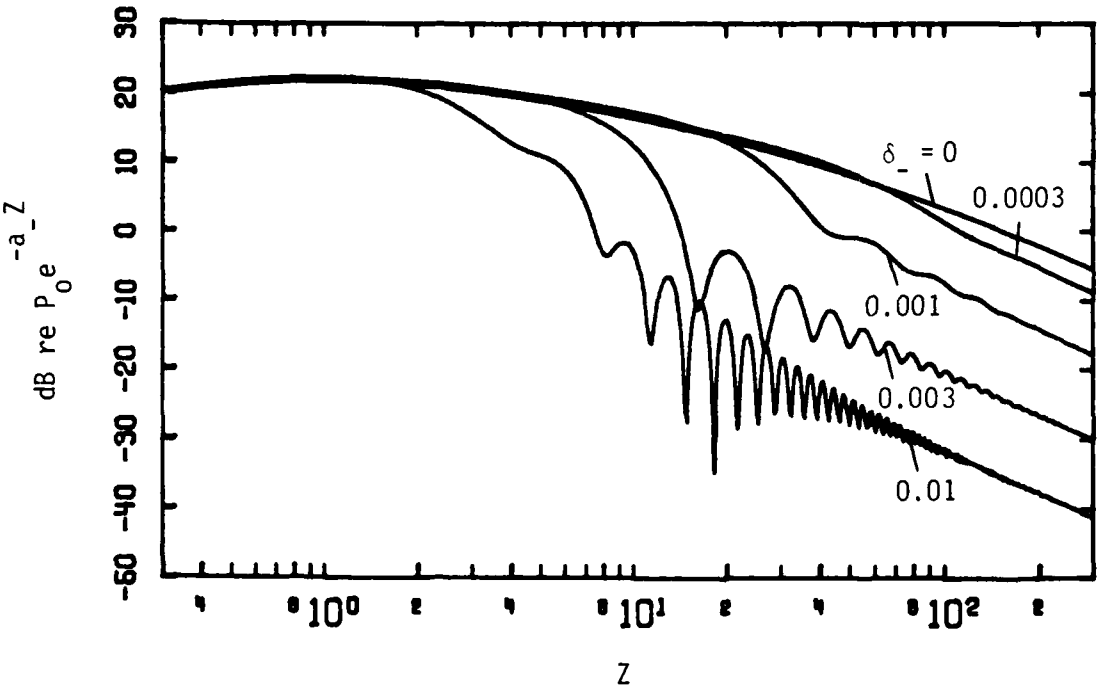

(a) $a_{T_-} = 0.01$

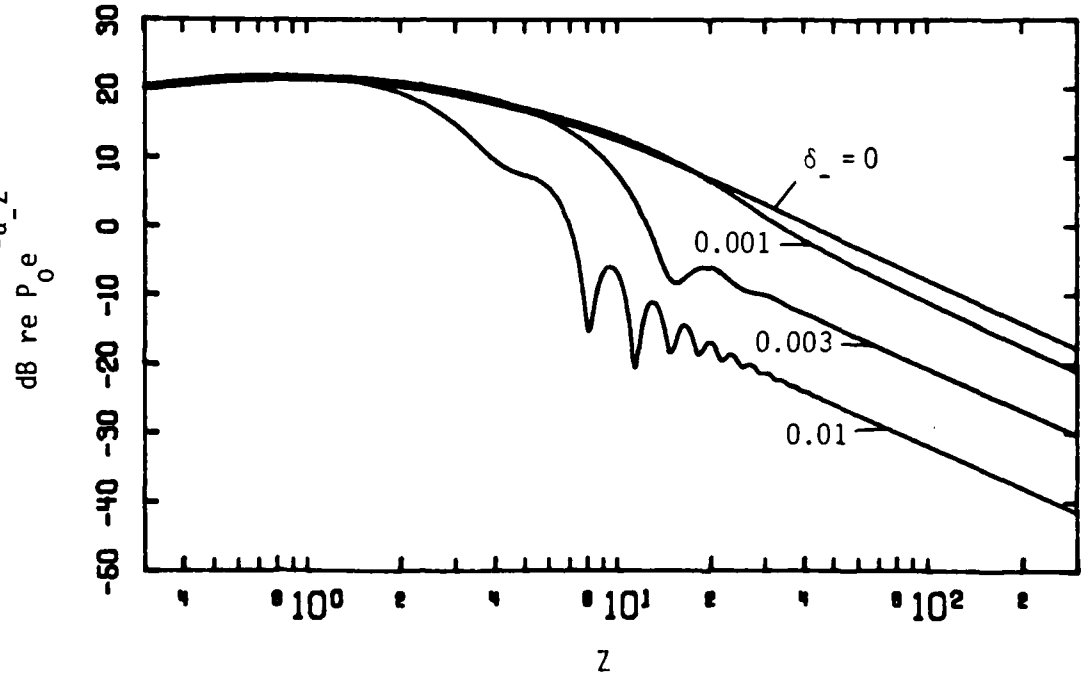

(b) $a_{T_-} = 0.1$

Figure 10. Effect of Dispersion on the Axial Difference-Frequency Field ($\Omega_- = 0.1$, $D = 30$).

AS-83-708

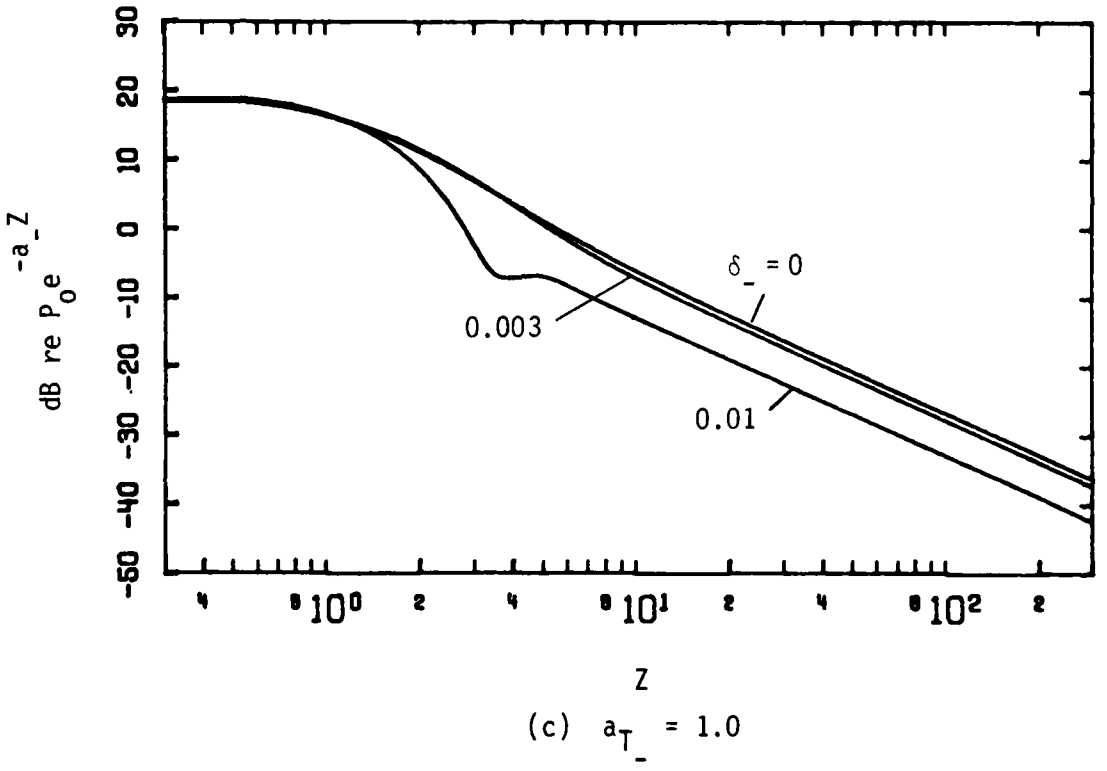

(c) $a_T = 1.0$

Figure 10. (continued)

thus the periods of spatial oscillation decrease. Reduced peak amplitudes within the oscillations accompany the shorter periods, and, as a result, less energy is transferred to the difference-frequency signal. The conversion efficiency of the parametric interaction is thus severely diminished, as evidenced by the amplitudes in the farfield of the array.

Given the rapid amplitude variations in the difference-frequency field which are caused by dispersion, the question arises as to what extent the paraxial wave equation remains valid. Equations (3.10) and (3.15) are based on the assumption that the amplitude of p_ω varies sufficiently slowly with z that $|\partial^2 p_\omega/\partial z^2| << 2k|\partial p_\omega/\partial z|$. To evaluate this inequality for the difference-frequency component, we assume for simplicity that $p_- = A \sin(\delta k_- z/2)$, as given by Equation (4.20) when there is no attenuation. Calculation of the derivatives yields $|\partial^2 p_-/\partial z^2| = |A\delta^2 k_-^2/4|$ and $2k_-|\partial p_-/\partial z| = |A\delta k_-^2|$, from which it can be deduced that Equations (3.10) and (3.15) are valid when

$$|\delta| << 4 \quad . \tag{4.34}$$

In practice, the condition in Equation (4.34) is likely to be violated only in inhomogeneous media such as bubbly water.

The mechanism that competes with dispersion is, of course, absorption of the primaries, and the relative significance of the latter is measured by comparing a_T with $|2\delta\Omega_- D^2|$. In Figure 11 (where $2\delta\Omega_- D^2 = 0.54$), it is seen that when $a_T < |2\delta\Omega_- D^2|$, the spatial oscillations are damped as a_T increases, but the farfield

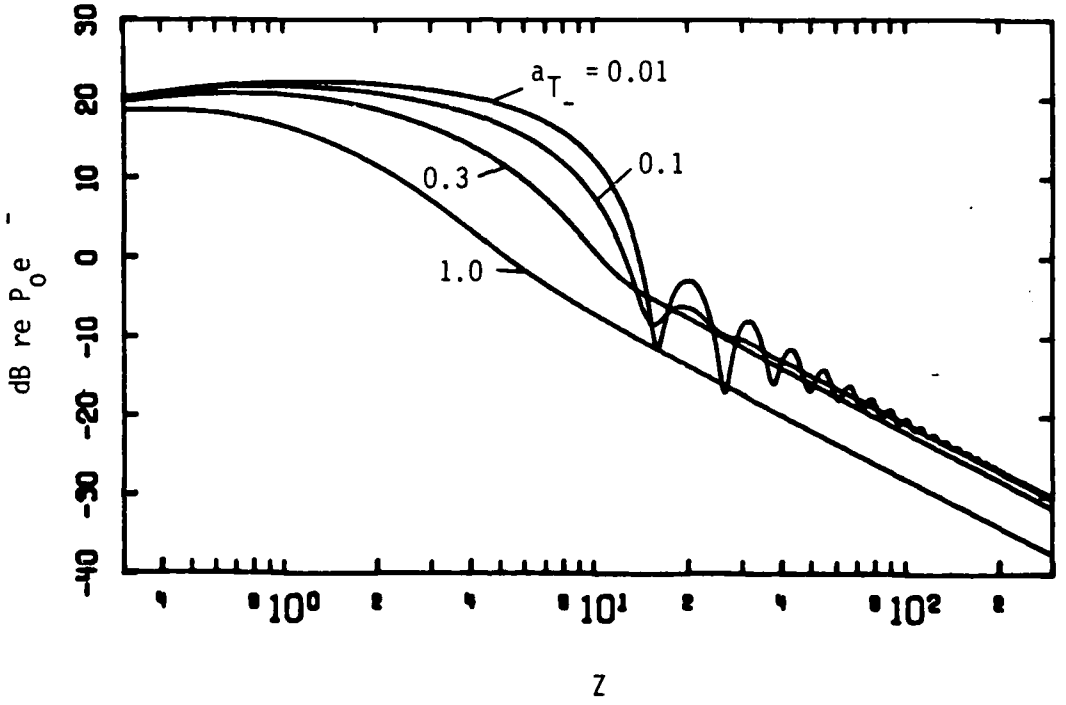

Figure 11. Effect of Dissipation on the Axial Difference-Frequency Field ($\delta_- = 0.003$, $\Omega_- = 0.1$, $D = 30$, $2\delta_-\Omega_- D^2 = 0.54$).

AS-83-710

level is relatively unaffected. When $a_T \simeq |2\delta\Omega_- D^2|$, the oscillations are entirely suppressed, whereas for higher attenuation of the primaries where a_T is larger, the farfield amplitude of the difference-frequency signal is decreased. For sufficiently high dissipation ($a_T >> |2\delta\Omega_- D^2|$) , the farfield amplitude is proportional to $1/a_T$. Conversely, when $|\delta| < a_T/2\Omega_- D^2$, variations in $|\delta|$ have virtually no effect on the nonlinear interaction. In short, from Figures 10 and 11, we find that dispersion becomes an important factor only when $|\delta| > a_T/2\Omega_- D^2$, or equivalently when

$$|\delta| > \frac{\alpha_T}{k_-} \quad . \tag{4.35}$$

The effect of changing the frequency-downshift ratio is illustrated in Figure 12. It is well known that increasing the difference frequency improves the efficiency of parametric interactions. For example, the farfield difference-frequency pressure amplitude for an absorption-limited array varies as Ω_-^2 , and tends toward Ω_- for a diffraction-limited array. When there is dispersion, however, increasing Ω_- while δ is constant shortens the periods of spatial oscillation and thus diminishes gains which would be expected in the absence of dispersion. As we see by comparing Figure 12a with Figure 12b, the increase of the farfield amplitude with Ω_- becomes less as $|\delta|$ is increased. In fact, when dispersion is large compared to both dissipation ($|\delta| >> \alpha_T/k_-$) and diffraction ($|\delta| >> 1/4D^2$) , the axial farfield is given by

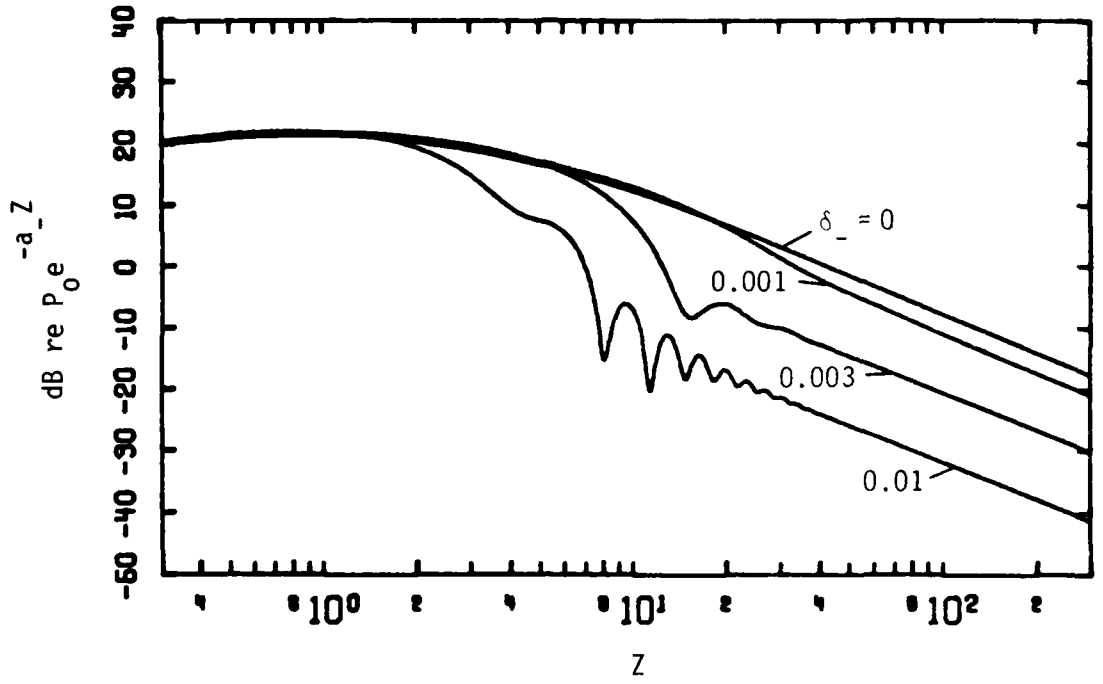

(a) $\Omega_- = 0.1$

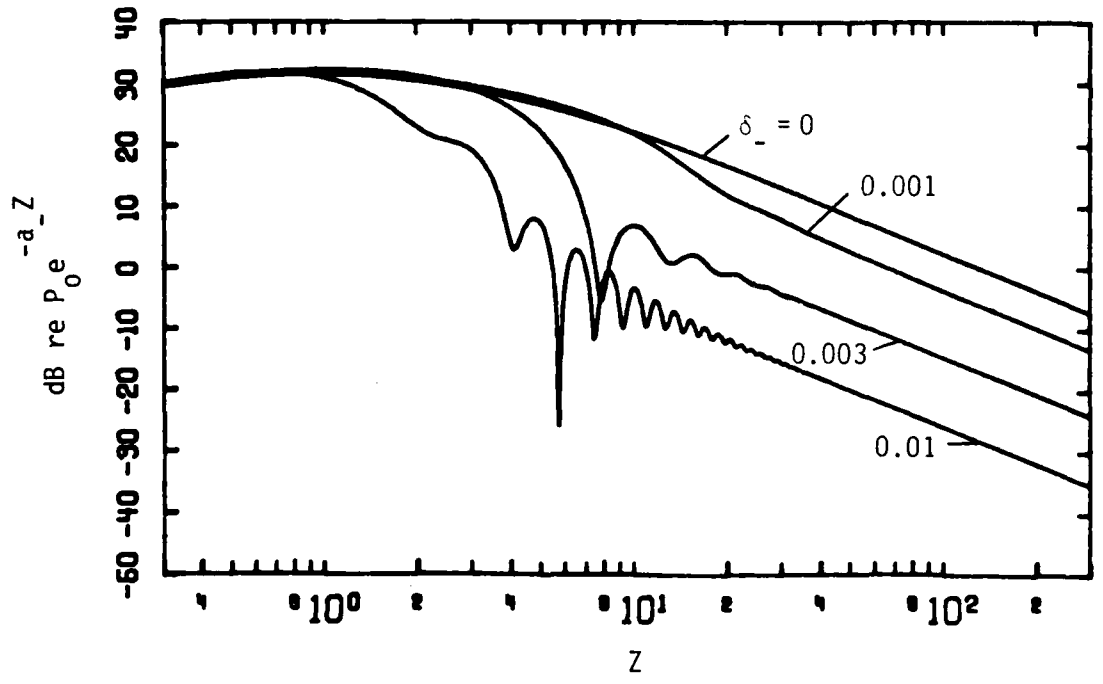

(b) $\Omega_- = 0.2$

Figure 12. Effect of the Frequency-Downshift Ratio on the Axial Difference-Frequency Field ($a_{T_-} = 0.1$, D = 30).

$$p_-(0,Z) \sim -i \frac{\Omega_- P_o}{4\delta} \frac{e^{-a_- Z}}{Z} \quad , \quad Z \to \infty \quad , \quad |\delta| >> \alpha_T/k_- \quad , \quad 1/4D^2 \quad . \tag{4.36}$$

An array behaving in this fashion may be called a dispersion-limited array.

In Figure 13 we see how changing the sign of δ affects the axial field. Numerical examination of Equation (4.17) reveals that, for the same value of $|\delta|$, the farfield amplitude is always greater when $\delta > 0$ than when $\delta < 0$. The difference approaches zero, however, as either $|\delta|$ or a_T becomes large. In the nearfield (the interaction region), the differences are greater than in the farfield. Close to the source, the amplitude of the difference-frequency wave increases slightly with δ. That is, amplification of the difference-frequency signal is initially more efficient when $\delta > 0$ than when $\delta \leq 0$. In fact, when δ is small and positive, the farfield amplitude may be greater than that for $\delta = 0$. When dispersion is large enough that oscillations are induced in the field, the spatial beating in two fields whose parameters differ only in the sign of δ tends to be 180° out of phase. It is near the onset of the oscillations that differences on axis arising from positive and negative δ are most significant.

The reason certain nonzero values of δ give rise to farfield pressures that exceed those occurring when $\delta = 0$ is that dispersion can offset the slight phase mismatch caused by diffraction. Compensation for this phase mismatch, referred to as diffraction-induced dispersion, was discussed earlier in this section. Presented

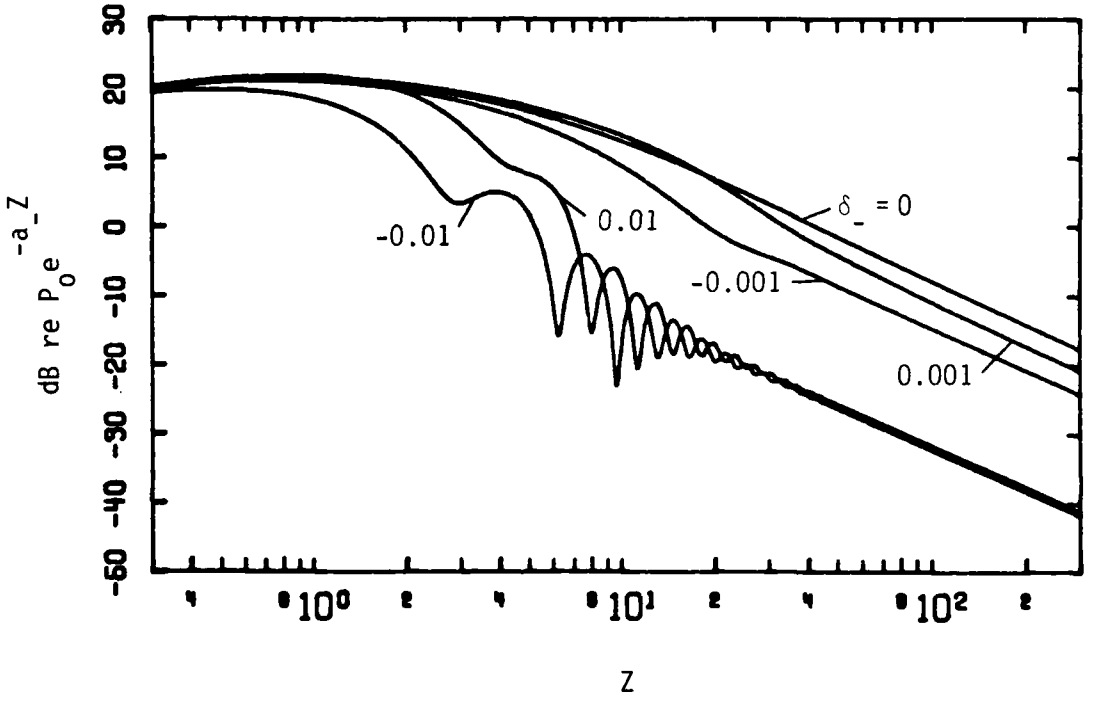

Figure 13. Effect of Anomalous ($\delta < 0$) Versus Normal ($\delta > 0$) Dispersion on the Axial Difference-Frequency Field ($a_{T_-} = 0.1$, $\Omega_- = 0.1$, $D = 30$).

AS-83-712

in Figure 14a is a family of curves, for different values of a_T/Ω_-, which shows how dispersion, through the term δD^2, can improve the farfield axial amplitude. As δ increases from zero, the amplitude passes through a maximum, after which any additional dispersion overcompensates for the diffraction-induced phase mismatch. We note again that only normal dispersion ($\delta > 0$) can compensate for diffraction effects. Others have asserted[7,9] that anomalous dispersion is required. In the case of Novikov's result,[9] the apparent error arises from a mistake in the sign of the dispersion parameter. However, the conclusion[7] reached by Karamzin, Sukhorukov, and Sukhorukova results from a numerical analysis, and therefore the discrepancy is not as easily understood. In Figure 14b, it is seen to what extent the phase mismatch caused by diffraction affects the farfield amplitude. For a given dissipation (i.e., value of a_T/Ω_-), the value of δD^2 which maximizes the farfield amplitude can be found. The improvement is never more than about 0.5 dB.

4.3 Difference-Frequency Farfield

In the paraxial farfield of the parametric array, ε can be replaced by $z\theta$ (i.e., $\xi = DZ\theta$), whereby Equation (4.10) assumes the asymptotic form

$$p_-(\theta,Z) \sim i\Omega_- D^2 P_o \frac{e^{-a_- Z}}{Z} \exp\{-4\delta D^2 - i2a_T/\Omega_- - (2 + \Omega_-^2)D^2\theta^2 - i\Omega_- D^2 Z\theta^2\}$$

$$\cdot \int_1^{i\infty} \exp\{(4\delta D^2 + i2a_T/\Omega_-)\chi + (2 + \Omega_-^2/2)D^2\theta^2 \frac{1}{\chi}\}\frac{d\chi}{\chi} \quad , \quad Z \to \infty \quad . \tag{4.37}$$

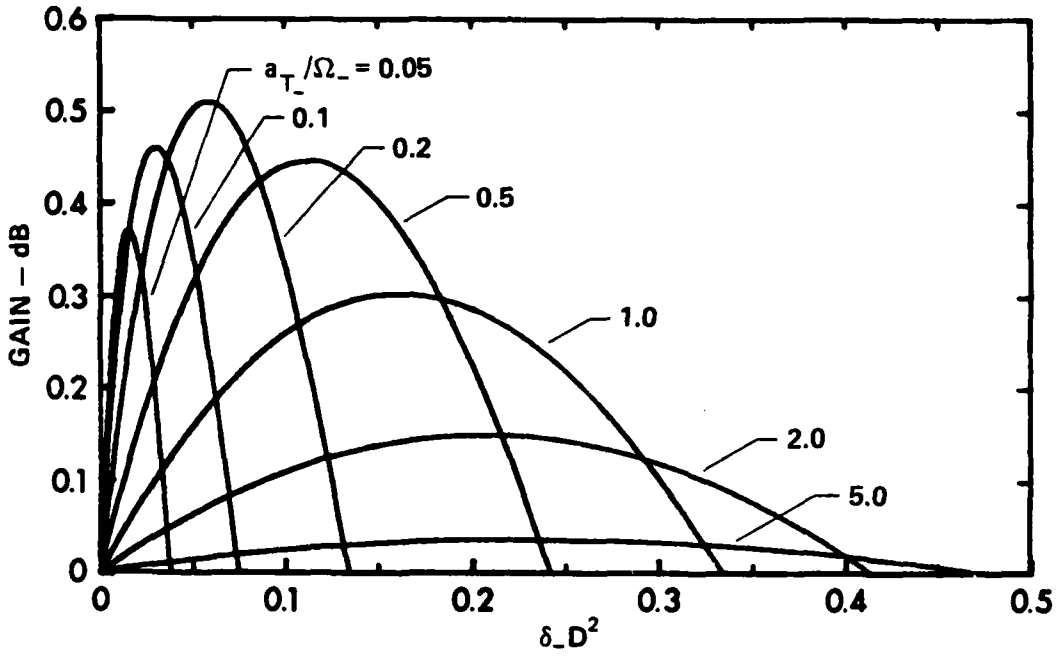

(a) Ranges of δ_D^2 Where Gain Occurs.

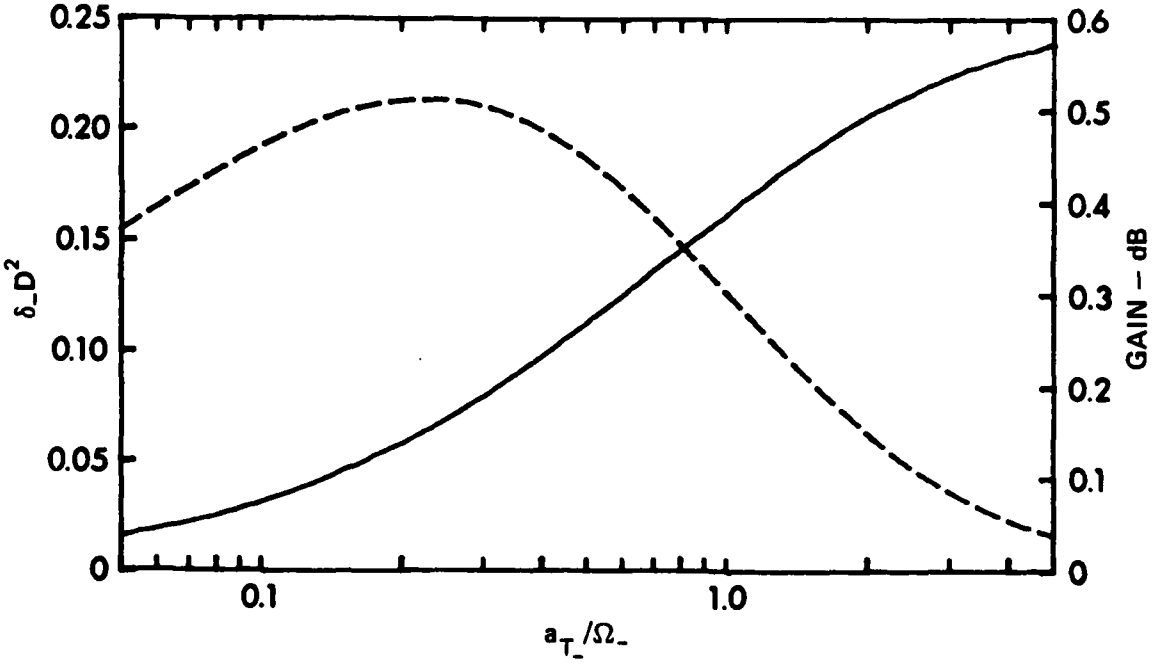

(b) Optimal Values of δ_D^2 as a Function of $a_{T\_}/\Omega\_$ (solid line), and Resulting Gain (Dashed Line).

Figure 14. Gain Achieved in Axial Difference-Frequency Farfield by Using Dispersion to Compensate for Phase Mismatch Caused by Diffraction.

AS-83-713

Either by performing the same limiting procedure on Equation (4.12) or else using Equations (4.11) and (4.13) to expand Equation (4.37), we obtain

$$p_-(\theta,Z) \sim i\Omega_- D^2 P_o \frac{e^{-a_- Z}}{Z} \exp\{-\Omega_-^2 D^2\theta^2/2 - i\Omega_- D^2 Z\theta^2\}$$

$$\cdot \sum_{n=-\infty}^{\infty} \exp\{-(4 + \Omega_-^2)D^2\theta^2\} I_n\{(4 + \Omega_-^2)D^2\theta^2\}$$

$$\cdot \exp\{2D^2[(1 + \Omega_-^2/4)\theta^2 - 2\delta] - i2a_T/\Omega_-\}$$

$$\cdot E_{1-n}\{2D^2[(1 + \Omega_-^2/4)\theta^2 - 2\delta] - i2a_T/\Omega_-\} \quad , \quad Z \to \infty \quad . \tag{4.38}$$

For an absorption-limited array, where $2a_T/\Omega_- \gg 1$, Equations (4.37) and (4.38) reduce to

$$p_-(\theta,Z) \sim -\frac{\Omega_-^2 D^2 P_o}{2a_T} \frac{e^{-a_- Z}}{Z} D_a(\theta) e^{-i\Omega_- D^2 Z\theta^2} \quad , \quad Z \to \infty \quad , \quad 2a_T/\Omega_- \gg 1 \, , \tag{4.39}$$

where

$$D_a(\theta) = \frac{\exp\{-\Omega_-^2 D^2\theta^2/2\}}{1 + i(\Omega_- D^2/a_T)(\theta^2 - 2\delta)} \quad , \tag{4.40}$$

and where, as usual, it has been assumed that $\Omega_-^2 \ll 1$. Equation (4.39) can be obtained from Equation (4.38) by assuming that $2a_T/\Omega_- \gg |n|$ as $|n| \to \infty$ so that Equation (4.14) can be used for all values of n, after which the identity

$$\sum_{n=-\infty}^{\infty} I_n(x) = e^x$$

is employed, which is obtained by setting $t = 1$ in Equation (4.11). However, numerical evaluation reveals that Equations (4.37) and (4.38) converge quite rapidly to Equation (4.39) as $2a_T/\Omega_-$ becomes large compared to unity. In Appendix G, a different limiting procedure is used which also leads to Equation (4.39). Although Novikov[9] obtained results which are similar to both Equations (4.37) and (4.39), the sign of his dispersion parameter is consistently wrong. In fact, the mistake is introduced in his governing inhomogeneous paraxial wave equation.

Note that Equation (4.39) is identical to Equation (2.33), which was derived under the assumption that the primaries do not experience diffraction. Such a result is to be expected because in an absorption-limited array, dissipation restricts nonlinear interaction to the nearfield of the primaries. Conditions are thus created which approximate collimated plane-wave interaction. The normalized aperture factor $A(\theta)$ in Equation (4.40) is

$$A(\theta) = e^{-\Omega_-^2 D^2 \theta^2/2}, \qquad (4.41)$$

which is a manifestitation of Gaussian primary beams. Equation (4.41) is the directivity function of a difference-frequency signal radiated by a source having an excitation formed by the product of two Gaussian primary excitations, i.e., $e^{-2\xi^2}$. On the basis of Figure 8, the factor factor

$$e^{-i\Omega_- D^2 Z\theta^2} \tag{4.42}$$

in Equation (4.39) can be identified as the phase factor which accounts for the spherical shape of the difference-frequency wave. Finally, since in the paraxial region $\theta/2$ may be replaced by $\sin(\theta/2)$, we have

$$\frac{1}{1 + i(\Omega_- D^2/a_T)(\theta^2 - 2\delta)} \simeq \frac{1}{1 + i(4\Omega_- D^2/a_T)[\sin^2(\theta/2) - \delta/2]} = D_\delta^W(\theta) \quad , \tag{4.43}$$

where $D_\delta^W(\theta)$ is the modified Westervelt directivity function which is defined in Equation (2.31). The similarity between our absorption-limited array and collimated plane-wave interaction, which gives rise to Equation (2.33), is thus complete.

In general, the normalized aperture factor for a difference-frequency signal is close to unity throughout the paraxial field. For example, if $\Omega_- = 0.1$ and $D = 30$, then Equation (4.41) accounts for attenuation of less than 3 dB at $\theta = 15°$. On the other hand, when there is no dispersion, we find from Equation (4.43) that the half-power point is located at

$$\theta = \frac{1}{D}\sqrt{\frac{a_T}{\Omega_-}} \quad ,$$

which is 6° for $a_T = 1.0$, $\Omega_- = 0.1$, and $D = 30$. Half-power angles derived from Equation (4.43) when $\delta \neq 0$ are given in Equation (2.37). As attenuation of the primaries increases, the

directivity function of the difference-frequency signal thus approaches $D_\delta^W(\theta)$, from which the direction of maximum radiation is found to be

$$\theta_o = \sqrt{2\delta} \tag{4.44}$$

or, equivalently,

$$\theta_o = \cos^{-1}\left(\frac{k_1 - k_2}{k_-}\right) \quad ,$$

as given in Equation (2.36). When $\delta < 0$, Equation (4.44) is replaced by $\theta_o = 0$. The detailed discussion of $D_\delta^W(\theta)$ in Section 2.3 therefore applies to the limiting case of an absorption-limited array formed by Gaussian primary beams.

In contrast to an absorption-limited array, a diffraction-limited array is one in which dissipation is low and the nonlinear interaction region is terminated because of spreading losses suffered by the primaries. Such a situation arises when $a_T' \to 0$, and as shown in Appendix E, the farfield of a diffraction-limited array is given by

$$p_-(\theta,Z) \sim i\Omega_- D^2 P_o \frac{e^{-a_- Z}}{Z} \exp\{-4\delta D^2 - i2a_T/\Omega_-\} E_1\{-4\delta D^2 - i2a_T/\Omega_-\}$$

$$\cdot D_d(\theta) e^{-i\Omega_- D^2 Z\theta^2} \quad , \quad Z \to \infty \quad , \quad |2a_T'/\Omega_-| << 1 \quad , \tag{4.45}$$

where

$$D_d(\theta) = e^{-(\Omega_1^2 + \Omega_2^2)D^2\theta^2} \quad . \tag{4.46}$$

Here we find that the directivity function, $D_d(\theta)$, is simply the product of the primary-beam directivity functions [see Equation (4.5)].

The directivity functions given in Equations (4.40) and (4.46) are consistent with the results obtained first by Blue[50] and subsequently generalized by Berktay and Leahy.[14] By clever manipulation of the field integral, it was shown that if nonlinear interaction is assumed to take place in the farfield of the primaries, then the directivity function of the difference-frequency signal is given essentially by the convolution

$$[D_1(\theta)D_2(\theta)] * D_\delta^W(\theta) \quad , \tag{4.47}$$

where $D_j(\theta)$ is given in Equation (4.5). When the primaries are highly collimated, $D_1(\theta)D_2(\theta)$ approaches a delta function, and Equation (4.47) yields $D_\delta^W(\theta)$. The lack of an aperture factor is a consequence of neglecting interaction in the nearfield of the primaries. On the other hand, as $a_T \to 0$, $D_\delta^W(\theta)$ assumes the form of a delta function, and Equation (4.47) yields $D_1(\theta)D_2(\theta)$. The conclusion to be drawn is that the directivity of the difference-frequency signal is at best only as good as that given by either the product of the primaries or the Westervelt result, whichever is less directional.

In Figure 15 is presented the directivity patterns obtained from Equations (4.37) and (4.38) for the same parameters as in Figure 10. Here the directivity function is defined as

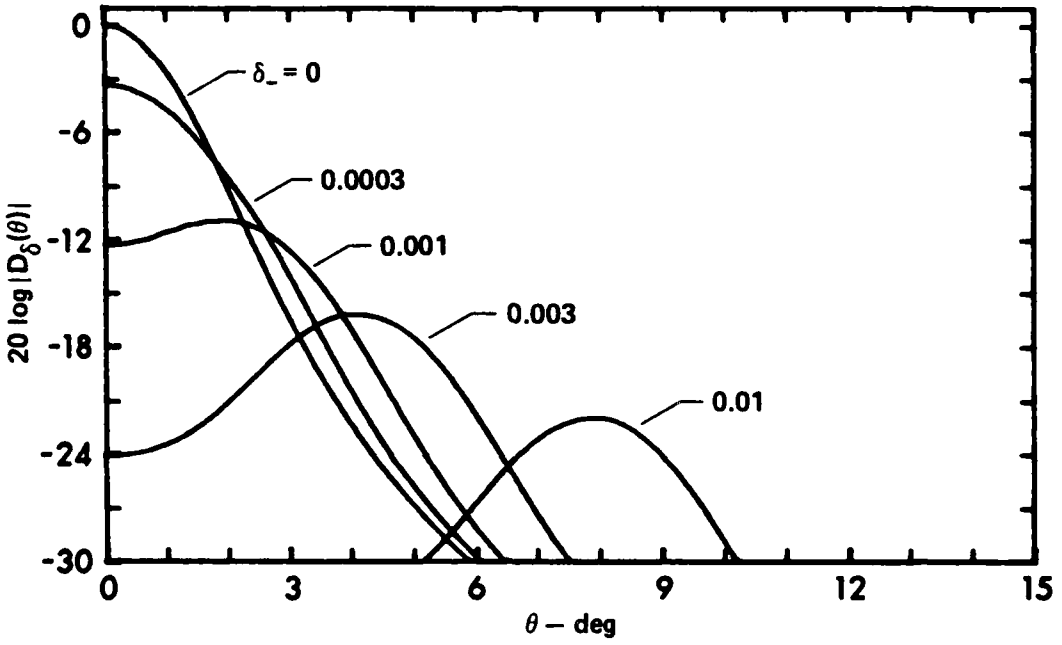

(a) $a_{T_-} = 0.01$

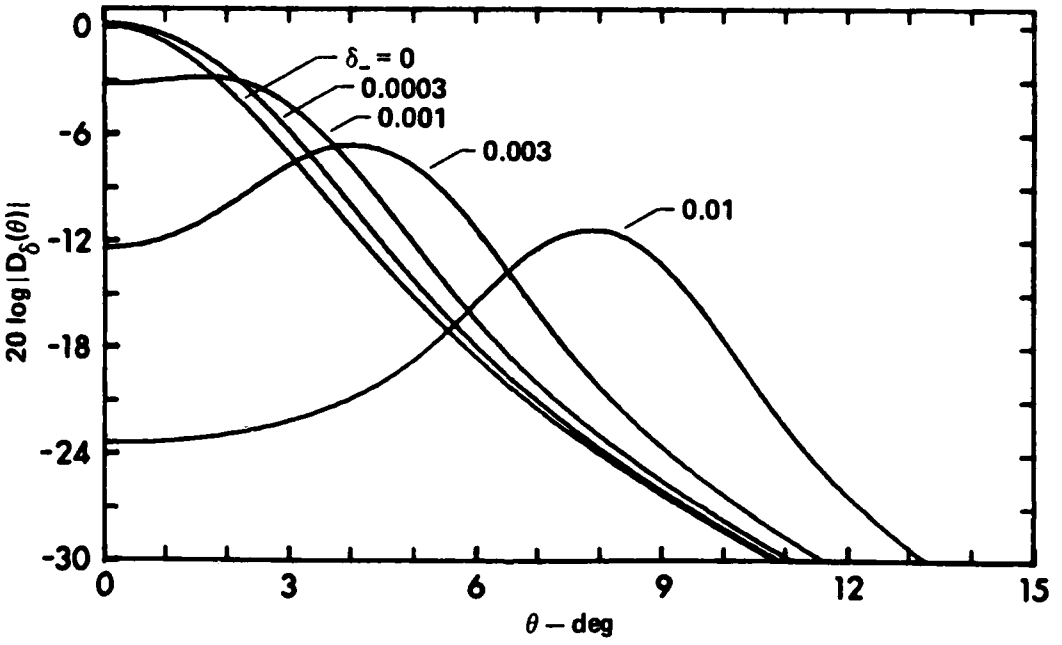

(b) $a_{T_-} = 0.1$

Figure 15. Effect of Dispersion on the Difference-Frequency Field Directivity Pattern ($\Omega_- = 0.1$, $D = 30$).

AS-83-714

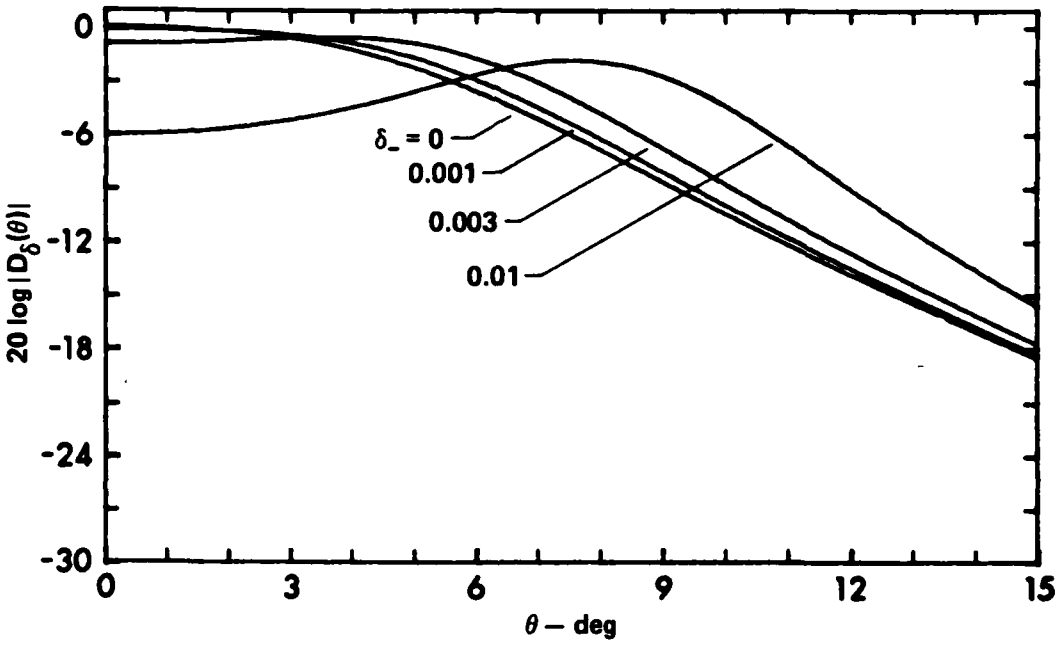

(c) $a_{T_-} = 1.0$

Figure 15. (continued)

AS-83-715

$$D_\delta(\theta) = \lim_{Z\to\infty} \frac{p_-(\theta,Z;\delta)}{p_-(0,Z;0)} \quad . \tag{4.48}$$

Note that this is not the conventional definition for a directivity function, where in the denominator, δ would not ordinarily be set equal to zero. By comparing the farfield pressure to the maximum farfield pressure obtained when there is no dispersion (which is at $\theta = 0$), we emphasize the effect of variations in δ. Equation (4.48) is therefore not a true directivity function in the sense that when $\delta \neq 0$, the maximum value of $|D_\delta(\theta)|$ is in general not equal to unity. In fact, when δD^2 and a_T/Ω_- are related as in Figure 14b, there are values of θ for which $|D_\delta(\theta)| > 1$. To calculate $D_\delta(\theta)$, it is more efficient to use Equation (4.38) rather than Equation (4.37). However, as discussed in Appendix B, for low absorption when $4D^2\theta^2 > 1$ and $\theta^2 \simeq 2\delta$, the series in Equation (4.38) converges very slowly and Equation (4.37) must be used. Finally, we note that

$$D_\delta(\theta) \sim \exp\{-\Omega_-^2 D^2\theta^2/2 - i\Omega_- D^2 Z\theta^2\} D_\delta^W(\theta) \quad , \quad 2a_T/\Omega_- >> 1 \quad ,$$

$$\sim \exp\{-2D^2\theta^2 - i\Omega_- D^2 Z\theta^2\} \quad , \quad |2a_T'/\Omega_-| << 1 \quad ,$$

since $\Omega_1^2 + \Omega_2^2 \simeq 2$.

Referring now to Figure 15a, we observe two salient effects of dispersion on the farfield directivity patterns. First, there is attenuation not only on axis, but also at the maximum in the directivity pattern. Second, for reasons that were discussed in Section 2.3, the direction of maximum radiation, θ_o, is shifted off

axis. In fact, for large values of δ, we find that θ_o approaches $\sqrt{2\delta}$, which is the angle predicted for an absorption-limited array. This is because in a dispersion-limited array, as in an absorption-limited array, significant energy transfer due to nonlinear interaction is confined to the nearfield of the primaries where the conditions for collimated plane-wave interaction are approximately satisfied.

As absorption increases, the maxima asymptotically approach levels given by $\exp\{-\Omega_-^2 D^2 \theta_o^2/2\}$, and Equation (4.39) becomes applicable. However, as seen in Figure 15c, the radiation pattern then becomes so broad that the locations of the off-axis maxima are hard to identify. In other words, when absorption becomes high enough that $|\delta| < a_T/2\Omega_- D^2$ (i.e., $|\delta| < \alpha_T/k_-$), then as noted in Section 4.2, the effects of dispersion may, for all practical purposes, be neglected. It is interesting to note again that (e.g., where $\delta = 0.0003$ in Figure 15b) because of diffraction, it is possible for dispersion to increase the efficiency of nonlinear interaction. In Figure 16 is presented a comparison of directivity patterns for anomalous and normal dispersion. Because of diffraction, the axial amplitudes in Figures 16a and 16b are not the same, in contrast to the results in Figure 6.

Evolution of the farfield radiation patterns is dramatically illustrated in Figures 17a-17c, which are three-dimensional field plots calculated by using Equation (4.10). When there is no dispersion, as in Figure 17a, resonance is achieved within the nonlinear interaction zone, and therefore constructive reinforcement of the difference-frequency signal occurs, which results in the end-fire radiation pattern. In contrast, for $\delta \neq 0$, it is seen from Figures 17b and 17c

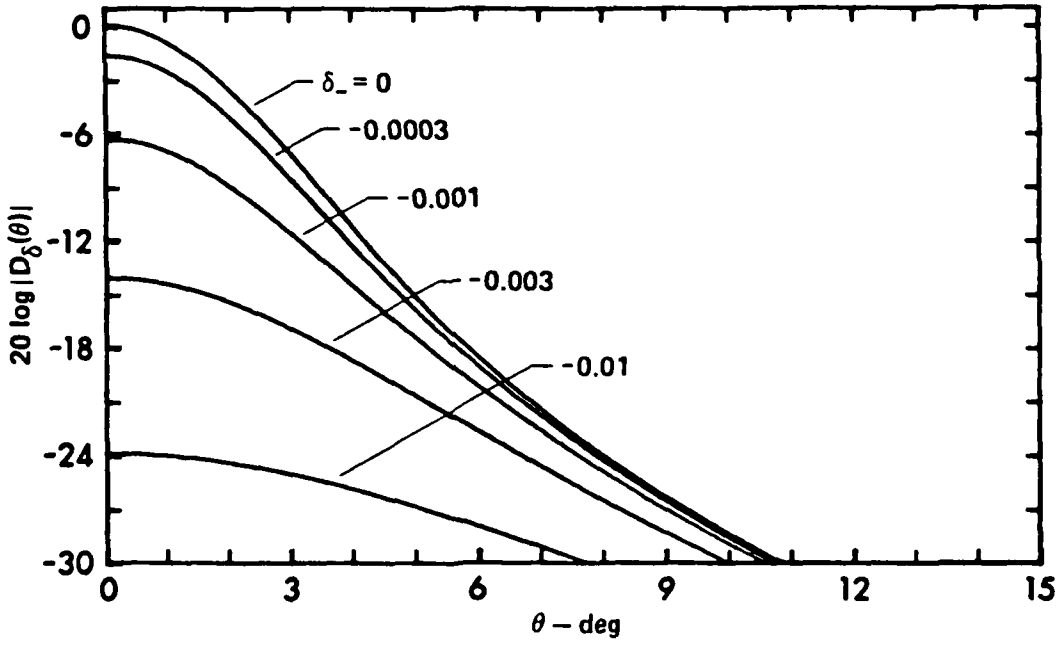

(a) Anomalous Dispersion

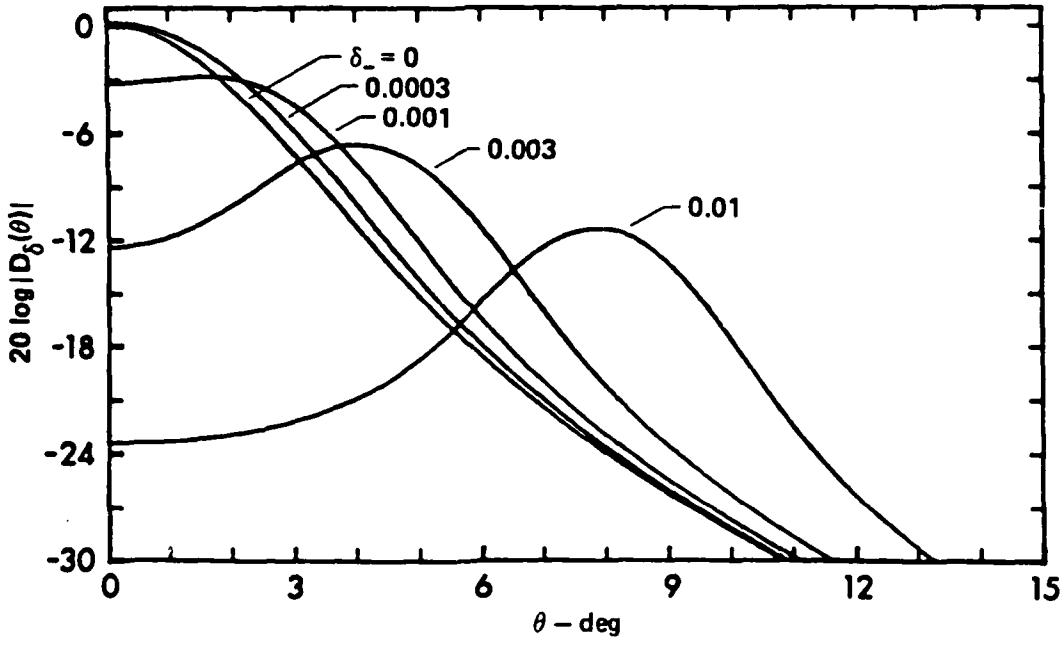

(b) Normal Dispersion

Figure 16. Effect of Anomalous ($\delta < 0$) Versus Normal ($\delta > 0$) Dispersion on the Difference-Frequency Field Directivity Pattern ($\Omega_- = 0.1$, $D = 30$).

AS-83-716

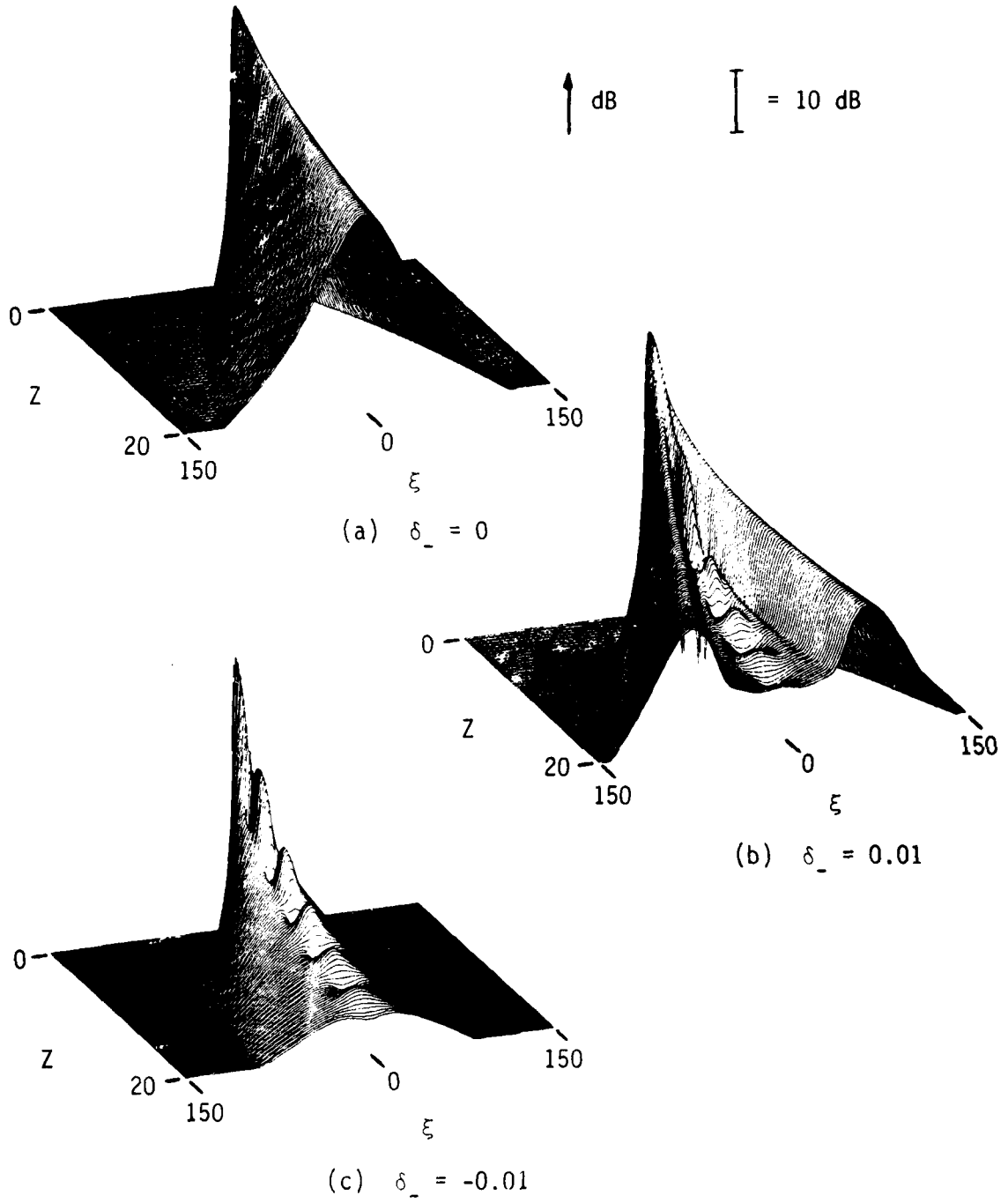

Figure 17. Effect of Dispersion on Difference-Frequency Pressure Field Resulting from Interaction of Gaussian Beams ($\Omega_- = 0.1$, $D = 30$, $a_{T_-} = 0.1$)

AS-83-717

that synchronism conditions are not realized within the nonlinear interaction region. The interaction region is clearly defined by the resulting spatial oscillations. For normal dispersion ($\delta > 0$), Figure 17b displays the radiation of a free difference-frequency wave from the interaction region. Referring now to Figure 17c, we see that for anomalous dispersion ($\delta < 0$), evanescent radiation outside of the interaction zone contributes virtually nothing to the difference-frequency field.

4.4 Sum-Frequency Field

Rewriting Equation (4.16), we obtain for the sum-frequency field

$$P_+(\xi,Z) = -2D^2P_o \frac{e^{-a_+Z}}{1 - iZ} \exp\{4\delta_+D^2 + ia_{T_+} - \frac{2\xi^2}{1 - iZ}\}$$

$$\cdot [E_1\{4\delta_+D^2 + ia_{T_+}\} - E_1\{(4\delta_+D^2 + ia_{T_+})(1 - iZ)\}] \quad , \tag{4.49}$$

where

$$a_{T_+} = a_1 + a_2 - a_+$$

and

$$\delta_+ = 1 - \frac{k_1 + k_2}{k_+} \quad ,$$

and where we let

$$c_o = c_+ \quad ,$$

so that $a'_+ = a_+$. As discussed in Section 4.1, Equation (4.49) is easily modified for application to the second-harmonic fields. Henceforth in this section, when Equation (4.49) is discussed with respect to the second harmonic, it is assumed that the necessary

modifications have been made. To the best of this author's knowledge, Equation (4.49) is a new result even when dispersion is neglected. This is rather remarkable considering the number of solutions of Equation (3.1) which have been published for the difference frequency. When $a'_{T_+} = 0$, Equation (4.49) reduces to the result obtained by Rudenko, Soluyan, and Khokhlov[51] for the second harmonic. Also, the solution for the second harmonic resulting from plane-wave propagation in a relaxing fluid was obtained by Polyakova.[52] However, it appears that no existing solutions account for dissipation, dispersion, and diffraction.

In contradistinction to the case of p_-, for which α_{T_-} is always positive, it is possible for α_{T_+} to be negative. In fact, although α_{T_+} may be positive or negative, it is usually negative. For the purpose of the discussion that follows, we shall assume the attenuation coefficient depends on frequency according to the relation

$$\alpha_\omega \propto \omega^n \quad . \tag{4.50}$$

Therefore, α_{T_+} is negative when $n > 1$, and it is positive when $n < 1$.

Depending on whether a_{T_+} is positive or negative, Equation (4.49) yields one of two different expressions for the farfield. When $n > 1$ in Equation (4.50) so that $a_{T_+} < 0$, Equation (4.49) reduces to

$$p_+(\theta,Z) \sim \frac{i2D^2P_o}{a_{T_+}-i4\delta_+D^2}\,\frac{e^{-(a_1+a_2)Z}}{Z^2}\exp\{-2D^2\theta^2-i2D^2Z\theta^2\}\ ,\quad Z\to\infty\ ,\quad a_{T_+}<0\ , \tag{4.51}$$

where ε has been replaced by $z\theta$. Likewise, when $n < 1$ and therefore $a_{T_+} > 0$, Equation (4.49) becomes

$$p_+(\theta,Z) \sim -i2D^2P_o\frac{e^{-a_+Z}}{Z}\exp\{4\delta_+D^2 + ia_{T_+}\}E_1\{4\delta_+D^2 + ia_{T_+}\}$$

$$\cdot \exp\{-2D^2\theta^2 - i2D^2Z\theta^2\} \quad , \quad Z \to \infty \quad , \quad a_{T_+} > 0 \; . \quad (4.52)$$

The salient difference between Equations (4.51) and (4.52) is that when $a_{T_+} < 0$, p_+ decays as $Z^{-2}e^{-(a_1+a_2)Z}$, whereas when $a_{T_+} > 0$, p_+ decays as $Z^{-1}e^{-a_+Z}$. An explanation of this phenomenon was given by Webster and Blackstock,[29] but since their discussion has not been published, we repeat it here. The heart of the analysis is based on the concept of virtual sources. Specifically, it matters whether the virtual sources (i.e., the particular solution) decay faster or slower with distance than the freely propagating component (i.e., the homogeneous solution) of the nonlinearly generated signal. Because the virtual source strength is determined by the product of the primary wave fields, its decay in the farfield is given by $Z^{-2}e^{-(a_1 + a_2)Z}$. On the other hand, a small-signal wave having frequency ω_+ (i.e., the free wave) decays as $Z^{-1}e^{-a_+Z}$.

We first consider the case where $a_{T_+} < 0$, i.e., $a_+ > a_1 + a_2$. At any arbitrary point in the field, the sum-frequency wave is formed by the addition of the signals radiated by all of the virtual sources between that observation point and the projector. At great distances, however, when $a_+ > a_1 + a_2$, the signals that were radiated by virtual sources near the projector will have suffered more attenuation

than did the actual virtual sources which are close to the observation point. As a result, far away from the projector, the radiation from neighboring virtual sources always exceeds the radiation from virtual sources which are closer to the projector. In other words, the particular solution is much more important than the homogeneous solution at sufficiently great distances. This explains why Equation (4.51) describes p_+ decaying at the same rate as the virtual sources, that is, as $Z^{-2}e^{-(a_1 + a_2)Z}$. Also, that the sum-frequency wave propagates according to the wave number $k_1 + k_2$ rather than k_+ is another manifestation of the particular solution. Thus, it may be said that when $a_{T_+} < 0$, there is no farfield for the sum frequency in the sense that p_+ never behaves as a small-signal wave of frequency ω_+.

When $a_{T_+} > 0$, i.e., $a_+ < a_1 + a_2$, the preceding argument is reversed. Now the radiation from virtual sources near the projector exceeds the contribution from those in the farfield. The homogeneous solution thus outlasts the particular solution. In the farfield, p_+ therefore behaves as a small-signal wave and decays according to $Z^{-1}e^{-a_+Z}$, as shown by Equation (4.52). This, of course, is always the case for the difference-frequency signal, i.e., p_- decays as $Z^{-1}e^{-a_-Z}$ because we always have $a_- < a_1 + a_2$. Incidentally, one may thus identify the homogeneous and particular solutions in the general field integral given in Equation (4.9); they are the functions which arise from the evaluation of the integral at the lower and upper limits, respectively.

Of particular interest are the directivity functions in Equations (4.51) and (4.52). Specifically, we find that the directivity function is always given by

$$D_+(\theta) = e^{-2D^2\theta^2} \quad , \tag{4.53}$$

which is equivalent to the product of the primary-beam directivity functions when $\Omega_1 \simeq \Omega_2 \simeq 1$. As was first reported by Westervelt and Radue,[53] the directivity function of a second harmonic, under weak finite-amplitude conditions, is equal to the square of the directivity function of the fundamental. Subsequent generalization by Lockwood, Muir, and Blackstock[54] yielded the result that, under similar conditions, the directivity function of the nth harmonic is $D^n(\theta)$, where $D(\theta)$ is the directivity function of the fundamental.

A noticeable absence in the directivity functions of the second-harmonic and sum-frequency components is the Westervelt directivity function. When $a_{T_+} < 0$, the sum-frequency signal never escapes from the interaction region, and its directivity is therefore that of the virtual sources. However, a Westervelt function might be expected when $a_{T_+} > 0$. If the analysis in Section 2.3 is repeated for the second-harmonic and sum-frequency components, we obtain, when $a_{T_+} > 0$,

$$D_+^a(\theta) = \frac{\exp\{-2D^2\theta^2\}}{1 + i(2D^2/a_{T_+})(\theta^2 - 2\delta_+)} \tag{4.54}$$

for the directivity function of an absorption-limited array. Note that the normalized aperture factor in the numerator of Equation (4.54) is identical to Equation (4.53); i.e., the normalized aperture factor is equal to the product of the primary-beam directivity functions. One can easily demonstrate that, compared to the numerator, the denominator of Equation (4.54) depends very weakly on θ . In fact, the denominator contributes significantly to the directivity function only when a_{T_+} is extremely small, in which case a diffraction-limited array is obtained for which Equation (4.54) no longer applies. Thus, whether we have a diffraction- or an absorption-limited array, the directivity function for the second-harmonic and sum-frequency components is always given by Equation (4.53). This result is not surprising because, unlike the difference-frequency signal for which the wavelength is large compared to the width of the interaction region, that of the sum-frequency signal is small. Radiation of the sum-frequency signal from the interaction region therefore never appears as though it comes from a line array of point sources.

Recall that in obtaining Equations (4.16) and (4.49), we neglected various terms containing ξ^2 on the basis that $\Omega_1\Omega_2 \simeq 1$. The validity of this approximation may be evaluated by considering to what extent the directivity function is affected. Had we retained all of our terms, we would have discovered for an absorption-limited array the presence of a Westervelt-type directivity function, namely,

$$D(\theta) = \left\{ 1 + i \frac{2D^2}{a_{T_+}} \left[\left(1 - \frac{1}{\Omega_1\Omega_2} \right) \theta^2 - 2\delta_+ \right] \right\}^{-1} \quad . \qquad (4.55)$$

When $\Omega_1\Omega_2 \simeq 1$, Equation (4.55) exhibits significantly weaker dependence on θ than does the denominator of Equation (4.54), and our approximation thus appears to be justified. In light of the discussion in the preceding paragraph, it should not be surprising that Equation (4.55) and the denominator of Equation (4.54) are dissimilar. Since diffraction is accounted for by our wave equation and it was found, from physical considerations, that we cannot have a Westervelt directivity function for the second-harmonic and sum-frequency waves, we should not expect our results to yield Equation (4.54). Consequently, no shift should be expected in the direction of maximum radiation due to dispersion.

A typical family of curves that depicts the axial sum-frequency pressure field as given by Equation (4.49) is presented in Figure 18, where we have set $a_{T_+} = -a_+/2 < 0$ to represent a thermoviscous fluid. For normal dispersion, δ_+ is negative, while for anomalous dispersion, δ_+ is positive. Here the pressure is referred to $P_o e^{-(a_1 + a_2)Z}$ so that the exponential attenuation of the farfield pressure is factored out. In general, the discussion in Section 4.2 of the axial difference-frequency field applies to the axial sum-frequency field as well. For example, the effects of dispersion become significant only when $|\delta_+| > |a_{T_+}/4D^2|$, or equivalently when $|\delta_+| > |\alpha_{T_+}/k_+|$. Again, compensation for the phase mismatch caused by diffraction is achieved with normal $(\delta_+ < 0)$, not anomalous $(\delta_+ > 0)$, dispersion.

When $a_{T_+} < 0$, there is a most striking difference between the sum- and difference-frequency fields. Notice that in Figure 18, there is a region around $Z = 40$ where the nulls due to dispersion are

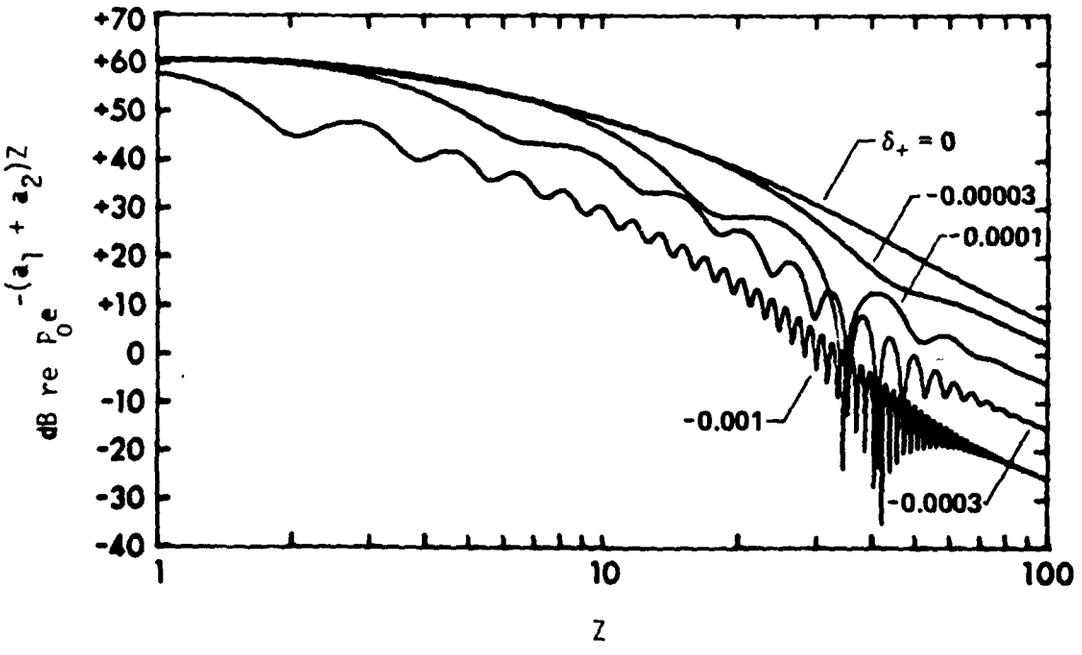

Figure 18. Effect of Dispersion on the Axial Sum-Frequency Field ($\Omega_- = 0.1$, $a_{T_+} = -0.1$, $a_+ = 0.2$, D = 30).

AS-83-718

deeper than anywhere else in the field. In the difference-frequency field, however, the relative amplitudes of oscillation always decrease with distance. The difference in behavior of the sum- and difference-frequency fields results from the decay rate of the virtual sources.

For example, Equation (2.18) gives the amplitude of the difference-frequency signal which results from dispersive plane-wave interaction. It is clear from Equation (2.18) that when $a_{T_-} \neq 0$, there is no place in the field where perfect cancellation can occur (compare Figures 1 and 3). Perfect cancellation occurs for plane-wave interaction, and reoccurs repeatedly with period $2\pi/|k_1 - k_2 - k_-|$, only when $a_{T_-} = 0$. When $a_{T_-} = 0$, we have $a_1 + a_2 = a_-$. Since there are no spreading losses, the virtual sources, which are determined by the product of the primaries, decay as $e^{-(a_1 + a_2)Z}$. Likewise, a freely propagating difference-frequency plane wave decays as e^{-a_-Z}, which is equal to $e^{-(a_1 + a_2)Z}$ when $a_{T_-} = 0$. Perfect cancellation of the difference-frequency plane wave is achieved whenever the virtual sources withdraw exactly the same amount of energy that they had previously pumped into the difference-frequency signal. This perfect balance occurs only when the attenuation of the virtual sources and of the free wave are identical.

When there are spreading losses, the decay rates are more complicated. In the farfield, the spreading losses are proportional to Z^{-2} for the virtual sources and Z^{-1} for the free sum-frequency wave. Thus, the rates of attenuation due to $Z^{-2}e^{-(a_1 + a_2)Z}$ and $Z^{-1}e^{-a_+Z}$ can never be the same at more than one point. In fact, for the difference frequency, where $a_- < a_1 + a_2$, the free wave decays

as $Z^{-1}e^{-a_- Z}$ in the farfield. This decay rate is always less than the decay rate of the virtual sources, i.e., $Z^{-2}e^{-(a_1 + a_2)Z}$. However, for the sum frequency where $a_+ > a_1 + a_2$, the decay rate of the free wave, given by $Z^{-1}e^{-a_+ Z}$, indeed matches that of the virtual sources at some point in the field. After the point where the decay rates match, the free wave thereafter decays faster than the virtual sources. Perfect cancellation does not necessarily occur at the location where the decay rates match. For perfect cancellation, the virtual sources must, in some interval, withdraw all of the remaining energy in the free wave before the relative phase between the two components reverses and the virtual sources begin pumping energy back into the free wave. Efficient cancellation of the free wave is thus more likely in the region where the decay curves cross. In fact, we find that the optimal location also depends on the amount of dispersion. Regardless, when $a_+ > a_1 + a_2$, conditions are such that the relative amplitudes of the spatial oscillations behave as in Figure 18. On the contrary, since we always have $a_- < a_1 + a_2$, a similar phenomenon does not occur in the difference-frequency field.

CHAPTER V

PARAMETRIC ARRAYS FORMED BY NONDIFFRACTING NONCOLLINEAR PRIMARY WAVES

By dispersion of sound is usually meant the dependence of the sound speed on frequency. When dispersion depends on inherent physical properties of the fluid, it is sometimes referred to as inherent dispersion. Examples of media which are inherently dispersive are relaxing fluids, bubbly liquids, two-phase media, and media subject to boundary layer effects. In Section 4.2, we discussed dispersion which was said to be diffraction-induced. Although it too exhibits a frequency dependence, the cause of diffraction-induced dispersion is the geometry of the source of radiation. Specifically, wavelets which arrive from different points on a source combine to form a wavefront which propagates at a speed that can be different from that of the individual wavelets. Because the direction from which each wavelet arrives is affected by diffraction, diffraction-induced dispersion must therefore exhibit a dependence on frequency. Sufficiently far away from any source of radiation, the wave field becomes spherical because of diffraction, so that diffraction-induced dispersion is manifested only in the nearfield.

Diffraction-induced dispersion may be regarded as a special case of geometric dispersion, which is a term often used to describe the trace speed of a wave. The trace speed is the phase speed of a wave along a direction which forms an arbitrary angle with the direction of propagation. For example, the trace speed along a

direction which forms an angle ϕ with the propagation direction of a plane wave is given by

$$c_{tr} = \frac{c}{\cos\phi} \quad , \tag{5.1}$$

where c is the propagation speed. Geometric dispersion is probably most well known in connection with the propagation of modes in waveguides.[55] Obviously, inherent and geometric dispersion are independent and can exist simultaneously. In Section 4.2 we showed that diffraction-induced dispersion can compensate for the effects of inherent dispersion. However, the amount of compensation was found to be insignificant and therefore of only academic interest. As seen from Equation (5.1), we can change the phase speed of the primaries along a particular direction by simply varying ϕ. Both this and the next chapter are devoted to an investigation of the use of geometric dispersion to compensate for inherent dispersion. In what follows, we shall refer to fluids exhibiting no inherent dispersion as dispersionless fluids, and to effects caused by noncollinear interaction as geometric dispersion.

The analysis in this chapter is simply an extension of that in Chapter II to the case of noncollinear interaction. In Section 5.1 we investigate the interaction region by way of an analysis of noncollinear infinite plane-wave interaction. Westervelt's analysis[1] is extended in Section 5.2 to encompass noncollinear interaction of collimated plane waves.

5.1 Interaction Region

In this section we consider noncollinear interaction of infinite plane waves where, for simplicity, we neglect both attenuation and variations in amplitude across the wavefronts. Both of these factors were included when we analyzed collinear interaction in Section 2.2, the discussion of which is easily extended to the analysis which follows.

We begin our analysis of infinite plane-wave interaction by rewriting Equation (2.4) as

$$\nabla^2 p_\omega + k_\omega^2 p_\omega = \frac{\beta\omega^2}{\rho_o c_o^4} Q_\omega \quad , \tag{5.2}$$

where $Q_\omega = p_\omega * p_\omega$. The first-order solution of Equation (5.2) for a plane wave propagating in an arbitrary direction is

$$p_\omega(\vec{r}) = p_0 e^{-i\vec{k}_\omega \cdot \vec{r}} \quad . \tag{5.3}$$

Combining Equations (5.2) and (5.3), we obtain the inhomogeneous wave equation for the difference-frequency field,

$$\nabla^2 p_- + k_-^2 p_- = \frac{\beta\omega_-^2}{\rho_o c_o^4} p_{01} p_{02} e^{-i(\vec{k}_1 - \vec{k}_2)\cdot\vec{r}} \quad . \tag{5.4}$$

The virtual-source distribution represented on the right-hand side of Equation (5.4) resembles a plane wave of frequency ω_- which is propagating in the direction of $\vec{k}_1 - \vec{k}_2$ at speed $\omega_-/|\vec{k}_1 - \vec{k}_2|$. Equation (5.4) is therefore a one-dimensional plane-wave problem of

the type which was considered in Section 2.2. In fact, if we employ a new axis, η, which is collinear with $\vec{k}_1 - \vec{k}_2$ as shown in Figure 19, we may rewrite Equation (5.4) as

$$\left(\frac{\partial^2}{\partial\eta^2} + k_-^2\right) p_-(\eta) = \frac{\beta\omega_-^2}{\rho_o c_o^4} p_{01} p_{02} e^{-i|\vec{k}_1 - \vec{k}_2|\eta} , \qquad (5.5)$$

because by definition, we have

$$(\vec{k}_1 - \vec{k}_2)\cdot\vec{\eta} = |\vec{k}_1 - \vec{k}_2|\eta \quad .$$

The solution of Equation (5.5) is

$$p_-(\eta) = \frac{i2\beta\omega_-^2 p_{01} p_{02}}{\rho_o c_o^4} \frac{\sin[(|\vec{k}_1 - \vec{k}_2| - k_-)\eta/2]}{|\vec{k}_1 - \vec{k}_2|^2 - k_-^2} e^{-i(|\vec{k}_1 - \vec{k}_2| + k_-)\eta/2} . \qquad (5.6)$$

Equation (5.6) is formally equivalent to Equation (2.19), and the discussion following the latter thus applies to Equation (5.6) as well. Specifically, the difference-frequency signal given by Equation (5.6) is a plane wave propagating in the direction of $\vec{k}_1 - \vec{k}_2$. The amplitude of the signal experiences spatial beating of period

$$\lambda_q = \frac{2\pi}{|\vec{k}_1 - \vec{k}_2| - k_-} , \qquad (5.7)$$

where λ_q is the distance over which the phase of the virtual sources relative to that of a freely propagating difference-frequency signal passes through 360°. From Equation (5.7), we deduce that resonant interaction, which occurs when there is phase matching, is possible only when

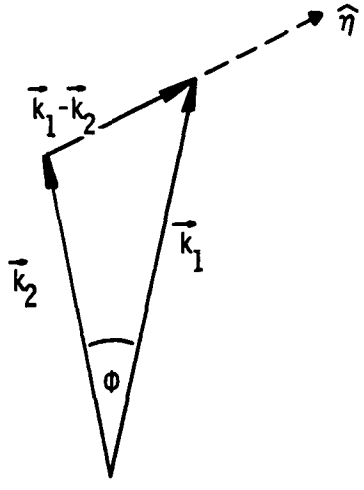

Figure 19. Geometry for Noncollinear Interaction of Two Plane Waves.

$$|\vec{k}_1 - \vec{k}_2| = k_- \quad . \tag{5.8}$$

Because the difference-frequency signal travels in the direction of $\vec{k}_1 - \vec{k}_2$, we have

$$\vec{k}_- \cdot \vec{\eta} = k_- \eta \quad ,$$

so that we may rewrite Equation (5.8) in more general notation as

$$\vec{k}_1 - \vec{k}_2 = \vec{k}_- \quad . \tag{5.9}$$

A three-wave interaction in which momentum is conserved must satisfy Equation (5.9). Likewise, the conservation of energy requires

$$\omega_1 - \omega_2 = \omega_- \quad . \tag{5.10}$$

Equations (5.9) and (5.10) together constitute the necessary and sufficient conditions for resonant interaction.[56] Finally, we may define a new dispersion coefficient, which accounts for both inherent and geometric dispersion, as

$$\delta_\phi = 1 - \frac{|\vec{k}_1 - \vec{k}_2|}{k_-} \quad ,$$

where δ_ϕ is a function of the angle of intersection. When $\phi = 0$, δ_ϕ reduces to δ, where δ is given as usual by Equation (2.20).

If ϕ is the angle formed by $\vec{k}_1$ and $\vec{k}_2$, then

$$|\vec{k}_1 - \vec{k}_2| = \sqrt{k_1^2 + k_2^2 - 2k_1k_2\cos\phi} \quad . \tag{5.11}$$

Combining Equations (5.8) and (5.11) to solve for the phase-matching angle ϕ_o, we obtain

$$\phi_o = 2 \sin^{-1} \sqrt{\frac{k_-^2 - (k_1 - k_2)^2}{4k_1k_2}} \quad . \tag{5.12}$$

Phase matching of plane waves can therefore be accomplished via geometric dispersion only when

$$k_1 - k_2 \leq k_- \quad , \tag{5.13}$$

which is a condition satisfied by fluids exhibiting normal dispersion, that is, $c_1 \geq c_2 > c_-$. When $k_1 - k_2 = k_-$, Equation (5.12) yields $\phi_o = 0$ as required.

A very graphic representation of the difference-frequency field resulting from noncollinear interaction of two plane waves having nearly equal wave numbers is given by Zverev and Kalachev,[57,58] and is reproduced[58] in Figure 20. The justification for using Figure 20 to represent the difference-frequency field within the interaction region is based on Equation (5.7), which we can rewrite in terms of wavelengths as

$$\lambda_q = \frac{\lambda_1\lambda_2}{\sqrt{\lambda_1^2+\lambda_2^2 - 2\lambda_1\lambda_2\cos\phi} - \lambda_1\lambda_2/\lambda_-} \quad . \tag{5.14}$$

If the intersecting plane waves depicted in Figure 20 have the same wave number and therefore the same wavelength, λ , it can be shown quite easily that the distance between adjacent Moiré bands is given by

$$\lambda_q = \frac{\lambda}{2 \sin(\phi/2)} \quad , \quad \lambda_1 = \lambda_2 \quad . \tag{5.15}$$

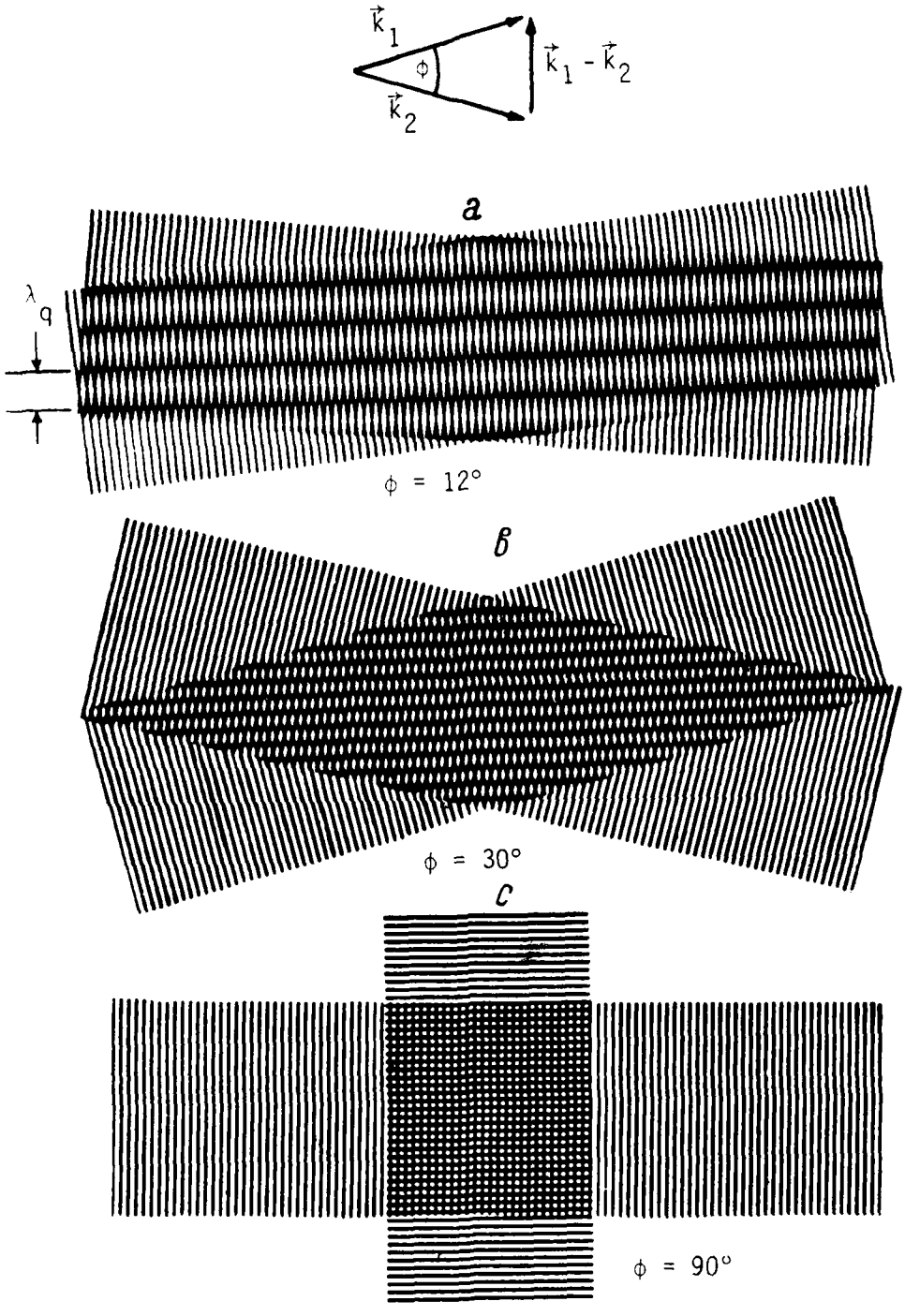

Figure 20. Representation of Difference-Frequency Field Resulting from Noncollinear Interaction of Two Plane Waves Having Nearly Equal Wave Numbers

As $\lambda_1 \to \lambda_2 = \lambda$, $\lambda_- \to \infty$, and Equation (5.14) reduces to Equation (5.15). Thus, when $\lambda_1 \simeq \lambda_2$, the Moiré bands in Figure 20 indeed represent the amplitude of the difference-frequency field, because the bands are separated according to the period of spatial oscillation given in Equations (5.7) and (5.14). The centers of the light bands may be interpreted as maxima in the difference-frequency field, and the centers of the dark bands may be interpreted as nulls (for comparison, see Figure 1).

The difference-frequency signal propagates in the direction of $\vec{k}_1 - \vec{k}_2$, which is perpendicular to the line of symmetry between $\vec{k}_1$ and $\vec{k}_2$ when $k_1 \simeq k_2$. This explains the orientation of the Moiré bands in Figure 20. When $\phi = 0$, there is no geometric dispersion so that in the absence of inherent dispersion, $\lambda_q = \infty$, and the difference-frequency signal grows linearly with range. Increasing ϕ causes λ_q to decrease. Aside from the direction of propagation of the difference-frequency signal, the net result is therefore identical to that obtained by increasing inherent dispersion in the collinear interaction of plane waves. In fact, when there is no inherent dispersion, δ_ϕ reduces to

$$\delta_\phi = 1 - \sqrt{1 + 4 \frac{k_1 k_2}{k_-^2} \sin^2(\phi/2)} \quad , \quad k_1 - k_2 = k_- \quad ,$$

where in this case, $\delta_\phi \leq 0$. When the length of the interaction region along the direction of $\vec{k}_1 - \vec{k}_2$ is longer than $\lambda_q/2$, energy transfer to the difference-frequency signal becomes extremely

inefficient. Recently, TenCate[59] reported results for wave interaction in a rectangular waveguide which indisputably support Equation (5.7).

In light of the above discussion, it is surprising how much attention has been devoted to the phenomenon first referred to by Ingard and Pridmore-Brown[60] as the scattering of sound by sound. The usual connotation of the scattering of sound by sound refers to radiation of sum- and difference-frequency signals from the interaction region formed by two primary beams which intersect at an arbitrary angle. When there is no inherent dispersion, we see clearly from Figure 20 that even small angles of intersection can cause asynchronous conditions. For large angles of intersection, we therefore expect only insignificant levels of radiation from the interaction region. In 1956, Ingard and Pridmore-Brown[60] reported results from a theoretical and experimental investigation of the sum- and difference-frequency signals radiated from the interaction region formed by two sound beams intersecting at 90°. Using Lighthill's[23] acoustic analog equation, they derived predictions for the levels of the scattered signals which exceeded their measured levels by about 10 dB. Discussion in the literature regarding both the theoretical model and experimental procedure employed by Ingard and Pridmore-Brown continues to this day, detailed accounts of which are given by Beyer[61] and Fenlon.[62] By far the most fruitful response was that of Westervelt,[63,64] whose series of papers on the subject led to his discovery in 1960[22] of the parametric array. Indeed, Equation (5.12) indicates that resonant interaction in a dispersionless fluid is possible only with collinear interaction. In context, it is therefore somewhat ironic that the

parametric array was belatedly conceived as a special case of the scattering of sound by sound.

To conclude this section, we consider the validity of using Equation (2.1) for the problem of noncollinear interaction. This question of validity arises because the form of the nonlinear term in Equation (2.1) was obtained subject to restrictions consistent with use of the plane-wave impedance relation. We therefore derive an inhomogeneous wave equation, for the specific case of noncollinear interaction of two infinite plane waves, where all second-order terms are retained. As shown in Appendix F, an equation is obtained for both the sum and difference frequencies, which is identical in form to Equation (5.4), but where β is replaced by

$$\beta_{\pm}(\phi) = \frac{B}{2A} + \cos\phi \pm 4 \frac{\omega_1\omega_2}{\omega_{\pm}^2} \sin^4(\phi/2) \quad . \tag{5.16}$$

Equation (5.16) is a modified coefficient of nonlinearity, which for collinear interaction reduces to $\beta_{\pm} = 1 + B/2A$.

The extent to which Equation (5.16) differs from $\beta_{\pm} = 1 + B/2A$ indicates how appropriate it is to use Equation (2.1) in an analysis of noncollinear interaction. We first consider the physical significance of each term in Equation (5.16). The first term represents the nonlinearity in the equation of state relating the pressure and density. If the acoustic pressure and density were related linearly by $p = c_o^2\rho$, the first term would disappear. The second term in Equation (5.16) represents convection. Because of the finite amplitude of the particle velocity, a small current is set in motion by the passage of the sound

wave. Since we are considering two waves which are propagating in different directions, the particle velocities add vectorially, and the convection therefore depends on the angle of intersection. At this time, the physical significance of the third term in Equation (5.16) is uncertain. Experimental results which support the angular dependence of the second term in Equation (5.16) have been reported recently by TenCate,[59] while verification of the third term was not possible because of the nature of his experiment. In any event, we are concerned with intersection angles of only a few degrees. Use of Equation (2.1) for noncollinear interaction is therefore justified insofar as the deviation of Equation (5.16) from $\beta_{\pm} = 1 + B/2A$ is small.

5.2 Farfield of the Parametric Array

Here we extend the analysis in Section 2.3 to encompass noncollinear interaction of nondiffracting, collimated primary beams. Specifically, we assume the primaries are given by

$$p_j(x,y,z) = f_j(x,y,z)\, e^{-i\vec{\chi}_j \cdot \vec{r}} \quad , \tag{5.17}$$

where $\chi_\omega = k_\omega - i\alpha_\omega$. The function $f(x,y,z)$, which is determined from the boundary condition, defines the pressure amplitude of the beam. Without loss of generality, we restrict the directions of $\vec{\chi}_1$ and $\vec{\chi}_2$ to the x-z plane. If the angles formed by $\vec{\chi}_1$ and $\vec{\chi}_2$ with the z axis are, respectively, ϕ_1 and ϕ_2 , then

$$\vec{\chi}_j \cdot \vec{r} = \chi_j z \cos\phi_j + \chi_j x \sin\phi_j \quad , \tag{5.18}$$

which for small ϕ_j is given approximately by

$$\vec{\chi}_j \cdot \vec{r} \simeq k_j z \cos\phi_j + k_j x \sin\phi_j - i\alpha_j z \quad . \tag{5.19}$$

We therefore write our boundary condition as

$$p_j(x,y,0) = P_j(x,y)\, e^{-ik_j x \sin\phi_j} \quad , \tag{5.20}$$

where $P_j(x,y)$ is the amplitude of the beam at $z = 0$. In other words, to steer a beam at an angle ϕ relative to the z axis in the x-z plane, a linear phase delay at the source given by $-kx \sin\phi$ is required. If we follow any ray which is parallel to such a beam, we find that the ray travels a distance $d \tan\phi$ in the x direction for each distance d traveled in the z direction. Combining Equations (5.17) and (5.20), we thus obtain

$$p_j(x,y,z) = P_j(x - z \tan\phi_j, y)\, e^{-i\vec{\chi}_j \cdot \vec{r}} \quad , \tag{5.21}$$

because of the assumption that there is no diffraction or spreading.

The solution of the inhomogeneous wave equation for the difference-frequency field is therefore given to a first approximation by

$$p_-(r,\theta_x,\theta_y) = \frac{\beta\omega_-^2}{4\pi\rho_o c_o^4} \int_{V'} \frac{e^{-i\chi_- |\vec{r} - \vec{r}'|}}{|\vec{r} - \vec{r}'|} \cdot P_1(x' - z' \tan\phi_1, y')\, P_2(x' - z' \tan\phi_2, y')\, e^{-i(\vec{\chi}_1 - \vec{\chi}_2^*)\cdot \vec{r}'}\, dV' \quad , \tag{5.22}$$

where V' is the volume of integration, and θ_x and θ_y are azimuthal angles in the x-z and y-z planes, respectively. Our coordinate system is defined by the relations

$$x = r \sin\theta_x \quad , \quad y = r \sin\theta_y \quad , \quad z = r \cos\theta \quad , \tag{5.23}$$

where

$$\sin^2\theta_x + \sin^2\theta_y = \sin^2\theta \quad . \tag{5.24}$$

The angle θ, which is formed by $\vec{r}$ and the z axis, is the same as that used in previous sections. We must now evaluate $|\vec{r} - \vec{r}'|$:

$$|\vec{r} - \vec{r}'| = \sqrt{(x - x')^2 + (y - y')^2 + (z - z')^2}$$

$$= r \sqrt{1 - \frac{2}{r^2}(xx' + yy' + zz') + O[(r'/r)^2]} \quad . \tag{5.25}$$

For observation points which are far away from the interaction region, we may neglect $O[(r'/r)^2]$ and rewrite Equation (5.25), using Equation (5.23), as

$$|r - r'| \simeq r - x' \sin\theta_x - y' \sin\theta_y - z' \cos\theta \quad . \tag{5.26}$$

Combining Equations (5.19), (5.22), and (5.26), and assuming all angles are sufficiently small that

$$\alpha r \simeq \alpha z \quad ,$$

we obtain

$$p_-(r,\theta_x,\theta_y) = \frac{\omega_-^2}{4\pi\rho_o c_o^4} \frac{e^{-ik_- r}}{r} \int_{V'} P_1(x'-z' \tan\phi_1, y') \; P_2(x'-z' \tan\phi_2, y')$$

$$\cdot \exp\{ik_- x' \psi_x + ik_- y' \sin\theta_y\}$$

$$\cdot \exp\{-\alpha_1 z' - i(k_1 \cos\phi_1 - k_2 \cos\phi_2 - k_- \cos\theta) z'\} \, dV' \; , \tag{5.27}$$

where

$$\psi_x = \sin\theta_x - \frac{k_1}{k_-} \sin\phi_1 + \frac{k_2}{k_-} \sin\phi_2 \quad . \tag{5.28}$$

The first case we consider is that of rectangular primary beams for which the amplitude distribution at the source is given by

$$P_j(x,y) = p_{0j} \; \text{rect}\left(\frac{x}{a}\right) \; \text{rect}\left(\frac{y}{b}\right) \quad , \tag{5.29}$$

where

$$\text{rect}(t) = 1 \quad , \quad |t| \leq 1$$

$$= 0 \quad , \quad \text{elsewhere} \; .$$

That is, both primary beams have width $2a$ in the x direction and $2b$ in the y direction. The volume of integration is simply the volume which is common to both beams. Referring to Figure 21 and assuming

$$\phi_1 \geq \phi_2 \quad ,$$

we find that the volume of integration is defined by

$$-a + z' \tan\phi_1 \leq x' \leq a + z' \tan\phi_2 \quad ,$$

$$-b \leq y' \leq b \quad ,$$

$$0 \leq z' \leq L \quad .$$

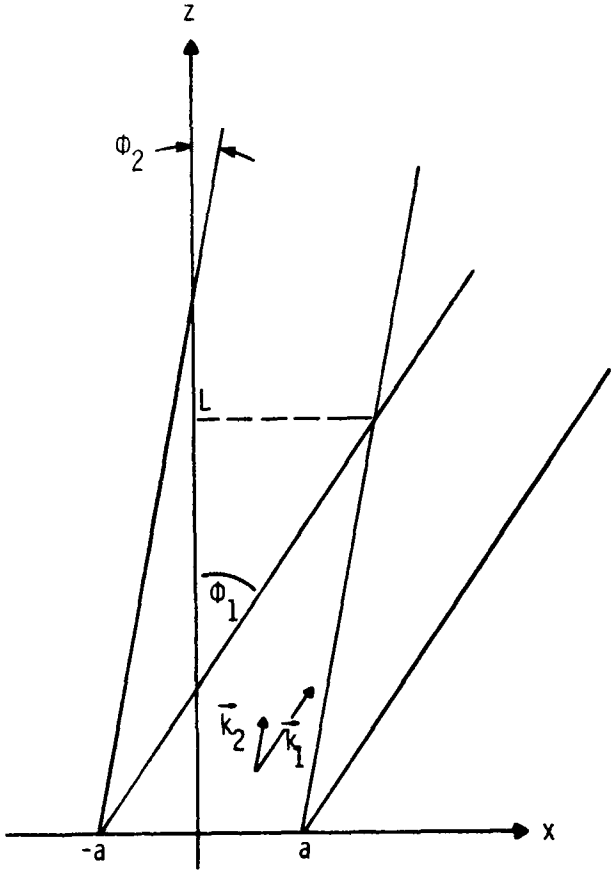

Figure 21. Geometry for Noncollinear Interaction of Nondiffracting Rectangular Primary Beams.

AS-83-721

The length L of the array, which is finite whenever $\phi_1 \neq \phi_2$, is given by

$$L = \frac{2a}{\tan\phi_1 - \tan\phi_2} \quad . \tag{5.30}$$

The difference-frequency field integral thus becomes

$$p_-(r,\theta_x,\theta_y) = \frac{\beta\omega_-^2 ab\, p_{01}p_{02}}{\pi\alpha_T\rho_o c_o^4} \frac{e^{-i\chi_- r}}{r} \frac{\sin(k_- b\sin\theta_y)}{k_- b\sin\theta_y} F_\delta^R(\theta_x,\theta_y;\phi_1,\phi_2) \quad , \tag{5.31}$$

where

$$F_\delta^R(\theta_x,\theta_y;\phi_1,\phi_2) = \frac{1}{i2k_- a\psi_x}\left\{e^{ik_- a\psi_x}\left[\frac{1 - e^{-(\alpha_T + i\kappa_2)L}}{1 + i\kappa_2/\alpha_T}\right] - e^{-ik_- a\psi_x}\left[\frac{1 - e^{-(\alpha_T + i\kappa_1)L}}{1 + i\kappa_1/\alpha_T}\right]\right\} \quad , \tag{5.32}$$

and

$$\kappa_j = k_1\cos\phi_1 - k_2\cos\phi_2 - k_-(\cos\theta + \psi_x\tan\phi_j) \quad . \tag{5.33}$$

ψ_x and L are defined in Equations (5.28) and (5.30), respectively.

When $\phi_1 = \phi_2 = \Phi$, F_δ^R reduces to

$$F_\delta^R(\theta_x,\theta_y;\Phi) = \frac{\sin\{k_- a[\sin\theta_x - (1 - \delta)\sin\Phi]\}}{k_- a[\sin\theta_x - (1 - \delta)\sin\Phi]} \frac{1}{1 + i\kappa_o/\alpha_T} \quad , \tag{5.34}$$

where

$$\kappa_o = \kappa_j\Big|_{\phi_j=\Phi} \quad . \tag{5.35}$$

Thus, only when $\phi_1 = \phi_2$ does F_δ^R separate into an aperture factor and a modified Westervelt directivity function. The aperture factors are then maximized when $\theta_x = \Phi$ and $\theta_y = 0$, which is, of course, the direction in which the primaries are radiated. We now check to see if $(1 + i\kappa_o/\alpha_1)^{-1}$, the modified Westervelt directivity function, is similarly oriented. From Equations (5.33) and (5.35) we obtain

$$\kappa_o/k_- = 2\sin^2(\theta/2) - \delta - \sin\theta_x \tan\Phi + (1-\delta)[\sin\Phi\tan\Phi - 2\sin^2(\Phi/2)] \ . \tag{5.36}$$

When both θ and Φ are small, we can replace the trigonometric functions in Equation (5.36) by their arguments to get

$$\frac{1}{1 + i\kappa_o/\alpha_T} \approx \frac{1}{1 + i(k_-/2\alpha_T)[(\theta_x - \Phi)^2 + \theta_y^2 - 2\delta - \delta\Phi^2]} \ . \tag{5.37}$$

Aside from the factor of $\delta\Phi^2$, Equation (5.37) is equivalent to $D_\delta^W(\theta_x - \Phi, \theta_y)$, as required.

In Figure 22 we plot F_δ^R for $\theta_y = 0$ to show the effect of noncollinear interaction in the absence of dispersion. The parameter k_o given in the figure captions is a mean primary wave number, where

$$k_o = \frac{k_1 + k_2}{2} \ .$$

For even small values of Φ, where

$$\Phi = \phi_1 - \phi_2$$

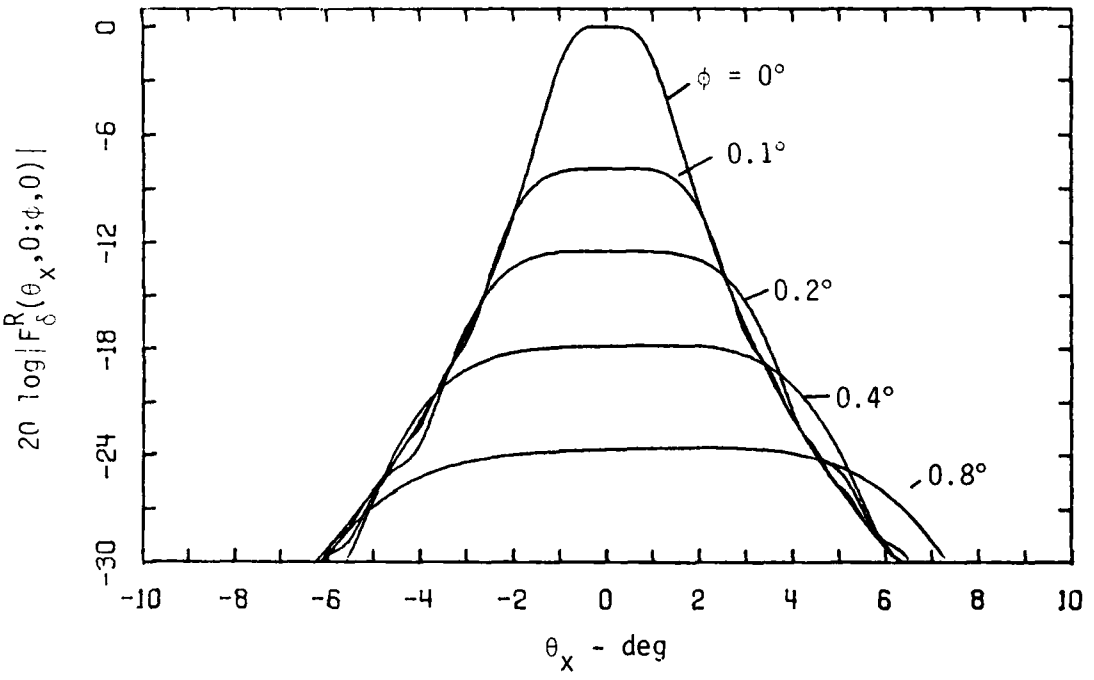

Figure 22. Difference-Frequency Field Directivity Pattern Resulting from Noncollinear Interaction of Nondiffracting Rectangular Primary Beams in a Dispersionless Fluid ($\phi_1 = \phi$, $\phi_2 = 0$, $\theta_y = 0$, $k_o/k_- = 10$, $k_-a = 5$, $k_-/\alpha_T = 5000$, $\delta = 0$).

AS-83-722

is the angle of intersection, the farfield suffers significant losses of both level and directivity. Two factors contribute to the deterioration of the farfield radiation pattern. First is the fact that when $\phi \neq 0$, the array is terminated at $z = L$, and has a well-defined triangular shape. If α_T is large and ϕ is small, the width of the interaction region remains relatively constant and attenuation effectively terminates the array at $z << L$. In such a case, noncollinear interaction does not significantly shorten the length of the interaction region. Otherwise, the width of the array gradually decreases with z up to the abrupt termination at $z = L$. The ripples observed in the directivity patterns of Figure 22 are manifestations of the finite length of the array when $\phi \neq 0$. As mentioned in Section 2.3, there are no sidelobes in the difference-frequency field radiated by collinear primary beams because attenuation (or spreading) provides a gradual termination of the array. Note that when $\phi \neq 0$, the directivity patterns exhibit slight asymmetry and are shifted in the direction of positive θ_x. This occurs not only because the interaction region is oriented in the direction of positive θ_x when $\phi_2 = 0$ and $\phi_1 = \phi$; in addition, the direction of $\vec{k}_1 - \vec{k}_2$, along which the difference-frequency signal is amplified, is oriented toward positive θ_x.

The second factor which contributes to deterioration of the farfield radiation pattern is phase mismatching resulting from the noncollinearity of the primaries. We investigate the phase mismatching by seeing to what extent and under what conditions it can be used to offset the inherent dispersivity of a fluid. In Figure 23 are presented farfield radiation patterns, obtained from Equation (5.32),

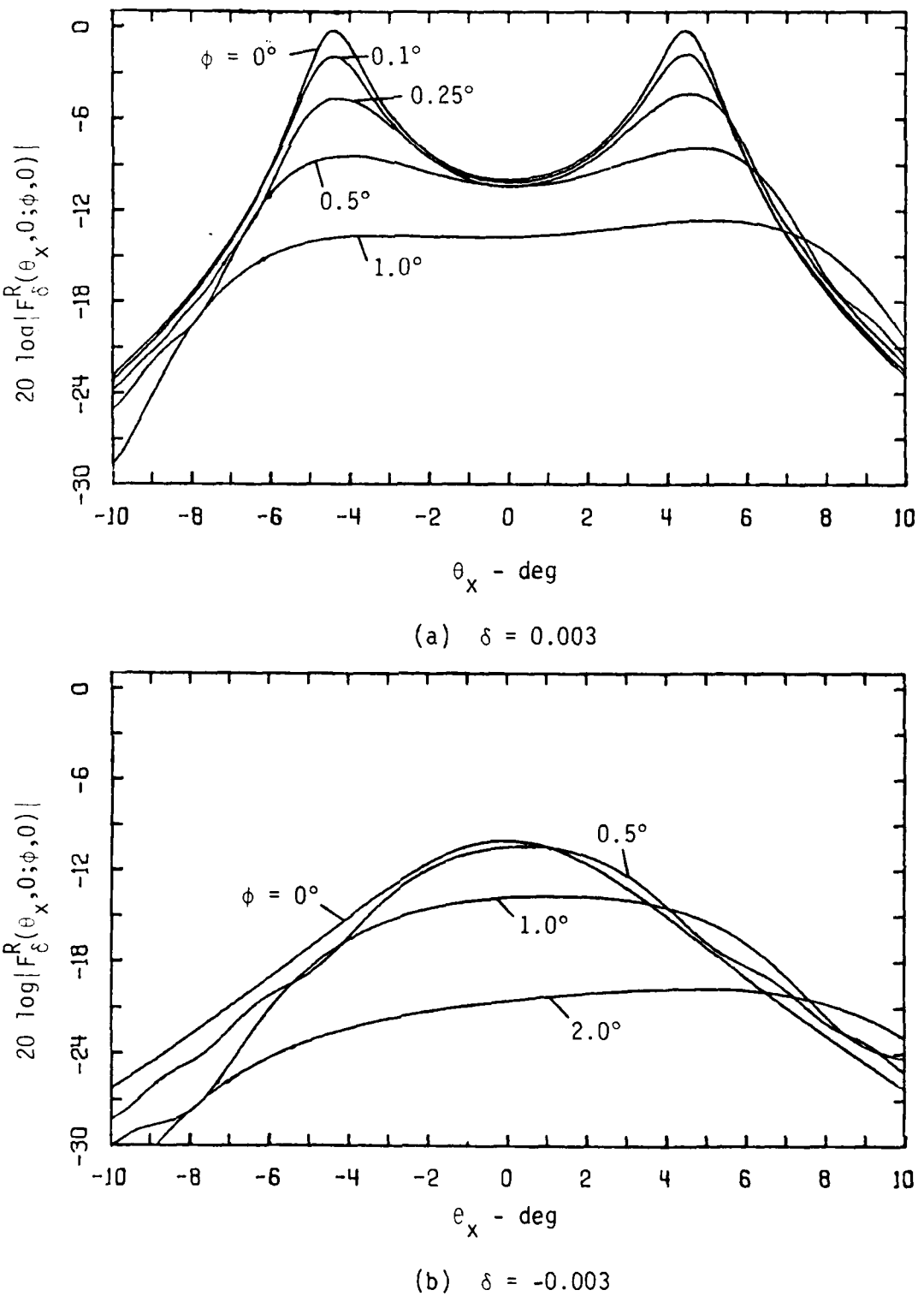

Figure 23. Difference-Frequency Field Directivity Pattern Resulting from Noncollinear Interaction of Nondiffracting Rectangular Primary Beams in a Dispersive Fluid ($\phi_1 = \phi$, $\phi_2 = 0$, $\theta_y = 0$, $k_o/k_- = 10$, $k_-a = 5$, $k_-/\alpha_T = 1000$).

AS-83-723

for noncollinear interaction in fluids which exhibit both normal (Figure 23a) and anomalous (Figure 23b) dispersion. The level of 0 dB refers to that which can be attained when $\delta = 0$ and $\phi = 0$, with all other parameters being equal. For $\delta = 0.003$, we use Equation (5.12) to find that the angle ϕ_o for which there is resonant interaction within the interaction region is $\phi_o = 0.44°$. However, in Figure 23a, it is seen that for no value of ϕ is there any improvement in the radiation pattern. In fact, we found that such improvement is never possible when $\delta > 0$. On the other hand, it is seen in Figure 23b that the effects of noncollinear interaction on the radiation pattern are less detrimental when $\delta < 0$. Moreover, for $\phi < 0.5°$ there appears to be no significant adverse effects. Indeed, in Figure 24, where the attenuation is lower than that in Figure 23, slight compensation for the inherent dispersivity of the fluid is seen to be possible when $\delta < 0$, but only for small ϕ. For ϕ increases, the size of the interaction region is reduced, thus offsetting any potential gains resulting from phase matching. We therefore find that compensation for inherent dispersion with the parametric array is possible only when $\delta < 0$, but not for $\delta > 0$, which is the condition required for resonant interaction within the interaction region. Before resolving this paradox, we consider one more example.

Since an undesirable consequence of noncollinear interaction of rectangular beams is the abrupt termination of the interaction region, we now consider nondiffracting Gaussian primary beams because of their gradual amplitude distributions. We thus prescribe the boundary condition

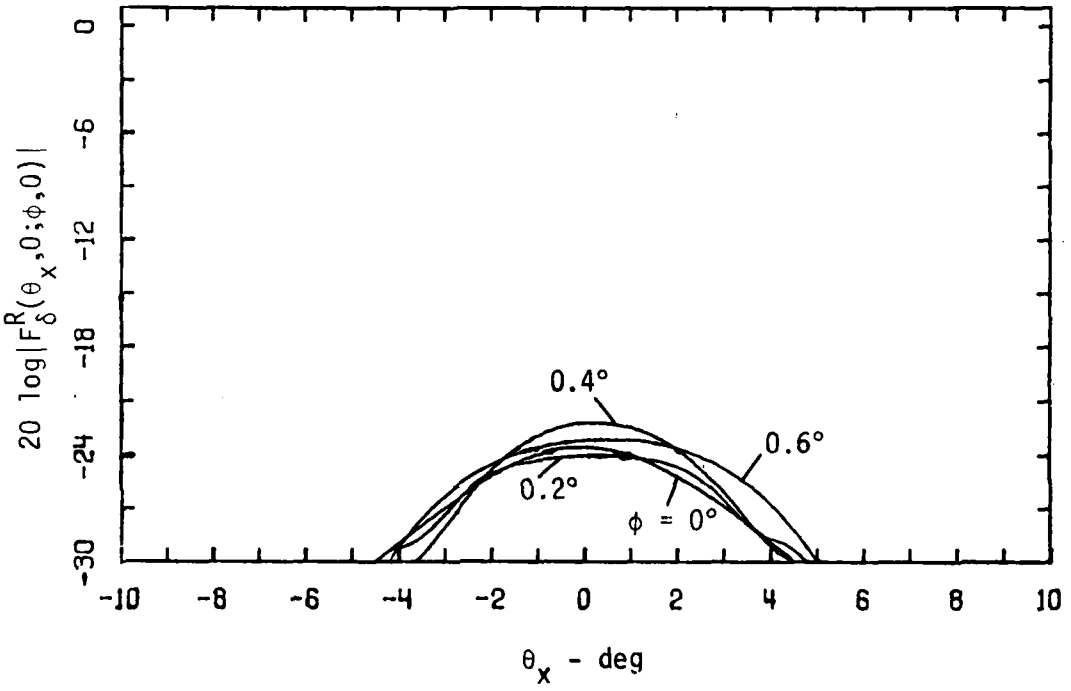

Figure 24. Difference-Frequency Field Directivity Pattern Resulting from Noncollinear Interaction of Nondiffracting Rectangular Primary Beams in a Dispersive Fluid ($\phi_1 = \phi$, $\phi_2 = 0$, $\theta_y = 0$, $k_o/k_- = 10$, $k_-a = 5$, $k_-/\alpha_T = 5000$, $\delta = -0.003$).

AS-83-724

$$p_j(x,y,0) = p_{Gj} \exp\{-(\frac{x}{x_o})^2 - (\frac{y}{y_o})^2 - ik_j x \sin\phi_j\} \quad , \qquad (5.38)$$

for which the primaries are given by

$$p_j(x,y,z) = p_{Gj} \exp\left\{-\left(\frac{x - z\tan\phi_j}{x_o}\right)^2 - (\frac{y}{y_o})^2\right\} e^{-i\vec{\chi}_j\cdot\vec{r}} \quad . \qquad (5.39)$$

Our field integral becomes

$$p_-(r,\theta_x,\theta_y) = \frac{\beta\omega_-^2 p_{G1} p_{G2}}{4\pi\rho_o c_o^4} \frac{e^{-i\chi_- r}}{r} I_y I_{xz} \quad , \qquad (5.40)$$

where

$$I_y = \int_{-\infty}^{\infty} \exp\{-2(\frac{y'}{y_o})^2 + ik_- y' \sin\theta_y\}\, dy'$$

$$= y_o\sqrt{\frac{\pi}{2}} \exp\{-\frac{1}{8}(k_- y_o)^2 \sin^2\theta_y\} \quad ,$$

and

$$I_{xz} = \int_0^{\infty}\int_{-\infty}^{\infty} \exp\{-[\alpha_T + i(k_1\cos\phi_1 - k_2\cos\phi_2 - k_-\cos\theta)]\, z'\}$$

$$\cdot \exp\{-(\tan^2\phi_1 + \tan^2\phi_2)(\frac{z'}{x_o})^2\}$$

$$\cdot \exp\{-2(\frac{x'}{x_o})^2 + (2\frac{z'}{x_o^2}\tan\phi_1 + 2\frac{z'}{x_o^2}\tan\phi_2 + ik_-\psi_x)\, x'\}\, dx'\, dz' \quad ,$$

where ψ_x is given in Equation (5.28). Note that I_{xz} can be separated into independent integrals over x' and z' if

$$\phi_1 = -\phi_2 = \frac{\phi}{2} \quad .$$

We thus obtain

$$I_{xz} = I_x I_z \quad ,$$

where

$$I_x = \int_{-\infty}^{\infty} \exp\{-2(\frac{x'}{x_o})^2 + i[k_- \sin\theta_x - (k_1 + k_2)\sin\frac{\phi}{2}]\, x'\}\, dx'$$

$$= x_o \sqrt{\frac{\pi}{2}} \exp\{-\frac{1}{8}(k_- x_o)^2[\sin\theta_x - (\frac{k_1 + k_2}{k_-})\sin\frac{\phi}{2}]^2\} \quad ,$$

and

$$I_z = \int_0^{\infty} \exp\{-2\tan^2(\phi/2)(\frac{z'}{x_o})^2 - (\alpha_T + i\kappa)z'\}\, dz'$$

$$= \frac{\sqrt{\pi}\, x_o}{2\sqrt{2}\tan(\phi/2)} \exp\left\{\left[\frac{(\alpha_T + i\kappa)x_o}{2\sqrt{2}\tan(\phi/2)}\right]^2\right\} \operatorname{erfc}\left\{\frac{(\alpha_T + i\kappa)x_o}{2\sqrt{2}\tan(\phi/2)}\right\} \quad ,$$

where

$$\kappa = (k_1 - k_2)\cos\frac{\phi}{2} - k_- \cos\theta \quad .$$

Therefore, when $\phi_1 = -\phi_2 = \phi/2$, Equation (5.40) becomes

$$p_-(r,\theta_x,\theta_y) = \frac{\beta\omega^2 x_o y_o p_{G1} p_{G2}}{8\alpha_T \rho_o c_o^4} \frac{e^{-i\chi_- r}}{r} A_G(\theta_x,\theta_y;\phi)\, D_\delta^G(\theta;\phi) \quad , \quad (5.41)$$

where

$$A_G(\theta_x,\theta_y;\phi) = \exp\left\{-\frac{1}{8}(k_- x_o)^2\left[\sin\theta_x - \left(\frac{k_1+k_2}{k_-}\right)\sin\frac{\phi}{2}\right]^2 - \frac{1}{8}(k_- y_o)^2\sin^2\theta_y\right\} , \tag{5.42}$$

and

$$D_\delta^G(\theta;\phi) = \frac{\sqrt{\pi}\,\alpha_T x_o}{2\sqrt{2}\tan(\phi/2)} \exp\left\{\left[\frac{(\alpha_T+i\kappa)x_o}{2\sqrt{2}\tan(\phi/2)}\right]^2\right\} \operatorname{erfc}\left\{\frac{(\alpha_T+i\kappa)x_o}{2\sqrt{2}\tan(\phi/2)}\right\} . \tag{5.43}$$

We have thus been able to separate the normalized aperture factor, $A_G(\theta_x,\theta_y;\phi)$, from the Westervelt-type directivity function, $D_\delta^G(\theta;\phi)$. The latter is so-named because

$$D_\delta^G(\theta;0) = D_\delta^W(\theta) \quad .$$

For $\phi = 0$, $D_\delta^G(\theta;\phi)$ gives the radiation pattern of a phased line array. The parameter which controls the length of the line array is α_T . When $\phi \neq 0$, the length of the parametric array is governed not only by attenuation, but also the width of the primaries and the angle of intersection. The latter two factors are represented by the addition of the parameters x_o and ϕ , respectively, in the modified Westervelt directivity function, $D_\delta^G(\theta;\phi)$.

From Equation (5.42), we find that the aperture factor is maximized when

$$\sin\theta_x = \left(\frac{k_1 + k_2}{k_-}\right)\sin\frac{\phi}{2} \quad , \tag{5.44}$$

and

$$\theta_y = 0 \quad .$$

The geometry of the interaction when $\phi_1 = -\phi_2 = \phi/2$ is given in Figure 25, where ψ denotes the angle formed by $\vec{k}_1 - \vec{k}_2$ and the z axis. Invoking the laws of sines and cosines we find that

$$\psi = \frac{\phi}{2} + \sin^{-1}\left\{\frac{\sin\phi}{\sqrt{1 - 2(k_1/k_2)\cos\phi + (k_1/k_2)^2}}\right\}. \qquad (5.45)$$

Under conditions where both ϕ and ψ are sufficiently small that we need only retain the first terms in the expansions of the trigonometric functions in Equation (5.45), we obtain

$$\psi \simeq \frac{k_1 + k_2}{2k_-}\,\phi \quad . \qquad (5.46)$$

Comparing Equations (5.44) and (5.46) we find that $A_G(\theta_x,\theta_y;\phi)$ is maximized when

$$\theta_x \simeq \psi \quad , \quad \theta_y = 0 \quad , \qquad (5.47)$$

i.e., in the direction of $\vec{k}_1 - \vec{k}_2$. A_G is therefore a normalized aperture factor in the sense that it is the directivity function of a difference-frequency signal radiated by a source defined by

$$p_1(x,y,0)\; p_2^*(x,y,0) \quad . \qquad (5.48)$$

However, when $\phi \neq 0$ we cannot decompose the parametric array into a distribution of identical virtual sources which are described by Equation (5.48), as was done in Figure 5 for collinear interaction. The reason is, of course, that the cross-sectional area of the array

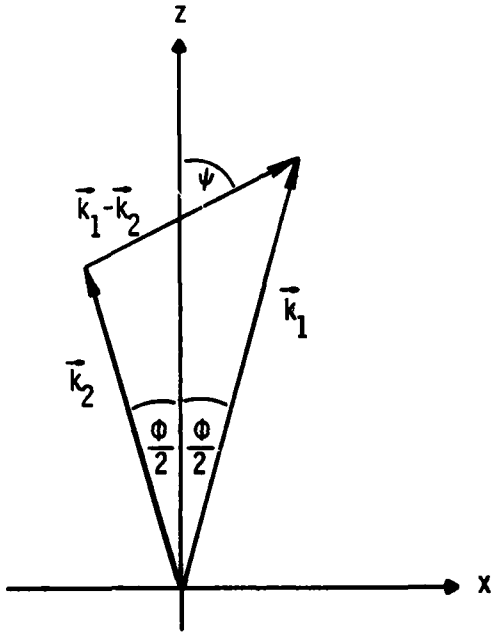

Figure 25. Geometry of Noncollinear Interaction of Nondiffracting Gaussian Primary Beams.

AS-83-725

decreases with z when $\phi \neq 0$. Moreover, D_δ^G is the directivity function of a line array only when $\phi = 0$.

In Figure 26 is plotted $A_G D_\delta^G$ for $\theta_y = 0$ and $\delta = 0$ to illustrate the effect of noncollinear interaction of Gaussian beams in a dispersionless fluid. The parameters used in Figure 26 are similar to those used in Figure 22. Except for the absence of ripples in the directivity patterns for noncollinear interaction of Gaussian beams, the results are much the same as those for rectangular beams. There are no ripples because the interaction region formed by Gaussian beams is theoretically infinite in extent even when $\phi \neq 0$. Referring now to Figure 27, we again find that compensation for inherent dispersion via noncollinear interaction is possible only when $\delta < 0$. In Figure 28, where attenuation is lower than that in Figure 27, we show a case where the improvement is about 2 dB. Thus, for Gaussian as well as rectangular primary beams, no cases were found where noncollinear interaction provides any compensation for the inherent dispersivity of a fluid when $\delta > 0$. However, when $\delta < 0$ and improvement is possible, Gaussian beams yield slightly better results than do rectangular beams. The reason appears to be the lack of abrupt boundaries on the interaction region when Gaussian beams are used.

We now offer an explanation for the paradoxical result that compensation for inherent dispersion with a parametric array appears possible via noncollinear interaction only when $\delta < 0$, whereas only when $\delta > 0$ can there be resonant interaction within the interaction region. Understanding comes from consideration of differences between plane-wave interaction and radiation from a parametric array. It was demonstrated in the previous section that resonant interaction occurs

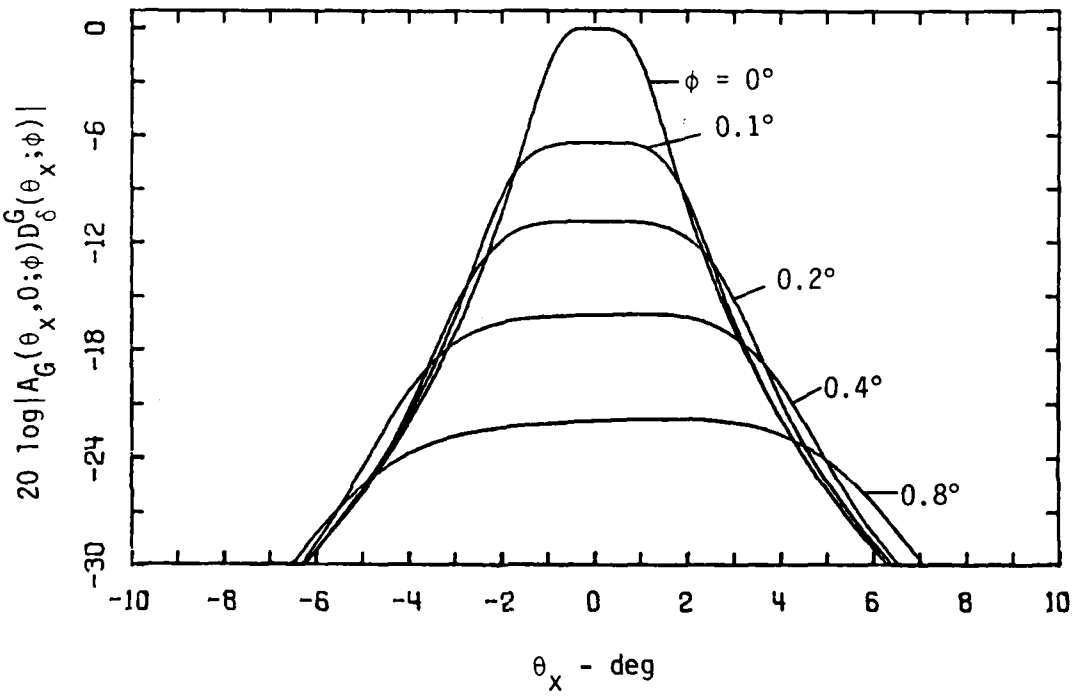

Figure 26. Difference-Frequency Field Directivity Pattern Resulting from Noncollinear Interaction of Nondiffracting Gaussian Primary Beams in a Dispersionless Fluid ($\phi_1 = \phi/2$, $\phi_2 = -\phi/2$, $\theta_y = 0$, $k_o/k_- = 10$, $k_- x_o = 5$, $k_-/\alpha_T = 5000$, $\delta = 0$).

AS-83-726

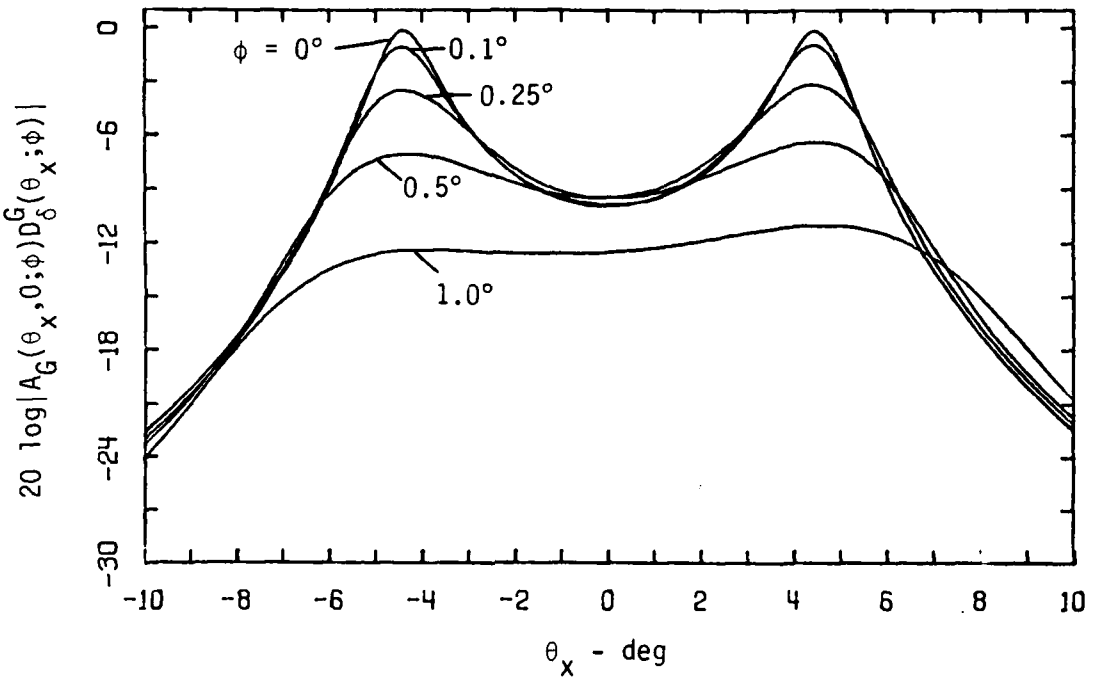

(a) $\delta = 0.003$

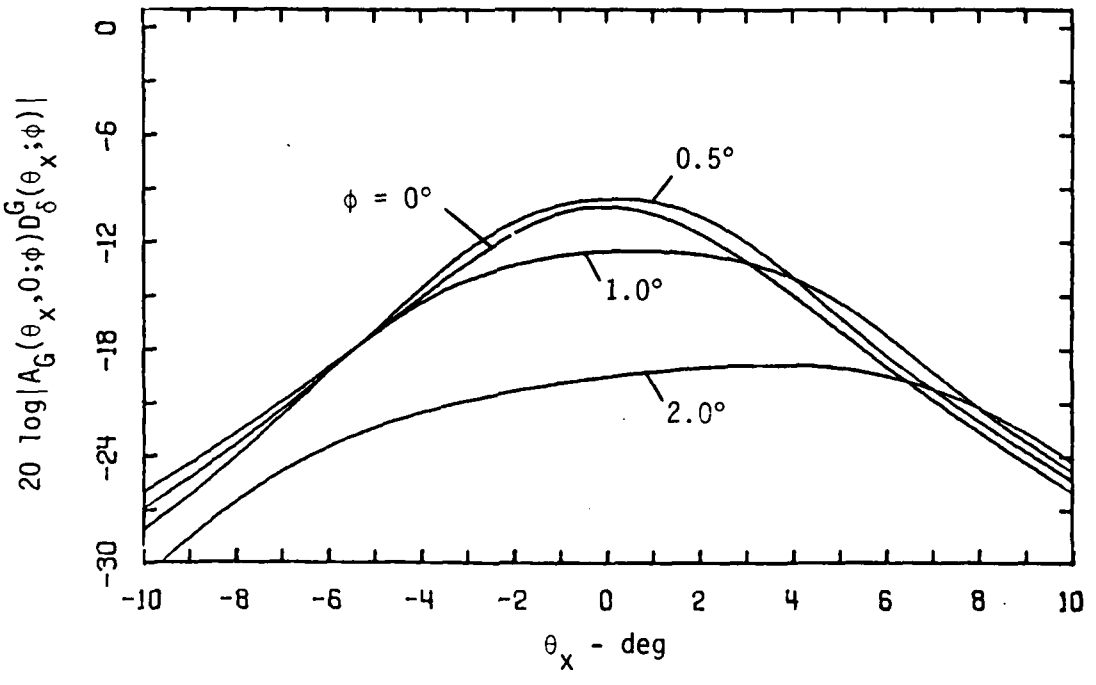

(b) $\delta = -0.003$

Figure 27. Difference-Frequency Field Directivity Pattern Resulting from Noncollinear Interaction of Nondiffracting Gaussian Primary Beams in a Dispersive Fluid ($\phi_1 = \phi/2$, $\phi_2 = -\phi/2$, $\theta_y = 0$, $k_o/k_- = 10$, $k_-x_o = 5$, $k_-/\alpha_T = 1000$).

AS-83-727

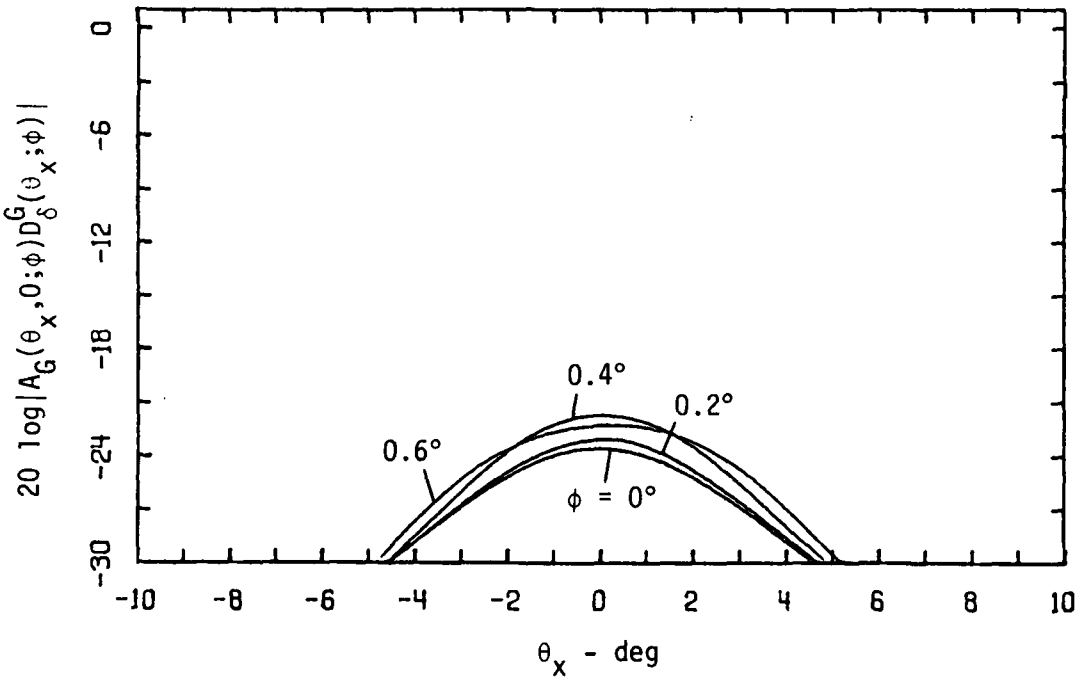

Figure 28. Difference-Frequency Field Directivity Pattern Resulting from Noncollinear Interaction of Nondiffracting Gaussian Primary Beams in a Dispersive Fluid ($\phi_1 = \phi/2$, $\phi_2 = -\phi/2$, $\theta_y = 0$, $k_o/k_- = 10$, $k_- x_o = 5$, $k_-/\alpha_T = 5000$, $\delta = -0.003$).

AS-83-728

when $|\vec{k}_1 - \vec{k}_2| = k_-$, and that the direction along which amplification of the difference-frequency signal occurs is $\vec{k}_1 - \vec{k}_2$. Since increasing ϕ causes $|\vec{k}_1 - \vec{k}_2|$ to increase, it is clear that resonant interaction can be attained in this fashion only when $k_1 - k_2 \leq k_-$, i.e., when $\delta \geq 0$. We should expect the same principle to hold for the parametric array, but herein lies the difference. In Figure 21 we see that the interaction region is aligned along a direction given approximately by $(\phi_1 + \phi_2)/2$. We therefore consider the geometry in Figure 25, where the interaction region is aligned approximately with the z axis, and the angle formed by $\vec{k}_1 - \vec{k}_2$ and the interaction region is approximately ψ , where ψ is defined in Equation (5.45). Such a configuration is illustrated in Figure 29, where the arrows are aligned with $\vec{k}_1 - \vec{k}_2$ to represent the phasing of virtual sources within the interaction region. The difference-frequency signal is amplified along the direction of $\vec{k}_1 - \vec{k}_2$ within the interaction region, as indicated in Figure 29a. However, we have $\psi \neq 0$ for noncollinear interaction, and therefore the path length along $\vec{k}_1 - \vec{k}_2$ is governed by the width of the interaction region and the angle ψ . In general, the width of the interaction region is no more than a few difference-frequency wavelengths. Also, when $k_1 \simeq k_2$, ψ becomes quite large for even small values of ϕ . As a result, the path length along $\vec{k}_1 - \vec{k}_2$ when $\phi \neq 0$ is too short to allow effective amplification of the difference-frequency signal, even when $|\vec{k}_1 - \vec{k}_2| = k_-$ within the interaction region. We now consider the narrow interaction region depicted in Figure 29b. If the width of the array is ignored, the interaction region may be interpreted as a line array of virtual

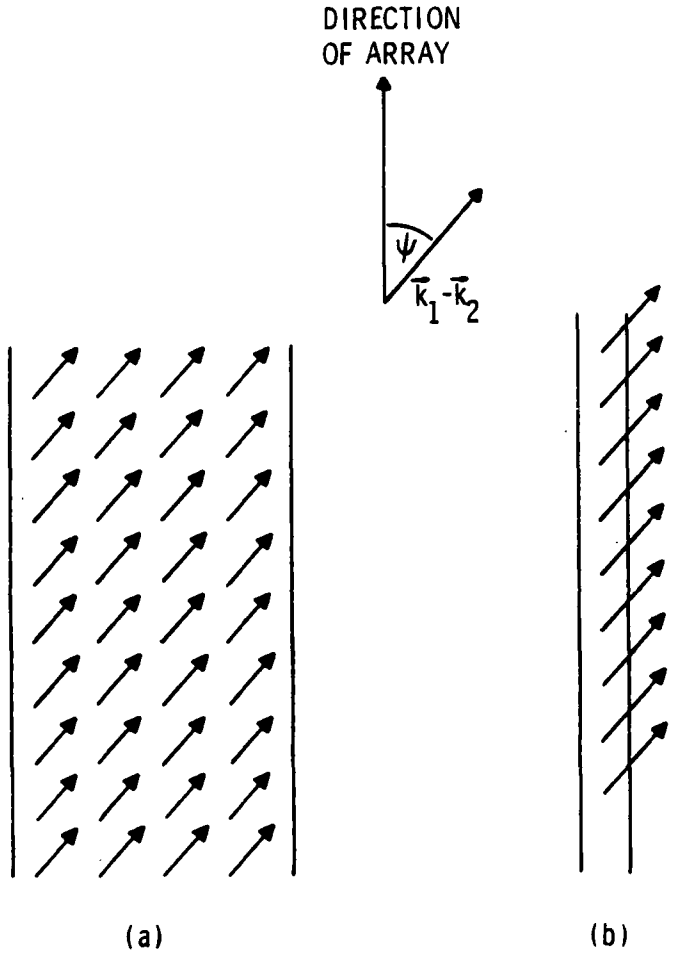

Figure 29. Phasing of Virtual Sources Within Wide (a) and Narrow (b) Interaction Regions.

point sources whose phasing is determined by the component of $\vec{k}_1 - \vec{k}_2$ along the array; i.e., $|\vec{k}_1 - \vec{k}_2| \cos\psi$. The condition for phase matching of the parametric array thus becomes

$$|\vec{k}_1 - \vec{k}_2| \cos\psi = k_- \quad . \tag{5.49}$$

As ϕ increases, the quantity $|\vec{k}_1 - \vec{k}_2| \cos\psi$ decreases. We thus expect phase matching for a narrow array to be possible only when $k_1 - k_2 \geq k_-$, i.e., when $\delta \leq 0$.

The question then arises as to why we cannot obtain greater compensation for dispersion via noncollinear interaction. Equation (5.49) holds only for a very narrow interaction region. If both the angle ψ and the width of the array are large, the virtual sources in any cross section of the interaction region do not have the same phase, and the phase-matching condition given by Equation (5.49) becomes invalid. On the other hand, to obtain a narrow interaction region requires narrow primaries. However, if the primaries are narrow, noncollinear interaction causes the length of the array to be significantly shortened. Indeed, we found that only for very small ϕ when $\delta < 0$ is there any improvement in the farfield radiation pattern. Eventually, gains attained by phase matching via noncollinear interaction are compromised by shortening of the interaction region.

We conclude by mentioning some results reported in the Soviet literature. In an analytical investigation of a parametric array formed by noncollinear interaction of narrow, nondiffracting primary beams in a dispersive fluid, Kozyaev and Naugol'nykh[8] obtained the directivity function

$$F(\theta) = \frac{\alpha_T}{\alpha_T + i(|\vec{k}_1 - \vec{k}_2| \cos\gamma - k_- \cos\theta)} \quad , \qquad (5.50)$$

where γ is the angle formed by $\vec{k}_1$ and $\vec{k}_1 - \vec{k}_2$, and θ is the angle formed by $\vec{r}$ and $\vec{k}_1$. They assert that when $|\vec{k}_1 - \vec{k}_2| = k_-$, radiation of the difference-frequency signal is maximized in the direction of $\vec{k}_1 - \vec{k}_2$, a result we have been unable to verify in our analysis. When $|\vec{k}_1 - \vec{k}_2| \cos\gamma = k_-$, Equation (5.50) is maximized when $\theta = 0$. The condition $|\vec{k}_1 - \vec{k}_2| \cos\gamma = k_-$ is the same as that given by Equation (5.49) when the interaction region is aligned with $\vec{k}_1$. However, the results in this section do not, in general, support Equation (5.50).

A somewhat different analysis was performed by Zverev and Kalachev[57] in their investigation of the scattering of sound by sound. They considered the case of plane waves in a perfectly collimated rectangular beam which, after propagating a distance L, encounter an acoustic filter which is opaque for the primaries but transparent for the difference-frequency signal. Interacting with the rectangular beam is a plane wave whose direction of propagation forms an angle ϕ with that of the beam. Because the plane wave completely overlaps the rectangular beam, the volume of the interaction region does not depend on ϕ. If we ignore attenuation and assume the primaries are given by

$$p_1(x,y,z) = p_{01} \text{ rect}\left(\frac{x}{a}\right) \text{ rect}\left(\frac{y}{b}\right) e^{-ik_1 z} \quad ,$$

$$p_2(x,y,z) = p_{02} \exp\{-ik_2 x \sin\phi - ik_2 z \cos\phi\} \quad ,$$

then from Equation (5.27) we obtain, for $\alpha_T = 0$, $\phi_1 = 0$, $\phi_2 = \phi$, and $0 \leq z' \leq L$,

$$p_-(r,\theta_x,\theta_y) = \frac{\beta\omega_-^2 abp_{01}p_{02}}{\pi\alpha_T\rho_o c_o^4} \frac{e^{-ik_-r}}{r} A_R(\theta_x,\theta_y;\phi)\, D_\delta^L(\theta;\phi) \quad , \tag{5.51}$$

where

$$A_R(\theta_x,\theta_y;\phi) = \frac{\sin\{k_-a[\sin\theta_x + (k_2/k_-)\sin\phi]\}}{k_-a[\sin\theta_x + (k_2/k_-)\sin\phi]} \frac{\sin(k_-b\sin\theta_y)}{k_-b\sin\theta_y} \quad , \tag{5.52}$$

and

$$D_\delta^L(\theta;\phi) = \frac{\sin\{k_-L[\sin^2(\theta/2) + (k_2/k_-)\sin^2(\phi/2) - 2\delta]\}}{k_-L[\sin^2(\theta/2) + (k_2/k_-)\sin^2(\theta/2) - 2\delta]} \quad . \tag{5.53}$$

When $\delta = 0$, Equation (5.51) becomes functionally equivalent to the result obtained by Zverev and Kalachev,[57] who verified Equation (5.51) experimentally for dispersionless fluids. The normalized aperture factor A_R is maximized in the direction of $\vec{k}_1 - \vec{k}_2$ [see, e.g., the discussion of Equation (5.42)]. Here, D_δ^L is the directivity function of a line array of length L . From Equation (5.53) we find that phase matching is achieved when

$$\frac{k_2}{k_-}\sin^2\left(\frac{\phi}{2}\right) = 2\delta \quad . \tag{5.54}$$

Phase matching is therefore possibly only when $\delta \geq 0$. However, suppose now that we reverse the roles of the primaries. That is, let the rectangular beam carry the high frequency, ω_1 , and let the plane wave be transmitted at the lower frequency, ω_2 . The resulting field

is then the same as that given by Equation (5.51), except that $-(k_1/k_-)$ replaces (k_2/k_-) in both Equations (5.52) and (5.53). Now the condition for phase matching becomes

$$\frac{k_1}{k_-} \sin^2\left(\frac{\phi}{2}\right) = -2\delta \quad , \tag{5.55}$$

and therefore phase matching is now possible only when $\delta \leq 0$.

The difference between the cases represented by the conditions given in Equation (5.54) and (5.55) is that in the former, the interaction region is aligned with $\vec{k}_1$, whereas in the latter, it is aligned with $\vec{k}_2$. Conditions for phase matching thus follow from the discussion relating to Figure 29b. When the interaction region is aligned with $\vec{k}_1$, an increase in ϕ causes the component of $\vec{k}_1 - \vec{k}_2$ along the array to increase. Likewise, when the interaction region is aligned with $\vec{k}_2$, an increase in ϕ causes the component of $\vec{k}_1 - \vec{k}_2$ along the array to decrease. We can therefore compensate for any type of inherent dispersion because we can adjust the frequency of the beam to be either higher or lower than that of the plane wave. Moreover, since there is no loss of volume in the interaction region as a result of noncollinear interaction, the beam can be made arbitrarily narrow to ensure that satisfaction of the phase-matching conditions given by Equations (5.54) and (5.55) yields measurable results. Indeed, one might conceivably use such an arrangement to measure dispersion by way of the directivity function in Equation (5.51). If attenuation is sufficiently high to terminate the beam, then Equation (5.53) must be replaced by

$$D_{\delta}^{W}(\theta;\phi) = \frac{1}{1 + i2(k_{-}/\alpha_{T})[\sin^{2}(\theta/2) + (k_{2}/k_{-})\sin^{2}(\phi/2) - 2\delta]} \quad . \tag{5.56}$$

A similar adjustment must be made for Equation (5.52) if something other than a rectangular beam is used. We note that Equation (5.56) is identical to Equation (5.50), and therefore comparison of the two sheds light on applicability of the latter.

CHAPTER VI

PARAMETRIC ARRAYS FORMED BY NONCOLLINEAR GAUSSIAN PRIMARY BEAMS

In this chapter we consider the effects of diffraction on noncollinear interaction of the primaries by resorting once again to an analysis of Gaussian beams. Solutions shall be obtained from the nonlinear paraxial wave equation, Equation (3.15), whose orientation is along the z axis. We justify our use of the paraxial wave equation when studying noncollinear interaction by requiring that the angles formed by the primaries and the z axis be small. Our attention here is restricted to angles of less than 5°.
For completeness, when deriving the field equations in Section 6.1, we allow both ϕ_1 and ϕ_2 to be nonzero, where ϕ_j $(j = 1,2)$ is the angle formed by the primary beam of frequency ω_j and the z axis. The important parameter is, of course, $\phi = \phi_1 - \phi_2$, so that no loss of generality results if either ϕ_1 or ϕ_2 is set equal to zero. For simplicity, we therefore let $\phi_2 = 0$ in the analysis of the difference-frequency field presented in Section 6.2.

6.1 Solutions for Primary and Secondary Components

As discussed in Section 5.2, to steer a beam at an angle ϕ relative to the z axis in the x-z plane, we need a phase distribution given by $-kx \sin\phi$ at the source. Because ϕ is assumed small, which is a necessary assumption when we use the paraxial wave equation, we may replace $\sin\phi$ by its argument and rewrite the phase distribution at the source as $-kx\phi$. This substitution is consistent with the approximation made when the

farfield of Gaussian beams is examined, where ε is replaced by $z\theta$ instead of $z\tan\theta$. Finally, the paraxial wave equation does not account for dispersion in the x and y directions, and therefore retaining $k = \omega/c_\omega$ instead of ω/c_o in the boundary condition is superfluous. The boundary condition, for beams steered as in Figure 21, is therefore

$$p_j(x,y,0) \simeq p_{Gj} \exp\left\{ - \left(\frac{x^2 + y^2}{\varepsilon_o^2}\right) - i\omega_j x\phi_j/c_o \right\} \quad . \qquad (6.1)$$

In dimensionless form, Equation (6.1) becomes

$$p_j(X,Y,0) \simeq p_{Gj} \exp\{-X^2 - Y^2 - i2\Omega_j DX\phi_j\} \quad . \qquad (6.2)$$

The dimensionless variables in Equation (6.2) are defined in Section 3.3. Inserting Equation (6.2) into Equation (3.37), we thus obtain for the primary wave fields

$$p_j(X,Y,Z) = p_{Gj} \frac{e^{-a_j' Z}}{1 - iZ/\Omega_j} \exp\left\{ - \frac{X^2 + Y^2 + i2\Omega_j DX\phi_j - i\Omega_j D^2 Z\phi_j^2}{1 - iZ/\Omega_j} \right\} . \qquad (6.3)$$

We now examine the asymptotic behavior of Equation (6.3). For the nearfield we have, in dimensional form,

$$p_j(x,y,z) \sim p_{Gj} e^{-\alpha_j' z} \exp\left\{ - \left(\frac{x - z\phi_j}{\varepsilon_o}\right)^2 - \left(\frac{y}{\varepsilon_o}\right)^2 \right\}$$

$$\cdot \exp\left\{ - i \frac{\omega_j}{c_o} x\phi_j + i \frac{\omega_j z\phi_j^2}{2c_o} - i \frac{2zc_o}{\omega_j \varepsilon_o^4} (x^2 + y^2) \right\} , \; Z << 1 . \qquad (6.4)$$

Note the similarity between the amplitude of p_j in the nearfield and the amplitude given by Equation (5.39) for nondiffracting Gaussian beams. Now, the equation describing a plane wave which travels in a direction forming an angle ϕ_j with the z axis is

$$p(x,y,z,t) = \exp\{i\omega_j(t - \frac{x}{c_o}\sin\phi_j - \frac{z}{c_o}\cos\phi_j)\}$$

$$= e^{i\omega_j t'} \exp\{- i \frac{\omega_j}{c_o} x \sin\phi_j + i \frac{\omega_j}{c_o} z(1 - \cos\phi_j)\} \quad , \tag{6.5}$$

where $t' = t - z/c_o$. For small ϕ_j , $(1 - \cos\phi_j) = 2\sin^2(\phi_j/2) \simeq \phi_j^2/2$ and $\sin\phi_j \simeq \phi_j$, whereby Equation (6.5) reduces to

$$p(x,y,z,t) \simeq e^{i\omega_j t'} \exp\left\{-i \frac{\omega_j}{c_o} x\phi_j + i \frac{\omega_j z \phi_j^2}{2c_o}\right\} \quad . \tag{6.6}$$

The angular dependence of Equation (6.6) is the same as that exhibited by the first two phase terms in Equation (6.4). In the paraxial nearfield, Equation (6.4) thus describes a plane wave propagating in the direction of ϕ_j , as required. The last phase term in Equation (6.4) indicates that the interpretation of the nearfield result as a plane wave is valid, at best, only very near the z axis.

As in Section 5.2, we let $x = z\tan\theta_x$ and $y = z\tan\theta_y$, where θ_x and θ_y are azimuthal angles in the x-z and y-z planes, respectively. In the paraxial farfield we may let $x \simeq z\theta_x$ and $y \simeq z\theta_y$, i.e.,

$$X \simeq DZ\theta_x \quad , \quad Y = DZ\theta_y \quad , \tag{6.7}$$

where the azimuthal angles satisfy the relation

$$\theta_x^2 + \theta_y^2 = \theta^2 \quad . \tag{6.8}$$

Equation (6.3) thus becomes

$$p_j(\theta_x,\theta_y,Z) \sim i\Omega_j P_{Gj} \frac{e^{-a_j' Z}}{Z} \exp\{-\Omega_j^2 D^2[(\theta_x - \phi_j)^2 + \theta_y^2] - i\Omega_j D^2 Z\theta^2\} \quad ,$$

$$Z >> 1 \quad . \tag{6.9}$$

We see that maximum radiation occurs in the direction where $\theta_x = \phi_j$ and $\theta_y = 0$, as expected. The phase term $-i\Omega_j D^2 Z\theta^2$ is a manifestation of spherically spreading wave fronts (see Figure 8).

We now derive solutions for the sum- and difference-frequency fields. It is helpful if, first, Equation (3.44) is rewritten as

$$p_{\pm}(X,Y,Z) = -\frac{1}{\pi}\Omega_{\pm}^2 D^2 \int_0^Z \iint_{-\infty}^{\infty} Q_{\pm}(X',Y',Z') \frac{e^{-a_{\pm}'(Z - Z')}}{Z - Z'}$$

$$\cdot \exp\left\{-i\Omega_{\pm}\left[\frac{(X - X')^2 + (Y - Y')^2}{Z - Z'}\right]\right\} dX'dY'dZ' \quad , \tag{6.10}$$

where

$$Q_{\pm}(X,Y,Z) = p_1(X,Y,Z)\, p_2^{(*)}(X,Y,Z) \quad .$$

As usual, (*) indicates that the complex conjugate applies only for the difference-frequency field. After a great deal of algebra to complete the square in X , we obtain

$$Q_{\pm}(X,Y,Z) = \frac{\Omega_1\Omega_2 P_{G1}P_{G2}}{(\Omega_1-iZ)(\Omega_2\mp iZ)} \exp\left\{ -(a_1'+a_2'^{(*)})Z+f_{\pm}(Z) \right.$$

$$\left. - \frac{2\Omega_1\Omega_2\mp i\Omega_{\pm}Z}{(\Omega_1-iZ)(\Omega_2\mp iZ)} \left[\left(X + \frac{i\Omega_1^2 D\phi_1(\Omega_2\mp iZ)\pm i\Omega_2^2 D\phi_2(\Omega_1-iZ)}{2\Omega_1\Omega_2\mp i\Omega_{\pm}Z} \right)^2 + Y^2 \right] \right\} , \tag{6.11}$$

where

$$f_{\pm}(Z) = \frac{i\Omega_1^2 D^2\phi_1^2 Z}{\Omega_1 - iZ} \pm \frac{i\Omega_2^2 D^2\phi_2^2 Z}{\Omega_2 \mp iZ}$$

$$- \frac{[\Omega_1^2 D\phi_1(\Omega_2 \mp iZ) \pm \Omega_2^2 D\phi_2(\Omega_1 - iZ)]^2}{(\Omega_1 - iZ)(\Omega_2 \mp iZ)(2\Omega_1\Omega_2 \mp i\Omega_{\pm}Z)} . \tag{6.12}$$

We therefore find that the integrals over X' and Y' in Equation (6.10) are simply convolutions of Gaussian functions. Combining Equations (6.10) and (6.11), and replacing Z' by η, we can reduce the field integral to

$$P_{\pm}(X,Y,Z) = i\Omega_1\Omega_2\Omega_{\pm}D^2P_o e^{-a_{\pm}'Z} \int_0^Z \exp\left\{ -a_{T_{\pm}}'\eta + f_{\pm}(\eta) \right.$$

$$\left. - \frac{2\Omega_1\Omega_2\mp i\Omega_{\pm}\eta}{A_{\pm}+B_{\pm}\eta} \left[\left(X + \frac{i\Omega_1^2 D\phi_1(\Omega_2\mp i\eta)\pm i\Omega_2^2 D\phi_2(\Omega_1-i\eta)}{2\Omega_1\Omega_2\mp i\Omega_{\pm}\eta} \right)^2 + Y^2 \right] \right\} \frac{d\eta}{A_{\pm}+B_{\pm}\eta} , \tag{6.13}$$

where

$$A_{\pm} = \Omega_1\Omega_2\left(1 - i\,\frac{2}{\Omega_{\pm}}\,Z\right) \tag{6.14}$$

and

$$B_{\pm} = \mp Z + i\left(2\,\frac{\Omega_1\Omega_2}{\Omega_{\pm}} \mp \Omega_{\pm}\right) . \tag{6.15}$$

Attenuation and dispersion are again combined in the factor

$$a'_{T_\pm} = a_{T_\pm} - i2\delta_\pm \Omega_\pm D^2 \quad , \tag{6.16}$$

where

$$a_{T_\pm} = \alpha_{T_\pm} z_o = (\alpha_1 + \alpha_2 - \alpha_\pm) z_o$$

and

$$\delta_\pm = 1 - \frac{k_1 \pm k_2}{k_\pm} \quad .$$

The normalized pressure coefficient is given as in Chapter IV by

$$P_o = \frac{\beta p_{G1} p_{G2}}{\rho_o c_o^2} \quad . \tag{6.17}$$

Finally, noting that for large Z ,

$$\frac{1}{A_\pm + B_\pm \eta} \sim \frac{i\Omega_\pm}{2\Omega_1\Omega_2 \mp i\Omega_\pm \eta} \frac{1}{Z} \quad , \quad Z >> 1 \quad ,$$

and using Equation (6.7), we find that the farfield asymptotic form of Equation (6.13) is given by

$$p_\pm(\theta_x, \theta_y, Z) \sim -\Omega_1\Omega_2\Omega_\pm^2 D^2 P_o \frac{e^{-a'_\pm Z}}{Z} \exp\{-\Omega_\pm^2 D^2 \theta^2 - i\Omega_\pm D^2 Z\theta^2\}$$

$$\cdot \int_0^Z \exp\left\{-a'_{T_\pm}\eta + f_\pm(\eta) + \Omega_1\Omega_2\Omega_\pm D^2\theta^2 \frac{\Omega_\pm - i2\eta}{2\Omega_1\Omega_2 \mp i\Omega_\pm\eta}\right.$$

$$\left. + 2\Omega_\pm D^2 \theta_x \frac{\Omega_1^2\phi_1(\Omega_2 \mp i\eta) \pm \Omega_2^2\phi_2(\Omega_1 - i\eta)}{2\Omega_1\Omega_2 \mp i\Omega_\pm\eta}\right\} \frac{d\eta}{2\Omega_1\Omega_2 \mp i\Omega_\pm\eta} \quad , \quad Z \to \infty \quad . \tag{6.18}$$

6.2 Difference-Frequency Field

Without loss of generality, we let the primary beam of frequency ω_2 be aligned with the z axis (i.e., $\phi_2 = 0$). For $\phi_1 = \phi$, as depicted in Figure 30, Equation (6.13) thus reduces to

$$p_-(X,Y,Z) = i\Omega_1\Omega_2\Omega_- D^2 P_o e^{-a_- Z} \int_0^Z \exp\left\{-a_T'\eta + \frac{i\Omega_1^2 D^2\phi^2\eta}{\Omega_1 - i\eta} - \frac{\Omega_1^4 D^2\phi^2(\Omega_2+i\eta)}{(\Omega_1-i\eta)(2\Omega_1\Omega_2+i\Omega_-\eta)}\right.$$
$$\left. - \frac{2\Omega_1\Omega_2+i\Omega_-\eta}{A_-+B_-\eta}\left[\left(X + \frac{i\Omega_1^2 D\phi(\Omega_2+i\eta)}{2\Omega_1\Omega_2+i\Omega_-\eta}\right)^2 + Y^2\right]\right\} \frac{d\eta}{A_-+B_-\eta} \quad , \qquad (6.19)$$

where

$$A_- = \Omega_1\Omega_2\left(1 - i\,\frac{2}{\Omega_-}\,Z\right)$$

and

$$B_- = Z + i\left(2\,\frac{\Omega_1\Omega_2}{\Omega_-} + \Omega_-\right) \quad .$$

As in Section 4.2, we have let $c_o = c_-$, and therefore $a_-' = a_-$. The subscripts on a_T and δ have again been omitted, where it is understood that

$$a_T' = a_T - i2\delta\Omega_- D^2 \quad ,$$

where

$$a_T = a_1 + a_2 - a_-$$

and

$$\delta = 1 - \frac{k_1 - k_2}{k_-} \quad .$$

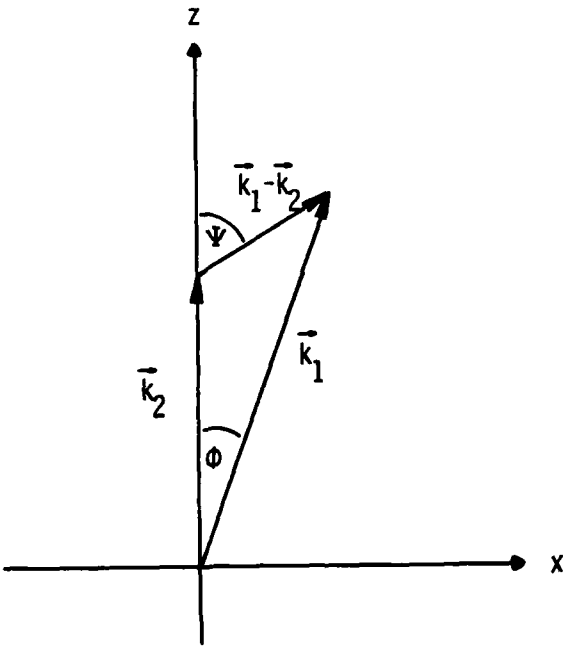

Figure 30. Geometry of Noncollinear Interaction of Gaussian Beams.

AS-83-730

Without making approximations, we have not been able to integrate Equation (6.19) analytically. Moreover, there appears to be no particular direction along which Equation (6.19) can be simplified when $\phi \neq 0$. We therefore begin by integrating Equation (6.19) numerically and investigating the difference-frequency pressure field via three-dimensional plots of the field in the x-z plane. Representative plots for a dispersionless fluid are presented in Figure 31, where $Y = 0$ and $\phi = 0°$, $2°$, and $4°$. The significant effects of noncollinear interaction are an overall attenuation of the pressure amplitude and a shift in the direction of maximum radiation. Note that when $\phi \neq 0$, there are no oscillations in the amplitude of the field. Based on the analysis in Section 5.1, oscillations might be expected as a result of noncollinear interaction. The slight irregular behavior of the amplitude near the origin in Figures 31b and 31c is due to an inadequacy in the number of points evaluated. Recall from Section 5.1 that spatial oscillations occur along the direction of $\vec{k}_1 - \vec{k}_2$. However, when ϕ is sufficiently large that the period of the spatial oscillations is on the order of the length of the interaction region, the angle formed by $\vec{k}_1 - \vec{k}_2$ and the direction of the array is so large that the oscillations go unnoticed.

A somewhat better perspective on the effects of noncollinear interaction is gained by examination of the farfield asymptotic form of Equation (6.19). For $\phi_1 = \phi$ and $\phi_2 = 0$, Equation (6.18) becomes

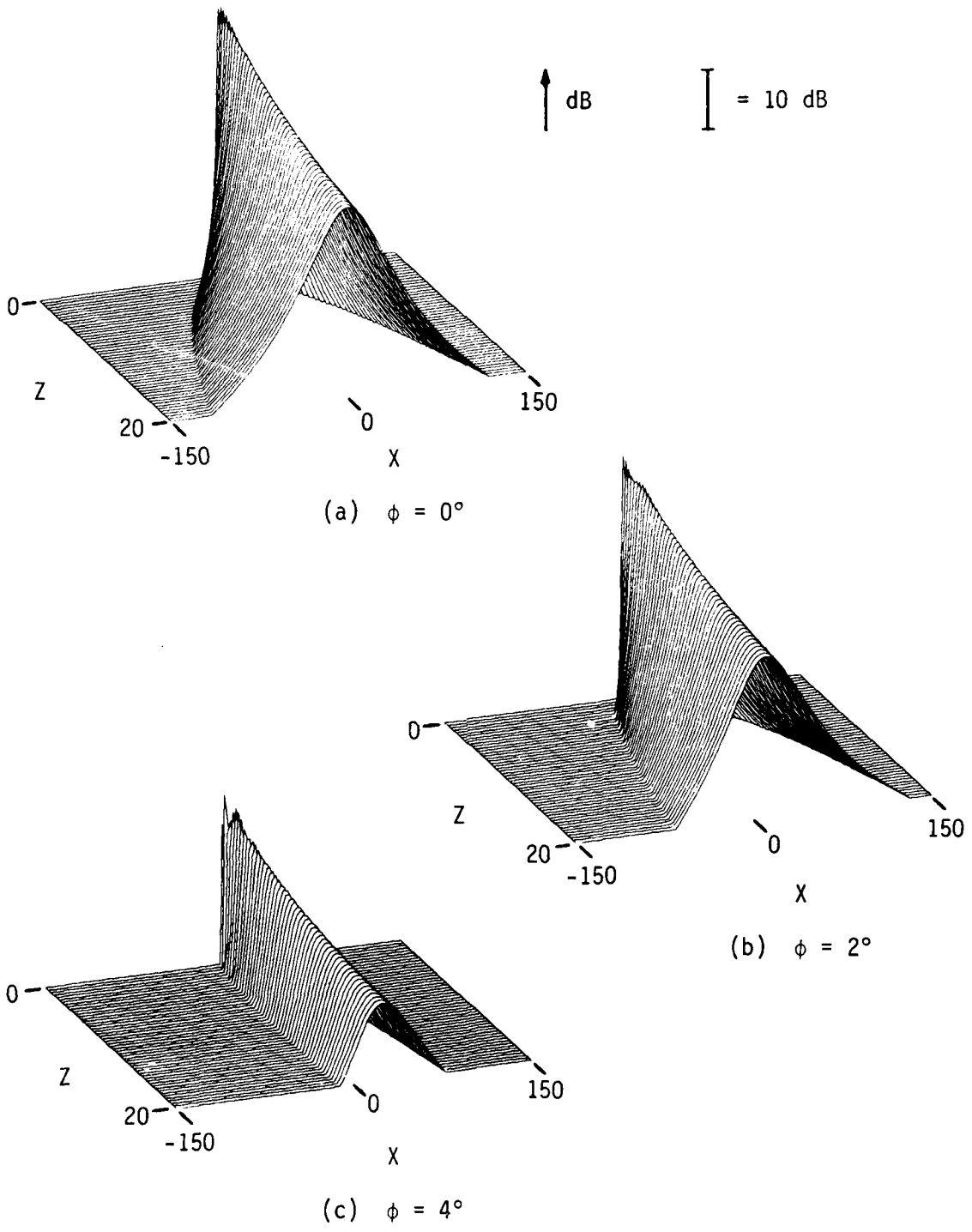

Figure 31. Difference-Frequency Pressure Field in the x-z Plane Resulting from Noncollinear Interaction of Gaussian Beams in a Dispersionless Fluid ($\Omega_- = 0.1$, $D = 30$, $a_{T_-} = 0.1$, $\delta_- = 0$, $\phi_1 = \phi$, $\phi_2 = 0$).

AS-83-731

$$p_-(\theta_x,\theta_y,Z)\sim-\Omega_1\Omega_2\Omega_-^2D^2P_o\,\frac{e^{-a_-Z}}{Z}\exp\{-\Omega_-^2D^2\theta^2-i\Omega_-D^2Z\theta^2\}$$

$$\cdot\int_0^\infty\exp\left\{-a_T'\eta+\frac{i\Omega_1^2D^2\phi^2\eta}{\Omega_1-i\eta}-\frac{\Omega_1^4D^2\phi^2(\Omega_2+i\eta)}{(\Omega_1-i\eta)(2\Omega_1\Omega_2+i\Omega_-\eta)}\right.$$

$$\left.+2\Omega_1^2\Omega_-D^2\phi\theta_x\,\frac{\Omega_2+i\eta}{2\Omega_1\Omega_2+i\Omega_-\eta}+\Omega_1\Omega_2\Omega_-D^2\theta^2\,\frac{\Omega_--i2\eta}{2\Omega_1\Omega_2+i\Omega_-\eta}\right\}\frac{d\eta}{2\Omega_1\Omega_2+i\Omega_-\eta}\,,$$

$$Z\to\infty\,. \qquad (6.20)$$

As shown in Appendix G, for an absorption-limited array where $\Omega_1\simeq\Omega_2$, Equation (6.20) reduces to

$$p_-(\theta_x,\theta_y,Z)\sim-\frac{\Omega_-^2D^2P_o}{2a_T}\,\frac{e^{-a_-Z}}{Z}\,\frac{\exp\{-(\Omega_-^2D^2/2)[(\theta_x-(\Omega_1/\Omega_-)\phi)^2+\theta_y^2]-i\Omega_-D^2Z\theta^2\}}{1+i(\Omega_-D^2/a_T)(\theta_x^2-\phi\theta_x+\theta_y^2-2\delta)}\,,$$

$$Z\to\infty\,,\quad 2a_T/\Omega_-\gg1\,. \qquad (6.21)$$

For collinear interaction, Equation (6.21) reduces to Equation (4.39).

The aperture factor in the numerator of Equation (6.21) is maximized when

$$\theta_x=\frac{\omega_1}{\omega_-}\phi\,,\quad\theta_y=0\,. \qquad (6.22)$$

Now the angle Ψ in Figure 30 is given by

$$\Psi=\phi+\sin^{-1}\left\{\frac{\sin\phi}{\sqrt{1-2(k_1/k_2)\cos\phi+(k_1/k_2)^2}}\right\}\,,$$

which for small ϕ and Ψ reduces to

$$\Psi \simeq \frac{k_1}{k_-} \phi \quad . \tag{6.23}$$

Comparing Equations (6.22) and (6.23), we find that the aperture factor is maximized when

$$\theta_x \simeq \Psi \quad , \quad \theta_y = 0 \quad .$$

The maximum therefore occurs in the approximate direction of $\vec{k}_1 - \vec{k}_2$. The same result was obtained in Section 5.2 for an array formed by nondiffracting Gaussian beams.

The modified Westervelt directivity function in Equation (6.21) is given, in the x-z plane (i.e., $\theta_y = 0$), by

$$D_\delta^G(\theta_x,0;\phi) = \frac{1}{1 + i(\Omega_- D^2/a_T)(\theta_x^2 - \phi\theta_x - 2\delta)} \quad . \tag{6.24}$$

Equation (6.24) is maximized when

$$\theta_x^2 - \phi\theta_x - 2\delta = 0 \quad . \tag{6.25}$$

The value of θ_x which satisfies Equation (6.25) is

$$\theta_x = \frac{1}{2} [\phi \pm \sqrt{\phi^2 + 8\delta}] \quad . \tag{6.26}$$

In a dispersionless fluid, where $\delta = 0$, $D_\delta^G(\theta_x,0;\phi)$ possesses two maxima, one at $\theta_x = 0$ and the other at $\theta_x = \phi$. That is, the maxima coincide with the directions of the primary beams. When the

discriminant $\phi^2 + 8\delta$ is positive, $D_\delta^G(\theta_x,0;\phi)$ always possesses two maxima. The two peaks merge into one when the discriminant is zero. For negative values of the discriminant, the maximum decreases in amplitude as $(\phi^2 + 8\delta)$ becomes increasingly negative. By comparison with our results for collinear interaction in dispersive fluids, we see that the combined effects of geometric and inherent dispersion resemble normal dispersion when $\phi^2 + 8\delta > 0$, and resemble anomalous dispersion when $\phi^2 + 8\delta < 0$. In this context, we are led to conclude that phase matching is accomplished only when $\phi^2 + 8\delta = 0$, i.e., when

$$\phi = \sqrt{-8\delta} \quad . \tag{6.27}$$

The result is again obtained that phase matching is possible with the parametric array only when $\delta \leq 0$. We note that solving the phase-matching condition given in Equation (5.49) yields a value for ϕ whi agrees with Equation (6.27) to within half of one percent for $-0.01 \leq \delta \leq 0$. The discussion in Section 5.2 of radiation from the interaction region is therefore supported by Equation (6.21).

As we found in Section 5.2, satisfaction of phase matching conditions by no means ensures that noncollinear interaction can be used to compensate for dispersion. The reason is that a price is paid for noncollinear interaction in that the length of the interaction region is shortened. Detrimental effects due to shortening of the interaction region are manifested through the combination of the aperture factor in Equation (6.21) and $D_\delta^G(\theta_x,0;\phi)$. When the phase matching condition given by Equation (6.27) is satisfied, we find from Equation (6.26) that $D_\delta^G(\theta_x,0;\phi)$ is maximized when $\theta_x = \phi/2$,

whereas the aperture factor is maximized when $\theta_x = (\Omega_1/\Omega_-)\phi$. The results in Chapter IV indicate that for high absorption, where Equation (6.21) is applicable, it is unlikely that the effects of dispersion are noticeable when $|\delta| < 0.001$. As an example, we thus let $\delta = -0.001$, for which the phase matching angle is found from Equation (6.27) to be $\phi \simeq 5°$. $D_\delta^G(\theta_x,0;\phi)$ is then maximized when $\theta_x \simeq 2.5°$, but if $\Omega_- = 0.1$, the aperture factor is maximized when $\theta_x \simeq 50°$. Unless the maxima of both $D_\delta^G(\theta_x,0;\phi)$ and the aperture factor coincide, the farfield pressure does not benefit from phase matching. The two contributions to the directivity function therefore compete in such a way that no significant compensation for dispersion can be attained by noncollinear interaction with an absorption-limited array.

As shown in Appendix H, Equation (6.20) reduces for a diffraction-limited array to

$$p_-(\theta_x,\theta_y,Z) \sim i\Omega_- D^2 P_o \frac{e^{-a_- Z}}{Z} \exp\{-i2a_T'/\Omega_-\}\, E_1\{-i2a_T'/\Omega_-\}$$

$$\cdot \exp\{-\Omega_1^2 D^2[(\theta_x - \phi)^2 + \theta_y^2] - \Omega_2^2 D^2\theta^2 - i\Omega_- D^2 Z\theta^2\} \quad ,$$

$$Z \to \infty \quad , \quad |2a_T'/\Omega_-| << 1 \quad . \qquad (6.28)$$

When $\phi = 0$, Equation (6.28) reduces to Equation (4.45). Again, the directivity function of a diffraction-limited array is given by the product of the primary-beam directivity functions. When $\phi \neq 0$, the direction of maximum radiation is shifted off axis, and the maximum pressure level is always less than that which occurs when $\phi = 0$.

Therefore, under no conditions should we expect to compensate for dispersion by noncollinear interaction with a diffraction-limited array.

As in Section 4.3, we need to define a directivity function for the difference-frequency field. For collinear interaction, we referred the pressure to that which occurs on axis in the absence of dispersion [see Equation (4.48)]. Here a similar ratio is employed, where the reference pressure on axis in the absence of dispersion is that which occurs when $\phi = 0$:

$$D_\delta(\theta_x,\theta_y;\phi) = \lim_{Z\to\infty} \frac{p_-(\theta_x,\theta_y,Z;\delta,\phi)}{p_-(0,0,Z;0,0)} \quad . \tag{6.29}$$

We therefore have for the two limiting cases

$$D_\delta(\theta_x,\theta_y;\phi) \sim \frac{\exp\{-(\Omega_-^2 D^2/2)[(\theta_x-(\Omega_1/\Omega_-)\phi)^2+\theta_y^2]-i\Omega_- D^2 Z\theta^2\}}{1+i(\Omega_- D^2/a_T)(\theta_x^2-\phi\theta_x+\theta_y^2-2\delta)} \quad , \quad 2a_T/\Omega_- >> 1 \ ,$$

$$\sim \exp\{-\Omega_1^2 D^2[(\theta_x-\phi)^2+\theta_y^2]-\Omega_2^2 D^2\theta^2-i\Omega_- D^2 Z\theta^2\} \quad , \quad |2a_T'/\Omega_-| << 1 \ .$$

The effect of noncollinear interaction in a dispersionless fluid on the farfield of the difference-frequency signal is shown in Figure 32. Discussion is restricted to directivity patterns for the x-z plane because ϕ does not affect the dependence of the directivity function on θ_y . Comparing Figure 32 with Figure 26, we find that diffraction of the primary beams causes the difference-frequency field to be far less sensitive to variations in ϕ than when the primaries do not experience diffraction. When there is no

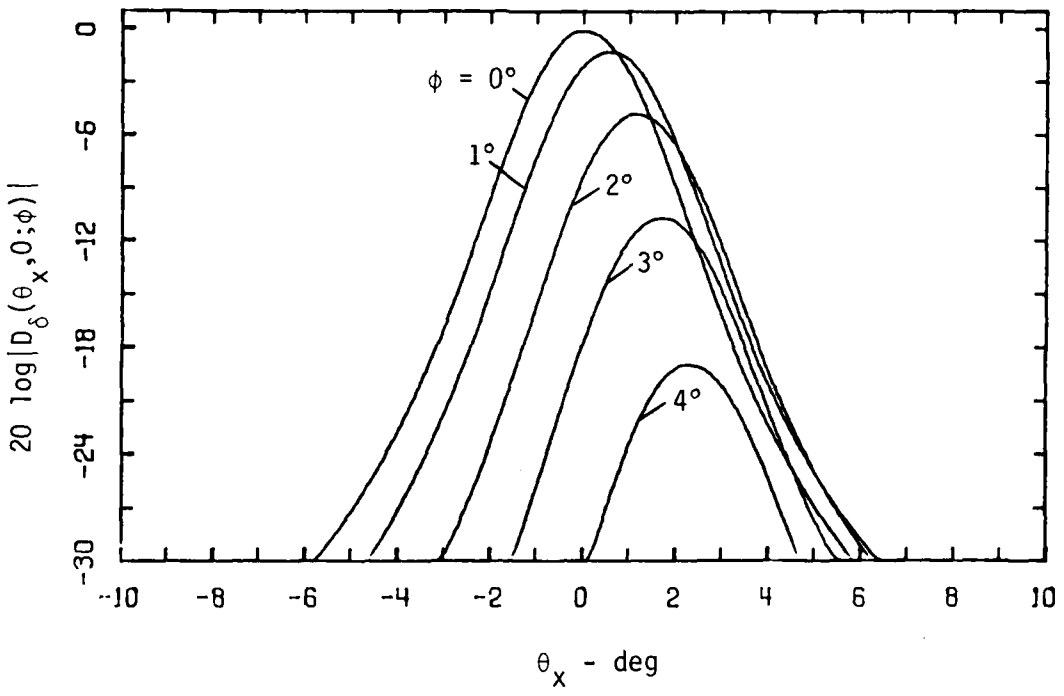

(a) $a_{T_-} = 0.01$

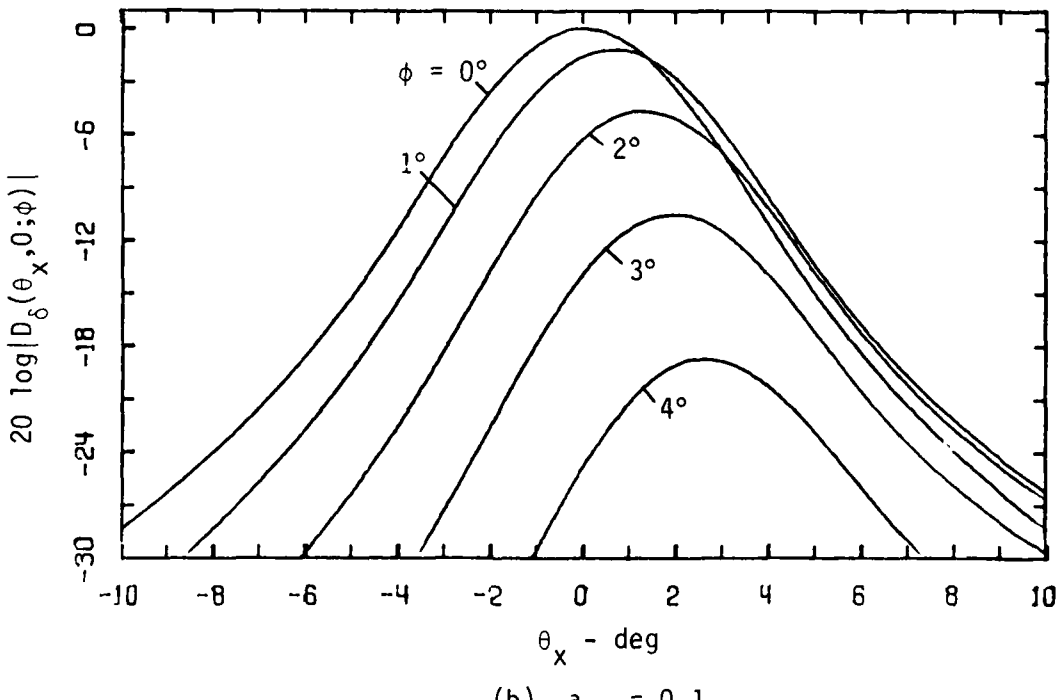

(b) $a_{T_-} = 0.1$

Figure 32. Difference-Frequency Field Directivity Pattern Resulting from Noncollinear Interaction of Gaussian Beams in a Dispersionless Fluid ($\Omega_- = 0.1$, D = 30, $\delta_- = 0$, $\phi_1 = \phi$, $\phi_2 = 0$).

AS-83-732

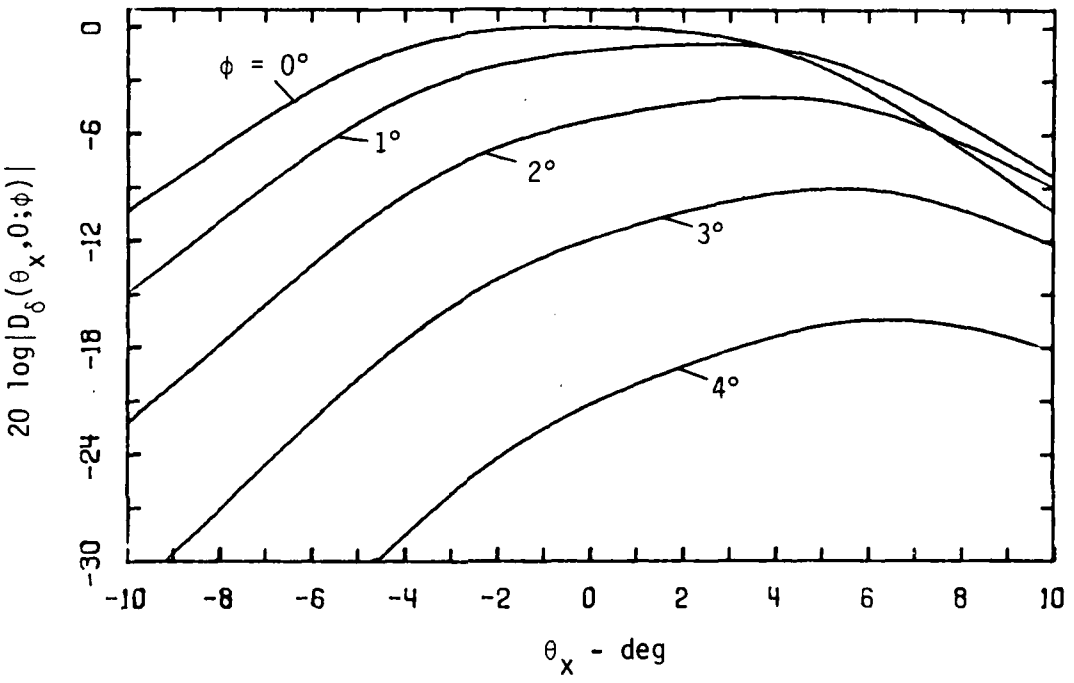

(c) $a_{T_-} = 1.0$

Figure 32. (continued)

AS-83-733

diffraction, noncollinear interaction produces significant shortening of the interaction region. Reduction of the interaction length diminishes the amplitude of the difference-frequency field. Because of diffraction, the width of the interaction region increases with distance, and therefore the amount by which the array is shortened as a result of noncollinear interaction is curtailed.

For a fixed nonzero value of ϕ, the direction of maximum radiation is shifted farther off axis as the absorption is increased. For low absorption, we find from Equation (6.28) that the difference-frequency signal is maximized at $\theta_x \simeq \phi/2$, i.e., at an angle half way between the maxima of the two primary beams. As absorption increases, the aperture factor in Equation (6.21) dominates the directivity function, and the direction of radiation of the difference-frequency signal thus tends toward that of $\vec{k}_1 - \vec{k}_2$, i.e., Ψ in Figure 30.

Presented in Figure 33 are results that are representative of the effect of noncollinear interaction in a dispersive fluid. For no combination of parameters did we observe any compensation for dispersion as a result of noncollinear interaction. Recall from Section 5.2 that for nondiffracting primaries, slight compensation is possible when $\delta < 0$. To obtain compensation requires that the interaction region be very narrow, a condition which is difficult to maintain when the primary beams experience diffraction.

In Section 5.1 we found that compensation for dispersion in plane-wave interaction can be achieved when $k_1 - k_2 \leq l_-$ by having the waves intersect at an angle for which $\vec{k}_1 - \vec{k}_2 = \vec{k}_-$ is satisfied. This method for phase matching of the difference-frequency signal does

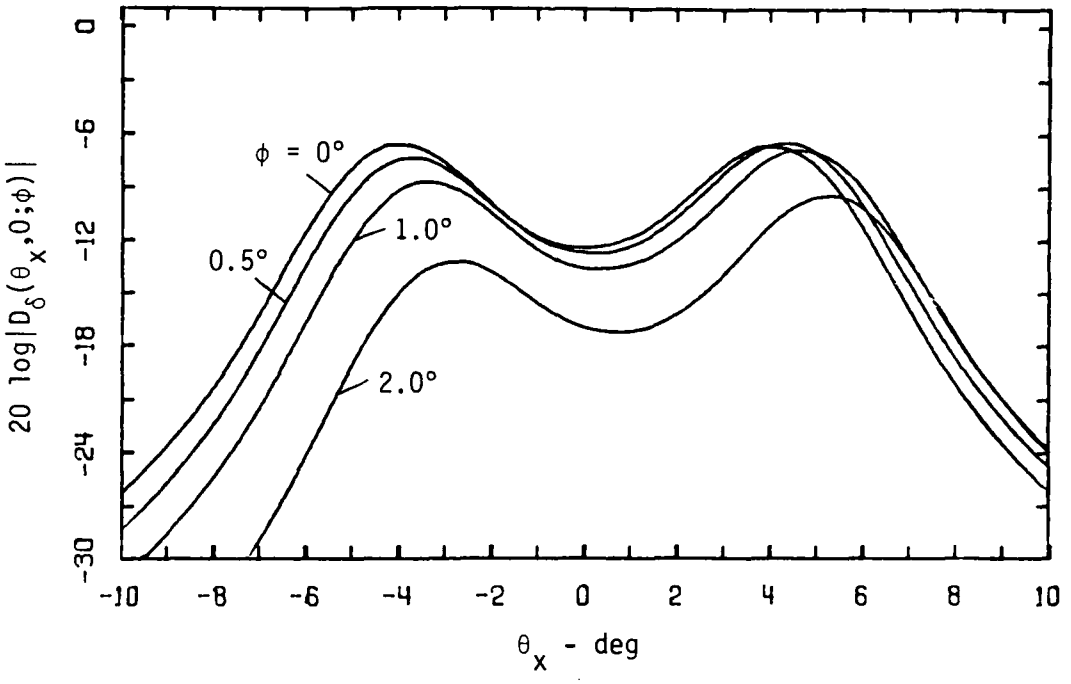

(a) $\delta_- = 0.003$

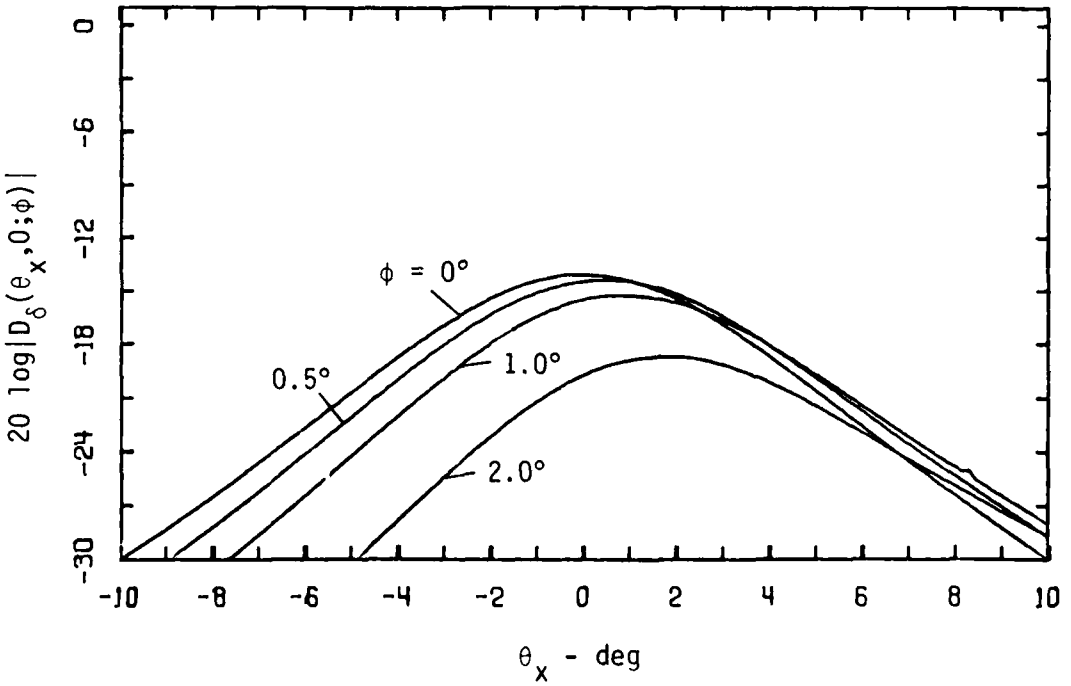

(b) $\delta_- = -0.003$

Figure 33. Difference-Frequency Field Directivity Pattern Resulting from Noncollinear Interaction of Gaussian Beams in a Dispersive Fluid ($\Omega_- = 0.1$, $D = 30$, $a_T = 0.1$, $\phi_1 = \phi$, $\phi_2 = 0$).

AS-83-734

not work for the parametric array because of the narrowness of the interaction region. When $k_1 \simeq k_2$, $\vec{k}_1 - \vec{k}_2$ is therefore not aligned with the interaction region. However, the vector sum $\vec{k}_1 + \vec{k}_2$ is always aligned with the interaction region. Now, the phase-matching condition for the sum frequency is

$$\vec{k}_1 + \vec{k}_2 = \vec{k}_+ \quad , \tag{6.30}$$

which is satisfied when the angle between the primaries is given by

$$\phi_o = 2 \sin^{-1} \sqrt{\frac{(k_1 + k_2)^2 - k_+^2}{4k_1k_2}} \quad . \tag{6.31}$$

We might therefore expect compensation for the effects of dispersion on sum-frequency generation to be possible for $k_1 + k_2 \geq k_+$ when ϕ is given by Equation (6.31). Preliminary results obtained from Equation (6.18) for the sum frequency do not indicate that compensation is possible. Because of time constraints, however, further investigation of this matter is necessary, because these results are, as yet, inconclusive.

In conclusion, it appears that noncollinear interaction of Gaussian beams cannot be used as a means of offsetting the detrimental effects of dispersion on generation of the difference-frequency signal. For $\delta > 0$, compensation for the effects of dispersion in infinite plane-wave interaction is achieved when $|\vec{k}_1 - \vec{k}_2| = k_-$. In Section 5.2, it was found that noncollinear interaction of highly collimated plane waves can be used to slight advantage when $\delta < 0$. Gaussian beams seem to fall somewhere in between. The interaction region is

too narrow to approximate infinite plane waves, yet spreading prohibits the beam from approximating highly collimated plane waves. In the event that the primaries are made so wide that the plane-wave case is approached, the purpose of the parametric array is defeated, that is, the difference-frequency signal is no longer radiated in a narrow beam. On the other hand, should the primaries be sufficiently narrow that the highly collimated plane-wave case is approached, the benefit obtained from noncollinear interaction when $\delta < 0$ is still very small.

CHAPTER VII

CONCLUSION

The original motivation for this investigation was to seek conditions for enhancing the efficiency of the parametric array.[65] The idea was to employ dispersive wave filtering, as suggested by Zabolotskaya and Soluyan[5] and discussed in Chapter I, to reduce energy transfer from the primaries to all components except the difference-frequency signal, and thus improve the efficiency of generation of the difference-frequency sound. When there is dispersion, the difference-frequency component is adversely affected as well as the other nonlinearly generated components. However, it is well known that for plane-wave interaction, the detrimental effects on the difference-frequency signal may be compensated by making the primary fields noncollinear. In particular, the angle should be chosen so that $\vec{k}_1 - \vec{k}_2 = \vec{k}_-$, where $\vec{k}_j$ is the wave vector for the plane wave of frequency ω_j.

The first part of this thesis is devoted to an investigation of the effect of dispersion on parametric arrays formed by collinearly interacting primary beams. There we note that dispersion causes the difference-frequency field to experience spatial oscillations within the interaction region. The spatial frequency of the oscillations increases with $|\delta|$, where $\delta = 1 - (k_1 - k_2)/k_-$ is the dispersion parameter. Diffraction of the primary beams also introduces slight phase mismatching, which affects the locations of the maxima and minima of the spatial oscillations. In particular, we find that in

the absence of dispersion, the phase speed of the lower-frequency primary is slightly greater than that of the higher-frequency primary within the paraxial region of Gaussian primary beams. This supports our result that the phase mismatch caused by diffraction can be offset by dispersion provided δ has a certain positive value. This conclusion contradicts that of both Karamzin, Sukhorukov, and Sukhorukova,[7] and Novikov,[9] who find that a negative value of δ is necessary. Given $\omega_1 > \omega_2$ (by convention), $c_1 \geq c_2 > c_-$ means that δ is positive, while $c_1 \leq c_2 < c_-$ means that δ is negative. Moreover, whereas it has been suggested[7] that the efficiency of the parametric array can be improved by offsetting the phase mismatch caused by diffraction, we find that the improvement is very small. For example, for Gaussian beams the maximum gain on axis is never more than 0.5 dB.

Dispersion also significantly affects the farfield radiation pattern. For an absorption-limited parametric array, where nonlinear interaction is restricted to the nearfield of the primaries, the directivity function may be written as the product of an aperture factor $A(\theta)$ and a modified Westervelt directivity function $D_\delta^W(\theta)$. The aperture factor, which depends on the cross-sectional shape of the primary beams, not on dispersion, is a weak function of θ throughout the paraxial region. The directivity function is thus determined primarily by $D_\delta^W(\theta)$. The Westervelt function gives the radiation pattern of a line array whose phasing depends on δ. When $\delta = 0$, the interaction region behaves as an end-fire array. For other values of δ the radiation behaves like that from bending waves on an infinite

plate. The case $\delta > 0$ corresponds to supersonic motion of the bending waves and $\delta < 0$ to subsonic motion. When $\delta > 0$, the direction of maximum radiation is shifted off axis to the angle $\cos^{-1}(1 - \delta)$, whereas when $\delta < 0$, radiation from the interaction region is of an evanescent nature, and the maximum, although diminished in amplitude, remains on axis. In both cases, dispersion causes the beamwidth to increase. Half-power angles for an absorption-limited array are given in Equation (2.37).

What are the prospects of observing these effects in practice? The striking effects of dispersion mentioned above occur only when $|\delta| > \alpha_T/k_-$, where $\alpha_T = \alpha_1 + \alpha_2 - \alpha_-$ is the combined attenuation coefficient. This condition seems to exclude most common acoustical media because it requires, in effect, strong dispersion and weak attenuation. For example, ordinary relaxing fluids have very small dispersion and large attenuation. Inhomogeneous fluids hold more promise. Bubbly water is perhaps the most readily available medium which combines strong dispersion with low attenuation. Another possibility is liquid-like viscoelastic solids of low shear modulus, for which dispersion is controlled by distributed inhomogeneities such as gas bubbles.

For the most part, dispersion affects the parametric array only in an adverse sense. That is, excluding compensation for the slight phase mismatch caused by diffraction, dispersion produces lower far-field levels and wider beam patterns. Conceivably, an understanding of the effect of dispersion on the parametric array may be used to evaluate various dispersion parameters in strongly dispersive fluids.

The second part of this thesis is an investigation of parametric arrays formed by noncollinear interaction. Specifically, we examine

conditions for which it may be possible to compensate for the effects of dispersion on the difference-frequency signal. Within the interaction region, phase matching occurs at the angle of intersection defined by $\vec{k}_1 - \vec{k}_2 = \vec{k}_-$. This condition can be satisfied only if $\delta \geq 0$. For noncollinear interaction, however, $\vec{k}_1 - \vec{k}_2$ is not aligned along the length of the interaction region. In fact, when $k_1 \simeq k_2$, $\vec{k}_1 - \vec{k}_2$ can form a very large angle with the array for even small angles formed by the two primaries. Therefore, since the difference-frequency signal is amplified along the direction of $\vec{k}_1 - \vec{k}_2$, the interaction length is significantly reduced when narrow primary beams interact noncollinearly. If the primaries are sufficiently wide that efficient amplification is possible for noncollinear interaction, the purpose of the parametric array is defeated. In other words, one no longer obtains a narrow directivity pattern. On the other hand, for a parametric array formed by highly collimated plane waves, compensation for the effect of dispersion on the farfield radiation is impossible when $\delta > 0$, whereas small compensation can occur when $\delta < 0$. Now the interaction region behaves as a line array whose phasing is given by the projection of $\vec{k}_1 - \vec{k}_2$ along its length. Theoretically, phase matching then occurs when the component of $\vec{k}_1 - \vec{k}_2$ along the array matches $\vec{k}_-$. The angle between the primary beams at which this occurs is approximately $\sqrt{-8\delta}$ radians. The price paid for noncollinear interaction of narrow primaries is significant shortening of the array. Therefore, only for very small angles of intersection does noncollinear interaction ever improve the farfield radiation. Because of spreading, a parametric array formed by Gaussian primary beams is far less sensitive to noncollinear interaction than is one formed by collimated plane waves.

AD-A130 533 PARAMETRIC ACOUSTIC ARRAY FORMATION VIA WEAK COLLINEAR AND NONCOLLINEAR I.. (U) TEXAS UNIV AT AUSTIN APPLIED RESEARCH LABS M F HAMILTON JUN 83 ARL-TR-83-19 3/3

UNCLASSIFIED N00014-79-C-0624 F/G 17/1 NL

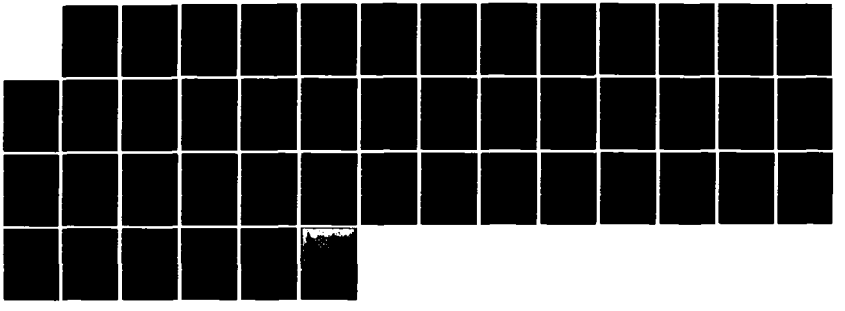

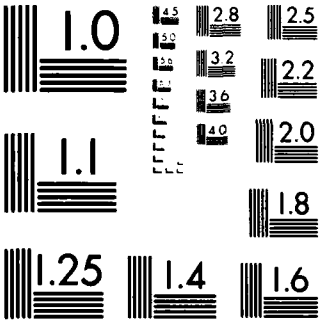

For the same reason, there appears to be no advantage resulting from noncollinear interaction of Gaussian beams.

Generation of the sum-frequency component poses a somewhat different situation. Whereas $\vec{k}_1 - \vec{k}_2$ is not aligned with the interaction region in the case of noncollinear interaction, $\vec{k}_1 + \vec{k}_2$ always appears to be properly aligned. One might therefore expect compensation for the effect of dispersion on the sum-frequency signal to be possible under certain conditions. Because of a lack of time, our results concerning phase matching for the sum-frequency signal via noncollinear interaction are inconclusive, and further work in this area is necessary.

In summary, this thesis provides a detailed analysis of the effect of dispersion on the parametric array, as well as an investigation of what happens when the primaries interact noncollinearly. Specifically, solutions are given for the difference-frequency components generated by weak collinear and noncollinear interaction of Gaussian beams in a dispersive fluid. In addition, solutions are obtained for sum-frequency and second-harmonic components. By way of the transformation in Appendix C, the solutions for collinear interaction approximate the paraxial region of fields resulting from primaries which are radiated by a uniformly excited circular piston. The results of the transformation are compared with data obtained from parametric arrays formed in water, where the dispersion is negligible.

A potentially fruitful avenue for future research might be to investigate ways of improving the conditions that result from noncollinear interaction. For example, a way to keep the difference-frequency signal within the interaction region as it propagates along the direction of $\vec{k}_1 - \vec{k}_2$ is to confine the array within a waveguide.

In fact, two parallel plane interfaces, separated by a distance less than the width of the primaries, provide the appropriate boundaries if the beams intersect in a plane that is perpendicular to the interfaces. Such a configuration may be exploited, for example, in a shallow water channel or other suitably layered media. Preliminary analyses by Ostrovskii and Papilova[66] and Yeager[67] have considered nonlinear interaction of modes in waveguides. A possible course of study is to extend these analyses and calculate the difference-frequency field resulting from noncollinear interaction of Gaussian beams in a waveguide. Results may then be compared with those obtained in this thesis. Because significant compensation for the effects of dispersion should be attainable with the use of a waveguide, more efficient amplification of the difference-frequency signal may be possible as a result of dispersive wave filtering. However, evaluation of the increase in efficiency, as well as extension of the analysis to strong nonlinear interactions, requires that all spectral components generated by the interaction be considered. The analysis then requires numerical solution of the nonlinear wave equation.

APPENDIX A

EIGENFUNCTIONS OF THE PARAXIAL WAVE EQUATION FOR AXISYMMETRIC RADIATION

As in Chapter III, here we shall obtain a solution of the nonlinear paraxial wave equation, Equation (3.15), for both the sum- and difference-frequency fields by the method of successive approximations. However, we now assume that the field is axisymmetric, and therefore the pressure depends only on the coordinate pair (ε,z), where $\varepsilon^2 = x^2 + y^2$. We again begin by deriving the Green's function, g_ω, for Equation (3.15), after which we shall obtain the eigenfunctions for the linearized paraxial wave equation. For axisymmetric fields, the Green's function problem becomes

$$\frac{\partial g_\omega}{\partial z} + (\alpha'_\omega + \frac{ic_o}{2\omega} \nabla_\perp^2) g_\omega = \frac{1}{\varepsilon} \delta(\varepsilon - \varepsilon') \delta(z - z') \quad , \tag{A1}$$

where $\delta(\cdot)$ is the Dirac delta function. The boundary condition is

$$g_\omega(\varepsilon,z|\varepsilon',z') = 0 \quad , \quad \text{for} \quad z \leq 0 \quad . \tag{A2}$$

Because the field is axisymmetric with respect to the z axis, we have

$$\nabla_\perp^2 g_\omega = \frac{1}{\varepsilon} \frac{\partial}{\partial \varepsilon} (\varepsilon \frac{\partial g_\omega}{\partial \varepsilon}) \quad .$$

By way of the Hankel transform pair

$$g_\omega(\varepsilon,z|\varepsilon',z') = \int_0^\infty G_\omega(k_\varepsilon,z) \, J_o(k_\varepsilon \varepsilon) \, k_\varepsilon dk_\varepsilon \quad , \tag{A3}$$

$$G_\omega(k_\varepsilon, z) = \int_0^\infty g_\omega(\varepsilon, z|\varepsilon', z')\ J_o(k_\varepsilon \varepsilon)\ \varepsilon d\varepsilon \quad , \tag{A4}$$

we can rewrite Equation (A1) in terms of G_ω as

$$\frac{\partial G_\omega}{\partial z} + (\alpha'_\omega - \frac{ic_o}{2\omega} k_\varepsilon^2)\ G_\omega = J_o(k_\varepsilon \varepsilon')\ \delta(z - z') \quad . \tag{A5}$$

The solution of Equation (A5) that satisfies Equation (A2) is

$$G_\omega(k_\varepsilon, z) = J_o(k_\varepsilon \varepsilon') \int_0^z \exp\left\{-(\alpha'_\omega - \frac{ic_o}{2\omega} k_\varepsilon^2)(z - \eta)\right\}\ \delta(\eta - z')\ d\eta$$

$$= J_o(k_\varepsilon \varepsilon')\ \exp\left\{-(\alpha'_\omega - \frac{ic_o}{2\omega} k_\varepsilon^2)(z - z')\right\}\ H(z - z') \quad , \tag{A6}$$

where $H(z)$ is the Heaviside unit step function. Combining Equations (A3) and (A6) yields

$$g_\omega(\varepsilon, z|\varepsilon', z') = e^{-\alpha'_\omega(z-z')}\ H(z - z') \int_0^\infty \exp\left\{\frac{ic_o}{2\omega}\ (z - z')\ k_\varepsilon^2\right\}$$

$$\cdot J_o(k_\varepsilon \varepsilon)\ J_o(k_\varepsilon \varepsilon')\ k_\varepsilon dk_\varepsilon \quad ,$$

which we can evaluate using integral tables[44] to obtain

$$g_\omega(\varepsilon, z|\varepsilon', z') = \frac{i\omega}{c_o} \frac{e^{-\alpha'_\omega(z-z')}}{z-z'} J_o\left\{\frac{\omega\varepsilon\varepsilon'}{c_o(z-z')}\right\} \exp\left\{-\frac{i\omega}{2c_o}\left[\frac{\varepsilon^2 + \varepsilon'^2}{z-z'}\right]\right\} H(z-z') \quad . \tag{A7}$$

We may now write the solution of the homogeneous paraxial wave equation,

$$\frac{\partial p_\omega}{\partial z} + (\alpha'_\omega + \frac{ic_o}{2\omega} \nabla_\perp^2)\ p_\omega = 0 \quad , \tag{A8}$$

in integral form as

$$p_\omega(\varepsilon,z) = \int_0^\infty p_\omega(\varepsilon',0)\ g_\omega(\varepsilon,z|\varepsilon',0)\ \varepsilon' d\varepsilon' \quad .$$

Since the eigenfunctions of Equation (A8) can be generated with orthogonal Gauss-Laguerre functions,[42,43] we expand the boundary condition for Equation (A8), $p_\omega(\varepsilon,0)$, accordingly:

$$p_\omega(\xi,0) = \sum_{n=0}^{\infty} P_n L_n(2\xi^2)\ e^{-\xi^2}, \tag{A9}$$

where $\xi = \varepsilon/\varepsilon_o$. The Laguerre polynomials are defined by[41]

$$L_n(x) = e^x \frac{d^n}{dx^n}(x^n e^{-x}) \quad ,$$

and satisfy the orthogonality relation[41]

$$\int_0^\infty L_m(2x^2)L_n(2x^2)e^{-2x^2}\, x\, dx = \delta_{mn}\left(\frac{n!}{2}\right)^2 \quad , \tag{A10}$$

where δ_{mn} is the Kronecker delta function. Using Equation (A10), we can evaluate the coefficients in Equation (A9):

$$P_n = \left(\frac{2}{n!}\right)^2 \int_0^\infty p_\omega(\xi,0)L_n(2\xi^2)e^{-\xi^2}\ \xi d\xi \quad .$$

Using the integral form of Equation (A8), we thus obtain, after inserting Equations (A7) and (A9),

$$p_\omega(\xi,Z) = i2\Omega \frac{e^{-a'_\omega Z}}{Z} e^{-i\frac{\Omega\xi^2}{Z}} \sum_{n=0}^{\infty} P_n \int_0^{\infty} L_n(2\xi'^2)$$

$$\cdot J_o(2\Omega\xi\xi'/Z)\ \exp\left\{-(1 + i\frac{\Omega}{Z})\ \xi'^2\right\} \xi' d\xi' \quad . \qquad \text{(A11)}$$

The dimensionless parameters in Equation (A11) are defined as in Section 3.3:

$$Z = \frac{z}{z_o} \quad , \quad a'_\omega = \alpha'_\omega z_o \quad , \quad z_o = \frac{\omega_o \varepsilon_o^2}{2c_o} \quad , \Omega = \frac{\omega}{\omega_o} \quad .$$

Resorting once again to integral tables,[44] we can express Equation (A11) as

$$p_\omega(\xi,Z) = \sum_{n=0}^{\infty} P_n E_n(\xi,Z;\Omega) \quad , \qquad \text{(A12)}$$

where

$$E_n(\xi,Z;\Omega) = \frac{e^{-a'_\omega Z}}{1-iZ/\Omega} L_n\left\{\frac{2\xi^2}{1+(Z/\Omega)^2}\right\} \exp\left\{-\frac{\xi^2}{1-iZ/\Omega} + i2n \tan^{-1}(Z/\Omega)\right\} \quad .$$

The orthogonality relation satisfied by the eigenfunctions is

$$\int_0^{\infty} E_m(\xi,Z;\Omega)\ E_n^*(\xi,Z;\Omega)\ \xi d\xi = \delta_{mn}\left(\frac{n!}{2}\right)^2 e^{-2a_\omega Z} \quad .$$

Now we solve the inhomogeneous paraxial wave equation for the sum- and difference-frequency pressure:

$$\frac{\delta p_\pm}{\delta z} + \left(\alpha'_\pm + \frac{ic_o}{2\omega_\pm}\nabla_\perp^2\right) p_\pm = \frac{i\beta\omega_\pm}{2\rho_o c_o^3} Q_\pm \quad . \qquad \text{(A13)}$$

In the second approximation, the source term is $Q_{\pm} = p_1 p_2^{(*)}$, where p_1 and p_2 are solutions of Equation (A8), and $(*)$ indicates that the complex conjugate applies only for the difference frequency. Using Equation (A12), we can express the source term as

$$Q_{\pm}(\xi,Z) = \sum_{m=0}^{\infty}\sum_{n=0}^{\infty} P_m P_n^{(*)} \; E_m(\xi,Z;\Omega_1)E_n^{(*)}(\xi,Z;\Omega_2) \; . \quad \text{(A14)}$$

The solution of Equation (A13) is given by

$$p_{\pm}(\varepsilon,z) = \frac{i\beta\omega_{\pm}}{2\rho_o c_o^3} \iint_0^{\infty} Q_{\pm}(\varepsilon',z')g_{\pm}(\varepsilon,z|\varepsilon',z') \; \varepsilon' d\varepsilon' dz' \quad , \quad \text{(A15)}$$

where we have assumed $p_{\pm}(\varepsilon,0) = 0$. After inserting Equations (A7) and (A14) into Equation (A15), we obtain

$$p_{\pm}(\xi,Z) = -2\Omega_{\pm}^2 D^2 \sum_{m=0}^{\infty}\sum_{n=0}^{\infty} P_{mn} \int_0^Z\int_0^{\infty} E_m(\xi',Z';\Omega_1) \; E_n^{(*)}(\xi',Z';\Omega_2)$$
$$\cdot \frac{e^{-a_{\pm}'(Z-Z')}}{Z-Z'} J_o\left[\frac{2\Omega_{\pm}\xi\xi'}{Z-Z'}\right] \exp\left\{-i\Omega_{\pm}\left[\frac{\xi^2+\xi'^2}{Z-Z'}\right]\right\} \; \xi' d\xi' dZ' \quad ,$$

where $D = \omega_o\varepsilon_o/2c_o$, and

$$P_{mn} = \frac{\beta P_m P_n^{(*)}}{\rho_o c_o^2} \quad .$$

APPENDIX B

COMPLEX EXPONENTIAL INTEGRALS

The complex exponential integrals are defined by[46]

$$E_n(z) = \int_1^\infty \frac{e^{-zt}}{t^n}\, dt \quad , \quad \mathrm{Re}(z) > 0 \quad , \tag{B1}$$

where n is any integer. The recurrence relations for Equation (B1) are

$$E_{n-1}(z) = \frac{1}{z}\left[e^{-z} + (1-n)\, E_n(z)\right] \quad , \quad n = 0,-1,-2, \ldots \tag{B2}$$

$$E_{n+1}(z) = \frac{1}{n}\left[e^{-z} - zE_n(z)\right] \quad , \quad n = 1,2,3, \ldots \quad . \tag{B3}$$

All of the exponential integrals can thus be calculated, at least in theory, if we have $E_o(z)$ and $E_1(z)$ to begin Equations (B2) and (B3), respectively.

If we assume $\mathrm{Re}(z) > 0$, then Equation (B1) yields

$$E_o(z) = \frac{e^{-z}}{z} \quad . \tag{B4}$$

However, in equations such as (4.12) and (4.16), the arguments of the exponential integrals can be located anywhere in the complex plane. The dilemma is resolved by noting that exponential integrals usually come in pairs as a result of integrals of the form

$$\int_{\alpha}^{\beta} \frac{e^{-zt}}{t^n}\,dt = \int_{\alpha}^{\infty} \frac{e^{-zt}}{t^n}\,dt - \int_{\beta}^{\infty} \frac{e^{-zt}}{t^n}\,dt$$

$$= \alpha^{1-n}E_n(\alpha z) - \beta^{1-n}E_n(\beta z) \quad . \tag{B5}$$

If the integral on the left-hand side of Equation (B5) is bounded, there are no restrictions on the arguments αz and βz (excluding the obvious singularities at zero and $-\infty$). For example, when $n = 0$, the exponential integrals in Equation (B5) are given by Equation (B4), even when the real parts of the arguments are negative.

Likewise, if we assume $\mathrm{Re}(z) > 0$ and make a simple change of variable, we obtain from Equation (B1)

$$E_1(z) = \int_{z}^{\infty} \frac{e^{-t}}{t}\,dt \quad , \quad |\arg z| < \pi \quad , \tag{B6}$$

which has a branch cut along the negative real axis. Like Equation (B4), Equation (B6) can be evaluated anywhere in the complex plane. At the end of this appendix is listed a computer program which evaluates $E_1(z)$ for arbitrary complex arguments.

Care must always be taken when using recurrence formulas. Although Equation (B2) is stable and can be used in either ascending or descending order, Equation (B3) becomes unstable when $|z| \gg n$, and should then be used in descending order. Unfortunately, we must use Equation (B3) in ascending order because the only function to which we have access is $E_1(z)$. Problems with Equation (B3) occur because

$$E_n(z) \sim \frac{e^{-z}}{z} \quad , \quad |z| >> |n| \quad .$$

Specifically, if by recursion we obtain $E_n(z) \simeq z^{-1}e^{-z}$, then from Equation (B3) we have $E_{n+1}(z) \simeq 0$ which, along with all subsequent values, is useless. This particular numerical difficulty can often be avoided by using the large $|z|$ asymptotic expansion[46]

$$E_n(z) \sim \frac{e^{-z}}{z}\left[1 - \frac{n}{z} + \frac{n(n+1)}{z^2} - \frac{n(n+1)(n+2)}{z^3} + \ldots\right] \quad . \qquad (B7)$$

Evaluation of exponential integrals for which n is negative can be performed quite accurately with Equation (B2). However, when $-n >> |z|$, $|E_n(z)|$ tends to grow as $(-n)!$. The problem which arises is of course the convergence of a series such as

$$\sum_{n=-\infty}^{\infty} \alpha_n E_n(z) \quad .$$

Equation (4.38) is a case in point, for which the series can be written as

$$\sum_{n=-\infty}^{\infty} I_{1-n}(4D^2\theta^2)\; E_n\{2D^2(\theta^2 - 2\delta) - i2a_T/\Omega_-\} \quad , \qquad (B8)$$

where I_n are modified Bessel functions of the first kind. When $4D^2\theta^2 < 1$, I_n approaches zero rapidly as $|n|$ increases, and Equation (B8) converges rapidly. It is when $4D^2\theta^2 > 1$ that the behavior of E_n becomes important, because for small $|n|$, I_n approaches zero very slowly. Not until $|n|$ becomes large does I_n eventually go to zero as $|n|^{-|n|}$. Problems can thus arise

when the argument of E_n becomes small, which for Equation (B8) occurs around $\theta^2 = 2\delta$. Specifically, if $2a_T/\Omega_-$ is small and $4D^2\theta^2 > 1$, Equation (B8) converges slowly when $\theta^2 \simeq 2\delta$.

In Figure 34 is listed a program, designed by McKendree,[68] which evaluates $E_1(z)$ as defined in Equation (B6). For any complex number z, the routine returns $E_1(z)$ with five places of accuracy. When $|z| < 3$, the exact expansion[46]

$$E_1(z) = -\gamma - \ln z - \sum_{n=1}^{\infty} \frac{(-z)^n}{nn!} \qquad \text{(B9)}$$

is used, where $\gamma = 0.57721$ is Euler's constant. When $|z| > 15$, the asymptotic expansion in Equation (B7) is used with $n = 1$. For $3 < |z| < 15$, the polynomial approximation described by Hershey[69] is used.

Note that when the value of z is such that the program uses Equation (B9) to evaluate $E_1(z)$, a branch cut exists along the negative real axis because of the presence of the term $\ln z$. When the branch cut is crossed, the phase of $E_1(z)$ changes by 2π. Therefore, when generating curves depending on arguments of $E_1(z)$ which cross the negative real axis, one might have to add or subtract 2π from the phase term in line 33 of the program.

```
      COMPLEX FUNCTION E1(Z)
      REAL APO(14),CPO(14)
      COMPLEX Z, GLZ, CTERM, ZINV, CORR, ZN, RE1, CSUM, ARG, P, Q
      REAL ZPR, ZPI, ZR, ZI, SUMR, SUMI, DENOM, DFACT, SIGN, ZDR, ZDI,
     1 DN
      DATA GAMMA /0.577215664/, RMX/15./, RMN/3./
      DATA AINF/7.E75/,ALIM/174.6/,BLIM/-177.3/
C
C     COEFFICIENTS FOR RATIONAL POLYNOMIAL APPROXIMATION.
C
      DATA     APO/-51.84471746, 1113.21866, -13030.1734, 92167.7640,
     1             -413031.176, 1196450.66, -2246393.77, 2701660.92,
     2             -2025134.77, 901637.337, -219656.339, 25224.8375,
     3             -983.262854, 2.84007982/
      DATA     CPO/-52.84471746, 1164.06604, -14094.5451, 104227.260,
     1             -494905.409, 1545152.90, -3195508.10, 4354093.96,
     2             -3834455.23, 2119769.51, -693517.213, 122583.807,
     3             -9871.30676, 244.9130177/
C
C     DETERMINE IF LARGE Z OR SMALL Z SERIES IS REQUIRED,
C     AND WHICH FORM FOR THE CORRECTION, IF EITHER, IS NEEDED.
C
      R=CABS(Z)
      IF (R .EQ. 0.) GO TO 6000
      IF (R .GT. RMX) GO TO 4000
      IF (REAL(Z) .LT. 0.) GO TO 900
      IF (RMN .LT. R) GO TO 2000
C
C     SET UP FIRST TWO TERMS OF E1(Z) IN GLZ,
C     AND INITIALIZE THE LOOP VARIABLES.
C
900   AMP=-ALOG(R)-GAMMA
      PHS=-ATAN2(AIMAG(Z),REAL(Z))
      GLZ=CMPLX(AMP,PHS)*Z
      TEST=1.E-6 * CABS(GLZ)
      SIGN=1.00
      N=1
      ZR=REAL(Z)
      ZI=AIMAG(Z)
      ZPR=ZR
      ZPI=ZI
      DFACT=1.00
      SUMR=0.00
      SUMI=0.00
C
C     LOOP TO EVALUATE THE SERIES TERM BY TERM.  ASCENDING POWERS OF Z
C     ARE COMPUTED IN ZPR AND ZPI, VALUES OF N FACTORIAL IN DFACT.
C
1000  N=N+1
      SIGN=-SIGN
      DN=FLOAT(N)
      DFACT=DFACT*DN
      DENOM=SIGN/(DFACT*DN)
      ZDR=ZPR*ZR-ZPI*ZI
      ZDI=ZPR*ZI+ZPI*ZR
      ZPR=ZDR
      ZPI=ZDI
```

Figure 34. Complex $E_1(z)$ Subroutine.

AS-83-735

```
      ZDR=ZDR*DENOM
      ZDI=ZDI*DENOM
      SUMR=SUMR+ZDR
      SUMI=SUMI+ZDI
      TERM=ABS(ZDR)+ABS(ZDI)
C
C     THE SERIES IS FINISHED IF THE CURRENT TERM IS LESS THAN .00001
C     OF THE FIRST TERM.  ALSO, IF N HAS GROWN TO 54, THE FACTORIAL WILL
C     FAIL AT THE NEXT TERM, AND THE LARGE Z EXPANSION MUST BE USED.
C
      IF (N .GT. 53) GO TO 4000
      IF (TERM .GT. TEST) GO TO 1000
C
C     ADD FIRST TWO TERMS TO THE REMAINDER, AND RETURN.
C
      E1=GLZ+CMPLX(SUMR,SUMI)
 8888 RETURN
C
C     RATIONAL POLYNOMIAL APPROXIMATION TO THE CORRECTION TERM.
C
 2000 ZINV=1./Z
      ZN=ZINV
      P=ZINV
      Q=ZINV
      K=0
C
C     LOOP TO ACCUMULATE NUMERATOR AND DENUMINATOR TERMS OF THE RATIONAL
C     POLYNOMIAL.
C
      DO 2500 K=1,14
      ZN=ZN*ZINV
      P=P+APQ(K)*ZN
      Q=Q+CPQ(K)*ZN
 2500 CONTINUE
      CORR=P/Q
      ZINV=-ZINV
      GO TO 5500
C
C     HERE THE COMPLEX EXPONENTIAL FORM IS USED.
C
 4000 ZN=CMPLX(1.,0.)
      ZINV=ZN/Z
      RS=1.
      FACTI=1.
      N=0
      NMAX=IFIX(R+0.5)
      IF (NMAX .GT. 20) NMAX=20
      CORR=CMPLX(1.,0.)
      N1=NMAX-2
C
C     TO THE EXPONENTIAL LARGE Z EXPANSION.  IF THE CORRECTION TERM,
C     WHICH IS IN DESCENDING POWERS OF Z, BECOMES LESS THAN 1.E-6
C     THE CORRECTION TERM IS CONSIDERED EVALUATED.
C
 4500 RS=-RS
      N=N+1
      IF (N .GT. N1) GO TO 4700
      FACTI=FACTI*FLOAT(N)
      ZN=ZN*ZINV
      CTERM=RS*ZN*FACTI
```

Figure 34. (continued)

AS-83-736

```
      CORR=CONJG(CTERM)
      IF (CABS(CTERM) .GT. 1.E-6) GO TO 4500
4700  IF (NMAX .EQ. 20) GO TO 5500
C
C     COMPUTE APPROXIMATION TO REMAINDER TERM.
C
      N1=NMAX-1
      ZN=-1./Z
      ZN=ZN**N1
      FACTI=0.5
      DO 5200 I=2,N1
      FACTI=FACTI*FLOAT(I)
5200  CONTINUE
      RE1=ZN*FACTI
      CORR=CONJG(RE1)
C
C     ASYMPTOTIC LARGE Z EXPANSION.
C     CHECK FOR DATA OUT OF RANGE.
C
5500  R=REAL(Z)
      IF (R .GE. ALIM) GO TO 5700
      CLIM=ALOG(CABS(Z))+BLIM
      IF (R .LE. CLIM) GO TO 5600
C
C     EXPONENTIAL WILL BE 'FINITE' USE CONNECTED EXPONENTIAL FORM.
C
      E1=ZINV*CEXP(-Z)*CORR
      GO TO 8888
C
C     DATA OUT OF RANGE COMPUTATION.
C     EXPONENTIAL WOULD HAVE BLOWN DOWN SO RETURN ZERO.
C
5600  E1=0.
      GO TO 8888
C
C     EXPONENTIAL WOULD HAVE BLOWN UP SO RETURN
C     'AINF' IN PROPER PHASE.
C
5700  AI=AIMAG(Z)
      E1=AINF*ZINV*CMPLX(COS(AI),SIN(AI))
      GO TO 8888
C
C     THIS PATCH PREVENTS THE ALOG(0.) FUNCTION FROM GIVING TROUBLE.
C
C     THE LOGARITHM OF 10**(-100) IS RETURNED FOR Z=0.
C
6000  E1=CMPLX(-2.302585E2,0.)
      GO TO 8888
      END
```

Figure 34. (continued)

APPENDIX C

FIELD EQUATIONS FOR THE SUM AND DIFFERENCE FREQUENCY COMPONENTS RESULTING FROM COLLINEAR BESSEL PRIMARY BEAMS

As shown by Fenlon[19] and McKendree,[10] Equation (4.2) approximates the paraxial field of a circular piston projector having radius a and uniform source amplitude p_0 if

$$\varepsilon_o = \frac{a}{\sqrt{2}} \quad , \quad p_G = 2p_0 \quad . \tag{C1}$$

The justification for Equation (C1) is as follows. After replacing ε by $r\theta$ in Equation (4.4), we obtain for the paraxial farfield of a Gaussian beam

$$|p_\omega(r,\theta)| \simeq \frac{1}{2} k\varepsilon_o^2 p_G \frac{e^{-\alpha r}}{r} \exp\{-(\tfrac{1}{2} k\varepsilon_o\theta)^2\}$$

$$= \frac{1}{2} k\varepsilon_o^2 p_G \frac{e^{-\alpha r}}{r} \{1 - \tfrac{1}{4} k^2\varepsilon_o^2\theta^2 + O[(k\varepsilon_o\theta)^4]\} \quad . \tag{C2}$$

Likewise, the paraxial farfield of a Bessel beam is given by

$$|p_\omega(r,\theta)| \simeq \frac{1}{2} ka^2 p_0 \frac{e^{-\alpha r}}{r} \left|\frac{2J_1(ka\theta)}{ka\theta}\right|$$

$$= \frac{1}{2} ka^2 p_0 \frac{e^{-\alpha r}}{r} |1 - \tfrac{1}{8} k^2 a^2\theta^2 + O[(ka\theta)^4]| \quad . \tag{C3}$$

Equations (C2) and (C3) are made equivalent up to $O[(ka\theta)^4]$ by way of Equation (C1).

We thus obtain the following transformations for our normalized Gaussian beam parameters:

$$P_o \to \frac{4\beta p_{01} p_{02}}{\rho_o c_o^2} \quad , \quad D \to \frac{\omega_o a}{2\sqrt{2} c_o} = 2.22 \frac{a}{\lambda_o}$$

$$Z \to \frac{4c_o}{\omega_o a^2} r \quad , \quad a_{T_\pm} \to \frac{\omega_o a^2}{4c_o} \alpha_{T_\pm} \quad . \tag{C4}$$

Through use of the relations in Equation (C4), the results based on Gaussian primary beams in Chapters IV and VI may be transformed for application to arrays formed by primaries radiated from a circular piston. The following equations, which result from the analysis of collinear interaction in Chapter IV, have been so transformed. As usual, the effects of dispersion are retained only in the parameter $\delta_\pm$. Consequently, because it has been assumed that $\Omega_-^2 << 1$, we may replace $(\omega_o/c_o)^2$ by $k_1 k_2$.

For the difference-frequency field, we obtain

$$p_-(r,\theta) = \frac{k_-^2 a^2 \beta p_{01} p_{02}}{4\rho_o c_o^2} \frac{e^{-\alpha_- r}}{1 - i \dfrac{2k_-}{k_1 k_2 a^2} r} \exp\left\{-(\alpha_{T_-} - ik_-\delta_-) \frac{k_1 k_2 a^2 A_r}{8k_- B_r} - k_-^2 r^2 \theta^2 / B_r\right\}$$

$$\cdot \int_1^{1 - \frac{8k_- r B_r}{k_1 k_2 a^2 A_r}} \exp\left\{(\alpha_{T_-} - ik_-\delta_-) \frac{k_1 k_2 a^2 A_r}{8k_- B_r} \chi - \frac{ik_-^2 (4k_1 k_2 + k_-^2) a^2 r^2 \theta^2}{A_r B_r} \frac{1}{\chi}\right\} \frac{d\chi}{\chi} \quad , \tag{C5}$$

where

$$A_r = 8k_- r + ik_-^2 a^2$$

and

$$B_r = (k_1 k_2 + k_-^2/2)a^2 - i2k_- r \quad .$$

Equation (C5) reduces on axis to

$$p_-(r,0) = \frac{k_-^2 a^2 \beta p_{01} p_{02}}{4\rho_o c_o^2} \frac{e^{-\alpha_- r}}{1-i\dfrac{2k_-}{k_1 k_2 a^2} r} \exp\left\{-(\alpha_{T_-} - ik_-\delta_-) \frac{k_1 k_2 a^2 A_r}{8k_- B_r}\right\}$$

$$\cdot \left[E_1\left\{-(\alpha_{T_-} - ik_-\delta_-) \frac{k_1 k_2 a^2 A_r}{8k_- B_r}\right\} - E_1\left\{-(\alpha_{T_-} - ik_-\delta_-)\left(\frac{k_1 k_2 a^2 A_r}{8k_- B_r} - r\right)\right\}\right] \quad . \tag{C6}$$

For the farfield of the array, Equation (C5) becomes

$$p_-(r,\theta) = \frac{ik_1 k_2 k_- a^4 \beta p_{01} p_{02}}{8\rho_o c_o^2} \frac{e^{-\alpha_- r}}{r}$$

$$\cdot \exp\left\{-(\alpha_{T_-} - ik_-\delta_-) \frac{ik_1 k_2 a^2}{2k_-} - (2k_1 k_2 + k_-^2) \frac{a^2\theta^2}{8} - ik_- r\theta^2/2\right\}$$

$$\cdot \int_1^{i\infty} \exp\left\{(\alpha_{T_-} - ik_-\delta_-) \frac{ik_1 k_2 a^2}{2k_-} \chi + (4k_1 k_2 + k_-^2) \frac{a^2\theta^2}{16} \frac{1}{\chi}\right\} \frac{d\chi}{\chi} \quad , \tag{C7}$$

which for a diffraction-limited array reduces to

$$p_-(r,\theta) = \frac{ik_1 k_2 k_- a^4 \beta p_{01} p_{02}}{8\rho_o c_o^2} \frac{e^{-\alpha_- r}}{r} \exp\{-k_1 k_2 a^2\theta^2/4 - ik_- r\theta^2/2\}$$

$$\cdot \exp\left\{-(\alpha_{T_-} - ik_-\delta_-) \frac{ik_1 k_2 a^2}{2k_-}\right\} E_1\left\{-(\alpha_{T_-} - ik_-\delta_-) \frac{ik_1 k_2 a^2}{2k_-}\right\} \quad . \tag{C8}$$

When $\theta = 0$, Equation (C8) reduces to the farfield form of Equation (C6). By way of Equations (4.11) and (4.13), Equations (C5) and (C7) can be written in terms of modified Bessel functions and exponential integrals, as was done in Chapter IV. For the farfield of an absorption-limited array, Equation (C7) reduces to

$$p_-(r,\theta) = -\frac{k_-^2 a^2 \beta p_{01} p_{02}}{4\alpha_{T_-}\rho_o c_o^2}\,\frac{e^{-\alpha_- r}}{r}\,\frac{\exp\{-(k_- a/4)^2\theta^2 - ik_- r\theta^2/2\}}{1 + i(k_-/2\alpha_{T_-})(\theta^2 - 2\delta_-)} \quad . \tag{C9}$$

Likewise, for the sum-frequency field we obtain

$$p_+(r,\theta) = -\frac{k_+^2 a^2 \beta p_{01} p_{02}}{4\rho_o c_o^2}\,\frac{e^{-\alpha_+ r}}{1-i8r/k_+a^2}\,\exp\left\{(\alpha_{T_+} - ik_+\delta_+)ik_+a^2/8 - \frac{4r^2\theta^2/a^2}{1-i8r/k_+a^2}\right\}$$

$$\cdot\left[E_1\left\{(\alpha_{T_+} - ik_+\delta_+)\ ik_+a^2/8\right\} - E_1\left\{(\alpha_{T_+} - ik_+\delta_+)\left(ik_+a^2/8 + r\right)\right\}\right] \quad . \tag{C10}$$

Equation (C10) yields two different results for the farfield. When $\alpha_{T_+} < 0$, Equation (C10) reduces in the farfield to

$$p_+(r,\theta) = \frac{ik_+^3 a^4 \beta p_{01} p_{02}}{32\rho_o c_o^2(\alpha_{T_+} - ik_+\delta_+)}\,\frac{e^{-(\alpha_1+\alpha_2)r}}{r^2}\,\exp\{-(k_+a/4)^2\theta^2 - ik_+r\theta^2/2\} \quad , \tag{C11}$$

while for $\alpha_{T_+} > 0$ we obtain

$$p_+(r,\theta) = -\frac{ik_+^3 a^4 \beta p_{01} p_{02}}{32\rho_o c_o^2} \frac{e^{-\alpha_+ r}}{r} \exp\{-(k_+ a/4)^2\theta^2 - ik_+ r\theta^2/2\}$$

$$\cdot \exp\{(\alpha_{T_+} - ik_+\delta_+)\, ik_+ a^2/8\}\, E_1\{(\alpha_{T_+} - ik_+\delta_+)\, ik_+ a^2/8\} \,. \tag{C12}$$

As discussed in Section 4.1, a simple transformation permits application of Equations (C10) - (C12) to second-harmonic fields.

Although the effect of dispersion on the parametric array has not been investigated experimentally, the utility of the above equations may be demonstrated by comparing our results with data obtained in water, where the dispersion is negligible. Axial data obtained by Muir and Willette[70] for the sum- and difference-frequency fields that resulted from a parametric array operated in fresh water may be used for this purpose. Primary beams at 482 kHz and 418 kHz were radiated by a circular source of radius 3.8 cm, each at a peak source level of 207 dB re 1 μPa at 1 m. The water for the difference-frequency experiment was isothermal at 55°F,[12] and therefore the attenuation coefficients are $\alpha_1 = 0.00755\ m^{-1}$, $\alpha_2 = 0.00568\ m^{-1}$, and $\alpha_- = 0.00013\ m^{-1}$. If it is assumed that the water for the sum-frequency experiment was the same temperature, then $\alpha_+ = 0.0263\ m^{-1}$. For comparison, we find from Equation (C4) that the equivalent Gaussian beam parameters are $\Omega_- = 0.14$, $D = 26$, $a_{T_-} = 0.009$ and $a_{T_+} = -0.009$. Theoretical predictions obtained from Equations (C6) and (C10), together with the data obtained by Muir and Willette, are presented in

Figure 35a. Agreement between theory and experiment is seen to be very good. We note that whereas the axial solutions of Muir and Willette require two complex integrations, Equations (C6) and (C10) require none if the subroutine in Appendix B is used to evaluate the complex exponential integral.

Data obtained for beam patterns may be used to check our far-field results. For the difference-frequency beam pattern we use the data from an experiment performed in sea water by Moffett and Mellen.[71] Primaries were radiated at 270 kHz and 220 kHz by a circular source of radius 5.1 cm, with $\alpha_{T_-} \simeq \alpha_1 + \alpha_2 \simeq 0.0173\ m^{-1}$. The data are compared in Figure 35b with the results obtained from Equation (C7). The agreement is excellent. In this case, the simple analytical expression derived by Moffett and Mellen for the difference-frequency beam pattern is easier to use than our results. However, we find from Equations (C11) and (C12) that our directivity function for the sum-frequency signal is extremely simple. It is given by $\exp\{-(k_+ a/4)^2\theta^2\}$. Similarly, for the second harmonic the prediction is $\exp\{-(ka/2)^2\theta^2\}$, where k is the wave number of the fundamental. We therefore use data for the second harmonic taken by Lockwood, Muir, and Blackstock[54] in a harmonic distortion experiment. The source was the same as that described by Muir and Willette[70] but was driven at the single frequency 454 kHz. As seen in Figure 35b, the agreement between theory and experiment is again very good. Beam patterns were also measured by Muir and Willette for sum- and difference-frequency signals, but it is difficult to read the data points with certainty because of inconsistencies in the scales.

The results in Figure 35 thus lend credibility to the equations presented in this appendix. However, one should beware of applying the equations to regions very far off axis. Further support of the transformation given in Equation (C1) is provided by Fenlon[19] and McKendree.[10]

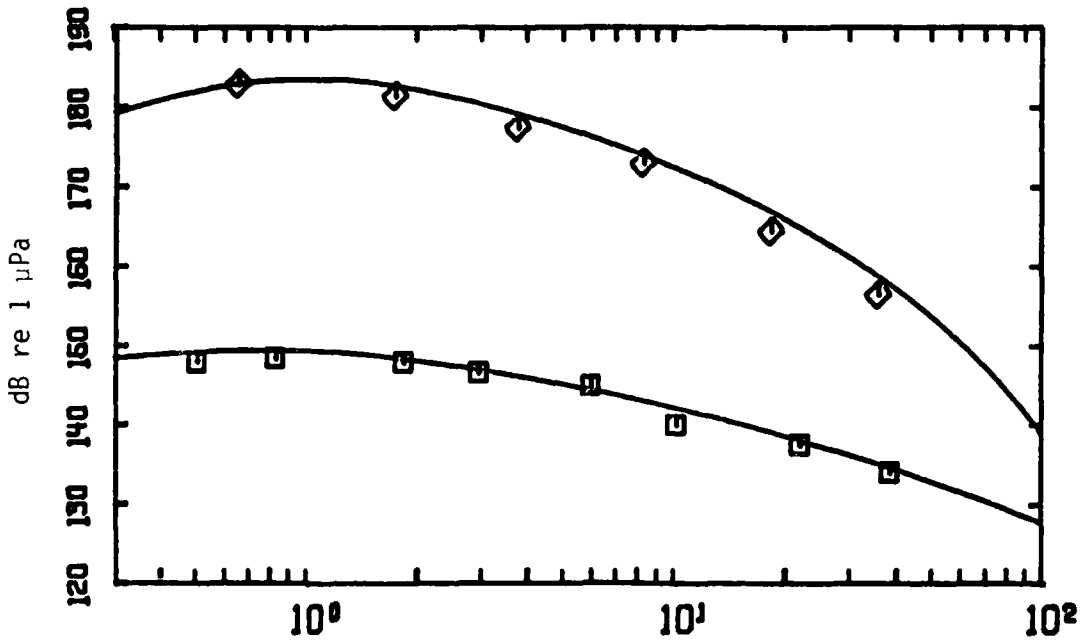

(a) Axial Field

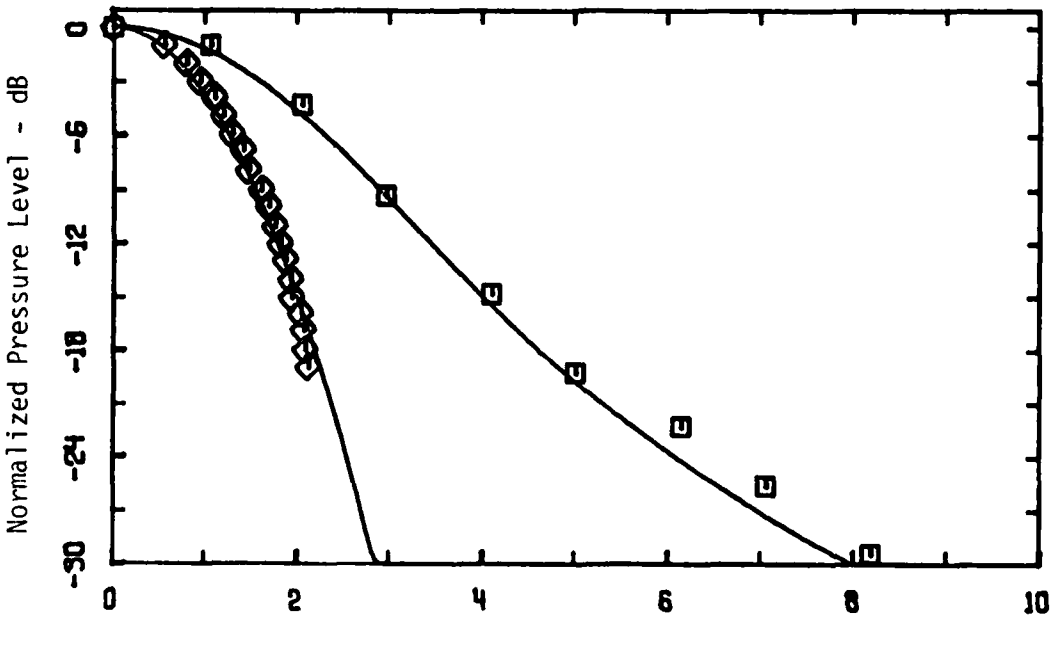

(b) Beam Pattern

Figure 35. Comparison of Theoretical and Experimental Results for Collinear Interaction in a Dispersionless Fluid. (a) Axial Field: Diamonds--Sum Frequency,[70] Squares--Difference Frequency;[70] (b) Farfield Directivity: Diamonds--Second Harmonic,[49] Squares--Difference Frequency.[71] Solid Lines Represent Present Theory.

AS-83-738

APPENDIX D

DIFFERENCE-FREQUENCY FIELD RESULTING FROM SPHERICAL PRIMARY WAVES

Here we solve the inhomogeneous wave equation for the difference-frequency field resulting from spherical primary waves which are radiated from a spherical source of radius a. Our wave equation thus becomes (see, e.g., Equations (2.4) and (2.8))

$$(\nabla^2 + \chi_-^2)p_-(r) = (k_-a)^2 P_o \frac{e^{-i(\chi_1 - \chi_2^*)r}}{r^2} , \qquad (D1)$$

where we assumed that the primaries are given by

$$p_j(r) = p_{0j}\left(\frac{a}{r}\right) e^{-i\chi_j r} ,$$

with $\chi = k - i\alpha$ and where

$$P_o = \frac{\beta p_{01} p_{02}}{\rho_o c_o^2} .$$

Because of spherical symmetry we have

$$\nabla^2 = \frac{\partial^2}{\partial r^2} + \frac{2}{r}\frac{\partial}{\partial r} ,$$

so that we can rewrite Equation (D1) as

$$\left(\frac{\partial^2}{\partial r^2} + \chi_-^2\right)\psi_-(r) = (k_-a)^2 P_o \frac{e^{-i(\chi_1 - \chi_2^*)r}}{r} , \qquad (D2)$$

where

$$p_-(r) = \frac{1}{r}\,\psi_-(r) \quad . \tag{D3}$$

Since the Green's function for Equation (D2) is

$$g_-(r|r') = \frac{e^{-i\chi_-(r-r')}}{i2\chi_-} \quad ,$$

we can immediately write the solution as

$$\psi_-(r) = \frac{(k_-a)^2 P_o}{i2\chi_-}\, e^{-i\chi_- r} \int_a^r e^{-i(\chi_1 - \chi_2^* - \chi_-)r'}\, \frac{dr'}{r'} \quad , \tag{D4}$$

where we have assumed that $p_-(a) = 0$. Equation (D4) can be expressed in terms of exponential integrals, so that using Equation (D3) we obtain

$$p_-(r) = i\,\frac{k_-a^2}{2}\, P_o\, \frac{e^{-i\chi_- r}}{r} \left[E_1\{i(\chi_1 - \chi_2^* - \chi_-)r\} - E_1\{i(\chi_1 - \chi_2^* - \chi_-)a\}\right] \quad , \tag{D5}$$

for $k_-/\chi_- \simeq 1$.

The first term in Equation (D5) is the particular solution and the second term is the homogeneous solution. Only the homogeneous solution survives in the farfield, where Equation (D5) reduces to

$$p_-(r) \sim -i\,\frac{k_-a^2}{2}\, E_1\{i(\chi_1 - \chi_2^* - \chi_-)a\}\, P_o\, \frac{e^{-i\chi_- r}}{r} \quad , \quad r \to \infty \quad .$$

Note that p_- is proportional to ω_- , whereas for directional primaries [see, for example, Equations (2.32) and (2.33)] p_- is proportional to ω_-^2 .

APPENDIX E

DIFFERENCE-FREQUENCY FARFIELD OF A DIFFRACTION-LIMITED ARRAY FORMED BY COLLINEAR GAUSSIAN PRIMARY BEAMS

In a diffraction-limited array, the nonlinear interaction region is terminated because of spreading losses suffered by the primaries, rather than dissipative losses. We therefore seek the asymptotic farfield form of the difference-frequency field equation when $a_T' \simeq 0$. For this purpose, it is convenient to use the farfield form of Equation (4.8), which we can write as

$$p_-(\theta,Z) \sim -\Omega_1\Omega_2\Omega_-^2 D^2 P_o \frac{e^{-a_- Z}}{Z} \exp\{-\Omega_-^2 D^2\theta^2 - i\Omega_- D^2 Z\theta^2\} I \quad , \qquad (E1)$$

where

$$I = \int_0^\infty \exp\left\{ \frac{\Omega_-^2 - i2\Omega_-\eta}{2\Omega_1\Omega_2 + i\Omega_-\eta} \Omega_1\Omega_2 D^2\theta^2 - a_T'\eta \right\} \frac{d\eta}{2\Omega_1\Omega_2 + i\Omega_-\eta} \quad .$$

After making the variable substitution $\psi = a_T'\eta$, we obtain

$$I = \int_0^{(1\pm i)\infty} \exp\left\{ \frac{\Omega_-^2 a_T' - i2\Omega_-\psi}{2\Omega_1\Omega_2 a_T' + i\Omega_-\psi} \Omega_1\Omega_2 D^2\theta^2 - \psi \right\} \frac{d\psi}{2\Omega_1\Omega_2 a_T' + i\Omega_-\psi} \quad , \qquad (E2)$$

where the factor $\pm i\infty$ in the upper limit indicates that the imaginary part of a_T', which depends on δ, can take on any value. If we assume $|2a_T'/\Omega_-| << 1$, then

$$\frac{\Omega_-^2 a_T' - i2\Omega_-\psi}{2\Omega_1\Omega_2 a_T' + i\Omega_-\psi} \sim -2 \quad ,$$

so that Equation (E2) reduces to

$$I \sim e^{-2\Omega_1\Omega_2 D^2\theta^2} \int_0^{(1 \pm i)\infty} e^{-\psi} \frac{d\psi}{2\Omega_1\Omega_2 a_T' + i\Omega_- \psi} \quad . \tag{E3}$$

Note that the contribution due to a_T' in the denominator of the integral is critical and cannot be neglected. Now we let $\chi = 2\Omega_1\Omega_2 a_T' + i\Omega_- \psi$ and rewrite Equation (E3) as

$$I \sim \frac{1}{i\Omega_-} \exp\{-2\Omega_1\Omega_2 D^2\theta^2 - i2\Omega_1\Omega_2 a_T'/\Omega_-\} \int_{2\Omega_1\Omega_2 a_T'}^{(i \pm 1)\infty} e^{-\frac{\chi}{i\Omega_-}} \frac{d\chi}{\chi}$$

$$= \frac{1}{i\Omega_-} \exp\{-2\Omega_1\Omega_2 D^2\theta^2 - i2\Omega_1\Omega_2 a_T'/\Omega_-\} E_1\{-i2\Omega_1\Omega_2 a_T'/\Omega_-\} \quad . \tag{E4}$$

Combining Equations (E1) and (E4) after setting $\Omega_1\Omega_2 = 1$ everywhere except in the directivity function, we obtain

$$p_-(\theta, Z) \sim i\Omega_- D^2 P_o \frac{e^{-a_- Z}}{Z} \exp\{-i2a_T'/\Omega_-\} E_1\{-i2a_T'/\Omega_-\}$$

$$\cdot \exp\{-(\Omega_1^2 + \Omega_2^2) D^2\theta^2 - i\Omega_- D^2 Z\theta^2\} \quad , \quad |2a_T'/\Omega_-| << 1 \quad ,$$

because

$$2\Omega_1\Omega_2 + \Omega_-^2 = 2\Omega_1\Omega_2 + (\Omega_1 - \Omega_2)^2$$

$$= \Omega_1^2 + \Omega_2^2 \quad .$$

APPENDIX F

THE COEFFICIENT OF NONLINEARITY FOR NONCOLLINEAR PLANE-WAVE INTERACTION

In this appendix we expand on Zverev and Kalachev's[57] analysis of the noncollinear interaction of two finite-amplitude plane waves of infinite extent. We begin with the complete second-order wave equation for inviscid, irrotational fluids, which can be written as[63]

$$\left(\nabla^2 - \frac{1}{c_o^2}\frac{\partial^2}{\partial t^2}\right)p = -\rho_o\left[(\vec{\nabla}\cdot\vec{u})^2 + \vec{u}\cdot\nabla^2\vec{u} + \frac{1}{2}\nabla^2 u^2\right] - \frac{1}{\rho_o c_o^4}\frac{B}{2A}\frac{\partial^2 p^2}{\partial t^2} \quad , \qquad \text{(F1)}$$

where $\vec{u}$ is the particle velocity vector. The ratio $B/2A$ arises from coefficients[24] in the equation of state relating the pressure and density. For ideal gas, $B/2A$ is equal to $(\gamma - 1)/2$, where γ is the ratio of specific heats. Without loss of generality, the analysis is restricted to two dimensions so that the particle velocity may be expressed as

$$\vec{u} = \hat{i}\, u_x + \hat{j}\, u_y \quad ,$$

where u_x and u_y are the components in the x and y directions, respectively. The terms in Equation (F1) containing $\vec{u}$ thus become

$$(\vec{\nabla}\cdot\vec{u})^2 = \left(\frac{\partial u_x}{\partial x}\right)^2 + 2\left(\frac{\partial u_x}{\partial x}\right)\left(\frac{\partial u_y}{\partial y}\right) + \left(\frac{\partial u_y}{\partial y}\right)^2 \quad ,$$

$$\vec{u}\cdot\nabla^2\vec{u} = u_x\frac{\partial^2 u_x}{\partial x^2} + u_x\frac{\partial^2 u_x}{\partial y^2} + u_y\frac{\partial^2 u_y}{\partial x^2} + u_y\frac{\partial^2 u_y}{\partial y^2} \quad ,$$

$$\nabla^2 u^2 = \frac{\partial^2 u_x^2}{\partial x^2} + \frac{\partial^2 u_x^2}{\partial y^2} + \frac{\partial^2 u_y^2}{\partial x^2} + \frac{\partial^2 u_y^2}{\partial y^2} \quad .$$

Combining the above equations we obtain, after manipulating the derivatives,

$$\left(\nabla^2 - \frac{1}{c_o^2}\frac{\partial^2}{\partial t^2}\right) p = -\rho_o \left\{ \frac{\partial^2 u_x^2}{\partial x^2} + 2\frac{\partial u_x}{\partial x}\frac{\partial u_y}{\partial y} + \frac{\partial^2 u_y^2}{\partial y^2} + 2u_x \frac{\partial^2 u_x}{\partial y^2} + 2u_y \frac{\partial^2 u_y}{\partial x^2} + \left(\frac{\partial u_x}{\partial y}\right)^2 + \left(\frac{\partial u_y}{\partial x}\right)^2 \right\} - \frac{1}{\rho_o c_o^4}\frac{B}{2A}\frac{\partial^2 p^2}{\partial t^2} \quad . \tag{F2}$$

We now consider a primary wave field in which one plane wave propagates in the x direction while the direction of propagation of a second plane wave forms an angle ϕ with the x axis. Such a field can be expressed by

$$p = p_{01}\cos\psi_1 + p_{02}\cos\psi_2 \quad , \tag{F3}$$

where

$$\psi_1 = \omega_1 t - k_1 x$$

and

$$\psi_2 = \omega_2 t - k_2 x \cos\phi - k_2 y \sin\phi \quad .$$

To determine the particle velocity we may use the first-order relation

$$\vec{u} = -\frac{1}{\rho_o}\int \vec{\nabla} p \, dt \quad , \tag{F4}$$

because use of a more exact relation for the terms containing $\vec{u}$ would only generate third- and higher-order quantities. Combining Equations (F3) and (F4) we obtain

$$u_x = \frac{p_{01}}{\rho_o c_o}\cos\psi_1 + \frac{p_{02}}{\rho_o c_o}\cos\phi\cos\psi_2 \quad ,$$

$$u_y = \frac{p_{02}}{\rho_o c_o}\sin\phi\cos\psi_2 \quad . \tag{F5}$$

We are concerned here only with the sum- and difference-frequency fields. The third, fifth, sixth, and seventh terms on the right-hand side of Equation (F2) are not forcing functions for these fields. The sum- and difference-frequency parts of the remaining terms are

$$\frac{\partial^2 u_x^2}{\partial x^2} = -\frac{p_{01}p_{02}}{\rho_o^2 c_o^2}(k_1 \pm k_2\cos\phi)^2 \cos\phi \cos\psi_\pm \quad ,$$

$$2\frac{\partial u_x}{\partial x}\frac{\partial u_y}{\partial y} = \mp\frac{p_{01}p_{02}}{\rho_o^2 c_o^2} k_1 k_2 \sin^2\phi \cos\psi_\pm \quad ,$$

$$2u_x\frac{\partial^2 u_x}{\partial y^2} = -\frac{p_{01}p_{02}}{\rho_o^2 c_o^2} k_2^2 \sin^2\phi \cos\phi \cos\psi_\pm \quad ,$$

$$\frac{\partial^2 p^2}{\partial t^2} = -p_{01}p_{02}\omega_\pm^2 \cos\psi_\pm \quad ,$$

where

$$\psi_\pm = \omega_\pm t - (k_1 \pm k_2\cos\phi)x - k_2 y \sin\phi \quad .$$

After replacing the terms on the right-hand side of Equation (F2) and making some trigonometric substitutions, we find that the wave equation for the sum- and difference-frequency fields is

$$\left(\nabla^2 - \frac{1}{c_o^2}\frac{\partial^2}{\partial t^2}\right)p_\pm = \beta_\pm(\phi)\frac{k_\pm^2 p_{01}p_{02}}{\rho_o c_o^2}\cos\psi_\pm \quad , \qquad \text{(F6)}$$

where

$$\beta_\pm(\phi) = \frac{B}{2A} + \cos\phi \pm 4\frac{\omega_1\omega_2}{\omega_\pm^2}\sin^4(\phi/2) \quad . \qquad \text{(F7)}$$

Westervelt's equation,[1] Equation (2.1), comes from using the plane-wave impedance relation to reduce the right-hand side of Equation (F1). The result is that Westervelt's equation is of the same form as Equation (F6), except that Equation (F7) is simply $\beta_{\pm} = 1 + B/2A$. It is of interest to note that had we derived an equation similar to Equation (F6) but in terms of density rather than pressure, we would have obtained a coefficient which is the same as that given in Equation (F7), except with the first term replaced by

$$\frac{B}{2A}\left[1 \mp 4\,\frac{\omega_1\omega_2}{\omega_{\pm}^2}\sin^2(\phi/2)\right] \quad .$$

In fact, various inhomogeneous wave equations in the literature[2,57] differ slightly depending on whether they pertain to pressure or density.

APPENDIX G

DIFFERENCE-FREQUENCY FARFIELD OF AN ABSORPTION-LIMITED ARRAY FORMED BY NONCOLLINEAR GAUSSIAN PRIMARY BEAMS

We begin with the farfield result presented in Equation (6.20) for $\phi_1 = \phi$ and $\phi_2 = 0$, where ϕ_j is the angle formed by the primary beam of frequency ω_j and the z axis:

$$p_-(\theta_x,\theta_y,Z) \sim -\Omega_1\Omega_2\Omega_-^2 D^2 P_o \frac{e^{-a_- Z}}{Z} \exp\{-\Omega_-^2 D^2\theta^2 - i\Omega_- D^2 Z\theta^2\}$$

$$\cdot \int_0^\infty \exp\left\{-a_T'\eta + \frac{i\Omega_1^2 D^2\phi^2\eta}{\Omega_1 - i\eta} - \frac{\Omega_1^4 D^2\phi^2(\Omega_2+i\eta)}{(\Omega_1-i\eta)(2\Omega_1\Omega_2+i\Omega_-\eta)}\right.$$

$$\left. + 2\Omega_1^2\Omega_- D^2\phi\theta_x \frac{\Omega_2+i\eta}{2\Omega_1\Omega_2+i\Omega_-\eta} + \Omega_1\Omega_2\Omega_- D^2\theta^2 \frac{\Omega_- - i2\eta}{2\Omega_1\Omega_2+i\Omega_-\eta}\right\} \frac{d\eta}{2\Omega_1\Omega_2+i\Omega_-\eta} , \tag{G1}$$

where

$$\theta^2 = \theta_x^2 + \theta_y^2 .$$

The variable of integration in Equation (G1) represents the dimensionless coordinate Z. In an absorption-limited array, dissipation restricts nonlinear interaction to the nearfield of the primaries, where $Z < 1$. We now assume that a_T is sufficiently large that the factor $a_T\eta$ dominates the integrand when $\eta > 1$. In other words, we assume that major contributions to the integral occur only when $\eta << 1$. We may therefore perform expansions for small η, discarding all terms of order η^2 or higher:

$$\frac{i\Omega_1^2 D^2\phi^2\eta}{\Omega_1 - i\eta} \sim i\Omega_1 D^2\phi^2\eta$$

$$-\frac{\Omega_1^4 D^2\phi^2(\Omega_2 + i\eta)}{(\Omega_1 - i\eta)(2\Omega_1\Omega_2 + i\Omega_-\eta)} \sim -\frac{\Omega_1^2}{2} D^2\phi^2 - i(3\Omega_2 + \Omega_1)\frac{\Omega_1 D^2\phi^2}{4\Omega_2}\eta$$

$$2\Omega_1^2\Omega_- D^2\phi\theta_x \frac{\Omega_2 + i\eta}{2\Omega_1\Omega_2 + i\Omega_-\eta} \sim \Omega_1\Omega_- D^2\phi\theta_x + i(2\Omega_1 - \Omega_-)\frac{\Omega_- D^2\phi\theta_x}{2\Omega_2}\eta$$

$$\Omega_1\Omega_2\Omega_- D^2\theta^2 \frac{\Omega_- - i2\eta}{2\Omega_1\Omega_2 + i\Omega_-\eta} \sim \frac{\Omega_-^2}{2} D^2\theta^2 - i\left(1 + \frac{\Omega_-^2}{4\Omega_1\Omega_2}\right)\Omega_- D^2\theta^2\eta$$

$$\frac{d\eta}{2\Omega_1\Omega_2 + i\Omega_-\eta} \sim \frac{d\eta}{2\Omega_1\Omega_2} \quad .$$

Inserting the asymptotic relations in Equation (G1) and regrouping terms we obtain

$$p_-(\theta_x,\theta_y,Z) \sim -\Omega_-^2 D^2 P_o \frac{e^{-a_- Z}}{2Z} \exp\{-(\Omega_-^2 D^2/2)[(\theta_x - (\Omega_1/\Omega_-)\phi)^2 + \theta_y^2] - i\Omega_- D^2 Z\theta^2\}$$

$$\cdot \int_0^\infty \exp\left\{-\left[a_T - i2\delta\Omega_- D^2 + i\left(1 + \frac{\Omega_-^2}{4\Omega_1\Omega_2}\right)\Omega_- D^2\theta^2\right.\right.$$

$$\left.\left. - i(2\Omega_1 - \Omega_-)\frac{\Omega_- D^2\phi\theta_x}{2\Omega_2} - i\left(1 - \frac{\Omega_1}{\Omega_2}\right)\frac{\Omega_1}{4} D^2\phi^2\right]\eta\right\} d\eta \quad . \qquad \text{(G2)}$$

The integral in Equation (G2) is easily evaluated, and the result is

$$p_-(\theta_x,\theta_y,Z) \sim -\frac{\Omega_-^2 D^2 P_o}{2a_T}\frac{e^{-a_- Z}}{Z}\frac{\exp\{-(\Omega_-^2 D^2/2)[(\theta_x - (\Omega_1/\Omega_-)\phi)^2 + \theta_y^2] - i\Omega_- D^2 Z\theta^2\}}{1 + i(\Omega_- D^2/a_T)F(\theta,\phi)} \quad , \qquad \text{(G3)}$$

where

$$F(\theta,\phi) = (1 + \frac{\Omega_-^2}{4\Omega_1\Omega_2})\theta^2 - (2\Omega_1 - \Omega_-)\frac{\phi\theta_x}{2\Omega_2} - (1 - \frac{\Omega_1}{\Omega_2})\frac{\Omega_1\phi^2}{4\Omega_-} - 2\delta \quad .$$

When $\Omega_1 \simeq \Omega_2$, $F(\theta,\phi)$ reduces to

$$F(\theta,\phi) \simeq \theta^2 - \phi\theta_x - 2\delta \quad ,$$

and Equation (G3) becomes

$$p_-(\theta_x,\theta_y,Z) \sim -\frac{\Omega_-^2 D^2 P_o}{2a_T}\frac{e^{-a_- Z}}{Z}\frac{\exp\{-(\Omega_-^2 D^2/2)[(\theta_x-(\Omega_1/\Omega_-)\phi)^2+\theta_y^2]-i\Omega_- D^2 Z\theta^2\}}{1+i(\Omega_- D^2/a_T)(\theta_x^2-\phi\theta_x+\theta_y^2-2\delta)} \quad .$$

APPENDIX H

DIFFERENCE-FREQUENCY FARFIELD OF A DIFFRACTION-LIMITED ARRAY FORMED BY NONCOLLINEAR GAUSSIAN PRIMARY BEAMS

We begin, as in Appendix G, with the farfield result for $\phi_1 = \phi$ and $\phi_2 = 0$, where ϕ_j is the angle formed by the primary beam of frequency ω_j and the z axis. Following the procedure in Appendix E, we let $\psi = a_T'\eta$, whereby Equation (G1) becomes

$$p_-(\theta_x,\theta_y,Z) \sim -\Omega_1\Omega_2\Omega_-^2 D^2 P_o \frac{e^{-a_- Z}}{Z} \exp\{-\Omega_-^2 D^2\theta^2 - i\Omega_- D^2 Z\theta^2\} \int_0^{a_T'\infty} \exp\left\{-\psi + \frac{i\Omega_1^2 D^2\phi^2\psi}{\Omega_1 a_T' - i\psi}\right.$$

$$- \frac{a_T'\Omega_1^4 D^2\phi^2(\Omega_2 a_T' + i\psi)}{(\Omega_1 a_T' - i\psi)(2\Omega_1\Omega_2 a_T' + i\Omega_-\psi)} + 2\Omega_1^2\Omega_- D^2\phi\theta_x \frac{\Omega_2 a_T' + i\psi}{2\Omega_1\Omega_2 a_T' + i\Omega_-\psi}$$

$$\left. + \Omega_1\Omega_2\Omega_- D^2\theta^2 \frac{\Omega_- a_T' - i2\psi}{2\Omega_1\Omega_2 a_T' + i\Omega_-\psi}\right\} \frac{d\psi}{2\Omega_1\Omega_2 a_T' + i\Omega_-\psi} \quad , \tag{H1}$$

where

$$\theta^2 = \theta_x^2 + \theta_y^2 \quad .$$

By writing $a_T'\infty$, we keep track of the relation between the real and imaginary parts of the upper limit in the integral. In a diffraction-limited array, attenuation of the primaries is so low (or the nearfield is so short) that the nonlinear interaction region is terminated because of spreading rather than dissipative losses suffered by the primary beams. Therefore, if we assume $|2a_T'/\Omega_-| \ll 1$, then

$$\frac{i\Omega_1^2 D^2\phi^2\psi}{\Omega_1 a_T' - i\psi} \sim -\Omega_1^2 D^2\phi^2$$

$$- \frac{a_T' \Omega_1^4 D^2 \phi^2 (\Omega_2 a_T' + i\psi)}{(\Omega_1 a_T' - i\psi)(2\Omega_1 \Omega_2 a_T' + i\Omega_- \psi)} \sim \frac{a_T' \Omega_1^4 D^2 \phi^2}{2\Omega_1 \Omega_2 a_T' + i\Omega_- \psi}$$

$$2\Omega_1^2 \Omega_- D^2 \phi \theta_x \frac{\Omega_2 a_T' + i\psi}{2\Omega_1 \Omega_2 a_T' + i\Omega_- \psi} \sim 2\Omega_1^2 D^2 \phi \vartheta_x$$

$$\Omega_1 \Omega_2 \Omega_- D^2 \theta^2 \frac{\Omega_- a_T' - i2\psi}{2\Omega_1 \Omega_2 a_T' + i\Omega_- \psi} \sim -2\Omega_1 \Omega_2 D^2 \theta^2 \quad .$$

After letting $\chi = 2\Omega_1 \Omega_2 a_T' + i\Omega_- \psi$ and rearranging terms, we obtain the following asymptotic form for Equation (H1):

$$p_-(\theta_x, \theta_y, Z) \sim i\Omega_- D^2 P_o \frac{e^{-a_- Z}}{Z} \exp\{-\Omega_1^2 D^2 [(\theta_x - \phi)^2 + \theta_y^2] - \Omega_2^2 D^2 \theta^2 - i\Omega_- D^2 Z \theta^2\}$$

$$\cdot \exp\left\{-i2 \frac{a_T'}{\Omega_-}\right\} \int_{2a_T'}^{ia_T'\infty} \exp\left\{-\frac{\chi}{i\Omega_-} + a_T' \Omega_1^4 D^2 \phi^2 \frac{1}{\chi}\right\} \frac{d\chi}{\chi} \quad , \quad \text{(H2)}$$

where we assumed $\Omega_1 \Omega_2 \simeq 1$. Expanding the integral in Equation (H2) by way of Equation (4.11), we find

$$\int_{2a_T'}^{ia_T'\infty} \exp\left\{-\frac{\chi}{i\Omega_-} + a_T' \Omega_1^4 D^2 \phi^2 \frac{1}{\chi}\right\} \frac{d\chi}{\chi}$$

$$= \sum_{n=-\infty}^{\infty} I_n\{2a_T' \Omega_1^4 D^2 \phi^2\} \int_{2a_T'}^{ia_T'\infty} \exp\left\{-\left(\frac{1}{i\Omega_-} + a_T' \Omega_1^4 D^2 \phi^2\right)\chi\right\} \frac{d\chi}{\chi^{1-n}}$$

$$= \sum_{n=-\infty}^{\infty} (2a_T')^n I_n\{2a_T' \Omega_i^4 D^2 \phi^2\} E_{1-n}\left\{-i \frac{2a_T'}{\Omega_-} + 2(a_T')^2 \Omega_1^4 D^2 \phi^2\right\} \quad .$$

(H3)

The assumption $|2a_T'/\Omega_-| << 1$ requires in general that $|a_T'| < 0.01$, so that we can safely omit all terms in Equation (H3) for which $n \neq 0$. Moreover, since $|2(a_T')^2\Omega_1^4 D^2\phi^2| << |2a_T'/\Omega_-|$ we have simply

$$\int_{2a_T'}^{ia_T'\infty} \exp\left\{-\frac{\chi}{i\Omega_-} + a_T'\Omega_1^4 D^2\phi^2\,\frac{1}{\chi}\right\}\frac{d\chi}{\chi} \simeq E_1\left\{-i\,\frac{2a_T'}{\Omega_-}\right\} \quad .$$

Therefore, Equation (H2) becomes

$$p_-(\theta_x,\theta_y,Z) \sim i\Omega_- D^2 P_o \frac{e^{-a_- Z}}{Z} \exp\{-i2a_T'/\Omega_-\}\, E_1\{-i2a_T'/\Omega_-\}$$

$$\cdot \exp\{-\Omega_1^2 D^2[(\theta_x-\phi)^2+\theta_y^2]-\Omega_2^2 D^2\theta^2 - i\Omega_- D^2 Z\theta^2\} \quad , \quad |2a_T'/\Omega_-| << 1 \quad .$$

REFERENCES

1. P. J. Westervelt, "Parametric Acoustic Array," J. Acoust. Soc. Am. 35, 535-537 (1963).

2. O. V. Rudenko and S. I. Soluyan, Theoretical Foundations of Nonlinear Acoustics, New York: Plenum Press, 1977, pp. 85-88.

3. N. Bloembergen, Nonlinear Optics, New York: W. A. Benjamin, Inc., 1982.

4. F. Zervike and J. E. Midwinter, Applied Nonlinear Optics, New York: Wiley-Interscience, 1973.

5. E. A. Zabolotskaya and S. I. Soluyan, "A Possible Approach to the Amplification of Sound Waves," Sov. Phys-Acoust. 13, 254-256 (1967).

6. B. K. Novikov, "Nonlinear Interaction of Sound Waves in Weakly Dispersive Media," Sov. Phys-Acoust. 22, 45-48 (1976).

7. Yu. N. Karamzin, A. P. Sukhorukov, and A. K. Sukhorukova, "Influence of Dispersion of the Medium on the Characteristics of a Parametric Ultrasonic Radiator," Sov. Phys-Acoust. 24, 77-78 (1978).

8. E. F. Kozyaev and K. A. Naugol'nykh, "Parametric Sound Radiation in a Two-Phase Medium," Sov. Phys-Acoust. 26, 48-51 (1980).

9. B. K. Novikov, O. V. Rudenko, and V. I. Timoshenko, Nonlinear Hydroacoustics (in Russian), Leningrad: Sudostroyeniye, 1981, pp. 89-92.

10. F. H. Fenlon and F. S. McKendree, "Axisymmetric Parametric Radiation - A Weak Interaction Model," J. Acoust. Soc. Am. 66, 534-547 (1979).

11. J. N. Tjøtta and S. Tjøtta, "Nonlinear Interaction of Two Sound Beams," J. Acoust. Soc. Am. 37, 174-175(L) (1965).

12. T. G. Muir, "An Analysis of the Parametric Acoustic Array for Spherical Wave Fields," Ph.D. Thesis, The University of Texas at Austin, Austin, Texas, May 1971.

13. F. H. Fenlon, "On the Performance of a Dual Frequency Parametric Source via Matched Asymptotic Solutions of Burgers' Equation," J. Acoust. Soc. Am. 55, 35-46 (1974).

14. H. O. Berktay and D. J. Leahy, "Farfield Performance of Parametric Transmitters," J. Acoust. Soc. Am. 55, 539-546 (1974).

15. R. H. Mellen and M. B. Moffett, "A Model for Parametric Sonar Radiator Design," U. S. Navy Journal of Underwater Acoustics 22, 105-116 (1972).

16. B. K. Novikov, O. V. Rudenko, and S. I. Soluyan, "Parametric Ultrasonic Radiators," Sov. Phys-Acoust. 21, 365-368 (1976).

17. V. P. Kuznetsov, "Equations of Nonlinear Acoustics," Sov. Phys-Acoust. 16, 467-470 (1971).

18. B. K. Novikov, M. S. Rybachek, and V. I. Timoshenko, "Interaction of Diffracting Sound Beams and the Theory of Highly Directional Ultrasonic Radiators," Sov. Phys-Acoust. 23, 354-357 (1977).

19. F. H. Fenlon, "A Weak Interaction Model for the Axial Difference-Frequency Field of Symmetric and Asymmetric Parametric Acoustic Transmitting Arrays," J. Sound Vib. 64, 17-30 (1979).

20. F. H. Fenlon and M. F. Hamilton, "Parametric Acoustic Array Formation in Relaxing Fluids," J. Acoust. Soc. Am. 69, S81(A) (1981).

21. M. F. Hamilton and F. H. Fenlon, "Parametric Acoustic Array Formation in Dispersive Fluids," J. Acoust. Soc. Am. 72, S41(A) (1982).

22. P. J. Westervelt, "Parametric End-Fire Array," J. Acoust. Soc. Am. 32, 934-935(A) (1960).

23. M. J. Lighthill, "On the Sound Generated Aerodynamically," Proc. R. Soc. London A222, 564-587 (1952).

24. R. T. Beyer, "Parameter of Nonlinearity in Fluids," J. Acoust. Soc. Am. 32, 719-721 (1960).

25. J. N. Tjøtta and S. Tjøtta, "Nonlinear Equations of Acoustics, with Application to Parametric Acoustic Arrays," J. Acoust. Soc. Am. 69, 1644-1652 (1981).

26. H. O. Berktay and B. V. Smith, "End-Fire Array of Virtual Sound Sources Arising from the Interaction of Sound Waves," Elect. Let. 1, 6 (1965).

27. D. J. Dunn, M. Kuljis, and V. G. Welsby, "Non-Linear Effects in a Focused Underwater Standing Wave Acoustic System," J. Sound Vib. 2, 471-476 (1965).

28. M. O'Donnell, E. T. Jaynes, and J. G. Miller, "Kramers-Kronig Relationship Between Ultrasonic Attenuation and Phase Velocity," J. Acoust. Soc. Am. 69, 696-701 (1981).

29. D. A. Webster and D. T. Blackstock, "Asymptotic Decay of Periodic Spherical Waves in Dissipative Media," J. Acoust. Soc. Am. 64, S33(A) (1978).

30. J. W. Goodman, Introduction to Fourier Optics, New York: McGraw-Hill, 1968, p. 59.

31. J. N. Tjøtta and S. Tjøtta, "Nonlinear Interaction of Two Collinear, Spherically Spreading Sound Beams, J. Acoust. Soc. Am. 67, 484-490 (1980).

32. R. J. Urick, Principles of Underwater Sound, second edition, New York: McGraw-Hill, 1975, p. 57.

33. L. L. Beranek, Noise and Vibration Control, New York: McGraw-Hill, 1971, p. 274.

34. E. A. Zabolotskaya and R. V. Khokhlov, "Quasi-Plane Waves in the Nonlinear Acoustics of Confined Beams," Sov. Phys-Acoust. 15, 35-40 (1969).

35. P. J. Westervelt, "Virtual Sources in the Presence of Real Sources," in "Nonlinear Acoustics," Proceedings of the 1969 Symposium held at Applied Research Laboratories, The University of Texas at Austin, 1970 (AD 719936).

36. D. T. Blackstock, "Thermoviscous Attenuation of Plane, Periodic, Finite-Amplitude Sound Waves," J. Acoust. Soc. Am. 36, 534-542 (1964).

37. D. T. Blackstock, "Generalized Burgers Equation for Plane Waves," in Book of Abstracts, Ninth International Symposium on Nonlinear Acoustics, University of Leeds, England, July 1981, p. 7.

38. O. V. Rudenko, S. I. Soluyan, and R. V. Khokhlov, "Problems in the Theory of Nonlinear Acoustics," Sov. Phys-Acoust. 20, 271-275 (1974).

39. R. Klinman, "Propagation of Finite Amplitude Acoustic Waves in Nonlinear Relaxing Fluids," Ph.D. Thesis, Drexel University, Philadelphia, Pennsylvania, 1971.

40. F. H. Fenlon, "On the Amplification of Modulated Acoustic Waves in Gas-Liquid Mixtures," in Cavitation and Inhomogeneities in Underwater Acoustics, edited by W. Lauterborn, New York: Springer-Verlag, 1980, pp. 141-150.

41. P. M. Morse and H. Feshbach, Methods of Theoretical Physics, New York: McGraw-Hill, 1953.

42. H. Kogelnik, "Coupling and Conversion Coefficients for Optical Modes," in Proceedings of the Symposium on Quasi-Optics, New York: Polytechnic Press, Brooklyn, 1974, p. 333.

43. H. Kogelnik and T. Li, "Laser Beams and Resonators," Appl. Opt. 5, 1550-1567 (1966).

44. I. S. Gradshteyn and I. M. Ryzhik, Table of Integrals, Series, and Products, 4th edition, New York: Academic Press, 1965.

45. B. D. Cook and W. J. Arnoult, "Gaussian-Laguerre/Hermite Formulation for the Nearfield of an Ultrasonic Transducer," J. Acoust. Soc. Am. 59, 9-11 (1976).

46. M. Abramowitz and I. A. Stegun, Handbook of Mathematical Functions, 9th edition, New York: Dover Publications, 1972.

47. O. V. Rudenko, S. I. Soluyan, and R. V. Khokhlov, "Nonlinear Theory of Paraxial Sound Beams," Sov. Phys-Doklady 20, 836-837 (1976).

48. N. S. Bakhvalov, Ya. M. Zhileikin, and E. A. Zabolotskaya, "Nonlinear Propagation of Sound Beams with a Uniform Amplitude Distribution," Sov. Phys-Acoust. 26, 95-100 (1980).

49. D. G. Browning and R. H. Mellen, "Finite-Amplitude Distortion of 150-kHz Acoustic Waves in Water," J. Acoust. Soc. Am. 44, 644-646 (1968).

50. J. E. Blue, "Farzone Beam Pattern and Source Level for the Parametric Array," Applied Research Laboratories Technical Memorandum No. 74-21 (ARL-TM-74-21), Applied Research Laboratories, The University of Texas at Austin, 1974.

51. O. V. Rudenko, S. I. Soluyan, and R. V. Khokhlov, "Confinement of a Quasiplane Beam of Periodic Perturbations in a Nonlinear Medium," Sov. Phys-Acoust. 19, 556-559 (1974).

52. A. L. Polyakova, "Propagation of Finite-Amplitude Waves in Relaxing Media," Sov. Phys-Acoust. 6, 356-359 (1961).

53. P. J. Westervelt and J. Radue, "Nonlinear Diverging Waves," J. Acoust. Soc. Am. 33, 1672(A) (1961).

54. J. C. Lockwood, T. G. Muir, and D. T. Blackstock, "Directive Harmonic Generation in the Radiation Field of a Circular Piston," J. Acoust. Soc. Am. 53, 1148-1153 (1973).

55. P. M. Morse and K. U. Ingard, Theoretical Acoustics, New York: McGraw-Hill, 1968, p. 498.

56. L. D. Landau and E. M. Lifshitz, Theory of Elasticity, New York: Addison-Wesley, 1959, pp. 115-117.

57. V. A. Zverev and A. I. Kalachev, "Sound Radiation from the Region of Interaction of Two Sound Beams," Sov. Phys-Acoust. 15, 322-327 (1970).

58. V. A. Zverev and A. I. Kalachev, "Scattering of Sound by Sound When Two Sound Beams Intersect One Another," Proceedings of the 1975 International Symposium on Nonlinear Acoustics, Moscow University Press, Moscow, 1976, pp. 330-341.

59. J. A. TenCate, "Nonlinear Interaction of Two Noncollinear Sound Waves in a Waveguide," M. S. Thesis, The University of Texas at Austin, 1983.

60. K. U. Ingard and D. C. Pridmore-Brown, "Scattering of Sound by Sound," J. Acoust. Soc. Am. 28, 367-369 (1956).

61. R. T. Beyer, Nonlinear Acoustics, Naval Sea Systems Command, Washington, D. C., 1976, pp. 299-311.

62. F. H. Fenlon, "Nonlinear Acoustics," Short Course on Underwater Acoustics, The Pennsylvania State University, University Park, Pennsylvania, 1976.

63. P. J. Westervelt, "Scattering of Sound by Sound," J. Acoust. Soc. Am. 29, 199-203 (1957).

64. P. J. Westervelt, "Scattering of Sound by Sound," J. Acoust. Soc. Am. 29, 934-935 (1957).

65. F. H. Fenlon and J. E. Fahy, "Parametric Acoustic Conversion-Efficiency Enhancement via Boundary Induced and Inherent Dispersivity," Annual Summary Report for the Office of Naval Research, The Pennsylvania State University, University Park, Pennsylvania, 1980.

66. L. A. Ostrovskii and I. A. Papilova, "Nonlinear Mode Interaction and Parametric Amplification in Acoustic Waveguides," Sov. Phys-Acoust. 19, 45-50 (1973).

67. D. M. Yeager, "Nonlinear Acoustic Wave Interactions in Layered Media," M. S. Thesis, The Pennsylvania State University, University Park, Pennsylvania, 1980.

68. F. S. McKendree, personal communication, The Pennsylvania State University, University Park, Pennsylvania, 1980.

69. A. V. Hershey, "Computing Programs for the Complex Exponential Function," NPG Report No. 1646, U. S. Naval Proving Ground, Dahlgren, Virginia, 1959.

70. T. G. Muir and J. G. Willette, "Parametric Acoustic Transmitting Arrays," J. Acoust. Soc. Am. 52, 1481-1486 (1972).

71. M. B. Moffett and R. H. Mellen, "Model for Parametric Acoustic Sources," J. Acoust. Soc. Am. 61, 325-337 (1977).

DISTRIBUTION LIST FOR

ARL-TR-83-19

UNDER CONTRACT N00014-79-C-0624

Copy No.	
1 - 3	Office of Naval Research Physics Program Office (Code 412) 800 North Quincy Street Arlington, VA 22217
4	Office of Naval Research Director, Technology (Code 200) 800 North Quincy Street Arlington, VA 22217
5 - 7	Director Defense Advanced Research Projects Agency 1400 Wilson Blvd. Arlington, VA 22209 Attn: Technical Library
8 - 10	Naval Research Laboratory Department of the Navy Washington, DC 20375 Attn: Technical Library
11 - 13	Office of the Director of Defense Research and Engineering Information Office Library Branch The Pentagon Washington, DC 20301
14 - 15	U. S. Army Research Office Box 12211 Research Triangle Park, NC 27709
16 - 27	Defense Technical Information Center Cameron Station, Bldg. 5 5010 Duke Street Alexandria, VA 22314

Copy No.	
28	Director, National Bureau of Standards Department of Commerce Washington, DC 20234 Attn: Technical Library
29 - 31	Commanding Officer Office of Naval Research Western Regional Office 1030 East Green Street Pasadena, CA 91101
32 - 34	Commanding Officer Office of Naval Research Eastern/Central Regional Office 666 Summer Street Boston, MA 02210
35	Commandant of the Marine Corps Washington, DC 20380 Attn: Scientific Advisor (Code RD-1)
36	Naval Ordnance Station Indian Head, MD 20640 Attn: Technical Library
37	Naval Postgraduate School Monterey, CA 93940 Attn: Technical Library (Code 0212)
38	Naval Missile Center Point Mugu, CA 93010 Attn: Technical Library (Code 5632.2)
39	Naval Ordnance Station Louisville, KY 40214 Attn: Technical Library

Dist. List for ARL-TR-83-19 (cont'd)

Copy No.

Commanding Officer
Naval Ocean Research &
Development Activity
NSTL Station, MS 39529
40 Attn: Technical Library

Naval Explosive Ordnance
Disposal Facility
Indian Head, MD 20640
41 Attn: Technical Library

Naval Ocean Systems Center
Department of the Navy
San Diego, CA 92152
42 Attn: Technical Library

Naval Surface Weapons Center
White Oak Laboratory
Department of the Navy
Silver Spring, MD 20910
43 Attn: Technical Library

David W. Taylor Naval Ship
Research and Development
Center
Department of the Navy
Bethesda, MD 20084
44 Attn: Central Library
(Code L42 and L43)

Naval Avionics Facility
Department of the Navy
Indianapolis, IN 46218
45 Attn: Technical Library

Director
U. S. Army Engineering
Research and Development
Laboratories
Fort Belvoir, VA 22060
46 Attn: Technical Documents
Center

47 - 49 ODR&E Advisory Group on
Electron Devices
201 Varick Street
New York, NY 10014

Copy No.

50 Air Force Office of
Scientific Research
Department of the Air
Force
Bolling AFB, DC 22209

Air Force Weapons
Laboratory
Kirtland Air Force Base
Albuquerque, NM 87117
51 Attn: Technical Library

Air Force Avionics Laboratory
Air Force Systems Command
Wright-Patterson Air Force
Base
Dayton, OH 45433
52 Attn: Technical Library

Lawrence Livermore
Laboratory
University of California
P. O. Box 808
Livermore, CA 94550
53 Attn: Dr. W. F. Krupke

Harry Diamond Laboratories
2800 Powder Mill Road
Adelphi, MD 20783
54 Attn: Technical Library

Naval Air Development Center
Department of the Navy
Johnsville
Warminster, PA 18974
55 Attn: Technical Library

Naval Weapons Center
Department of the Navy
China Lake, CA 93555
56 Attn: Technical Library
(Code 753)

Naval Training Equipment
Center
Department of the Navy
Orlando, FL 32813
57 Attn: Technical Library

Dist. List for ARL-TR-83-19 (cont'd)

Copy No.

58 Naval Underwater Systems Center
New London Laboratory Detachment
Technical Center
New London, CT 06320

Brown University
Department of Physics
Providence, RI 02912
59 - 60 Attn: R. T. Beyer
P. J. Westervelt

Georgia Institute of Technology
School of Mechanical Engineering
Atlanta, GA 30332
61 - 62 Attn: J. H. Ginsberg
P. H. Rogers

Kalamazoo College
Department of Physics
Kalamazoo, MI 49007
63 Attn: W. M. Wright

New London Laboratory
Naval Underwater Systems Center
New London, CT 06320
64 Attn: M. B. Moffett

University of Tennessee
Department of Physics
Knoxville, TN 37916
65 Attn: M. A. Breazeale

Technical University of Denmark
Fluid Mechanics Department
Building 404
DK-2800 Lyngby
DENMARK
66 Attn: L. Bjørnø

Copy No.

University of Leeds
Department of Mathematics
Leeds, Yorkshire, LS2 9JT
ENGLAND
67 Attn: David G. Crighton

Institute of Sound and Vibration Research
The University
Southampton SO9 5NH
ENGLAND
68 Attn: Dr. C. L. Morfey

The Institute of Scientific & Industrial Research
Osaka University
Yamadakami, Suita-Shi
Osaka 565
JAPAN
69 Attn: Dr. Akira Nakamura

Instituto de Acústica
Centro de Fisica Aplicada
"Leonardo Torres Quevado"
Serrano, 144-Madrid-6
SPAIN
70 Attn: J. A. Gallego-Juárez

Department of Electrical Engineering
Nagoya University
Furo-Cho, Chikusa-Ku
Nagoya, 464
JAPAN
71 Attn: T. Kamakura

Yale University
Mason Laboratory
New Haven, CT 06511
72 Attn: Wesley N. Cobb

Matematisk Institutt
Allegaten 53-55
5014 Bergen-U
NORWAY
73 Attn: Sigve Tjøtta and
Jacqueline Naze Tjøtta

Dist. List for ARL-TR-83-19 (cont'd)

Copy No.	
	School of Physics University of Bath Claverton Down Bath BA2 7AY ENGLAND
74	Attn: Professor H. O. Berktay
	Hoover, Keith and Bruce, Inc. 9730 Town Park Houston, TX 77036
75	Attn: Herbert L. Kuntz
	Naval Research Laboratory Code 5135 Washington, DC 20375
76	Attn: D. Trivett
	Jet Propulsion Laboratory 4800 Oak Grove Pasadena, CA 91103
77	Attn: T. G. Wang
	MAR, Incorporated East Lyme, CT 06333
78	Attn: R. H. Mellen
	Department of Physics and Chemistry Naval Postgraduate School Monterey, CA 93940
79	Attn: S. L. Garrett
	Westinghouse Research and Development Center 1310 Beulah Road Pittsburgh, PA 15235
80	Attn: F. S. McKendree
	The Pennsylvania State University 331 Davey Laboratory University Park, PA 16802
81	Attn: J. D. Maynard

Copy No.	
	The Pennsylvania State University Applied Research Laboratory P. O. Box 30 State College, PA 16801
82	Attn: Librarian
83	Yves H. Berthelot
84 - 93	David T. Blackstock
94	James M. Estes
95 - 117	Mark F. Hamilton
118	Loyd D. Hampton
119	T. G. Muir
120	David A. Nelson
121	Richard L. Rolleigh
122	James A. TenCate
123	Suk Wang Yoon
124	Nonlinear Acoustics Project
125	Library, ARL:UT